UNIVERSIDAD NACIONAL AUTÓNOMA DE MÉXICO

POSGRADO EN CIENCIAS FÍSICAS

FROM QUANTUM RADIAL ANHARMONIC OSCILLATOR TO ZEEMAN EFFECT IN HYDROGEN ATOM

TESIS

QUE PARA OPTAR POR EL GRADO DE:

DOCTOR EN CIENCIAS (FÍSICA)

PRESENTA:

M. EN C. JUAN CARLOS DEL VALLE ROSALES

TUTOR PRINCIPAL:
DR. ALEXANDER TURBINER ROSENBAUM (ICN-UNAM)

COMITÉ TUTOR:
DR. JUAN CARLOS LÓPEZ VIEYRA (ICN-UNAM)
DR. JORGE ALEJANDRO REYES ESQUEDA (IF-UNAM)

CIUDAD DE MÉXICO, 2020

SEPTIEMBRE

Abstract

In the present thesis, two fundamental systems of quantum mechanics are studied: (*i*) the D-dimensional radial polynomial anharmonic potential, and (*ii*) a hydrogen atom subjected to a uniform constant magnetic field. For both systems, the corresponding Schrödinger equation is non-exactly solvable: closed analytical expressions (not in terms of infinite asymptotic series) for the energies and wave functions may be found only in approximate form. This thesis presents the general formalism to construct locally accurate approximations of the wave functions in the coordinate space, which leads to highly accurate energies and expectations values.

The first part of this thesis is devoted to constructing a locally accurate approximation, called the *Approximant*, for the wave functions of the low-lying states of the D-dimensional radial polynomial anharmonic potential. Perturbation Theory in the weak and strong coupling regimes, asymptotic expansions at small and large distances, and the *true* semi-classical approximation are basic ingredients of the formalism to construct the Approximant. The key result of this study is a compact expression for the exponential phase of the ground state wave function, which is parameter-dependent. This expression is the building block for constructing the Approximants of the excited states. To fix the value of some parameters, the exact reproduction of all growing terms of the exponential phase at large distances is imposed as constraint. This procedure effectively reduces the number of parameters. Taking the Approximant as trial function, the remaining free parameters are optimized in the framework of the Variational Method. In this manner, the energy is calculated as an expectation value of the Hamiltonian by means of a locally accurate Approximant.

Explicit calculations are carried out for the first four low-lying states of the cubic, quartic, and sextic anharmonic potentials of the form $V(r) = r^2 + g^{m-2} r^m$, with $m = 3, 4, 6$, respectively. For the cubic case, a one-parametric Approximant leads to unprecedented accurate energies with a relative accuracy of order $\lesssim 10^{-5}$ with respect to the *exact* result. In turn, the relative deviation of the Approximant from the *exact* wave function is $\lesssim 10^{-2}$ at any point of the r-space. For the case of the quartic/sextic anharmonicity, a 2/4-parametric Approximant leads to energies with a relative accuracy of order $\lesssim 10^{-8}$, while the relative accuracy of the Approximant is of order 10^{-6} for any point of the r-space. Consistency of those results is checked inside the Non-Linearization Procedure and the Lagrange-Mesh method.

In the second part, the formalism used for the radial anharmonic potential is employed to construct a locally accurate Approximant for the ground state ($1s_0$) of the hydrogen atom in a uniform constant magnetic field. A non-relativistic consideration with a static proton is assumed. The natural extension of the *true* semi-classical expansion was obtained for this system. The main result of this part is a compact 8-parametric expression for the Approximant of the ground state. When it is used as a trial function in the Variational Method, it leads to highly accurate energy (relative accuracy $\lesssim 10^{-6}$), and an accurate quadrupole moment in the whole domain of accessible magnetic fields in Nature.

Resumen

En la presente tesis se estudian dos sistemas fundamentales de mecánica cuántica: (i) el potencial anarmónico radial D-dimensional, y (ii) un átomo de hidrógeno en presencia de un campo magnético constante y uniforme. Para ambos sistemas, la ecuación de Schrödinger correspondiente no admite soluciones exactas: las energías y las funciones de onda solamente se pueden encontrar de forma aproximada. Esta tesis presenta el formalismo general para construir aproximaciones localmente precisas de las funciones de onda en el espacio de coordenadas, esto conduce a energías y valores de expectacíon altamente precisos.

La primera parte de la tesis está dedicada a construir una aproximación localmente precisa (llamada Aproximante) para las funciones de onda de los primeros estados ligados del potencial anarmónico radial D-dimensional. La teoría de perturbaciones en los regímenes de acoplamiento débil y fuerte, las expansiones asintóticas a pequeñas y grandes distancias, y la *verdadera* aproximación semiclásica son los ingredientes básicos del formalismo para construir el Aproximante. El resultado principal de este estudio es una expresión compacta para la fase exponencial de la función de onda del estado base, la cual depende de ciertos parámetros. Esta expresión es la pieza clave para construir Aproximantes de estados excitados. Para fijar el valor de algunos parámetros, se impone como constricción la reproducción exacta de todos los términos crecientes de la fase exponencial a grandes distancias. Este procedimiento reduce efectivamente el número de parámetros. Tomando el Aproximante como función de prueba, los parámetros restantes se optimizan usando el Método Variacional. De esta manera, la energía se calcula como el valor esperado del Hamiltoniano evaluado por medio de un Aproximante localmente preciso.

Se realizan cálculos explícitos para los primeros cuatro estados ligados de los potenciales anarmónicos cúbico, cuártico, y séxtico de la forma $V(r) = r^2 + g^{m-2}r^m$, con $m = 3, 4, 6$, respectivamente. Para el caso cúbico, un Aproximante con un solo parámetro conduce a energías sin precedentes de una precisión relativa de orden 10^{-5} en cualquier punto del espacio r. A su vez, la desviación relativa del Aproximante con respecto a la función de onda exacta es de orden 10^{-2}. Para los casos de anarmonicidad cuártica/sextica, un Aproximante de 2/4 parámetros conduce a energías de una precisión relativa de orden 10^{-8}, mientras que la precisión relativa del Aproximante es de orden 10^{-6} para cualquier punto del espacio r. La consistencia de esos resultados se verifica usando el Procedimiento de No-Linealización y por medio del método de la malla de Lagrange.

En la segunda parte, el mismo formalismo utilizado para el potencial anarmónico radial se emplea para construir un Aproximante localmente preciso para el estado base ($1s_0$) del átomo de hidrógeno en un campo magnético constante y uniforme. Las consideraciones del estudio son no-relativistas con un protón estático. El resultado principal de esta parte es una expresión compacta para el Aproximante del estado base. Cuando el Aproximante se usa como una función de prueba en el Método Variacional, este conduce a una energía altamente precisa (de precisión relativa 10^{-6}), y a un momento cuadrupolar preciso en todo el dominio de campos magnéticos accesibles en la Naturaleza ($\lesssim 2.35 \times 10^{13}$G).

Contents

Overview

It is well-known that the time-independent Schrödinger equation can be solved exactly for a few physical systems. Therefore, we need to use different approximation methods to handle the overwhelming majority of quantum-mechanical problems. In fact, much of the success of quantum mechanics has been achieved thanks to approximation methods. Among them, the Variational Method is one of the most powerful tools which allow us to deal with many physical systems of different nature. In all books on quantum mechanics, e.g. [1–3], the Variational Method plays a central role among the approximation methods presented. In the variational approach, the *trial function* is key for leading to approximations of the spectrum of a given system. A natural question is: how to choose an *adequate* trial function that yields reliable approximate energies and wave functions? The Variational Method *per se* does not provide a prescription about the choice of a trial function. Thus, the construction of a trial function is handmade, usually based on physical intuition. Symmetries of the system, perturbation theory, asymptotic analysis, semi-classical approximations, features of nodal surfaces, etc., are sources of information of the exact function that may be *coded* in the trial one. Nevertheless, one could choose a trial function based on technical arguments. For example, one may choose a trial function in such a way that all integrals involved in the realization of the Variational Method are calculated in closed analytical form or reduced to one-dimensional integrals. In fact, most of the trial functions chosen in atomic physics follow this line.

Any trial function represents an approximate solution of the Schrödinger equation. With an approximate solution, one can calculate the expectation values of relevant operators. It is known that a high accuracy reached in the variational energy does not guarantee high accuracy in such expectation values, see [4]. This reflects one fact: a trial function may be close to the exact one in the domain where the dominant contribution of the integrals (involved in the Variational Method) occurs, but it may differ in the domains required by the calculation of the expectation value. Let us discuss a simple example, see [5], that illustrates these phenomena described above.

We consider a particular system where the exact solutions are known: a hydrogen atom. The exact ground state wave function is well-known[1]

$$\psi_{exact}(r) \;=\; e^{-r} \;,$$

[1]Atomic units used: $\hbar = m_e = -e = 1$, where m_e and e are the mass and the electric charge of the electron, respectively.

as well as its energy[2]

$$E \;=\; -1\,\mathrm{Ry}\;.$$

Suppose we are not aware of the exact solution, and we want to use the Variational Method to estimate the ground state energy. In particular, we can consider a Gaussian trial function

$$\psi_I(r) \;=\; e^{-\alpha\, r^2}$$

where α is a positive variational parameter. With this trial function, the realization of the Variational Method is completely analytical. The optimal parameter α turns out to be $\alpha = \dfrac{8}{9\pi}$, and it leads to the following variational energy

$$E_{var} \;=\; -0.849\,\mathrm{Ry}\;.$$

This variational estimate deviates from the exact value around 15%. This result is surprising due to the high accuracy of the variational estimate and the simplicity of the trial function. The deviation can be dramatically reduced to 3% by considering a two-term superposition of the previous trial function, namely

$$\psi_{II}(r) \;=\; e^{-\alpha\, r^2} \;+\; \gamma\, e^{-\beta\, r^2}\;, \qquad \alpha, \beta \;> 0\;.$$

Here α, β, and γ are free parameters that are fixed by means of the Variational Method.[3] With this new trial function, the variational estimate of the energy is

$$E_{var} \;=\; -0.972\,\mathrm{Ry}\;.$$

One could continue to reduce the deviation taking as trial function a larger combination of Gaussian functions. However, no matter how many Gaussian functions we consider, it is clear that their sum will never converge to ψ_{exact}. This simple example evidences one important fact: although a trial function can provide an accurate estimate of the energy, the trial function with optimal parameters may not be very *close* to the exact one. In our particular example, it can be roughly seen if we plot the exact solution and compare it with the trial ones, see Fig. 1.

The closeness of the trial functions to the exact one may be qualitatively studied by means of the *relative deviation* (*Rd*), which is defined as

$$Rd(r) \;=\; \left|\frac{\psi_{exact}(r) - \psi_i(r)}{\psi_i(r)}\right|\;, \qquad i \;=\; I, II\;. \tag{1}$$

For both ψ_I and ψ_{II}, the plot of *Rd* as a function of r is presented in Fig. 2. In the domain $0 \leq r \lesssim 3.5$, the dominant contribution of the integrals (required by the Variational Method) occurs for both trial functions. Inside this domain, the relative deviation reaches a local maximum: ~ 0.6 and ~ 0.3 for ψ_I and ψ_{II}, respectively. Therefore, in percentage terms, ψ_{exact} may deviate from ψ_I around 60%, and 30% from ψ_{II}. Outside this domain, the relative deviation is a monotonically increasing function for both trial functions. Due to the large relative deviation

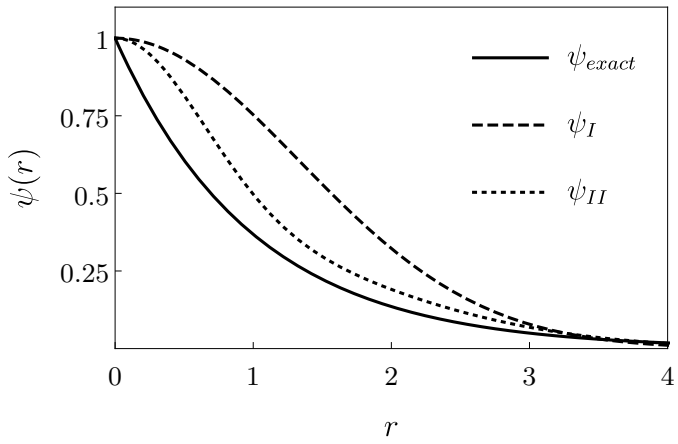

Figure 1: Plot of ψ_{exact}, ψ_I, and ψ_{II}. As normalization, we set $\psi_{exact}(0) = \psi_I(0) = \psi_{II}(0) = 1$.

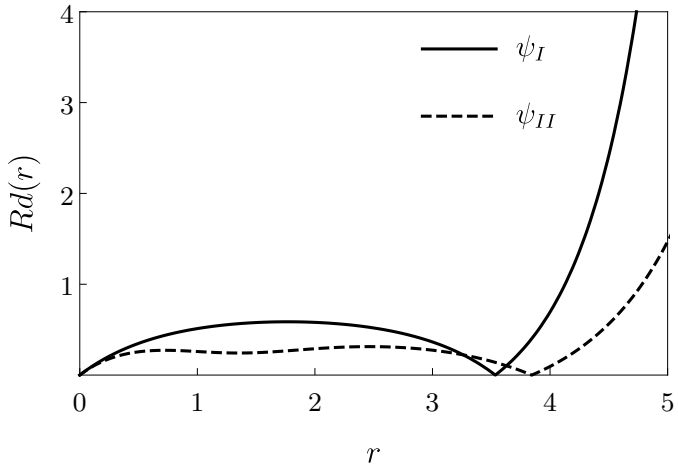

Figure 2: Relative deviation of the functions ψ_I and ψ_{II} (from ψ_{exact}) as a function of r

throughout the domain, we may say that neither ψ_I nor ψ_{II} are *locally accurate* approximations of ψ_{exact}.

Non-locally accurate approximation may lead to inaccurate estimates of some expectation values. For instance, let us now compute $\langle r^{2-n} \rangle$ using ψ_{exact}, ψ_I, and ψ_{II}. The numerical results are presented in Table 1. One can note that the deviation of the variational results, compared with the exact one, is significant for $n > 5$: it exceeds 30%. This deviation contrasts with the fact that for the trial functions ψ_I and ψ_{II}, the deviation of the variational energy from the exact one is 15% and 3%, respectively. The calculation of expectation values of more complex functions than simple monomials could be *catastrophic* for reaching highly accurate results. For example, one relevant quantity which involves expectation values is the *cusp parameter* C,

$$C \equiv \frac{\left\langle \psi \,\middle|\, \delta(\vec{r}) \frac{\partial}{\partial r} \,\middle|\, \psi \right\rangle}{\langle \psi \,|\, \delta(\vec{r}) \,|\, \psi \rangle} \ ,$$

[2]Ry stands for the Rydberg constant, 1 Ry $\approx$ 13.6 eV.

[3]The optimal choice of (rounded) parameters is $\alpha = 0.20$, $\beta = 1.33$, and $\gamma = 1.38$. The integration required by the Variational Method can be done analytically, while the optimization of parameters is a numerical procedure.

Table 1: Expectation values $\langle r^{n-2} \rangle$ for different values of n using ψ_{exact}, ψ_I, and ψ_{II}. Interestingly, at $n = 3$ the trial function ψ_I provides the exact result. Results rounded to first displayed s. d. Atomic units used.

n	ψ_{exact}	ψ_I	ψ_{II}
0	2	1.13	1.71
1	1	0.85	0.97
3	1.5	1.5	1.48
4	3	2.65	2.80
5	7.5	5.30	6.28
6	22.5	11.71	16.01
7	78.75	28.11	44.90

see [6]. In atomic physics, this parameter is usually employed to *measure* the local quality of the approximate wave function near the Coulomb singularities. Using the exact wave function of the hydrogen atom ψ_{exact}, the exact cusp parameter results in

$$C_{exact} = -1 \ .$$

This is an exact number that the ground state wave function of the hydrogen atom must provide. On the other hand, if we compute the cusp parameter associated with the approximate functions ψ_I and ψ_{II}, it is zero for both! This is nothing but a reflection of the fact that the logarithmic derivative of ψ_I and ψ_{II} do not have the correct asymptotic behavior at small r. In fact, the difference between ψ_{exact}, ψ_I, and ψ_{II} is more pronounced when we plot their corresponding logarithmic derivatives, see Fig. 3.

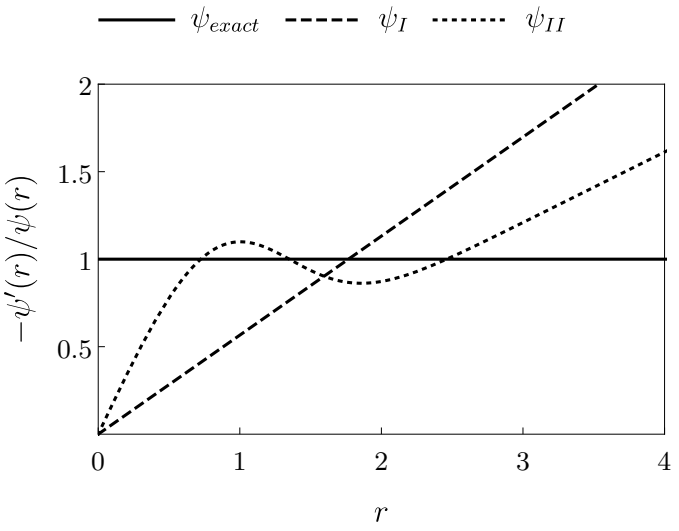

Figure 3: Logarithmic derivative of ψ_{exact}, ψ_I, and ψ_{II}.

This simple and illustrative example exhibits some important niceties that should be taken

into account when designing trial functions. However, it has to be noted that the above discussion is based on the knowledge of the exact energy and wave function, which is frequently unknown. So, the question is: how to estimate the accuracy of the approximate energy (wave function) that the Variational Method provides when the exact energy (wave function) is not available? The answer to this highly non-trivial question lies in the connection between the variational energy and perturbation theory discovered in [7]. This connection plays a fundamental role in this thesis.

The present work aims to construct locally accurate trial functions for one fundamental system: the quantum radial polynomial anharmonic oscillator in arbitrary dimension D. This study is strongly motivated by the work presented in [8]. Due to the separation of the angular variables, this D-dimensional system is reduced to a one-dimensional problem. We present a formalism to design locally accurate trial functions of any state for an arbitrary anharmonic potential. The formalism culminates in a simple expression that produces trial functions that lead to unprecedented results in the weak and strong coupling regime: highly accurate estimates of the exact energies, and locally accurate approximate wave functions. It is demonstrated that an extension of these ideas and the formalism may be applied to a different physical system: the hydrogen atom in a constant uniform magnetic field in its ground state. The formalism leads to an adequate trial function that yields highly accurate results for the energy and quadrupole moment for all magnetic fields available in Nature. For both systems, the obtained approximate wave functions actually represent approximate *solutions* of the corresponding Schrödinger equation. In fact, they can be considered as *exact and compact* solutions inside their domain of applicability. This will be discussed in detail for both systems.

The thesis is divided in two parts. Part I is devoted to the D-dimensional quantum radial anharmonic oscillator. The hydrogen atom in a constant magnetic field is studied in the Part II. It is worth mentioning that Part I and II can be read independently since they are self-contained. Each one begins with a short Introduction and ends with Conclusions. Regarding Part I, some of the results shown in this thesis were presented in [9, 10]. For Part II, they will appear in [11].

Chapter 1

The Basic Tool: Variational Method in Quantum Mechanics

In this Chapter, we present a brief and general description of the Variational Method (VM) in the framework of quantum mechanics. We focus the discussion on the ground state. However, when additional information about the nodal surface is available, it may be extended to study excited states.

1.1 Variational Principle and Upper Bounds for the Energy

Let us consider an arbitrary Hamiltonian $\hat{H}$ which describes a particular system of interest. We assume that the wave function of the ground state, as well as the corresponding energy, are unknown. If the Schrödinger equation of $\hat{H}$ is non-solvable, the natural question is: *How to find the energy and wave function approximately?* The variational principle gives us an answer in terms of the *variational energy*, which is defined as

$$E_{var}[\psi] \;=\; \frac{\int \psi_t^* \hat{H} \psi_t \, dV}{\int \psi_t^* \psi_t \, dV} \; . \tag{1.1}$$

Here, ψ_t is an arbitrary normalizable function,

$$\int \psi^* \psi \, dV \quad < \infty \; , \tag{1.2}$$

usually called *trial function*. The importance of the variational energy is established via the Variational Principle.

Variational Principle. *Consider a system described by the Hamiltonian $\hat{H}$ with exact ground state energy E_0, then the variational energy satisfies the inequality*

$$E_{var}[\psi_t] \;\geq\; E_0 \tag{1.3}$$

for any trial function ψ_t. Besides, the equality is fulfilled if and only if ψ_t is the exact ground state wave function of the system.

Proof. The trial function ψ_t can be expanded in terms of the (unknown) exact basis of orthonormal eigenfunctions $\{\psi_k\}$ of $\hat{H}$. Thus,

$$\psi_t \;=\; \sum_k c_k \psi_k \;, \qquad \hat{H}\psi_k \;=\; E_k \psi_k \;, \tag{1.4}$$

where c_k are some coefficients, and E_k is the eigenvalue associated to ψ_k. Without loss of generality, we assume that eigenvalues are sorted, $E_0 \leq E_1 \leq E_2 \leq \ldots$. Hence, the variational energy (1.1) reads

$$E_{var}[\psi_t] \;=\; \frac{\sum_k |c_k|^2 E_k}{\sum_k |c_k|^2} \;. \tag{1.5}$$

Since E_0 is the lowest energy, the following inequality holds

$$\sum_k |c_k|^2 E_k \geq E_0 \sum_k |c_k|^2 \;. \tag{1.6}$$

Using it in (1.5), it follows the variational principle

$$E_{var}[\psi_t] \;\geq\; E_0 \;. \tag{1.7}$$

From another side, it is clear that the equality is fulfilled if and only if ψ_t is the exact ground state wave function of $\hat{H}$. In this case, all coefficient c_k is zero except c_0. □

As one could imagine, the variational principle is a useful tool to estimate upper bounds of the exact ground state energy. The lower upper bound, the closer E_{var} is to the exact energy. In practice, the trial function can depend on a finite number of free parameters. In this manner, the variational energy will also be parameter-dependent. A proper choice of parameters may lead to the lowest upper bound that a given trial function can provide. This choice of parameters is known as *the optimal configuration*. The efficient way to find it is through an optimization procedure, which is, for most of the *adequate* trial functions, a numerical procedure. The Variational Method covers from the construction of the trial function to the calculation of the lowest upper bound.

1.2 Variational Energy and Perturbation Theory

We now discuss an interesting connection between the variational energy and Perturbation Theory (PT). For a given trial function ψ_t, it is straightforward to calculate the Hamiltonian $\hat{H}_t$ for which ψ_t is an *exact* ground state eigenfunction. We call this procedure *the Inverse Problem*. In fact, since the kinetic operator $\hat{T}$ of the Hamiltonian is usually given, we can

focus only on the construction of the *associated* potential[1] V_t of such Hamiltonian. Thus, let us assume that $\hat{H}_t$ is of the form

$$\hat{H}_t \;=\; \hat{T} \;+\; V_t \;. \tag{1.8}$$

Since ψ_t is the exact eigenfunction of $\hat{H}_t$, it is clear that it obeys

$$\hat{H}_t\psi_t \;=\; \hat{T}\psi_t \;+\; V_t\psi_t \;=\; E_0^{(t)}\psi_t \;, \tag{1.9}$$

where $E_0^{(t)}$ is the ground state energy[2] of $\hat{H}_t$. From equation (1.9) we can trivially solve for the (unknown) V_t,

$$V_t \;= E_0^{(t)} - \frac{\hat{T}\psi_t}{\psi_t} \;. \tag{1.10}$$

Since $E_0^{(t)}$ can be absorbed in the definition of V_t, its value is unimportant. It is evident that when solving the inverse problem, we can generate zillions of potentials for which a single eigenstate - the lowest - is known exactly. Once V_t is known, the connection between the variational energy and PT can be established.

Suppose that we are interested in the ground state of the operator

$$\hat{H} \;=\; \hat{T} \;+\; V \;. \tag{1.11}$$

However, it turns out that the corresponding Schrödinger equation

$$\hat{H}\psi \;= E\psi \tag{1.12}$$

is non-solvable. To estimate E, we use the VM with a trial function ψ_t as entry. Thus, we calculate the variational energy associated to ψ_t

$$E_{var}[\psi_t] \;=\; \frac{\int \psi_t^*(\hat{T}\psi_t + V\psi_t)\, dV}{\int \psi_t^*\psi_t\, dV} \;. \tag{1.13}$$

Using (1.10), we can write (1.13) as follows

$$E_{var}[\psi_t] \;=\; E_0^{(t)} \;+\; \frac{\int \psi_t^*(V - V_t)\psi_t\, dV}{\int \psi_t^*\psi_t\, dV} \;. \tag{1.14}$$

If we define

$$E_1^{(t)} \;=\; \frac{\int \psi_t^*(V - V_t)\psi_t\, dV}{\int \psi_t^*\psi_t\, dV} \;, \tag{1.15}$$

the expression shown in (1.14) acquires a more compact form,

$$E_{var}[\psi_t] \;=\; E_0^{(t)} \;+\; E_1^{(t)} \;. \tag{1.16}$$

This result suggests reinterpreting the variational energy as the first two terms of an expansion in PT developed for the *perturbed* Hamiltonian

$$\hat{H} \;=\; \hat{T} \;+\; V_t \;+\; \lambda\,(V - V_t) \;. \tag{1.17}$$

[1] In this work, potentials are always real functions.

[2] The meaning of the subscript will be clarified, for now, it is just notation.

Here, λ is a formal parameter that ultimately should be placed equal to one, $\lambda = 1$. The meaning of the superscripts placed in (1.16) is now clear: $E_0^{(t)}$ plays the role of the zero-order correction of the energy, while $E_1^{(t)}$ - the expectation value of perturbation potential $(V - V_t)$ - is the first order correction. To summarize,

The computation of the variational energy of a given Hamiltonian $\hat{H} = \hat{T} + V$, taking as trial function ψ_t, is equivalent to calculate the first two terms in a formal PT. The trial function ψ_t is the exact ground state of the unperturbed Hamiltonian $\hat{H}_t = \hat{T} + V_t$, while $V - V_t$ plays the role of perturbation.

If higher order corrections, $E_2^{(t)}, E_3^{(t)}, ...$, are known, they may be used to estimate the accuracy of the variational energy. In principle, the exact value of the lowest energy of $\hat{H}$ is the sum of those corrections,

$$E \;=\; \sum_{n=0}^{\infty} E_n^{(t)} \;. \tag{1.18}$$

In general, the question about the convergence of the expansion (1.18) is crucial but difficult to answer. We restrict ourselves by saying that if ψ_t is chosen with the appropriate asymptotic behavior at large distances, a convergent expansion will occur. In this situation, our initial variational estimate of the energy can be improved by adding next-order corrections. In practice, it is sufficient to calculate few terms in the expansion (1.18) to estimate rates of convergence as well as highly accurate estimates of the exact energy via partial sums. For all one dimensional physical systems, a considerable number of corrections $E_n^{(t)}$ can be calculated. This situation changes dramatically when we deal with *true* multidimensional systems.

The calculation of any energy correction, i.e. $E_2^{(t)}$, $E_3^{(t)}, ...$, requires the knowledge of the corrections to the wave function in PT. In this manner, using corrections for ψ_t, the deviation (between the trial function and exact one) can also be analyzed and, more important, estimated.

Part I

Radial Anharmonic Oscillator

Chapter 2

Introduction

2.1 Anharmonic Oscillator and Diatomic Molecules

The first *modern* study of the one-dimensional quantum anharmonic oscillator dates back to 1925. This study was carried out by Heisenberg and presented to the scientific community in [12]. In this work, Heisenberg considered the cubic and quartic anharmonic oscillators described by the classical equations of motion

$$\ddot{x} \; + \; w_0^2 \, x \; + \; \lambda \, x^2 \; = \; 0 \; ,$$

$$\ddot{x} \; + \; w_0^2 \, x \; + \; \lambda \, x^3 \; = \; 0 \; ,$$

respectively. We have denoted the coupling constant as λ, in turn, w_0 is the natural frequency of the harmonic oscillator. In the framework of what would later be called Matrix (quantum) Mechanics, he presented not only the energy spectrum of the harmonic oscillator ($\lambda = 0$) for the first time, but also gave the first corrections to the energy in PT in powers of λ. For the cubic case, a first order (vanishing) correction was obtained. For the quartic case, the first two corrections were presented. Results at $\lambda = 0$ were confirmed in the framework of quantum mechanics exposed by Schrödinger just one year later [13]. Around those years, the main motivation to study anharmonic perturbations of the harmonic oscillator came from atomic and molecular physics. A concrete example is the discovery of the spectral band at 1.76μm of the diatomic molecule HCl (hydrogen chloride). This result, obtained by Brinsmade and Kemble in 1917 [14], was of importance since it established that the HCl molecule behaves as an anharmonic oscillator and showed how this could be interpreted on the basis of the early quantum theory introduced by Planck. Once the Schrödinger equation was presented to the world in 1926, the diatomic molecule described by a 3-dimensional anharmonic potential was studied immediately, see e.g. [15]. Due to the exactly solvable *nature* of the one-dimensional Morse potential, it was widely used to model the interaction between the two atoms of a diatomic molecule near their equilibrium position [16, 17]. The Morse potential is given by

$$V(r) \; = \; V_0 (e^{-2a(r-r_0)} \; - \; 2 \, e^{-a(r-r_0)}) \; ,$$

where V_0 is the energy of dissociation, r the nuclear separation, r_0 the equilibrium value of r, and a is a positive constant. From the Taylor expansion of this potential around r_0,

$$V(r) \;=\; V_0\left(-1 \;+\; a^2(r-r_0)^2 \;-\; a^3(r-r_0)^3 \;+\; \frac{7a^4}{12}(r-r_0)^4 \;+\; \ldots\right) , \qquad (2.1.1)$$

one can easily check that the Morse potential contains an infinite number of anharmonic terms. Following the vibrational spectroscopic information, one can determine parameters a, V_0, and r_0. For example, the diatomic molecule BeO (beryllium oxide, see [16]) in the state Σ^1 is characterized by

$$a \;=\; 2.12\, a_0^{-1}, \qquad V_0 \;= 5.245\,\mathrm{eV}\ , \qquad r_0 \;=\; 1.27\, a_0\ ,$$

where $a_0 = 5.29\times 10^{-9}$cm is the Bohr radius. As far as vibrational energy levels are concerned, the Morse potential provides accurate results. However, when the information given by the rotational energy levels is taken into account, certain discrepancies are found [15]. A natural direction, to avoid such discrepancies, was to consider a more general radial anharmonic polynomial potential[1] of the form

$$V(r) \;=\; K(r-r_0)^2\left(1 \;+\; b\,(r-r_0) \;+\; c\,(r-r_0)^2 \;+\; d\,(r-r_0)^3 \;+\; \ldots\right) ,$$

with K, b, c, d, ..., being real parameters called anharmonic constants. With this kind of potential, the corresponding Schrödinger equation is non-exactly solvable: energies and wave functions can be found only in approximate form. The first approaches to solve it ($\sim$1926) were based on the Bohr theory [18], and second order PT [19]. Over the next years, several studies were focused on determining the first anharmonic constants of several diatomic molecules using those approaches.

2.2 Renewed Interest

As we have seen, immediately after the foundation of quantum mechanics, the study of anharmonic oscillators was strongly motivated by molecular physics. From a more general point of view, it was recognized that the spectral problem of a quantum anharmonic oscillator has very interesting properties. The publication of seminal papers by Bender and Wu [20] (from 1969) refreshed the interest in the quantum mechanical properties of anharmonic oscillators. First, they studied the one-dimensional quartic anharmonic oscillator characterized by the quantum Hamiltonian

$$\hat{H} \;=\; -\frac{d^2}{dx^2} \;+\; \frac{1}{4}x^2 \;+\; \frac{1}{4}\lambda\, x^4\ ,$$

where λ is a positive coupling constant. In particular, this Hamiltonian is interesting because it allows us to demonstrate that the perturbation series of the energy in powers of λ diverges for any state. They investigated the reason for this divergence using an analytical continuation of the energy levels into the complex λ-plane as well as the WKB approximation. It turned out

[1] Series are truncated up to some order.

that the presence of an infinite number of branch points with a limit point at $\lambda = 0$ was the reason for this divergence. A generalization of this study was presented a few months later by Bender [21]. This time he considered a more general case

$$\hat{H} \;=\; -\frac{d^2}{dx^2} \;+\; \frac{1}{4}x^2 \;+\; \frac{1}{2^M}\lambda\, x^{2M} \;,$$

where $M = 2, 3, \ldots$. Analytical features of the energy levels were investigated in this work. He concluded that those properties are qualitatively similar to the case $M = 2$. Interestingly, it was shown that the exact solution exists in the limit $M \to \infty$. In a following paper (1973), Bender and Wu [22] developed two independent mathematical techniques for determining the large-n behavior of PT for the quartic anharmonicity. In fact, asymptotic expressions at large n of perturbation coefficients were immediately called Bender-Wu formulas.

After the publication of their results, thousands of physical systems were suddenly connected in one way or another. For example, the Hamiltonian of the one-dimensional quantum quartic anharmonic oscillator represents a ϕ^4 scalar quantum field theory in $(0+1)$ dimensions. Many properties that appear in $(0 + 1)$ dimension, like divergence in PT, can also be present in a realistic field theory. The apparently simple problem of a quantum anharmonic oscillator revealed an extremely rich internal structure, which looks intrinsic for any non-trivial system in quantum mechanics. In particular, they formally evidenced the impossibility of finding the spectrum in PT in powers of λ. These facts encouraged the development of various numerical and analytical non-perturbative methods over the next years. Thus, the anharmonic oscillator became a basic system to test new methods. That explains why, from the early '70s until today, one can find many papers devoted to the exploration of the quantum spectra of the anharmonic potential[2]. It is worth mentioning some of the methods used throughout the years: Variational Method [23, 24], Rayleigh-Ritz method [25], PT in both the weak and strong coupling regimes [20,22,26–30], Padé Approximants [31], Hill Determinant method [32–34], WKB method [35,36], Self-Similar Approximations [37], the method of Characteristic Functions [38], among many, many others.

2.3 Present Work

From previous considerations, it is clear that the anharmonic oscillator has a fundamental interest in physics. The present study is devoted to studying the energy spectra of the D-dimensional radial polynomial anharmonic oscillator. One may ask: why to consider it in D-dimension? Of course, the physical spatial dimensions, $D = 1, 2, 3$, are evidently the most popular. However, as it will be shown, in our study the dimension D does not play an essential role in the formalism that we present below: it appears only as an *external* parameter. We may easily deal with an arbitrary D, and ultimately set its value to the dimension of interest. Furthermore, some non-trivial analytical properties of the energy as a function of D appear at both physical and not-physical dimensions, [39, 40].

[2]Specially in one-dimension for quartic and sextic cases.

This work aims primarily to study the ground state of the radial anharmonic oscillator in arbitrary D using as tools PT in the weak and strong coupling regimes, asymptotic series at small and large distances, and a *new version* of the semi-classical approximation. In general, here we present the formalism to study an arbitrary polynomial anharmonic oscillator. Nevertheless, as we will see in Part II, it can be applied to physical systems with different nature.

Our ultimate goal is to construct a locally-accurate approximation of the ground state wave function in arbitrary (integer) dimension $D > 0$. We will call this approximation the *Approximant*, and we will denote it by $\Psi^{(t)}_{0,0}$. Moreover, we will show how the Approximant $\Psi^{(t)}_{0,0}$ can be modified to construct Approximants for the wave functions of excited states. It will be demonstrated that when an Approximant is used as a trial function in the Variational Method (VM), it leads to a highly accurate estimate of the energy with a very small deviation from the *exact result* for all coupling constant. In fact, some of our results will serve as benchmarks for future works. Furthermore, a fast-convergent PT occurs for both the energy and the wave function if the trial function is used as the zeroth order approximation in a PT scheme[3]. This is explicitly checked for three anharmonicities: cubic, quartic, and sextic.

[3]By means of the connection between PT and the variational energy discussed in the previous Chapter.

Chapter 3

Generalities

In the forthcoming Sections, we present some general results that will be useful for our study of the D-dimensional anharmonic oscillator.

3.1 Radial Potential in D-dimension

The time-independent Schrödinger equation for a particle subjected to a spherical-symmetric potential $V(r)$ in a D-dimensional space ($D = 1, 2, ...$) has the form

$$\left[-\frac{\hbar^2}{2M}\nabla_D^2 \;+\; V(r)\right]\psi \;=\; E\,\psi\;. \tag{3.1.1}$$

Here $\hbar$ is the Planck constant, M is the mass of the particle,

$$\nabla_D^2 = \sum_{k=1}^{D}\partial_{x_k}^2 \tag{3.1.2}$$

is the D-dimensional Laplace operator in Cartesian coordinates $\{x_1, x_2, ...x_D\}$,

$$r \;=\; \sqrt{x_1^2 + x_2^2 + ... + x_D^2}\;, \qquad x_i \in (-\infty, \infty)\;, \tag{3.1.3}$$

$i = 1, ..., D$, is the radius in D-dimension[1], while ψ and E represent wave function and its corresponding energy, respectively. Due to the spherical symmetry of the potential $V(r)$, in $D > 1$ it is convenient to introduce D-dimensional hyperspherical coordinates[2] $\{r, \Omega\}$, with r as in (3.1.3) and Ω parameterized with $(D-1)$ Euler angles. In these coordinates, the Laplace operator ∇_D^2 takes the form

$$\nabla_D^2 \;=\; \partial_r^2 \;+\; \frac{D-1}{r}\partial_r \;+\; \frac{\Delta_{S^{D-1}}}{r^2}\;, \quad \partial_r \equiv \frac{\partial}{\partial r}\;, \tag{3.1.4}$$

[1] In the present work, we assume that at $D = 1$ the radius becomes $r = |x|$, see (3.1.3), thus $V = V(|x|)$.
[2] See [41, 42].

where $\Delta_{S^{D-1}}$ is the Laplacian on the S^{D-1} sphere. Naturally, if we choose in (3.1.4) a dimension $D = 2, 3$, we obtain the familiar expressions of the Laplacian in polar and spherical coordinates, respectively. For the purposes of the present work, the explicit form of the operator S^{D-1} is not needed. It is enough to know that the operator $\Delta_{S^{D-1}}$ is closely related with the D-dimensional orbital angular momentum $\hat{\mathbf{L}}$,[3]

$$\Delta_{S^{D-1}} \;=\; -\hat{\mathbf{L}}^2 \;. \tag{3.1.5}$$

This relation[4] brings two remarkable consequences at $D > 1$:

(*i*) For any spherically symmetric potential, the D-dimensional angular momentum $\hat{\mathbf{L}}$ is conserved.

(*ii*) In hyperspherical coordinates, we can separate the hyperradial coordinate r from the angular ones (Ω).

Hence, in $D > 1$ the wave function ψ and its energy E can be labeled by one radial quantum number n_r, one angular quantum momentum ℓ, and $(D-2)$ *magnetic* quantum numbers. As a consequence, the wave function is represented as the product of two functions

$$\psi_{n_r,\ell,\{m_\ell\}}(r,\Omega) \;=\; \Psi_{n_r,\ell}(r)\,\xi_{\ell,\{m_\ell\}}(\Omega) \;, \tag{3.1.6}$$

where $n_r = 0, 1, 2, \ldots$, $\ell = 0, 1, 2, \ldots$. The set of $(D-2)$ magnetic quantum numbers $\{m_\ell\}$, where each of them takes values from $-\ell$ to $+\ell$, contains $\mathcal{N}(D,\ell)$ different configurations, where

$$\mathcal{N}(D,\ell) \;=\; \begin{cases} \dfrac{(2\ell+D-2)\,(\ell+D-3)!}{\ell!\,(D-2)!} \;, & \ell \geq 1, \\ 1 \;, & \ell = 0 \;. \end{cases} \tag{3.1.7}$$

For $D > 1$, the *angular* part of the wave function $\xi_{\ell,\{m_\ell\}}(\Omega)$ corresponds to a D-dimensional spherical harmonic [41, 42] which satisfies the spectral problem

$$-\,\Delta_{S^{D-1}}\,\xi_{\ell,\{m_\ell\}} \;=\; \hat{\mathbf{L}}^2\,\xi_{\ell,\{m_\ell\}} \;=\; \ell\,(\ell+D-2)\,\xi_{\ell,\{m_\ell\}} \;. \tag{3.1.8}$$

Hence, for given ℓ this equation is satisfied by $\mathcal{N}(D,\ell)$ different linear independent spherical harmonics, which correspond to the eigenvalue $\ell\,(\ell+D-2)$ with degeneracy[5] equals to $\mathcal{N}(D,\ell)$.

[3]The $D(D-1)/2$ independent components of the D-dimensional angular momentum *tensor* are

$$L_{ij} \;=\; x_i p_j \;-\; x_j p_i \;, \qquad i < j \;,$$

where x_i and p_i are the ith coordinate and the linear quantum momentum, respectively.

[4]The operator $\hat{\mathbf{L}}^2$ is defined as

$$\hat{\mathbf{L}}^2 \;=\; \sum_{j=2}^{N} \sum_{i=1}^{j-1} L_{ij}^2$$

in terms of its components, see [43].

[5]Note that for $D = 3$, the eigenvalue of $\hat{\mathbf{L}}^2$ and its degeneracy are given by the familiar formulas $\ell(\ell+1)$ and $\mathcal{N}(3,\ell) = 2\ell+1$, respectively.

Not surprisingly, two spherical harmonics with different quantum numbers and same ℓ are orthogonal,

$$\int_{\Omega} \xi_{\ell,\{m_\ell\}} \xi_{\ell,\{m'_\ell\}} \, d\Omega \;=\; \delta_{m_\ell,m'_\ell} \tag{3.1.9}$$

where δ_{m_ℓ,m'_ℓ} is the Kronecker delta, and $d\Omega$ is the solid angle in $D-1$ dimensions. Furthermore, two spherical harmonics with different angular momentum, say ℓ and ℓ', are orthogonal too. Further properties of the spherical harmonics can be found in [41,42]. However, those properties do not play an important role in the present work. Since the theory of the spherical harmonics is well established, we have to focus solely on determining the *radial* part of the wave function $\Psi_{n_r,\ell}(r)$.

After substituting (3.1.4), (3.1.6) and (3.1.8) into (3.1.1), we arrive to a *radial* Schrödinger equation[6]

$$\left[-\frac{\hbar^2}{2M}\left(\partial_r^2 \;+\frac{D-1}{r}\,\partial_r - \frac{\ell\,(\ell+D-2)}{r^2}\right) + V(r)\right]\Psi_{n_r,\ell}(r) \;=\; E_{n_r,\ell}\,\Psi_{n_r,\ell}(r)\;, \tag{3.1.10}$$

which determines the *radial* wave function $\Psi_{n_r,\ell}(r)$. For any radial potential, the energy $E_{n_r,\ell}$ of an excited state is always degenerate with respect to the quantum numbers $\{m_\ell\}$. Specifically, for a given $(n_r,\, \ell)$ and $D > 1$ we have $\mathcal{N}(D,\ell)$ different wave functions with the same energy. Note that the magnetic quantum numbers do not play an essential role. For this reason, since now on, we get rid of the label $\{m_\ell\}$ in the energy and wave function.

3.2 Radial Polynomial Anharmonic Oscillator

From now on, we consider the radial polynomial anharmonic potential[7]

$$V(r) \;=\; \frac{1}{g^2}\sum_{k=2}^{m} a_k\, g^k\, r^k\;, \qquad m \geq 2\;, \tag{3.2.1}$$

where g is a non-negative coupling constant, a_k are real parameters. In addition, we consider only potentials such that $V(r) > 0$ at $r > 0$, with a_2 and a_m positive. Hence, the minimum at $r = 0$ is global. For $m > 3$ there may be some other (local) minimums at $r > 0$. For the sake of simplicity, we assume that none of them is degenerate. Evidently, under these considerations the Hamiltonian

$$\hat{H} \;=\; -\frac{\hbar^2}{2M}\nabla_D^2 \;+\; \frac{1}{g^2}\sum_{k=2}^{m} a_k\, g^k r^k, \tag{3.2.2}$$

[6]It is known that by means of a *gauge rotation*, equation (3.1.10) can be transformed into a one-dimensional Schrödinger one with an effective potential. However, we do not follow this approach since it does not provide advantages in the present study.

[7]Note that any radial polynomial potential, with a leading quadratic term at small r, can be rewritten as in (3.2.1) employing scalings in coefficients a_k.

has an infinite and discrete spectrum: the potential (3.2.1) admits bound states. Let us note that the potential (3.2.1) can be written in a *compact* form as

$$V(r) \;=\; \frac{1}{g^2}\hat{V}(gr)\;, \tag{3.2.3}$$

where we have defined

$$\hat{V}(gr) \;=\; \sum_{k=2}^{m} a_k\,(gr)^k\;. \tag{3.2.4}$$

As we discussed in the previous Section, separation of variables occurs for the Schrödinger equation associated to Hamiltonian (3.2.2). Therefore, we only have to determine the radial part of the wave function using the Schrödinger equation (3.1.10). We are not trying to find the complete spectra of the Hamiltonian operator (3.2.2). Our study is devoted to the low-lying states. However, as we will see through these pages, the ground state plays the most important role between the low-lying states.

3.3 The Ground State: Riccati Equation

The ground state of any spherical symmetric D-dimensional Hamiltonian is non-degenerate (and nodeless). It has zero angular momentum $\ell = 0$ (S-state) and zero radial quantum number $n_r = 0$. The angular part corresponds to the zeroth spherical harmonic (which is a constant) with zero eigenvalue in (3.1.8). From (3.1.10), it can be seen that the ground wave function depends only on the radial coordinate r, we will denote it without labels by $\Psi(r)$. For the D-dimensional radial anharmonic oscillator (3.2.1), the ground state wave function corresponds to the lowest energy eigenfunction of the radial Schrödinger operator

$$\hat{h}_r \;=\; -\frac{\hbar^2}{2M}\left(\partial_r^2 \;+\; \frac{D-1}{r}\,\partial_r\right) \;+\; \frac{1}{g^2}\hat{V}(gr)\;. \tag{3.3.1}$$

The corresponding spectral problem, with explicit boundary conditions, read

$$\hat{h}_r\,\Psi(r) \;=\; E\,\Psi(r)\;, \qquad \int_0^\infty \Psi^2\, r^{D-1}dr \;<\; \infty\;, \qquad \Psi(0) \;=\; 1, \quad \Psi(\infty) \;=\; 0\;. \tag{3.3.2}$$

Here E denotes the ground state energy. It is interesting to note that D may be considered as a continuous parameter in (3.3.2). It will be shown that some non-trivial analytical properties of the ground state energy as a function of D appear at non-physical dimensions, see e.g. [39] and [40].

To solve the spectral problem (3.3.2), it is convenient to adopt the so-called exponential representation,

$$\Psi(r) \;=\; e^{-\frac{1}{\hbar}\Phi(r)}. \tag{3.3.3}$$

The function $\Phi(r)$ has dimension of action, and it is usually called *the phase* of the wave function. Thus, instead of looking for Ψ, we have to find the phase Φ. From (3.3.2), it can

be shown that Φ satisfies a non-linear ordinary differential equation of first order and second degree,

$$\hbar\,\partial_r y(r) \;-\; y(r)\left(y(r) - \frac{\hbar(D-1)}{r}\right) \;=\; 2M\left[E \;-\; \frac{1}{g^2}\hat{V}(r)\right], \tag{3.3.4}$$

where the function $y(r)$ is nothing but the derivative of $\Phi(r)$

$$y(r) \;=\; \partial_r \Phi(r)\;. \tag{3.3.5}$$

In fact, $y(r)$ coincides with the logarithmic derivative of the wave function Ψ,

$$y(r) \;=\; -\hbar\,\partial_r\left(\log\Psi(r)\right). \tag{3.3.6}$$

Equation (3.3.4) is a particular case of the familiar Riccati (differential) equation. It shows that the logarithmic derivative $y(r)$ is *more fundamental* than the wave function Ψ, and even more than the phase. The Riccati equation is the key equation of this Chapter.

3.3.1 Riccati-Bloch Equation

The Riccati equation (3.3.4) can be transformed into one without the explicit dependence on the constants $\hbar$ and M. This is achieved by introducing the *quantum coordinate*[8]

$$v \;=\; \left(\frac{2M}{\hbar^2}\right)^{\frac{1}{4}} r\;, \tag{3.3.7}$$

and making the replacements

$$y \;=\; (2M\hbar^2)^{\frac{1}{4}}\,\mathcal{Y}(v) \quad , \qquad E \;=\; \frac{\hbar}{(2M)^{\frac{1}{2}}}\,\varepsilon\;. \tag{3.3.8}$$

In this way, the equation (3.3.4) becomes

$$\partial_v\mathcal{Y}(v) \;-\; \mathcal{Y}(v)\left(\mathcal{Y}(v) - \frac{D-1}{v}\right) \;=\; \varepsilon(\lambda) \;-\; \frac{1}{\lambda^2}\,\hat{V}(\lambda v) \quad , \quad \partial_v \equiv \frac{d}{dv}\;, \tag{3.3.9}$$

where

$$\lambda \;=\; \left(\frac{\hbar^2}{2M}\right)^{\frac{1}{4}} g \tag{3.3.10}$$

plays the role of the *effective* coupling constant replacing g. Using previous definitions, it is evident that

$$\lambda\, v = g\, r\;. \tag{3.3.11}$$

The boundary conditions which we impose to the equation (3.3.9) are

$$\partial_v\mathcal{Y}(v)\Big|_{v=0} \;=\; \frac{\varepsilon}{D} \quad , \quad \mathcal{Y}(+\infty) \;=\; +\infty\;. \tag{3.3.12}$$

[8]We call v *the quantum coordinate* because it depends explicitly on the Planck constant $\hbar$.

These two boundary conditions guarantee that the corresponding wave function is normalizable, leading to a bound state. Evidently, if $\hbar = 1$ and $M = 1/2$, the equations (3.3.9) and (3.3.4) coincide with the same coupling constant $\lambda = g$. We call the equation (3.3.9) the Riccati-Bloch (RB) equation. It governs the *dynamics* of the logarithmic derivative in the v-space.

The RB equation (3.3.9) allows us to construct the asymptotic expansions of $\mathcal{Y}(v)$ at small and large v.[9] For fixed $\lambda \neq 0$ and *small* v, we have the Taylor series[10]

$$\mathcal{Y}(v) \;=\; \frac{\varepsilon}{D}\,v + \frac{(\varepsilon^2 - a_2 D^2)}{D^2(D+2)}\,v^3 - \frac{a_3\lambda}{D+3}\,v^4 - \frac{a_4 D^3(D+2)\lambda^2 - 2\,\varepsilon\,(\varepsilon^2 - a_2 D^2)}{D^3(D+2)(D+4)}\,v^5 + \dots\,. \tag{3.3.13}$$

For *large* v,

$$\mathcal{Y}(v) = a_m^{1/2}\lambda^{(m-2)/2}v^{m/2} + \frac{a_{m-1}\lambda^{(m-4)/2}}{2a_m^{1/2}}v^{(m-2)/2} + \frac{(4a_m a_{m-2} \;-\; a_{m-1}^2)\lambda^{(m-6)/2}}{8a_m^{3/2}}v^{(m-4)/2} + \dots\,. \tag{3.3.14}$$

It is easy to check that for $\lambda = 0$, hence, for the harmonic oscillator potential $V(r) = a_2\,r^2$, the equation (3.3.9) has the exact solution

$$\mathcal{Y}(v) = \;\frac{\varepsilon}{D}\,v\;, \qquad \varepsilon \;=\; a_2^{1/2}\,D\;. \tag{3.3.15}$$

Not surprisingly, this solution leads to the well-known ground state *Gaussian* wave function of the harmonic oscillator.

Four remarks in a row:

(*i*) The expansion (3.3.13) at $\lambda = 0$ is terminated, and it consists of the first term alone, leading to $\mathcal{Y}(v) = (\varepsilon/D)\,v$, which is in agreement with (3.3.15).

(*ii*) In general, the majority of the coefficients in the expansion of $\mathcal{Y}(v)$ in powers of v, see (3.3.13), depends on the energy ε explicitly.

(*iii*) The fourth and subsequent (unwritten) terms in (3.3.14) can acquire explicit dependence on ε.

(*iv*) For M fixed, large v can be obtained in two situations: large r and fixed $\hbar$, or fixed r and small $\hbar$, see (3.3.7). Hence, the expansion (3.3.14) can describe the semi-classical limit $\hbar \to 0$.

Integrating (3.3.13) and (3.3.14) with respect to the coordinate v, both expansions are converted into series for $\frac{1}{\hbar}\Phi$, namely,

$$\frac{1}{\hbar}\Phi \;=\; \frac{\varepsilon}{2D}v^2 + \frac{(\varepsilon^2 - a_2 D^2)}{4D^2(D+2)}v^4 - \frac{a_3\lambda}{5(D+3)}v^5 - \frac{a_4 D^3(D+2)\lambda^2 - 2\varepsilon(\varepsilon^2 - a_2 D^2)}{6D^3(D+2)(D+4)}v^6 \;+\; \dots\;, \tag{3.3.16}$$

[9] Ultimately, it allows us to construct the expansion of $y(r)$ at large distances once variable r is restored.

[10] This is the expansion around the global minimum.

and

$$\frac{1}{\hbar}\Phi \;=\; \frac{2a_m^{1/2}}{m+2}\lambda^{(m-2)/2}v^{(m+2)/2}+\frac{a_{m-1}\lambda^{(m-4)/2}}{m\,a_m^{1/2}}v^{m/2}+\frac{(4a_ma_{m-2}-a_{m-1}^2)\lambda^{(m-6)/2}}{4(m-2)a_m^{3/2}}v^{(m-2)/2}+\ldots\,, \tag{3.3.17}$$

for small and large v, respectively. These two expansions contain the asymptotic information about the exact wave function that later will be used.

3.3.2 Generalized Bloch Equation

There exists an alternative way to transform the original Riccati equation (3.3.4) into a new one in which the constants $\hbar$ and M do not appear explicitly. This is achieved by introducing the *classical coordinate*[11]

$$u \;=\; g\,r\;, \tag{3.3.18}$$

and defining a new unknown function

$$\mathcal{Z}\,(u) \;=\; \left(\frac{g^2}{2M}\right)^{1/2} y\;. \tag{3.3.19}$$

It is straightforward to show that the function $\mathcal{Z}(u)$ satisfies a non-linear differential equation

$$\lambda^2\,\partial_u\mathcal{Z}(u) \;-\; \mathcal{Z}(u)\left(\mathcal{Z}(u)-\frac{\lambda^2(D-1)}{u}\right) \;=\; \lambda^2\,\varepsilon(\lambda) \;-\; \hat{V}(u) \quad,\quad \partial_u\equiv\frac{d}{du}\;, \tag{3.3.20}$$

c.f. (3.3.9). Here ε and λ are the same as in (3.3.8) and (3.3.10). Therefore, these two quantities play the role of energy and effective coupling constant in both spaces: the v-space and the u-space. Boundary conditions, which guarantee the normalizability of the wave function, are similar to those imposed for the RB equation,

$$\partial_u\mathcal{Z}(u)\Big|_{u=0} \;=\; \frac{\varepsilon}{D} \quad,\quad \mathcal{Z}(+\infty) \;=\; +\infty\;. \tag{3.3.21}$$

At $D=1$, the equation (3.3.20) was called in [44–46] the *(one-dimensional) Generalized Bloch equation*. Here, the equation (3.3.20) is a natural extension of the one-dimensional GB equation to the D-dimensional radial case. For this reason, we continue to call it as the *Generalized (radial) Bloch* equation. In contrast with the RB equation, by setting $\hbar=1$ and $M=1/2$ the GB equation does not take the form of the Riccati one shown in (3.3.4). This is one of the principal features that differentiate the RB equation from the GB one.

Naturally, (3.3.20) can also be used to construct the asymptotic expansions similar to (3.3.13) and (3.3.14) for *small* u,

$$\mathcal{Z}(u) \;=\; \frac{\varepsilon}{D}\,u+\frac{(\varepsilon^2-a_2D^2)}{D^2(D+2)\lambda^2}\,u^3-\frac{a_3}{(D+3)\lambda^2}\,u^4-\frac{a_4D^3(D+2)\lambda^2-2\,\varepsilon\,(\varepsilon^2-a_2D^2)}{D^3(D+2)(D+4)\lambda^4}\,u^5\;+\;\ldots\,, \tag{3.3.22}$$

[11] We called it like this since it is $\hbar$-independent. In fact, in the *classical counterpart* of the anharmonic oscillator, the classical equations of motion written in variable u are g-independent, see [44, 45].

and *large* u,

$$\mathcal{Z}(u) \;=\; a_m^{1/2}\, u^{m/2} \;+\; \frac{a_{m-1}}{2a_m^{1/2}}\, u^{(m-2)/2} \;+\; \frac{(4a_m a_{m-2} \;-\; a_{m-1}^2)}{8a_m^{3/2}}\, u^{(m-4)/2} \;+\; \ldots\;, \qquad (3.3.23)$$

respectively. We note the following:

(i) Small u can be obtained in two situations, small r and fixed g, or fixed r and small coupling constant g.

(ii) Large u occurs when r is large for fixed g, or for fixed r and g large.

Therefore, it is not a surprise that expansions in v-space (3.3.13) and (3.3.14) can be connected with (3.3.22) and (3.3.23) in u-space, respectively. This is achieved by using the remarkable relation

$$u \;=\; \lambda\, v\;, \qquad (3.3.24)$$

which connects the two spaces.

Chapter 4

The Weak Coupling Regime

Assuming a small effective coupling constant λ, we describe how to solve the RB and GB equations using PT in λ. In particular, we will show that the perturbative solution of the RB equation is an application of the Non-Linearization Procedure [7]. On the other hand, the perturbative approach developed for the GB equation leads to a purely algebraic procedure to calculate arbitrary corrections. Finally, we discuss the non-trivial connection between these two solutions and its relation with the WKB approximation.

4.1 Riccati-Bloch Equation

Let us take the RB equation (3.3.9) with an arbitrary potential $V(v;\lambda)$ in the right-hand side[1],

$$\partial_v \mathcal{Y}(v) \;-\; \mathcal{Y}(v)\left(\mathcal{Y}(v) - \frac{D-1}{v}\right) \;=\; \varepsilon\,(\lambda) \;- V(v;\lambda)\;, \tag{4.1.1}$$

We assume that potential $V(v;\lambda)$ admits a Taylor expansion in powers of the effective coupling constant λ, thus

$$V(v;\lambda) \;=\; \sum_{n=0}^{\infty} V_n(v)\,\lambda^n\;. \tag{4.1.2}$$

Here the *coefficient* functions $V_n(v)$, $n = 0, 1, ...$, are real functions in v. Let us now assume that the *unperturbed* equation at $\lambda = 0$,

$$\partial_v \mathcal{Y}_0(v) \;-\; \mathcal{Y}_0(v)\left(\mathcal{Y}_0(v) - \frac{D-1}{v}\right) \;=\; \varepsilon_0 \;-\; V_0(v)\;, \tag{4.1.3}$$

[1]We take (3.3.9) and make the replacement $\dfrac{1}{\lambda^2}\,\hat{V}\,(\lambda v) \to V(v;\lambda)$.

can be solved explicitly by any means.[2] Evidently, once we know $\mathcal{Y}_0(v)$, the wave function can be found since

$$\Psi_0 \;=\; \exp\left(-\int^v \mathcal{Y}_0(s)\,ds\right)\;. \tag{4.1.4}$$

The only constraint when finding $\mathcal{Y}_0(s)$ is that the function Ψ_0 should be normalizable.

Once the solution of the unperturbed problem is known, we can develop PT in powers of λ,

$$\varepsilon(\lambda) \;=\; \sum_{n=0}^{\infty} \varepsilon_n\,\lambda^n\;, \tag{4.1.5}$$

and

$$\mathcal{Y}(v) \;=\; \sum_{n=0}^{\infty} \mathcal{Y}_n(v)\,\lambda^n\;. \tag{4.1.6}$$

Now the task is to find the corrections ε_n and $\mathcal{Y}_n(v)$. To do so, we substitute (4.1.5) and (4.1.6) into the RB equation (4.1.1); it is easy to see that the nth correction $\mathcal{Y}_n(v)$ satisfies the first order linear ordinary differential equation[3]

$$\partial_v\left(\,v^{D-1}\Psi_0^2\;\mathcal{Y}_n(v)\right) \;=\; \left(\varepsilon_n - Q_n(v)\right)v^{D-1}\Psi_0^2\quad, \tag{4.1.7}$$

where

$$Q_1(v) \;=\; V_1(v)\;,\qquad\qquad Q_n(v) \;=\; V_n(v) \;-\; \sum_{k=1}^{n-1}\mathcal{Y}_k(v)\,\mathcal{Y}_{n-k}(v)\;,\quad n=2,3,\ldots\;. \tag{4.1.8}$$

Evidently, the exact solution for $\mathcal{Y}_n(v)$ is written in integral form

$$\mathcal{Y}_n(v) \;=\; \frac{1}{v^{D-1}\,\Psi_0^2}\left(\int_0^v \left(\varepsilon_n - Q_n\right)\Psi_0^2\,s^{D-1}\,ds\right)\;. \tag{4.1.9}$$

Since we are interested in finding bound states, it is necessary to impose the condition of the *absence of current of particles* for both $v\to 0$ and $v\to\infty$ as boundary condition [8],

$$\mathcal{Y}_n(v)\,v^{D-1}\,\Psi_0^2\Big|_{v=\{0,\infty\}} \;\to\; 0\;. \tag{4.1.10}$$

It can be easily checked that if $v\to 0$, the condition (4.1.10) is satisfied automatically, while at $v\to\infty$ the correction ε_n has to be chosen accordingly

$$\varepsilon_n \;=\; \frac{\int_0^\infty Q_n\,\Psi_0^2\,v^{D-1}\,dv}{\int_0^\infty \Psi_0^2\,v^{D-1}\,dv} \tag{4.1.11}$$

to satisfy (4.1.10). In $D=1$, PT developed to solve the Riccati equation (associated with a given Schrödinger equation) was called the *Non-Linearization Procedure* [8]. We have given its straightforward extension to radial potentials in arbitrary D. We will continue to call it the *Non-Linearization Procedure*. Some remarks:

[2] It can always be achieved via the *Inverse Problem* in the framework of the RB equation: we take some function $\mathcal{Y}_0(v)$ and then calculate the left-hand side of (4.1.3). Finally, we solve for the potential $V_0(v)$ and ε_0.

[3] The product $v^{D-1}\Psi_0^2$ is the integrating factor of the differential equation.

(*i*) In contrast with the Rayleigh-Schrödinger PT, see e.g. [1], the knowledge of the entire spectrum of the unperturbed problem is not required to find perturbative corrections in (4.1.5) and (4.1.6). It is sufficient to know the unperturbed state wave function of the unperturbed problem to which we are looking for corrections.

(*ii*) This approach gives the closed analytic expression for both corrections ε_n and $\mathcal{Y}_n(v)$ in the form of nested integrals. Therefore, this procedure is an efficient method to calculate several orders in PT, see e.g. [8] and [47].

(*iii*) In this framework, the convergence of the perturbation series (4.1.5) and (4.1.6) is guaranteed for any D if the first correction $\mathcal{Y}_1(v)$ is bounded

$$|\mathcal{Y}_1(v)| \;\leq\; C \tag{4.1.12}$$

where C is a positive constant, for discussion and details see [8].

(*iv*) Using the Non-Linearization Procedure we can exploit the connection between the variational energy and PT to calculate corrections of a given trial function and its variational estimate of the energy.

We have presented a brief review of the Non-Linearization Procedure applied to the ground state. This approach can be modified to study excited states by admitting a finite number of simple poles with residues equal to one in the corrections $\mathcal{Y}_n(v)$. The position of the poles is also found in PT in powers in λ. Explicit formulas can be found in [8] for the one-dimensional case. The generalization of the D-dimensional radial potential case is straightforward.

4.1.1 D-dimensional Radial Anharmonic Oscillator

Let us now consider the D-dimensional radial anharmonic oscillator potential (3.2.1). We study the weak coupling regime assuming that the effective coupling constant

$$\lambda = \left(\frac{\hbar^2}{2M}\right)^{\frac{1}{4}} g$$

is *small*. To apply the Non-Linearization Procedure, we choose in (4.1.2)

$$\begin{aligned} V_k &= a_{k+2}\, v^{k+2} \quad \text{for} \quad k = 0,\, 1, \ldots, m-2\ , \\ V_k &= 0 \quad \text{for} \quad k > m-2\ . \end{aligned} \tag{4.1.13}$$

Therefore, our potential is a polynomial of finite degree $m-2$ and m, in λ and v, respectively. The corresponding unperturbed equation (4.1.3) describes the $D-$dimensional spherical harmonic oscillator: an exactly solvable problem in any dimension $D > 0$, see e.g. [48]. The unperturbed ground state wave function is given by

$$\Psi_0 \;=\; e^{-\sqrt{\frac{M}{2\hbar^2}}\; a_2^{1/2} r^2} \;=\; e^{-\frac{1}{2} a_2^{1/2} v^2}\ , \tag{4.1.14}$$

and it does not depend on the dimension D.

In general, the explicit calculation of the perturbative corrections $\mathcal{Y}_n(v)$ and ε_n can be carried out analytically by using (4.1.9). However, the final expressions involve the incomplete gamma function and the Meijer G-function explicitly. Due to the form of those expressions, they are irrelevant for our study since the information that they may provide is hidden in cumbersome formulas. Hence, we take a different but more relevant approach: asymptotic series in particular domains.

Let us find the asymptotic expansions of the nth correction $\mathcal{Y}_n(v)$ in two limits: $v \to 0$, and $v \to \infty$. For small v, the correction $\mathcal{Y}_n(v)$ is given by the Taylor expansion

$$\mathcal{Y}_n(v) \;=\; v \sum_{k=0}^{\infty} b_k^{(n)}\, v^k \;, \tag{4.1.15}$$

where $b_k^{(n)}$ are some coefficients. It can be easily shown that the first coefficient $b_0^{(n)}$ is related to the energy correction ε_n,

$$b_0^{(n)} \;=\; \frac{\varepsilon_n}{D} \;. \tag{4.1.16}$$

The next coefficient always vanishes,

$$b_1^{(n)} \;=\; 0 \;, \tag{4.1.17}$$

due to the absence of the linear term in the radial anharmonic potential (3.2.1). On the other hand, for large v we have a Laurent-like series,

$$\mathcal{Y}_n(v) \;=\; v \sum_{k=0}^{\infty} c_k^{(n)}\, v^{n-k} \;, \qquad n > 0 \;, \tag{4.1.18}$$

where $c_k^{(n)}$ are some coefficients. Interestingly, the leading coefficient $c_0^{(n)}$ does not depend on D while the next-to-leading one always vanishes,

$$c_1^{(n)} \;=\; 0 \;. \tag{4.1.19}$$

Using expansions (4.1.15) and (4.1.18), it can be shown that in the non-physical dimension $D = 0$ all corrections ε_n vanish,

$$\varepsilon_n \;=\; 0 \;. \tag{4.1.20}$$

From the integral form of correction ε_n shown in (4.1.11), one can show that if $D \to 0$, the numerator of (4.1.11) is bounded,

$$\int_0^{\infty} Q_n\, \Psi_0^2\, v^{D-1}\, dv \;<\; \infty \;, \tag{4.1.21}$$

while the denominator behaves like

$$\int_0^{\infty} \Psi_0^2\, v^{D-1}\, dv \;=\; \frac{1}{D}\, a_2^{-\frac{D}{4}} \;+\; O(D^0) \tag{4.1.22}$$

for $D \to 0$. Consequently, the correction ε_n vanishes linearly in D when $D \to 0$. Note that the coefficient $b_0^{(n)}$ remains finite in this limit, see (4.1.16). If any correction ε_n vanishes for arbitrary n, then their formal sum (4.1.5) results in $\varepsilon = 0$, and the energy vanishes, $E = 0$. In general, for $D \neq 0$ it can be shown that expansion for ε is asymptotic: ε_n grows at least factorially as $n \to \infty$, see e.g. [20, 22, 28, 49]. Therefore, series (4.1.5) and (4.1.6) are divergent. This is not surprising since a Dyson [50] instability is present for most of the radial anharmonic oscillators of the form (3.2.1). The divergent nature of the series could discourage to calculate corrections in PT. However, for some particular cases of (3.2.1) it has been proved that perturbation series for the energy can be summed to the exact one by using different *summation techniques*: calculating the Borel sum [27], taking Padé approximants [31] and via renormalization [51]. These regularization procedures can lead to highly accurate estimates of the energy for some systems. In particular, it is successful for some cases of the anharmonic oscillator.

An interesting situation occurs when all odd monomial terms in r in potential (3.2.1) are absent, i.e. the potential is (formally) an even function in r, $V(r) = V(-r)$. In this case, all odd corrections $\mathcal{Y}_{2n+1}(v)$ and ε_{2n+1} vanish. Likewise, any even correction $\mathcal{Y}_{2n}(v)$ has the form of a polynomial of finite degree

$$\mathcal{Y}_{2n}(v) \;=\; v \sum_{k=0}^{n} c_{2k}^{(2n)} v^{2(n-k)} \;, \qquad \mathcal{Y}_{2n}(-v) \;=\; -\mathcal{Y}_{2n}(v) \;, \tag{4.1.23}$$

where

$$c_{2n}^{(2n)} \;=\; \frac{\varepsilon_{2n}}{D} \;. \tag{4.1.24}$$

This implies that ε_{2n} and $\mathcal{Y}_{2n}(v)$ can be calculated by linear algebra means[4]. In turn, the energy correction ε_{2n} is a finite-degree polynomial in D,

$$\varepsilon_{2n} = \sum_{k=1}^{n+1} d_k^{(2n)} D^k \;, \tag{4.1.25}$$

where $d_k^{(2n)}$ are real coefficients. However, it is enough to have a single odd monomial term $\sim v^{2q+1}$ in the potential (3.2.1) (with q positive and integer) to break the features (4.1.23) and (4.1.25). Hence, all coefficients in front of the singular terms in the expansion (4.1.18), as well as all higher order terms in the expansion (4.1.15) at $k > n$, are proportional to a_{2q+1}.

4.2 Generalized Bloch Equation

We can develop PT in powers of λ for the GB equation (3.3.20). Of course, the expansion of ε in powers of λ is the same as the one used in the RB equation, see (4.1.5),

$$\varepsilon(\lambda) \;=\; \sum_{n=0}^{\infty} \varepsilon_n \, \lambda^n \;.$$

[4] In this situation, a large number of corrections can be calculated by using a computational code, see e.g. [47].

In turn, the expansion for the function $\mathcal{Z}(u)$ reads

$$\mathcal{Z}(u) \;=\; \sum_{n=0}^{\infty} \mathcal{Z}_n(u)\,\lambda^n \;. \tag{4.2.1}$$

We assume that the energy corrections ε_n are already known: they can be found using the Non-Linearization Procedure, the standard Rayleigh-Schrödinger PT, or any other suitable method. It is immediate to see that the correction $\mathcal{Z}_n(u)$ is calculated by algebraic means. Its calculation depends on corrections of a smaller order, just like it happens in any perturbative approach. The first 3 corrections are

$$\begin{aligned} \mathcal{Z}_0(u) \;&=\; \pm\sqrt{\hat{V}(u)}\;, \\ \mathcal{Z}_1(u) \;&=\; 0\;, \\ \mathcal{Z}_2(u) \;&=\; \frac{u\,\partial_u\mathcal{Z}_0(u) \;+\; (D-1)\,\mathcal{Z}_0(u) \;-\; u\,\varepsilon_0}{2\,u\,\mathcal{Z}_0(u)}\;. \end{aligned} \tag{4.2.2}$$

In general, the nth correction is given by

$$\mathcal{Z}_n(u) \;=\; \frac{u\,\partial_u\mathcal{Z}_{n-2}(u) \;+\; (D-1)\,\mathcal{Z}_{n-2}(u) \;-\; u^2\sum_{i=2}^{n-2}\mathcal{Z}_i(u)\mathcal{Z}_{n-i}(u) \;-\; u\,\varepsilon_{n-2}}{2\,u\,\mathcal{Z}_0(u)}\;, \qquad n>2\;. \tag{4.2.3}$$

Note that the boundary condition (3.3.21), $\mathcal{Z}(\infty) = +\infty$, implies that the positive sign of the square root must be chosen in the expression for $\mathcal{Z}_0(u)$.

Analyzing the $\mathcal{Z}_n(u)$ correction (4.2.3), one can see that the boundary condition at $u = 0$, see (3.3.21), can *not* be fulfilled in the case of an arbitrary potential (3.2.1) without defined parity with respect to the change $r \to -r$. In this situation, any $\mathcal{Z}_n(u)$ (and its derivative) at $n > 1$ diverges at small u. For instance, for the cubic potential where $a_3 \neq 0$ the nth correction $\mathcal{Z}_n(u)$ with $n > 1$ behaves like

$$\mathcal{Z}_n(u) \sim u^{-n+2} \tag{4.2.4}$$

when $u \to 0$. In turn, for the quintic potential with $a_3 = 0$ but $a_5 > 0$ the nth correction at $n > 3$ behaves like

$$\mathcal{Z}_n(u) \sim u^{-n+4} \tag{4.2.5}$$

when u tends to zero. For the polynomial potential of degree $(2k + 1)$ in u, if all other odd terms are absent $a_3 = a_5 = \ldots = a_{2k-1} = 0$ but $a_{2k+1} > 0$, the function $\mathcal{Z}_n(u)$ behaves like

$$\mathcal{Z}_n(u) \sim u^{-n+2k} \tag{4.2.6}$$

for small u as long as $n > 2k - 1$. It might be an indication that the radius of convergence of the expansion of $\mathcal{Z}(u)$ (see (4.2.1)) in $1/u$ is finite. However, if the anharmonic potential $V(r)$ is formally even, $V(r) = V(-r)$ the boundary condition at $u = 0$ can always be satisfied. This allows us to determine the correction ε_n by imposing

$$\partial_u\mathcal{Z}_n(u)\Big|_{u=0} \;=\; \frac{\varepsilon_n}{D}\;. \tag{4.2.7}$$

At this point, it is worth mentioning that the expansion in powers of λ (4.2.1) is divergent for any anharmonic oscillator due to the Dyson instability mentioned below. This fact can be seen in the partial sums of (4.2.1), see Figs. 4.1 and 4.2.

Let us emphasize that the presence of a single odd degree monomial term in u in the potential $V(u)$ breaks the feature (4.2.7): the expansion for $\mathcal{Z}(u)$ in powers of λ only satisfies the single boundary condition at $u = \infty$. It is necessary to discuss the connection between the expansions (4.1.6) and (4.2.1) to explain why this happens.

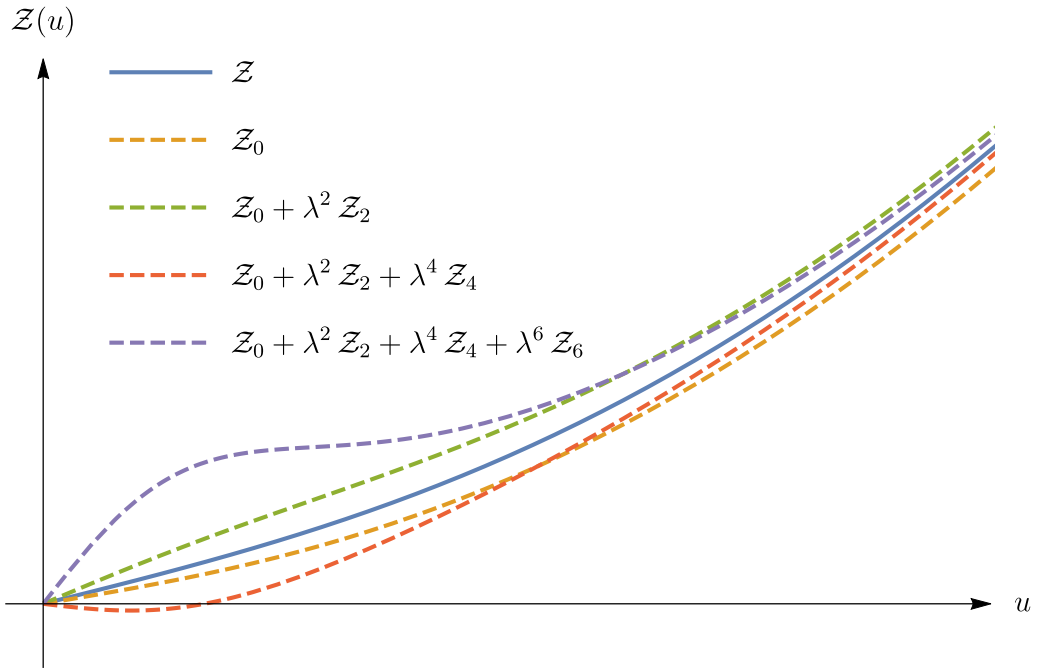

Figure 4.1: Partial sums of the expansion for $\mathcal{Z}(u)$ as functions of u for a general anharmonic potential with monomials of even degrees. The function $\mathcal{Z}(u)$ (solid blue line), represents the exact solution, see text. Near $u = 0$, the deviation of the partial sums from the exact solution is a consequence of the divergent nature of series (4.1.6).

4.3 Connection Between the Expansions for $\mathcal{Y}$ and $\mathcal{Z}$

Thus far, we have constructed two different representations for the logarithmic derivative $y(r)$, see (3.3.6). Due to the uniqueness of the solutions of the Schrödinger equation, there must be a connection between those representations. According to the RB equation, we have the

$$y(r) \;=\; (2M\hbar^2)^{\frac{1}{4}}\,\mathcal{Y}(v(r))\;, \qquad \mathcal{Y}(v) \;=\; \sum_{n=0}^{\infty}\mathcal{Y}_n(v)\,\lambda^n\;, \qquad v(r) \;=\; \left(\frac{2M}{\hbar^2}\right)^{\frac{1}{4}} r\;. \tag{4.3.1}$$

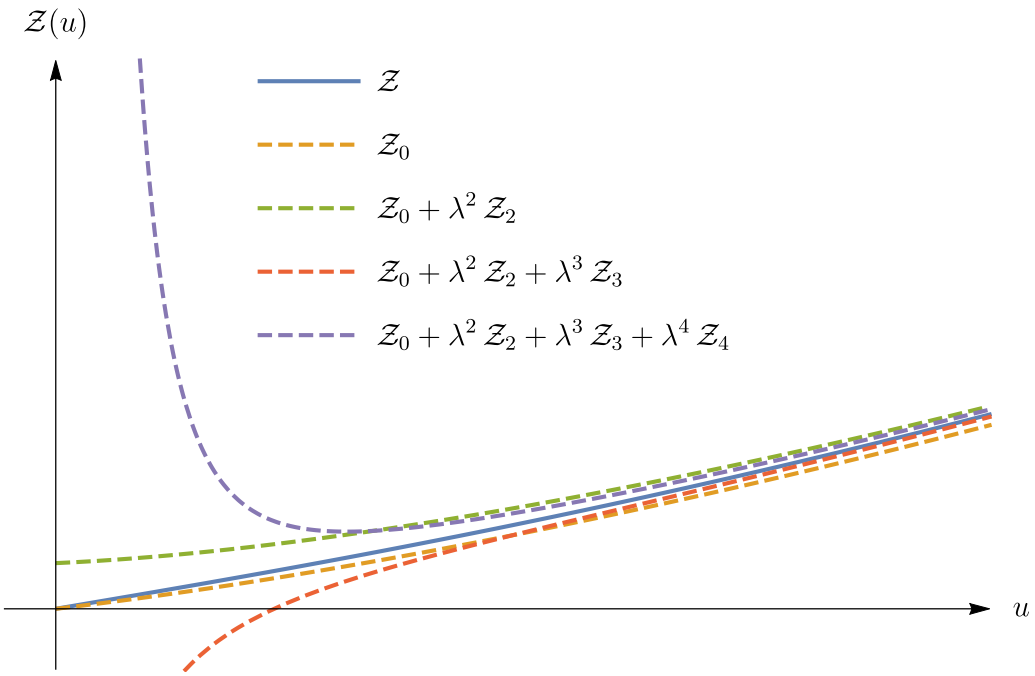

Figure 4.2: Partial sums of the expansion for $\mathcal{Z}(u)$ as functions of u for a generic anharmonic potential which includes odd monomials. The function $\mathcal{Z}(u)$ (solid blue line) represents the exact solution, see text. The divergence in the vicinity of $u = 0$ of the partial sums is the result of the impossibility of satisfying the boundary condition at $u = 0$.

From the other side, the GB equation leads to

$$y(r) \;=\; \left(\frac{2M}{g^2}\right)^{\frac{1}{2}} \mathcal{Z}(u(r)) \;, \qquad \mathcal{Z}(u) \;=\; \sum_{n=0}^{\infty} \mathcal{Z}_n(u)\,\lambda^n \;, \qquad u(r) \;=\; g\,r \;. \tag{4.3.2}$$

The coupling constant λ is defined in (3.3.10). The connection can be established if we use explicitly the expansion of $\mathcal{Y}_n(v)$ at large v, see (4.1.18). In this case, $y(r)$ is given formally by

$$y \;=\; (2M\,\hbar^2)^{\frac{1}{4}}\, v \sum_{n=0}^{\infty} \lambda^n \sum_{k=0}^{\infty} c_k^{(n)}\, v^{n-k} \;. \tag{4.3.3}$$

By using the relation between the v-space and u-space (3.3.24),

$$u \;=\; \lambda\, v \;,$$

and changing the order of summation, it follows that (4.3.3) is equivalent to

$$y \quad = \quad \left(\frac{2M}{g^2}\right)^{\frac{1}{2}} \sum_{n=0}^{\infty} \lambda^n (gr) \sum_{k=1}^{\infty} c_n^{(k)} (gr)^{k-n} \;. \tag{4.3.4}$$

Now, the connection is clear. If we compare the expansions (4.3.3) and (4.3.4), we can conclude that

$$\mathcal{Z}_n(u) \;=\; u \sum_{k=1}^{\infty} c_n^{(k)} u^{k-n} \tag{4.3.5}$$

due to the uniqueness of the Taylor series. Therefore, $\mathcal{Z}_n(u)$ is a generating function of the coefficients $c_k^{(n)}$, $k = 0, 1, \ldots$, see Fig. 4.3 for a graphical illustration. Equation (4.3.5) exhibits

$$
\begin{array}{rcccccccccc}
y(r) \;=\; \frac{(2M)^{\frac{1}{2}}}{g}\,(& & \boxed{c_0^{(0)}(gr)^1} & & & & & & & & \\
& + & c_0^{(1)}(gr)^2 & + & \boxed{\lambda^2\, c_2^{(1)}(gr)^0} & + & \boxed{\lambda^3\, c_3^{(1)}(gr)^{-1}} & + & \boxed{\lambda^4\, c_4^{(1)}(gr)^{-2}} & + & \ldots \\
& + & c_0^{(2)}(gr)^3 & + & \lambda^2\, c_2^{(2)}(gr)^1 & + & \lambda^3\, c_3^{(2)}(gr)^0 & + & \lambda^4\, c_4^{(2)}(gr)^{-1} & + & \ldots \\
& + & c_0^{(3)}(gr)^4 & + & \lambda^2\, c_2^{(3)}(gr)^2 & + & \lambda^3\, c_3^{(3)}(gr)^1 & + & \lambda^4\, c_4^{(3)}(gr)^0 & + & \ldots \\
& + & c_0^{(4)}(gr)^5 & + & \lambda^2\, c_2^{(4)}(gr)^3 & + & \lambda^3\, c_3^{(4)}(gr)^2 & + & \lambda^4 c_4^{(4)}(gr)^1 & + & \ldots \\
& + & \vdots & + & \vdots & + & \vdots & + & \vdots & + & \ldots\,) \\
& & \underbrace{\qquad\qquad} & & \underbrace{\qquad\qquad} & & \underbrace{\qquad\qquad} & & \underbrace{\qquad\qquad} & & \\
\equiv \frac{(2M)^{\frac{1}{2}}}{g}\,(& & \mathcal{Z}_0(gr) & + & \lambda^2\,\mathcal{Z}_2(gr) & + & \lambda^3\,\mathcal{Z}_3(gr) & + & \lambda^4\,\mathcal{Z}_4(gr) & + & \ldots\,)
\end{array}
$$

Figure 4.3: Representation of the generating functions $\mathcal{Z}_n$ constructed from the perturbative series in powers of λ for the function $y(r)$.

the reason why we cannot satisfy, in general, the boundary condition at $u = 0$: $\mathcal{Z}_n(u)$ is constructed from the expansion (4.1.18), which is valid in the limit $r \to \infty$ ($u \to \infty$ for fixed g). It also clarifies the reason why this boundary condition can be satisfied only for even potentials: when formally $V(r) = V(-r)$, the (finite) series of any $\mathcal{Y}_n(v)$ at small distances is the same than for large ones.

Some interesting properties of the corrections $\mathcal{Z}_n(u)$ occur when considering $r \to \infty$. It will be discussed in detail for the cubic, quartic, and sextic anharmonic oscillators, see below.

4.4 Connection with WKB

Let us conclude this Chapter by showing the relation between the perturbative approach implemented for the GB equation and the semi-classical WKB approximation. By integrating in r, the expansion (4.3.2) is converted into an expansion in terms of generating functions for the phase

$$\Phi(r) \;=\; \sum_{n=0}^{\infty} \lambda^n G_n(r) \quad , \qquad G_1(r) \;=\; 0 \; , \tag{4.4.1}$$

where $G_n(r)$ is equal to

$$G_n(r) \;=\; \left(\frac{2M}{g^2}\right)^{1/2} \int^r \mathcal{Z}_n(gr)\, dr \; . \tag{4.4.2}$$

Note that keeping g and M fixed, (4.4.1) can be regarded as a semi-classical expansion of the phase in powers of $\hbar^{\frac{1}{2}}$, see (3.3.10). The leading order of this expansion is given by

$$G_0(r) \;=\; \int^r \sqrt{2M\,V(r)}\,dr \;. \tag{4.4.3}$$

This leading order term is the classical action for vanishing energy[5] $E = 0$, and it is related to the zeroth order correction of the standard D-dimensional (radial) WKB method[6] (developed in the classically forbidden region), see below. This is the only term in the expansion (4.4.1) which contains no dependence on D. The second order term in (4.4.1) is

$$\lambda^2 G_2(r) \;=\; \hbar\left(\frac{D-1}{2}\log[r] + \;\frac{1}{4}\,\log\left[2M\,V(r)\right] \;-\; \frac{\varepsilon_0}{2}\int^r \frac{dr}{\sqrt{V(r)}}\right) \;. \tag{4.4.4}$$

Except for the integral - the third term - it looks like the first order correction to WKB at $E = 0$ and arbitrary D, see Appendix A. Thus, it defines the *functional determinant* of a path integral formalism [45]. The appearance of the extra term in the form of an integral can be explained as follows. Let us take the zeroth order term in the standard WKB method (in the forbidden region) and expand it in powers of $\hbar^{1/2}$ using the fact that the energy is $\hbar$-dependent, see (3.3.8) and (3.3.10), thus

$$\int^r \sqrt{2M\,(V(r)-E)}\,dr \;=\; \int^r \sqrt{2M\,V(r)}\,dr \;-\; \frac{\hbar\,\varepsilon_0}{2}\int^r \frac{dr}{\sqrt{V(r)}} \;+\; O(\hbar^{3/2}) \;. \tag{4.4.5}$$

Note that the first term is nothing but $G_0(r)$ while the second term is exactly the integral which appears in (4.4.4). Consequently, one can see that (4.4.1) is the standard semi-classical WKB expansion in the classically-forbidden region, re-expanded in powers of $\hbar^{1/2}$. Higher order generating functions $G_3(r), G_4(r), \ldots$, are related with higher order corrections of the WKB expansion in a similar way.

This is an alternative consideration to the one-dimensional case presented in [44–46]. In these papers, it was described how to obtain expansion (4.4.1) using a path integral formulation (in Euclidean time) considering a special classical solution of zero energy ($E = 0$) called *flucton*. In a quite straightforward way, this consideration can be extended to the D-dimensional radial case, where the flucton path appears in the radial direction. Hence, the perturbative approach developed for the GB Equation can be called the *true* semi-classical approximation: both $\varepsilon(\lambda)$ and $\Phi(r;\lambda)$ are expanded in powers $\hbar^{1/2}$.

[5] A vanishing energy corresponds to the classical energy of a particle located at the global minimum.
[6] We present a brief review of the WKB method in Appendix A.

Chapter 5

The Strong Coupling Regime

In Chapter 4, assuming a *small* effective constant

$$\lambda = \left(\frac{\hbar^2}{2M}\right)^{\frac{1}{4}} g,$$

we studied the ground state energy E and the phase in the form of a Taylor expansion around $\lambda = 0$. As a result, the harmonic oscillator was taken as the unperturbed problem. We now consider the opposite limit: large λ in both RB and GB equations. In this case, we take as unperturbed potential the leading monomial term $a_m g^{m-2} r^m$ in (3.2.1). It implies that all other terms in the potential (3.2.1), except for the leading one, are taken as perturbations. This situation can be achieved if we consider the expansion of the energy in fractional powers $1/\lambda$.

5.1 Riccati-Bloch Equation

To develop the strong coupling expansion in the framework of the RB equation, let us first introduce the new quantum coordinate[1]

$$w \;=\; \lambda^{\frac{m-2}{m+2}} v \;, \tag{5.1.1}$$

and define the new function

$$\tilde{\mathcal{Y}}(w) \;=\; \lambda^{\frac{2-m}{m+2}} \mathcal{Y}(v) \;. \tag{5.1.2}$$

When we introduce these two expressions in the RB equation (3.3.9), we have

$$\partial_w \tilde{\mathcal{Y}}(w) \;-\; \tilde{\mathcal{Y}}(w)\left(\tilde{\mathcal{Y}}(w) - \frac{D-1}{w}\right) \;=\; \tilde{\varepsilon}(\tilde{\lambda}) \;-\frac{1}{\tilde{\lambda}^m}\hat{V}\left(\tilde{\lambda}\, w\right) \;, \qquad \partial_w \equiv \frac{d}{dw} \;, \tag{5.1.3}$$

[1]The insertion of this coordinate in the RB equation is equivalent to perform a Symanzik scaling transformation to the Schrödinger equation, see [9].

where

$$\tilde{\varepsilon} \;=\; \lambda^{\frac{4-2m}{m+2}}\,\varepsilon\;, \qquad \tilde{\lambda} \;=\; \lambda^{\frac{4}{m+2}}\;, \tag{5.1.4}$$

cf. (3.3.9). This equation does not contain explicit dependence on $\hbar$ and M, while $\tilde{\varepsilon}$ plays the role of energy. Furthermore, (5.1.3) is the RB equation that is appropriate to construct the strong coupling expansion. This can be easily seen if we note that the potential is now given by

$$\frac{1}{\tilde{\lambda}^m}\,\hat{V}\left(\tilde{\lambda}\,w\right) \;=\; \frac{1}{\tilde{\lambda}^m}\sum_{k=2}^{m} a_k\,(\tilde{\lambda}\,w)^k \;=\; a_m w^m + \frac{a_{m-1}}{\tilde{\lambda}}\,w^{m-1} + \ldots + \frac{a_2}{\tilde{\lambda}^{m-2}}\,w^2\;. \tag{5.1.5}$$

Thus, the parameter $\tilde{\lambda}^{-1}$ is now the coupling constant. Therefore, when large $\tilde{\lambda}$ is considered, the potential becomes a single monomial in the variable w in power m. This monomial now represents the unperturbed potential. The latter implies that $\tilde{\mathcal{Y}}(w)$ and $\tilde{\varepsilon}(\tilde{\lambda})$ should eventually be expanded in series in the following form

$$\tilde{\mathcal{Y}}(w) \;=\; \sum_{n=0}^{\infty}\tilde{\mathcal{Y}}_n(w)\,\tilde{\lambda}^{-n}\;. \tag{5.1.6}$$

and

$$\tilde{\varepsilon}(\tilde{\lambda}) \;=\; \sum_{n=0}^{\infty}\tilde{\varepsilon}_n\,\tilde{\lambda}^{-n}\;, \tag{5.1.7}$$

respectively. Here $\tilde{\varepsilon}_n$, $n = 0, 1, \ldots$, are the coefficients of the strong coupling expansion. A similar expansion to (5.1.7) occurs for the excited states. Contrary to the weak coupling expansion, it has been demonstrated that, for some particular cases of the anharmonic potential (3.2.1), PT developed in the strong coupling regime (5.1.7) has a finite radius of convergence, see e.g. [52] and references therein. It is related to the fact that the dominant term in the potential (3.2.1) is r^m at $r \to \infty$ while other monomials are subdominant. Therefore, the phenomenon of the Dyson instability does not occur.

It has to be emphasized that the equation (5.1.3) has a similar form than the RB equation with arbitrary potential (4.1.1). This implies that all the formulas, derived in Section 4.1 in the framework of the Non-Linearization Procedure, are suitable to calculate $\tilde{\mathcal{Y}}_n(w)$ and $\tilde{\varepsilon}_n$: we only have to make the replacement $v \to w$ in (4.1.1). Thus, let us choose the potential that appears in (4.1.2) in the following form

$$\begin{aligned} V_k \;&=\; a_{m-k}\,w^{m-k} \quad \text{for} \quad k = 0,\,1,\,...,\,m-2\;, \\ V_k \;&=\; 0 \quad \text{for} \quad k > m-2\;. \end{aligned} \tag{5.1.8}$$

In this case, the unperturbed equation (4.1.3) is

$$\partial_v\tilde{\mathcal{Y}}_0(w) \;-\; \tilde{\mathcal{Y}}_0(w)\left(\tilde{\mathcal{Y}}_0(w) - \frac{D-1}{w}\right) \;=\; \tilde{\varepsilon}_0 \;-\; a_m\,w^m\;. \tag{5.1.9}$$

If the solution of this equation were known, the corresponding square-integrable unperturbed wave function Ψ_0 would be obtained using (4.1.4). Then, we would use the formulas (4.1.9) and

(4.1.11) to construct PT. As a result, we would obtain the coefficients $\tilde{\varepsilon}_k$ of the strong coupling expansion. However, since the exact solution of (5.1.9) for $m > 2$ is unknown, we need to find $\tilde{\mathcal{Y}}_0(w)$ in approximate form. In the spirit of the present work, there are two possible ways to find $\tilde{\mathcal{Y}}_0(w)$:

(*i*) One can choose the simplest physically relevant trial function for the potential

$$W_0(w) \;=\; a_{2p}\, w^{2p} \;, \qquad\qquad m \;=\; 2p \tag{5.1.10}$$

which defines the unperturbed dimensionless radial Schrödinger equation

$$-\,\frac{1}{2}\left(\partial_w^2 \;+\; \frac{D-1}{w}\partial_w\right)\Psi_{0,0} \;+\; W_0(w)\Psi_{0,0} \;=\; \tilde{\varepsilon}_{0,0}\Psi_{0,0}\;. \tag{5.1.11}$$

Then, we use the Non-Linearization Procedure employing the connection between PT and the variational energy, see (1.16).

(*ii*) We can construct a more sophisticated locally-accurate approximation of $\tilde{\mathcal{Y}}_0(w)$ for $w \geq 0$.

Let us describe both options.

5.1.1 Physically Relevant Trial Function

Probably, the simplest physically relevant trial function, see [8] for discussion, was proposed for the first time in [7, 53] handling the one-dimensional case. Undoubtedly, the similar trial function is also appropriate for the D-dimensional case of the radial potentials,

$$\Psi_{0,0}(w) \;=\; e^{-a_{2p}^{1/2}\,\frac{w^{p+1}}{p+1}} \quad , \quad \tilde{\mathcal{Y}}_{0,0}(w) \;=\; a_{2p}^{1/2}\, w^p \;, \tag{5.1.12}$$

where the second subscript marks the order of the correction to Ψ_0. By solving the *inverse problem*, one can find the potential $W_{0,0}(w)$ for which $\Psi_{0,0}$ is the exact solution, namely

$$W_{0,0}(w) \;=\; a_{2p}w^{2p} \;-\; a_{2p}^{1/2}(p+D-1)w^{p-1} \;, \qquad \tilde{\varepsilon}_{0,0} \;=\; 0\;. \tag{5.1.13}$$

Taking the difference between the potentials (5.1.10) and (5.1.13),

$$W_{0,1}(w) \;=\; W_0(w) \;-\; W_{0,0}(w) \;=\; a_{2p}^{1/2}(p+D-1)\, w^{p-1} \;, \tag{5.1.14}$$

one can expand PT as in (4.1.5) and (4.1.6) with $W_{0,1}(w)$ as the perturbative potential for $W_{0,0}(w)$, see Section 1.2 for details. In this manner, it allows us to calculate the zeroth order coefficient $\tilde{\varepsilon}_0$ in the strong coupling expansion (5.1.7) iteratively, which appears in the form of an expansion

$$\tilde{\varepsilon}_0 \;=\; \tilde{\varepsilon}_{0,0} \;+\; \tilde{\varepsilon}_{0,1} \;+\; \tilde{\varepsilon}_{0,2} \;+\; \ldots\;. \tag{5.1.15}$$

The first two coefficients can be found analytically,

$$\tilde{\varepsilon}_{0,0} \;=\; 0 \;, \tag{5.1.16}$$

$$\tilde{\varepsilon}_{0,1} \;=\; a_{2p}^{\frac{1}{p+1}}(p+D-1)\left(\frac{p+1}{2}\right)^{\frac{p-1}{p+1}}\;\frac{\Gamma(\frac{D+p-1}{p+1})}{\Gamma(\frac{D}{p+1})}\;. \tag{5.1.17}$$

The next ones can be obtained numerically[2]. The function $\tilde{\mathcal{Y}}_0(w)$ is expanded in a similar way as in (5.1.15),

$$\tilde{\mathcal{Y}}_0(w) \;=\; \tilde{\mathcal{Y}}_{0,0}(w) \;+\; \tilde{\mathcal{Y}}_{0,1}(w) \;+\; \tilde{\mathcal{Y}}_{0,2}(w) \;+\; \ldots \;, \tag{5.1.18}$$

where $\tilde{\mathcal{Y}}_{0,0}(w)$ is given by (5.1.12). Evidently, this expansion can be converted into the expansion of the phase,

$$\Phi_0 \;=\; \Phi_{0,0} \;+\; \Phi_{0,1} \;+\Phi_{0,2} \;+\; \ldots \tag{5.1.19}$$

where $\Phi_{0,0} = a_{2p}^{1/2}\,\hbar\,\dfrac{w^{p+1}}{p+1}$. Using $\Psi_{0,0}$ as entry one can also calculate explicitly the first approximation to $\tilde{\varepsilon}_1$, the subdominant coefficient in the strong coupling expansion (5.1.7), which results in

$$\tilde{\varepsilon}_{1,0} \;=\; a_{m-1}\left(\frac{p+1}{2a_{2p}^{1/2}}\right)^{\frac{2p-1}{p+1}}\;\frac{\Gamma(\frac{D+2p-1}{p+1})}{\Gamma(\frac{D}{p+1})}\;. \tag{5.1.20}$$

The next terms, e.g. $\tilde{\varepsilon}_{1,1}$, $\tilde{\varepsilon}_{1,2}$, ..., can be only written in the form of nested integrals, similar to those as in expression (4.1.11). Their computation is numerical. Of course, this procedure can be extended to calculate higher coefficients in the expansion (5.1.7).

In general terms, it can be shown that in this approach series (5.1.15) and (5.1.19) are convergent. However, the rate of convergence is very slow. It implies that several corrections are needed to obtain highly accurate results from their partial sums. Since corrections are calculated numerically, the accumulation of error in the computations is a drawback. This inconveniences can be avoided if we accelerate the convergence using a more appropriate zeroth order approximation than (5.1.12).

5.1.2 Interpolation: Locally Accurate Approximation

One can construct another physically relevant trial function for the RB Equation (5.1.9) that leads to a fast convergent series (5.1.15) and (5.1.19). To do so, we employ the asymptotic behavior of $\tilde{\mathcal{Y}}_0(w)$ at small w,

$$\tilde{\mathcal{Y}}_0(w) \;=\; \left(\frac{\tilde{\varepsilon}_0}{D}\,w \;+\; \frac{\tilde{\varepsilon}_0^2}{D^2\,(D+2)}w^3 - \frac{a_{2p}\,\delta_{p,3/2}}{D+3}w^4 \;+\; \frac{2\tilde{\varepsilon}_0^3 - a_{2p}D^3(D+2)\delta_{p,2}}{D^3(D+2)(D+4)}w^5 + \;\ldots\right)\;, \tag{5.1.21}$$

[2] In Section 7.2, which is devoted to the cubic anharmonic oscillator, the first coefficients will be presented explicitly.

and at large w

$$\tilde{\mathcal{Y}}_0(w) \;=\; \left(a_{2p}^{1/2}\, w^p + \;\frac{1}{2}\,(D+p-1)\, w^{-1} \;-\; \frac{1}{2}\,\tilde{\varepsilon}_0\, w^{-p} + \;\ldots \right) \;. \tag{5.1.22}$$

The dominant term in (5.1.22) corresponds to (5.1.12). A more sophisticated approximation of $\tilde{\mathcal{Y}}_{0,0}(w)$ is the result of the interpolation between expansions (5.1.21) and (5.1.22). The construction of such interpolation will be presented in Chapter 6. We show how this interpolation leads to a locally accurate approximation for the cubic, quartic, and sextic anharmonic oscillators. Furthermore, it leads to highly accurate estimates of the first two coefficients of the strong coupling expansion.

5.2 Generalized Bloch Equation

There is an interesting connection between the strong coupling expansion developed for the GB equation (3.3.20) and the expansion of $y(r)$ at small r, see (3.3.13). To construct the GB equation for the strong coupling regime, it is necessary to note that u and w are related in a very simple way,

$$u \;=\; \tilde{\lambda}\, w \;. \tag{5.2.1}$$

This can be checked straightforwardly just by noting that

$$\begin{aligned} \tilde{\lambda}\, w \;&=\; \lambda^{\frac{4}{m+2}} \left(\lambda^{\frac{m-2}{m+2}} v \right) \\ &=\; \lambda\, v \\ &=\; u \;, \end{aligned} \tag{5.2.2}$$

see (5.1.1) and (5.1.4). Interestingly, the equation (5.2.2) looks very similar to (3.3.24). This remark suggests introducing into the RB equation (5.1.3) the classical coordinate

$$u \;=\; \tilde{\lambda}\, w \;, \tag{5.2.3}$$

and a new function

$$\tilde{Z}(u) \;= \tilde{\lambda}\, \tilde{Y}(w) \;. \tag{5.2.4}$$

In this way, we obtain

$$\tilde{\lambda}^2\, \partial_u \tilde{\mathcal{Z}}(u) \;-\; \tilde{\mathcal{Z}}(u) \left(\tilde{\mathcal{Z}}(u) \;-\; \tilde{\lambda}^2 \frac{(D-1)}{u} \right) \;=\; \tilde{\lambda}^2\, \tilde{\varepsilon} \;-\; \tilde{\lambda}^{-m+2}\, \hat{V}(u) \;. \tag{5.2.5}$$

This equation is the GB Equation for the strong coupling regime: the left-hand side is the same as in (3.3.20) - the GB equation for weak coupling regime - while the right-hand side is different[3]. Now we can develop PT in inverse powers of $\tilde{\lambda}^{-1}$ in the form

$$\tilde{\varepsilon}(\tilde{\lambda}) \;=\; \sum_{n=0}^{\infty} \tilde{\varepsilon}_n\, \tilde{\lambda}^{-n}.$$

[3]Except when $m = 2$. In this irrelevant case - the harmonic oscillator - there is no coupling constant, see (3.2.1).

see (5.1.7), and

$$\tilde{\mathcal{Z}}(u) \;=\; \sum_{n=0}^{\infty} \tilde{\mathcal{Z}}_n(u)\;\tilde{\lambda}^{-n}\;, \tag{5.2.6}$$

This is nothing but the expansions at $\tilde{\lambda} = \infty$. We assume the coefficients $\tilde{\varepsilon}_n$ are known *a priori*. In particular, they may be computed from PT developed for the RB equation in the strong coupling regime. Inserting the series (5.1.7) and (5.2.6) in (5.2.5), one can determine corrections $\tilde{\mathcal{Z}}_n(u)$ iteratively by solving the same first order differential equation with a different right-hand side

$$\partial_u \tilde{\mathcal{Z}}_i(u) \;+\; \frac{(D-1)}{u}\,\tilde{\mathcal{Z}}_i(u) \;=\; \tilde{\varepsilon}_i\;, \qquad i = 0, 1\;, \tag{5.2.7}$$

and

$$\partial_u \tilde{\mathcal{Z}}_n(u) \;+\; \frac{(D-1)}{u}\,\tilde{\mathcal{Z}}_n(u) \;=\; \tilde{\varepsilon}_n + \sum_{i=0}^{n-2} \tilde{\mathcal{Z}}_i(u)\,\tilde{\mathcal{Z}}_{n-i-2}(u) \;-\; \delta_{m,n}\,\hat{V}(u)\;,\; n = 2, 3, \dots\;. \tag{5.2.8}$$

Imposing the boundary condition $\tilde{\mathcal{Z}}(0) = \tilde{\varepsilon}/D$ to the original equation (5.2.5), we can find the boundary condition for the nth correction,

$$\partial_u \tilde{\mathcal{Z}}(u)\Big|_{u=0} \;=\; \frac{\tilde{\varepsilon}_n}{D}\;. \tag{5.2.9}$$

The equations (5.2.7) and (5.2.8) are solved in an elementary way. In particular,

$$\begin{aligned}
\tilde{\mathcal{Z}}_0(u) \;&=\; \frac{\tilde{\varepsilon}_0}{D} u\;,\\
\tilde{\mathcal{Z}}_1(u) \;&=\; \frac{\tilde{\varepsilon}_1}{D} u\;,\\
\tilde{\mathcal{Z}}_2(u) \;&=\; \frac{\tilde{\varepsilon}_2}{D} u \;+\; \frac{\tilde{\varepsilon}_0^2}{D^2(D+2)} u^3\;,\\
\tilde{\mathcal{Z}}_3(u) \;&=\; \frac{\tilde{\varepsilon}_3}{D} u \;+\; \frac{2\,\tilde{\varepsilon}_0\,\tilde{\varepsilon}_1}{D^2(D+2)} u^3 \;-\; \delta_{m,3} \sum_{k=2}^{m} \frac{a_k}{D+k} u^{k+1}\;,\\
\tilde{\mathcal{Z}}_4(u) \;&=\; \frac{\tilde{\varepsilon}_4}{D} u \;+\; \frac{2\,\tilde{\varepsilon}_0\,\tilde{\varepsilon}_2 + \tilde{\varepsilon}_1^2}{D^2(D+2)} u^3 \;+\; \frac{2\,\tilde{\varepsilon}_0^3}{D^3(D+2)(D+4)} u^5 \;-\; \delta_{m,4} \sum_{k=2}^{m} \frac{a_k}{D+k} u^{k+1}\;.
\end{aligned}$$

The general nth correction is given by

$$\tilde{\mathcal{Z}}_n(u) \;=\; \frac{\tilde{\varepsilon}_n}{D} u \;+\; u^{1-D} \sum_{k=0}^{n-2} \int_0^u \tilde{\mathcal{Z}}_k(s)\,\tilde{\mathcal{Z}}_{n-k-2}(s)\,s^{D-1}\,ds \;-\; \delta_{m,n} \sum_{k=2}^{m} \frac{a_k\,u^{k+1}}{D+k} \tag{5.2.10}$$

at $n \geq 2$. Note that it is not guaranteed that the boundary condition $\tilde{\mathcal{Z}}(\infty) = +\infty$ is fulfilled for all these corrections. It implies that PT in inverse powers of $\tilde{\lambda}$ for $\tilde{\mathcal{Z}}(u)$ has a finite radius of convergence in u. Thus, the corrections $\tilde{\mathcal{Z}}_n(u)$ make sense in a bounded domain in u only, see

discussion below. From (5.2.10), one can see that any correction is a finite-degree polynomial in u,

$$\tilde{\mathcal{Z}}_n(u) \;=\; \begin{cases} \displaystyle\sum_{k=0}^{[\frac{n}{2}]} \alpha_{2k}^{(n)} u^{2k+1} \;-\; \delta_{m,n} \sum_{k=2}^{m} \frac{a_k\, u^{k+1}}{D+k} & \text{for} \quad n \le m+1 \;, \\ \displaystyle\sum_{k=0}^{n} \alpha_k^{(n)} u^{k+1} & \text{for} \quad n > m+1 \;, \end{cases} \tag{5.2.11}$$

where $\alpha_k^{(n)}$ are real coefficients, and the symbol [ ] denotes the *integer part function*. It is easy to see that

$$\alpha_0^{(n)} = \frac{\tilde{\varepsilon}_n}{D} \tag{5.2.12}$$

following (5.2.9). The next coefficient always vanishes,

$$\alpha_1^{(n)} = 0 \;, \tag{5.2.13}$$

for any n. The coefficient $\alpha_2^{(n)}$ can be found in the form of finite sum

$$\alpha_2^{(n)} = \frac{1}{D^2(D+2)} \sum_{k=0}^{n-2} \tilde{\varepsilon}_k \tilde{\varepsilon}_{n-k-2} \quad , \tag{5.2.14}$$

while the next coefficient again vanishes,

$$\alpha_3^{(n)} = 0 \;, \tag{5.2.15}$$

for any n, c.f. (5.2.13). From (5.2.11), one can see that $\tilde{\mathcal{Z}}_n(u)$ for $n < m$ and $n = m+1$ is always an odd polynomial in u:

$$\tilde{\mathcal{Z}}_n(-u) \;=\; -\tilde{\mathcal{Z}}_n(u) \;,$$

while for $n = m$ and $n > m+1$ this property may be lost. In the case of an even anharmonic potential, $V(r) = V(-r)$, all odd corrections $\tilde{\mathcal{Z}}_{2n+1}(u)$ and $\tilde{\varepsilon}_{2n+1}$ vanish. In turn, all even corrections $\tilde{\mathcal{Z}}_{2n}(u)$ are odd polynomials in u of degree $(2n+1)$ if $2n > m+1$.

The perturbative approach, which was used to calculate the strong coupling expansion of $\tilde{\mathcal{Z}}(u)$, is related to the asymptotic behavior of $\tilde{\mathcal{Z}}(u)$ at small u. Once we established the polynomial structure of the corrections $\tilde{\mathcal{Z}}_n(u)$, one can sum up some subseries of the perturbative expansion (5.2.6), keeping the degree of u fixed. For example, the sum

$$\left(\sum_{n=0}^{\infty} \alpha_0^{(n)} \tilde{\lambda}^{-n} \right) u \;=\; \frac{\tilde{\varepsilon}}{D} u \;, \tag{5.2.16}$$

corresponds to summing up all terms $O(u)$ in (5.2.6). The next sum is carried out with all terms $O(u^3)$. Using (5.2.14) one can show that it corresponds to

$$\sum_{n=2}^{\infty} \alpha_2^{(n)} \tilde{\lambda}^{-n} u^3 \;-\; \frac{a_2\, \tilde{\lambda}^{-m}}{D+2} u^3 \;=\; \frac{\tilde{\lambda}^{-2}\, \tilde{\varepsilon}^2 \;-\; a_2\, \tilde{\lambda}^{-m} D^2}{D^2(D+2)} u^3 \;. \tag{5.2.17}$$

The next sum contains coefficients in front of u^4 terms. Following (5.2.15), this sum has a single term,

$$- \frac{a_3 \, \tilde{\lambda}^{-m}}{D+3} u^4 \ . \tag{5.2.18}$$

This summation procedure can be extended to higher order terms $u^n, n > 4$. After performing such summations, we obtain the coefficients in front of all terms in the Taylor expansion in powers of u for the function $\tilde{\mathcal{Z}}(u)$, and, eventually, for $y(r)$. From another side, one can construct the expansion in powers of u directly from (5.2.5),

$$\begin{aligned} \tilde{\mathcal{Z}}(u) \ =& \frac{\tilde{\varepsilon}}{D} u \ + \ \frac{\tilde{\lambda}^{-2} \, \tilde{\varepsilon}^2 \ - \ a_2 \, \tilde{\lambda}^{-m} D^2}{D^2(D+2)} u^3 \ - \ \frac{a_3 \, \tilde{\lambda}^{-m}}{D+3} \, u^4 \ - \\ & \frac{a_4 \, \tilde{\lambda}^{-m} D^3(D+2) - 2 \, \tilde{\varepsilon} \, \tilde{\lambda}^{-2} (\tilde{\varepsilon}^2 \tilde{\lambda}^{-2} - a_2 \, \tilde{\lambda}^{-m} D^2)}{D^3(D+2)(D+4)} \, u^5 \ + \ \ldots \ . \end{aligned} \tag{5.2.19}$$

One can note the exact correspondence between the first three terms of the expansion (5.2.19) and the subseries previously defined in (5.2.16), (5.2.17) and (5.2.18). In this way, we can see the connection between the strong coupling expansion, developed on the basis of the GB equation, and the small u one: both expansions lead to the same representation - the Taylor series - of $\tilde{\mathcal{Z}}(u)$ and, eventually, of $y(r)$. Finally, this connection clarifies why the boundary condition $\tilde{\mathcal{Z}}(\infty) = +\infty$ can not always be fulfilled.

Chapter 6

The Approximant

Now we formulate a prescription for the construction of a locally-accurate, uniform approximation of the wave function of a given state. Such approximate function is called *The Approximant*.

6.1 The Approximant for the Ground State

We denote this approximation by $\Psi^{(t)}_{0,0}$ and call it the *Approximant*. Here, the subscripts indicate explicitly the quantum numbers of the ground state ($n_r = 0, l = 0$) at any D.[1] It is convenient to assume the exponential representation of the wave function,

$$\Psi^{(t)}_{0,0}(r) = e^{-\frac{1}{\hbar}\Phi_t(r)} \ , \tag{6.1.1}$$

since the phase Φ of the exponential representation is not that sharp as the wave function Ψ.[2] Hence, we focus on the construction of the approximate phase Φ_t. We follow the prescription that the phase Φ_t has to interpolate the expansions for small and large distances, (3.3.16) and (3.3.17), respectively. Besides, it should interpolate the same expansions constructed in the strong coupling regime (5.1.21) and (5.1.22). One of the simplest interpolations with these characteristics is of the following form

$$\frac{1}{\hbar}\Phi_t(r) \ = \ \frac{\tilde{a}_0 \ + \ \tilde{a}_1\, g\, r + \frac{1}{g^2} V(r\,;\tilde{a}_2,\ldots,\tilde{a}_m)}{\sqrt{\frac{1}{g^2\, r^2} V(r\,;\,\tilde{b}_2,\ldots,\tilde{b}_m)}} \ + \ \text{Logarithmic Terms}\,(r\,;\,\{\tilde{c}\}) \ . \tag{6.1.2}$$

[1] At $D = 1$, the angular quantum number is not defined. However, we may fix it (formally) to zero, $\ell = 0$.

[2] This was explicitly seen in a particular example described in the Overview.

Without loss of generality, we put $\tilde{b}_2 = 1$ as normalization. Here, $V(r;\{\tilde{a}\})$ and $V(r;\{\tilde{b}\})$ are modified potentials of the form of the original one (3.2.1): instead of the external given parameters $\{a\}$ some free parameters $\{\tilde{a}\}$ and $\{\tilde{b}\}$ are taken, respectively. The logarithmic terms can depend on free parameters $\{\tilde{c}\}$ as well. These terms will eventually insert a prefactor in (6.1.1). Parameters $\{\tilde{c}\}$ are chosen in such a way that this prefactor has no real nodes.

All those remaining free parameters will be fixed by making the variational calculation with (6.1.2) taken as the phase of the trial function.

At $g = 0$, the phase (6.1.2) becomes $\tilde{a}_0 + \tilde{a}_2 r^2$, which corresponds to the radial harmonic oscillator phase. Formula (6.1.2) is the key result of this Chapter.

The phase Φ_t has the outstanding property that, with an appropriate choice of parameters $(\tilde{a}_0, \tilde{a}_1; \tilde{a}_2, \tilde{b}_2, \ldots \tilde{a}_k, \tilde{b}_k; \{\tilde{c}\})$, the generating function $G_0(r)$ is partially (or exactly) reproduced. In particular, to reproduce exactly the dominant term in the expansion (3.3.17), the condition

$$\tilde{a}_m \;=\; \frac{2\, a_m^{1/2}}{m+2}\, \tilde{b}_{m-2} \tag{6.1.3}$$

is imposed[3]. Further constraints to parameters can be imposed in order to reproduce all growing terms in the expansion of the exact function $\mathcal{Y}(v)$, see (3.3.14). If such constraints are imposed, all the corrections in PT to $\mathcal{Y}_0 = \partial_r \Phi_t$ will be bounded, and it will guarantee the convergence of the perturbation series (1.18).

To mimic the possible appearance of logarithmic terms in the expansion (3.3.17), in particular, those which may occur in $G_0(r)$ and $G_2(r)$, some logarithmic terms to phase Φ_t should be added, see (4.4.4). For example, for the two-term anharmonic oscillator potential

$$V(r) \;=\; r^2 \;+\; g^{m-2}\, r^m \;, \tag{6.1.4}$$

the generating function $G_2(r)$ always contains logarithmic terms,

$$\frac{g^2\, G_2(r)}{(2M)^{1/2}} \;=\; \frac{1}{4}\, \log\left[1 + (gr)^{m-2}\right] \;+\; \frac{D}{m+2}\, \log\left[1 + \sqrt{1 + (gr)^{m-2}}\right] \;, \tag{6.1.5}$$

see (4.4.2). In this case, the logarithmic terms added in (6.1.2) should be a certain *minimal* modification of the logarithmic terms that appear in $G_0(r)$ and $G_2(r)$. For instance, a minimal modification of $g^2 G_2(r)/(2M)^{1/2}$ is of the form

$$\frac{1}{4}\, \log\left[1 + \tilde{c}\,(gr)^{m-2}\right] \;+\; \frac{D}{m+2}\, \log\left[1 + \sqrt{1 + \tilde{c}\,(gr)^{m-2}}\right] \;, \tag{6.1.6}$$

where $\tilde{c}$ is a free parameter. If $\tilde{c} = 1$, it coincides with (6.1.5).

In general, some constraints on parameters have to be imposed to guarantee that Φ_t has the structure of (3.3.16) and that $\Psi_{0,0}^{(t)}$ is a normalizable function. Other constraints come from

[3]Without loss of generality, this constraint is written for the case $\hbar = 1$ and $M = 1/2$.

the symmetry of the phase. For example, if the potential is formally even, $V(r) = V(-r)$, the function Φ_t has to be even too.

After imposing all the constraints described above, the remaining free parameters can be fixed by giving them the values of optimal parameters obtained in variational calculations. To realize it, we use the VM for the radial Hamiltonian (3.3.2) taking the Approximant[4]

$$\Psi^{(t)}_{0,0}(r) \;=\; \text{Prefactor}(r\,;\,\{\tilde{c}\}) \times \exp\left(-\frac{\tilde{a}_0 \;+\; \tilde{a}_1\, g\, r + \frac{1}{g^2} V(r\,;\tilde{a}_2,\ldots,\tilde{a}_m)}{\sqrt{\frac{1}{g^2\, r^2} V(r\,;\,\tilde{b}_2,\ldots,\tilde{b}_m)}}\right)\,, \tag{6.1.7}$$

as a trial function, see (6.1.1) and (6.1.2). The accuracy of variational calculations can be estimated using the connection between the variational energy and PT[5]. This kind of estimates will be presented in the forthcoming Chapter for particular anharmonicities.

6.2 Approximants for Excited States

Case $D = 1$

In the one-dimensional situation $r = |x|$, where $x \in (-\infty, \infty)$, see (3.1.3). Therefore, the potential is an even function $V = V(|x|)$. Due to the symmetry of the potential under the reflection $x \to -x$ the quantum number which indicates the *parity* $\nu = (-1)^p$, $p = 0, 1$, is well defined. It implies that we can use it to label any wave function[6], namely,

$$\Psi^{(t)}_{n_r,p}(x) \;=\; x^p P^{(p)}_{n_r}(x^2) e^{-\frac{1}{\hbar}\Phi_t(x)}\,, \qquad n_r \;=\; 0, 1, ..., \quad p \;=\; 0, 1\,, \tag{6.2.1}$$

where $P^{(p)}_{n_r}(x^2)$ is a polynomial of degree n_r with real coefficients and all real roots, and with $P^{(p)}_{n_r}(0) = 1$ chosen for normalization. The polynomial in (6.2.1) defines the nodal surface of the approximate wave function. With vanishing coupling constant ($g = 0$) the polynomial $x^p P^{(p)}_{n_r}(x^2)$ is well-known, it is written in terms of the Hermite polynomials

$$x^p P^{(p)}_{n_r}(x^2) \;=\; H_{2n_r+p}(x)\,. \tag{6.2.2}$$

The phase Φ_t has exactly the same form as in (6.1.2) but with a different set of free parameters $\{\tilde{a}\}, \{\tilde{b}\}, \{\tilde{c}\}$. The same constraints imposed on the parameters of the ground state should be

[4]It is beyond our purpose to study the analytical properties of the Approximant in the complex r-plane. However, except for the real axis, it is clear that the Approximant develops nodes in the complex plane.

[5]See Section 1.2

[6]The energies (which now are labeled as $E_{n_r,p}$) obey the following inequality $E_{n_r,0} < E_{n_r,1} < E_{n_r+1,0}$ for any coupling constant g.

imposed for the excited ones. To fix the value of the coefficients of $P_{n_r}^{(p)}(x^2)$, some orthogonality constraints are imposed. For fixed (n_r, p), the $(n_r - 1)$ free parameters of $P_{n_r}^{(p)}(x^2)$ are found by demanding[7]

$$\langle \Psi_{n_r,p}^{(t)} | \Psi_{k_r,p}^{(t)} \rangle \;=\; 0 \;, \qquad k_r = 0, \ldots, (n_r - 1) \;. \tag{6.2.3}$$

These constraints will ensure that the function $\Psi_{n_r,p}^{(t)}(r)$ has the *correct* number of nodes ($n = 2n_r + p$).[8] The remaining free parameters are fixed through the VM.

Case $D > 1$

Due to the separation of the Schrödinger equation (3.1.1) in spherical coordinates, it is sufficient to approximate the radial part of the wave function. One can label the eigenstates by the pair of quantum numbers (n_r, ℓ), omitting the magnetic quantum number. In this case, the Approximant is of the form

$$\Psi_{n_r,\ell}^{(t)}(r) \;=\; r^{\ell}\, P_{n_r}^{(\ell)}(r^2)\, e^{-\Phi_t} \;, \qquad n_r \;=\; 0, 1, ..., \quad \ell \;=\; 0, 1, ..., \tag{6.2.4}$$

where $P_{n_r}^{(\ell)}(r^2)$ is a polynomial of degree n_r with real roots. We set $P_{n_r}^{(\ell)}(0) = 1$ as normalization. Note that at $g = 0$, the polynomial $P_{n_r}^{(\ell)}(r^2)$ is given in terms of the Laguerre associated polynomials [48]

$$P_{n_r}^{(\ell)}(r^2) \;=\; L_{n_r}^{\ell - D/2 - 1}(r^2) \;. \tag{6.2.5}$$

Analogously to the one-dimensional case, in (6.2.4) Φ_t has the same form of the phase constructed for the ground state (6.1.2), but with a different set of parameters $\{\tilde{a}\}, \{\tilde{b}\}, \{\tilde{c}\}$. The same set of constraints imposed on the parameters of the ground state should be imposed for the excited ones. For a given (n_r, ℓ), the coefficients of the polynomial $P_{n_r}^{(\ell)}(r)$ are fixed imposing the orthogonality constraints

$$\langle \Psi_{n_r,\ell}^{(t)} | \Psi_{k_r,\ell}^{(t)} \rangle \;=\; 0 \;, \qquad k_r = 0, \ldots, (n_r - 1) \;. \tag{6.2.6}$$

These constraints will make sure that the function $\Psi_{n_r,p}^{(t)}(r)$ has the *correct* number of nodes ($n = 2n_r + l$). Note that two states with different angular momentum, say ℓ and ℓ' are already orthogonal, independently of the value of their radial quantum numbers, see Section 3.1. The remaining free parameters are fixed by means of the VM.

[7] We used the familiar *bra-ket* notation to represent the scalar product.

[8] In practice, n can be used as the only quantum number to label the states.

Chapter 7

Results for Two-Term Potentials

The formalism, described in the previous Chapters, is now applied to 3 particular cases of two-term radial anharmonic potentials: cubic, quartic, and sextic. Hence, the forthcoming discussion is focused on potentials of the form

$$V(r) \;=\; r^2 \;+\; g^{m-2} r^m \;, \tag{7.0.1}$$

with $m = 3, 4, 6$. For each anharmonicity, we present results of analytical and numerical nature in the following order. We begin by presenting some general features of the PT coming from the RB and GB equations developed in the weak coupling regime.[1] Then, we construct the Approximants of the first 4 low-lying states for which we estimate their corresponding energy by means of the VM at $g^{m-2} = 0.1, 1, 10$ in $D = 1, 2, 3, 6$. For some of those states, we use the connection between PT and the variational energy to estimate its accuracy, as well as the accuracy of the Approximant. Finally, employing the Approximant, we compute in VM the first two coefficients of the strong coupling expansion of the ground state energy. As we describe below, the realization of the VM and the estimation of its accuracy is a numerical procedure. In the next Section, we briefly describe the computational codes used in numerical computations. Full details can be found in [54], [55], and [56]. Finally, let us mention that the Section for each anharmonicity is self-contained, written in such a way that they can be read independently.

7.1 Numerical Realization of the Variational Method

It is not a surprise that the calculation of the variational energy $E_{var}[\psi_t]$ with trial function $\psi_t = \Psi^{(t)}_{0,0}$, shown in (6.1.7), requires to perform a one-dimensional numerical integration, see (1.13). In addition, a numerical minimization is needed in order to obtain the optimal configuration of parameters.

A computational code was written in FORTRAN 77. It uses the integration routine D01FCF

[1] Some general properties of the two-term potential are summarized in Appendix D.

from the NAG-LIB, which was built using the algorithm described in [57]. The routine of optimization that we used to find the optimal variational parameters was MINUIT of the CERN-LIB. Needless to say, the use of Approximants for excited states as trial functions in VM of the form (7.2.25) and (7.2.26) also require numerical integration and minimization.

Without loss of generality in (numerical) variational calculations we set $\hbar = 1$ and $M = 1/2$, thus $v = r$, $\varepsilon = E$, $\lambda = g$, and $\mathcal{Y} = y$ see (3.3.7), (3.3.8) and (3.3.10). With this setting, it is clear that E_{var} corresponds to a variational estimate of the exact *energy* ε.

For each anharmonicity in $D = 1$, we performed variational calculations for the first three low-lying states which are characterized by the quantum numbers $(0, 0)$, $(0, 1)$, and $(1, 0)$, see (6.2.1). In turn, at $D = 2, 3, 6$ we consider the first four states with quantum numbers (0,0), (1,0), (0,1), and (0,2), see (6.2.4). We calculate the variational energy

$$E_{var} = E_0^{(t)} + E_1^{(t)} \tag{7.1.1}$$

for those states. Using the connection between the variational energy and PT[2], we take $y_0 = \partial_r \Phi_t$ as zeroth order correction. Then, the accuracy of the variational estimate E_{var} is found by calculating the second correction[3]

$$E_2^{(t)} \tag{7.1.2}$$

in the expansion (1.18). Furthermore, we can define the *corrected variational energy*

$$E_{var} + E_2^{(t)} \tag{7.1.3}$$

which, in principle, should provide a more accurate estimate of the exact energy. Correction $E_2^{(t)}$ is found numerically using the formalism of the Non-Linearization Procedure presented in Section 4.1. The calculation of $E_2^{(t)}$ requires the knowledge of y_1, which is already known in integral form, see (4.1.9). A computational code in *Mathematica* package was designed; it includes all relevant formulas. Note that once y_1 is known, the accuracy of the Approximant itself can be estimated via the relative deviation from the exact wave function

$$\left| \frac{\Psi_{0,0}(r) - \Psi_{0,0}^{(t)}(r)}{\Psi_{0,0}^{(t)}(r)} \right| \lesssim 10^{-\delta} \ . \tag{7.1.4}$$

Here δ is a positive constant that is obtained numerically. In (7.1.4), the function $\Psi_{0,0}$ denotes the (unknown) *exact* one. If δ is *sufficiently* large, we will say that $\Psi_{0,0}^{(t)}$ is a locally accurate approximation of the *exact* wave function $\Psi_{0,0}$.

We can compare the corrected variational energies $E_{var} + E_2^{(t)}$ with those coming from an independent numerical method. We choose the Lagrange-Mesh method [58]: an approximate variational method simplified by a Gauss quadrature associated with the mesh. It is known that this method, in the form proposed and developed by D. Baye and co-authors, provides easily 12 - 13 s. d. in energies for various problems of atomic and molecular physics. A detailed and complete description can be found in [58]. At $D = 1$, we use the Hermite mesh, while for $D > 1$, the Laguerre one.

[2]Presented in Section 1.2

[3] It is the second correction in formal PT, but the first one to the variational energy.

7.2 Cubic Anharmonic Oscillator

The simplest radial anharmonic oscillator is characterized by a cubic anharmonicity,

$$V(r) \;=\; r^2 \;+\; g\,r^3 \;, \tag{7.2.1}$$

see (7.0.1) at $m = 3$. It is worth mentioning that many features that the cubic anharmonic potential exhibits are also present in the general potential without symmetry of reflection $r \to -r$, i.e. $V(r) \neq V(-r)$. Thus, the cubic anharmonic oscillator covers the basis of understanding of more complex potentials. Let us note that at $D = 1$, $r \to |x|$. Therefore, the one-dimensional version of the potential (7.2.1) is

$$V(x) \;=\; x^2 + g|x|^3 \;, \qquad -\infty < x < \infty \;, \tag{7.2.2}$$

which clearly holds bound states.

7.2.1 Perturbation Theory in the Weak Coupling Regime

For the cubic anharmonic oscillator, the perturbative expansions of ε and $\mathcal{Y}(v)$ can be derived for the RB equation (3.3.9),

$$\partial_v \mathcal{Y}(v) \;-\; \mathcal{Y}(v)\left(\mathcal{Y}(v) - \frac{D-1}{v}\right) \;=\; \varepsilon\,(\lambda) \;-\; v^2 \;-\; \lambda\, v^3 \quad , \quad \partial_v \equiv \frac{d}{dv} \;, \tag{7.2.3}$$

with v and λ defined in (3.3.7) and (3.3.10), respectively. Those expansions remain functionally the same as for the general oscillator,

$$\varepsilon \;=\; \varepsilon_0 \;+\; \varepsilon_1\,\lambda \;+\; \varepsilon_2\,\lambda^2 \;+\; \ldots \;, \qquad \varepsilon_0 = D \;,$$

and

$$\mathcal{Y}(v) \;=\; \mathcal{Y}_0(v) \;+\; \mathcal{Y}_1(v)\,\lambda \;+\; \mathcal{Y}_2(v)\,\lambda^2 \;+\; \ldots \;, \qquad \mathcal{Y}_0(v) \;=\; v \;.$$

Since potential (7.2.1) contains an odd degree monomial r^3, the correction $\mathcal{Y}_n(v)$ is characterized by the infinite series (4.1.15) and (4.1.18) at small and large v, respectively. The first three corrections $\mathcal{Y}_n(v)$, at both $v \to 0$ and $v \to \infty$, are presented in Appendix B. The first corrections ε_1 and $\mathcal{Y}_1(v)$ can be calculated in closed analytic form using (4.1.9) and (4.1.11),

$$\varepsilon_1 \;=\; \frac{\Gamma(\frac{D+3}{2})}{\Gamma(\frac{D}{2})} \quad , \quad \mathcal{Y}_1(v) \;=\; \frac{e^{v^2}}{2\,v^{D-1}}\left\{\varepsilon_1\,\gamma\left(\frac{D}{2}, v^2\right) - \gamma\left(\frac{D+3}{2}, v^2\right)\right\} \;, \tag{7.2.4}$$

where $\Gamma(a)$ and $\gamma(a,b)$ denote the complete and incomplete gamma functions, respectively, see [59]. Higher energy corrections ε_n can be computed only numerically.[4] For example, the first six corrections[5] at $D = 1$ are

$$\begin{aligned} \varepsilon_1 \;&=\; 0.564\,190 \;, \qquad \varepsilon_2 \;=\; -0.373\,405 \;, \qquad \varepsilon_3 \;=\; 0.512\,464 \;, \\ \varepsilon_4 \;&=\; -0.941\,502 \;, \qquad \varepsilon_5 \;=\; 2.051\,176 \;, \qquad \varepsilon_6 \;=\; -5.022\,987 \;. \end{aligned} \tag{7.2.5}$$

[4] Interestingly, the behavior of ε_n at large D can be obtained analytically in the $1/D$-expansion, see [29].

[5] Rounded to the first displayed s. d.

7.2.2 Generating Functions

We can determine the coefficients of the expansion of $\mathcal{Y}_n(v)$ at large v, $c_k^{(n)}$ in (4.1.18), by algebraic means. In general, they are written in terms of the corrections ε_0, ε_1, ..., ε_n, see Appendix B for explicit formulas for $n = 1, 2, 3$.

It was pointed out in [8,39,60,61] that the general expression for the coefficients $c_0^{(n)}$, $c_2^{(n)}$, ... can be obtained by solving recurrence relations. For example, $c_0^{(n)}$ satisfies non-linear recurrence relation

$$c_0^{(n)} \;=\; -\frac{1}{2}\sum_{k=1}^{n-1} c_0^{(k)} c_0^{(n-k)} \;, \qquad\qquad c_0^{(1)} \;=\; \frac{1}{2}\;. \tag{7.2.6}$$

In turn, the recurrence relation for $c_2^{(n)}$ is linear

$$c_2^{(n)} \;=\; \frac{1}{2}\,(2n+D)\,c_0^{(n)} \;-\; \sum_{k=1}^{n-1} c_0^{(k)} c_2^{(n-k)} \;, \qquad\qquad c_2^{(1)} \;=\; \frac{1}{4}(D+2)\;. \tag{7.2.7}$$

The solution of (7.2.7) requires the knowledge of the coefficients $c_0^{(n)}$. It is evident that in order to find $c_3^{(n)}$, the coefficients $c_0^{(n)}$ and $c_2^{(n)}$ are needed, and so on. The simplest way to solve these recurrence relations is by means of generating functions. Surprisingly, we can calculate these generating functions straightforwardly via the algebraic and iterative procedure derived from the GB equation in the weak coupling regime. For the cubic anharmonic oscillator, the GB equation reads

$$\lambda^2\,\partial_u \mathcal{Z}(u) \;-\; \mathcal{Z}(u)\left(\mathcal{Z}(u) - \frac{\lambda^2(D-1)}{u}\right) \;=\; \lambda^2\,\varepsilon(\lambda) \;-\; u^2 \;-\; u^3 \quad , \quad \partial_u \equiv \frac{d}{du}\;. \tag{7.2.8}$$

For the particular cubic anharmonicity, the function $\mathcal{Z}(u)$ admits an expansion of the form

$$\mathcal{Z}(u) \;=\; \mathcal{Z}_0(u) \;+\; \mathcal{Z}_2(u)\,\lambda^2 \;+\; \mathcal{Z}_3(u)\,\lambda^3 \;+\; \ldots \;, \tag{7.2.9}$$

with

$$\mathcal{Z}_k(u) \;=\; u\sum_{n=1}^{\infty} c_k^{(n)} u^{n-k}\;. \tag{7.2.10}$$

Evidently, the generating function of the coefficient $c_k^{(n)}$ is nothing but $\mathcal{Z}_k(u)$. Generating functions can be easily calculated using formulas presented in (4.2.2) and (4.2.3). For example, the first two are

$$\mathcal{Z}_0(u) \;=\; u\sqrt{1+u}\;, \tag{7.2.11}$$

$$\mathcal{Z}_2(u) \;=\; \frac{u + 2D\left(1+u-\sqrt{1+u}\right)}{4u(1+u)}\;. \tag{7.2.12}$$

From these expressions, the explicit solutions of the equations (7.2.6) and (7.2.7) may be easily derived,

$$c_0^{(n)} \;=\; \frac{(-1)^{n+1}\,\Gamma(2n+1)}{2^{2n-1}\Gamma(n)\,\Gamma(n+1)} \quad , \quad c_2^{(n)} \;=\; \frac{(-1)^{n+1}}{2}\left(1 + D\frac{\Gamma(2n+1)}{2^{2n}\,\Gamma(n+1)^2}\right)\;. \tag{7.2.13}$$

Note that the coefficients $c_0^{(n)}$ are D-independent, while $c_2^{(n)}$ depends on D linearly. As mentioned before, an important property of the generating functions $\mathcal{Z}_0(u)$, $\mathcal{Z}_2(u)$, $\mathcal{Z}_3(u)$, ... is related to the asymptotic expansion of the function $y(r)$ at large r, keeping fixed the effective coupling constant λ. This expansion is conveniently written in variable v,

$$y \;=\; (2M\hbar^2)^{\frac{1}{4}} \left(\lambda^{1/2} v^{3/2} + \frac{1}{2\lambda^{1/2}} v^{1/2} - \frac{1}{8\lambda^{3/2}} v^{-1/2} + \frac{2D+1}{4} v^{-1} - \frac{(8\lambda^2\varepsilon - 1)}{16\lambda^{5/2}} v^{-3/2} + \dots \right) \tag{7.2.14}$$

see (3.3.7). Note that the first four terms of this expansion are ε-independent, but only first three are D-independent. From another side, the expansion of $(\frac{2M}{g^2})^{1/2}\mathcal{Z}_0(u)$ at large u is

$$\left(\frac{2M}{g^2}\right)^{1/2} \mathcal{Z}_0(u) \;=\; \left(\frac{2M}{g^2}\right)^{1/2} \left(u^{3/2} \;+\; \frac{1}{2} u^{1/2} \;-\; \frac{1}{8} u^{-1/2} \;+\; \frac{1}{16} u^{-3/2} \;+\; \dots \right) . \tag{7.2.15}$$

To compare the expansions (7.2.14) and (7.2.15), let us replace the classical coordinate u by the quantum one v, taking into account that $u = \lambda v$, see (3.3.24). Then, the expansion (7.2.15) becomes

$$\left(\frac{2M}{g^2}\right)^{1/2} \mathcal{Z}_0(\lambda v) \;=\; (2M\hbar^2)^{\frac{1}{4}} \left(\lambda^{1/2} v^{3/2} + \frac{1}{2\lambda^{1/2}} v^{1/2} - \frac{1}{8\lambda^{3/2}} v^{-1/2} + \frac{1}{16\lambda^{5/2}} v^{-3/2} + \dots \right) . \tag{7.2.16}$$

One can intermediately see that it reproduces exactly the expansion (7.2.14) up to $O(v^{-1/2})$. With a similar approach, we can demonstrate that at large r the function $\left(\frac{2M}{g^2}\right)^{1/2} \lambda^2 \mathcal{Z}_2(\lambda v)$ contributes to the expansion (7.2.14) from $O(v^{-1})$, since

$$\left(\frac{2M}{g^2}\right)^{1/2} \lambda^2 \mathcal{Z}_2(\lambda v) \;=\; (2M\hbar^2)^{\frac{1}{4}} \left(\frac{2D+1}{4} v^{-1} \;-\; \frac{D}{2\lambda^{1/2}} v^{-3/2} \;-\; \frac{1}{4\lambda} v^{-2} \;+\; \dots \right) . \tag{7.2.17}$$

Note that the expansion of $(\frac{2M}{g^2})^{1/2}(\mathcal{Z}_0(gr) + \lambda^2\mathcal{Z}_2(gr))$ at large v reproduces exactly the first four terms in (7.2.14). The expansion of the next generating functions $(\frac{2M}{g^2})^{1/2}\lambda^3\mathcal{Z}_n(\lambda v)$, with $n > 2$, starts from $O(v^{-3/2})$. Explicitly,

$$\left(\frac{2M}{g^2}\right)^{1/2} \lambda^n \mathcal{Z}_n(\lambda v) \;=\; (2M\hbar^2)^{\frac{1}{4}} \left(-\frac{\varepsilon_{n-2}\, \lambda^{n-5/2}}{2}\, v^{-3/2} \;+\; \dots \right) , \quad v \to \infty \,,\; n \,>\, 2 \,, \tag{7.2.18}$$

where ε_{n-2} is the energy PT correction of the order $(n-2)$. As a consequence, no matter how many generating functions we consider in the expansion $(\frac{2M}{g^2})^{1/2}(\mathcal{Z}_0(\lambda v) + \lambda^2\mathcal{Z}_2(\lambda v) + ...)$, the term of order $O(v^{-3/2})$ in (7.3.18) can not be reproduced exactly.

7.2.3 The Approximant

By means of (4.4.2), we can calculate the first two[6] generating functions, $G_0(r)$ and $G_2(r)$ in the expansion (4.4.1). They are given by

$$G_0(r) \;=\; \frac{(2M)^{1/2}}{g^2}\left(\frac{2(-2+3gr)(1+gr)^{3/2}}{15}\right)\,, \tag{7.2.19}$$

$$G_2(r) \;=\; \frac{(2M)^{1/2}}{g^2}\left(\frac{1}{4}\log[1+gr]+D\log\left[1+\sqrt{1+gr}\right]\right)\,. \tag{7.2.20}$$

In contrast with $G_2(r)$, the function $G_0(r)$ contains no logarithmic terms. Theses generating functions serve as the building blocks for the construction of the Approximant. Following the general prescription (6.1.2), we write the Approximant of the ground state in the exponential representation $\Psi^{(t)}_{0,0} = e^{-\frac{1}{\hbar}\Phi_t}$ with

$$\frac{1}{\hbar}\Phi_t(r) \;=\; \frac{\tilde{a}_0+\tilde{a}_1\,gr+\tilde{a}_2\,r^2+\tilde{a}_3\,g\,r^3}{\sqrt{1+\tilde{b}_1\,g\,r}} \;+\; \frac{1}{4}\,\log[1+\tilde{b}_1\,g\,r] \;+\; D\log\left[1+\sqrt{1+\tilde{b}_1\,g\,r}\right]\,. \tag{7.2.21}$$

We set

$$\tilde{a}_3 \;=\; \frac{2}{5}\,\tilde{b}_1^{1/2}\,, \tag{7.2.22}$$

in order to reproduce exactly the leading term in the asymptotic behavior of the phase at $r\to\infty$. Here, the logarithmic terms in Φ_t represent a *minimal* modification of those coming $G_2(r)$, cf. (7.2.20). Additionally, we impose the constraint

$$\tilde{a}_1 \;=\; \frac{\tilde{b}_1}{4}\,(2\,\tilde{a}_0 \;-D\;-1) \tag{7.2.23}$$

in order to guarantee a vanishing Φ_t' at $r=0$. Thus, there is no linear term in the expansion of (7.2.21) at small distances, just as it is indicated in (3.3.16). Eventually, the Approximant in its final form depends on three free parameters $\{\tilde{a}_0,\tilde{a}_2,\tilde{b}_1\}$ *only*, and it reads

$$\Psi^{(t)}_{0,0}(r) \;=\; \frac{1}{\left(1+\tilde{b}_1\,g\,r\right)^{1/4}\left(1+\sqrt{1+\tilde{b}_1\,g\,r}\right)^{D}}\,\exp\left(-\frac{\tilde{a}_0+\tilde{a}_1\,g\,r+\tilde{a}_2\,r^2+\tilde{a}_3\,g\,r^3}{\sqrt{1+\tilde{b}_1\,g\,r}}\right)\,, \tag{7.2.24}$$

[6]The next two functions $G_3(r)$ and $G_4(r)$ are presented explicitly in Appendix B.

where $\tilde{a}_{3,1}$ are defined by constraints (7.2.22), (7.2.23). This is the eventual expression of the 3-parametric approximate ground state wave function.

To construct 3-parametric Approximants for excited states, we follow the prescription presented in Section 6.2. Hence, at $D = 1$ we have

$$\Psi^{(t)}_{n_r,p}(x) = \frac{x^p P^{(p)}_{n_r}(x^2)}{\left(1+\tilde{b}_1 g|x|\right)^{1/4}\left(1+\sqrt{1+\tilde{b}_1 g|x|}\right)^{D}} \exp\left(-\frac{\tilde{a}_0+\tilde{a}_1 g|x|+\tilde{a}_2 x^2+\tilde{a}_3 g|x|^3}{\sqrt{1+\tilde{b}_1 g|x|}}\right), \tag{7.2.25}$$

while at $D > 1$

$$\Psi^{(t)}_{n_r,\ell}(r) = \frac{r^\ell\, P^{(\ell)}_{n_r}(r^2)}{\left(1+\tilde{b}_1\, g\, r\right)^{1/4}\left(1+\sqrt{1+\ \tilde{b}_1\, g\, r}\right)^{D}} \exp\left(-\frac{\tilde{a}_0+\tilde{a}_1\, g\, r+\tilde{a}_2\, r^2+\tilde{a}_3\, g\, r^3}{\sqrt{1+\tilde{b}_1\, g\, r}}\right). \tag{7.2.26}$$

Definitions of $P^{(p)}_{n_r}(x^2)$ and $P^{(\ell)}_{n_r}(r^2)$ are presented in (6.2.1) and (6.2.4), explicitly.

7.2.4 Numerical Results: Variational Calculations

The calculations of the variational energy for the first low-lying states with quantum numbers $(0,0),(0,1),(0,2),(1,0)$ are presented in Tables 7.1 - 7.4 for different values of D and g. For some states, the variational energy $E_{var} = E^{(t)}_0 + E^{(t)}_1$, the first correction $E^{(t)}_2$ to it as well as its corrected value $E_{var} + E^{(t)}_2$ are shown. All states are studied in dimension $D = 1, 2, 3, 6$ and coupling constant $g = 0.1, 1, 10$. For all cases, the variational energy E_{var} is obtained with absolute deviation from the exact result of the order $10^{-7} - 10^{-8}$ ($7-8$ s.d.[7]). This deviation is found by calculating the second correction $E^{(t)}_2$ (the first correction to the variational energy).

To check the energies obtained in Non-Linearization Procedure, we calculated them numerically in the Lagrange-Mesh method. These numerical calculations show that all digits presented for $E_{var} + E^{(t)}_2$ - the variational energy with the first (second order in PT) correction $E^{(t)}_2$ taken into account - are exact. We obtain not less than 9 d.d.[8] correctly in Non-Linearization Procedure. This accuracy is confirmed independently by calculating the second correction $E^{(t)}_3$ to the

[7] From now on, s.d. stands for significant digits.

[8] Decimal digits is abbreviated as d.d.

variational energy: this correction is $\lesssim 10^{-9}$ for any D and g that we have studied. It indicates a very fast rate of convergence in Non-Linearization Procedure with trial functions (7.2.24), (7.2.25), and (7.2.26) taken as zeroth order approximations of the wave function. In general, the energies grow with the increase of D and/or g. At $D > 1$, we can classify the states by radial quantum number n_r and angular momentum ℓ as (n_r, ℓ); we mention the hierarchy of eigenstates which holds for any fixed integer $D > 1$ and $g > 0$: (0,0), (0,1), (0,2), (1,0).

It has to be noted that to the best of our knowledge, these results represent the first accurate calculations of the energy of the low-lying states for the D-dimensional cubic anharmonic oscillator. Hence, our results will serve as the benchmark for future studies. The Deviation of the Approximant from the exact (unknown) eigenfunction can be estimated via the Non-Linearization Procedure. It can be shown that for the ground state function the relative deviation is extremely small and bounded.

$$\left| \frac{\Psi_{0,0}(r) - \Psi^{(t)}_{0,0}(r)}{\Psi^{(t)}_{0,0}} \right| \lesssim 10^{-4} \ , \tag{7.2.27}$$

This small deviation occurs in the whole range of $r \in [0, \infty)$ at any dimension D that we explored and at any coupling constant $g > 0$ considered.

Therefore, the Approximant leads to a locally accurate approximation of the exact wave function $\Psi_{0,0}(r)$ once the optimal parameters for $\Psi^{(t)}_{0,0}$ are chosen. In general, optimal variational parameters are smooth and slow changing functions of g without a strong D dependence. As an example, for the ground state (0,0) the plots of the parameters $\tilde{a}_{0,2,3}$ vs g for $D = 2, 3, 6$ are shown in Appendix C, see Fig. C.1. A similar situation appears for the excited states for different D and g. Analyzing those plots, one can see the (accidental) appearance of another constraint,

$$\tilde{a}_0 \ = \ \frac{125\,\tilde{a}_3^2 + 12}{150\,\tilde{a}_3} \ . \tag{7.2.28}$$

It is fulfilled by the optimal parameters with high accuracy. This constraint guarantees an approximate reproduction of the subdominant term in the expansion (7.2.14). One can demand the Approximant to fulfill exactly this constraint. When doing so, no deterioration in the accuracy of the wave function and energy occurs.

In all cases studied, the first correction y_1 to the logarithmic derivative $y_0 = \partial_r \Phi_t$ is unbounded. The reason is clear: we have only imposed the constraint (7.2.22) to Φ_t, the exact reproduction of the dominant term in the expansion (7.2.14).[9] If in addition to constraints (7.2.22), (7.2.23), and (7.2.28), we impose

$$-\,g^2 \tilde{a}_1 \ = \ \frac{9375\,a_3^4 \ - \ 1000\,a_3^2 \ + \ 48}{15000\,a_3^3} \ , \tag{7.2.29}$$

Φ_t reproduces (exactly) all growing terms of the exact phase at $r \to \infty$: $r^{5/2}, r^{3/2}, r^{1/2}$, and $\log r$ see (7.2.14). Thus, y_1 will be bounded. Surprisingly, the accuracy of the variational estimate

[9] The approximate reproduction of the subdominant term was imposed by the VM.

Table 7.1: Ground state energy for the cubic potential $V(r) = r^2 + g\,r^3$ for $D = 1, 2, 3, 6$ and $g = 0.1, 1, 10$, labeled by quantum numbers (0,0) at any D. Variational energy $E_{var} = E_{var}$, the first correction $E_2^{(t)}$ (rounded to three s.d.) found with use of $\Psi_{0,0}^{(t)}$, see text, and the corrected energy $E_{var} + E_2^{(t)} = E_{var} + E_2^{(t)}$ shown. $E_{var} + E_2^{(t)}$ coincides with Lagrange Mesh results (see text) in 9 displayed d. d., hence all printed digits are exact.

g	$D = 1$			$D = 2$		
	E_{var}	$-E_2^{(t)}$	$E_{var} + E_2^{(t)}$	E_{var}	$-E_2^{(t)}$	$E_{var} + E_2^{(t)}$
0.1	1.053 120 300	5.39×10^{-7}	1.053 119 761	2.124 027 648	4.40×10^{-7}	2.124 027 208
1.0	1.387 428 891	4.00×10^{-8}	1.387 428 851	2.877 490 906	3.76×10^{-8}	2.877 490 868
10.0	2.729 533 139	6.56×10^{-7}	2.729 532 483	5.794 213 459	5.58×10^{-7}	5.794 212 901
g	$D = 3$			$D = 6$		
	E_{var}	$-E_2^{(t)}$	$E_{var} + E_2^{(t)}$	E_{var}	$-E_2^{(t)}$	$E_{var} + E_2^{(t)}$
0.1	3.208 922 743	4.00×10^{-7}	3.208 922 343	6.528 432 540	2.02×10^{-7}	6.528432338
1.0	4.442 965 260	3.15×10^{-8}	4.442 965 229	9.465 319 951	1.85×10^{-8}	9.465319933
10.0	9.094 985 589	4.23×10^{-7}	9.094 985 166	19.981 458 504	1.96×10^{-7}	19.981 458 308

Table 7.2: The first excited state energy for the cubic potential $V(r) = r^2 + g\,r^3$ for different D and g. Variational energy E_{var}, the first correction $E_2^{(t)}$ found with use of $\Psi_{0,1}^{(t)}$ for $D = 1$ and $\Psi_{0,1}^{(t)}$ for $D > 1$, see (7.2.25) and (7.2.26). The corrected energy $E_{var} + E_2^{(t)} = E_{var} + E_2^{(t)}$ shown, the correction $E_2^{(t)}$ rounded to 3 s.d. All printed digits for $E_{var} + E_2^{(t)}$ are exact.

g	$D = 1$			$D = 2$		
	E_{var}	$-E_2^{(t)}$	$E_{var} + E_2^{(t)}$	E_{var}	$-E_2^{(t)}$	$E_{var} + E_2^{(t)}$
0.1	3.208 922 765	4.21×10^{-7}	3.208 922 343	4.305 557 665	3.55×10^{-7}	4.305 557 309
1.0	4.442 965 265	3.59×10^{-8}	4.442 965 229	6.068 723 537	2.92×10^{-8}	6.068 723 507
10.0	9.094 985 630	4.64×10^{-7}	9.094 985 166	12.579 594 377	3.48×10^{-7}	12.579 594 029
g	$D = 3$			$D = 6$		
	E_{var}	$-E_2^{(t)}$	$E_{var} + E_2^{(t)}$	E_{var}	$-E_2^{(t)}$	$E_{var} + E_2^{(t)}$
0.1	5.412 425 220	2.86×10^{-7}	5.412 424 933	8.784 695 351	1.21×10^{-7}	8.784 695 230
1.0	7.745 092 165	2.41×10^{-8}	7.745 092 141	13.018 486 318	1.49×10^{-8}	13.018 486 303
10.0	16.215 748 127	2.66×10^{-7}	16.215 747 861	27.841 430 199	1.37×10^{-7}	27.841 430 061

Table 7.3: The second excited state energy for the cubic potential $V(r) = r^2 + g\,r^3$ for different D and g. Variational energy E_{var} found with use of $\Psi^{(t)}_{1,0}$ for $D = 1$ and $\Psi^{(t)}_{0,2}$ for $D > 1$, see (7.2.25) and (7.2.26). The first correction $E^{(t)}_2$ and the corrected energy $E_{var}+E^{(t)}_2 = E_{var}+E^{(t)}_2$ shown. Correction $E^{(t)}_2$ rounded to 3 s.d. All 9 printed d. d. in $E_{var} + E^{(t)}_2$ are exact.

g	$D=1$	$D=2$		
	E_{var}	E_{var}	$-E^{(t)}_2$	$E_{var} + E^{(t)}_2$
0.1	5.436 849 553	6.528 432 582	2.43×10^{-7}	6.528 432 338 34
1.0	7.879 141 644	9.465 319 955	2.21×10^{-8}	9.465 319 932 56
10.0	16.641 305 904	19.981 458 531	2.23×10^{-7}	19.981 458 308 14

g	$D=3$			$D=6$		
	E_{var}	$-E^{(t)}_2$	$E_{var} + E^{(t)}_2$	E_{var}	$-E^{(t)}_2$	$E_{var} + E^{(t)}_2$
0.1	7.652 743 974	1.87×10^{-7}	7.652 743 787	11.069 434 802	6.73×10^{-8}	11.069 434 735
1.0	11.224 406 591	1.87×10^{-8}	11.224 406 573	16.699 837 135	1.22×10^{-8}	16.699 837 123
10.0	23.860 743 313	1.78×10^{-7}	23.860 743 135	36.070 426 676	1.01×10^{-7}	36.070 426 576

Table 7.4: The third excited state energy for the cubic potential $V = r^2 + g\,r^3$ for different D and g. The radial node r_0 calculated in Lagrange-Mesh method with 9 correct d.d. Variational energy E_{var} and its radial node $r^{(0)}_0$ given by underlined digits, both found with $\Psi^{(t)}_{1,0}$, see (7.2.26).

g	$D=2$		$D=3$		$D=6$	
	E_{var}	$r^{(0)}_0$	E_{var}	$r^{(0)}_0$	E_{var}	$r^{(0)}_0$
0.1	6.570 941 476	0.953 355 772	7.709 696 057	1.162 462 764	11.158 149 471	1.626 259 519
1.0	9.690 376 045	0.780 270 156	11.517 370 455	0.942 382 083	17.128 462 904	1.289 488 891
10.0	20.681 622 942	0.532 038 126	24.758 598 047	0.638 712 790	37.346 045 150	0.865 039 246

will not be dramatically deteriorated for the ground state: it can provide not less than 5 s.d for the energy in the whole domain studied. Furthermore, the Approximant results in a locally accurate approximation of the exact ground state wave function. The relative deviation does not exceed ~ 0.02. This is surprising, taking into account that the Approximant will be one parametric. Interestingly, the dependence of the single parameter as function of D and g is very weak, see Fig. 7.1.

Results of similar accuracy occur for excited states.

In our present calculations[10], the ratio $|y_1/y_0|$ is bounded and small. Thus, y_1 is a *small* function in comparison with y_0. In Fig. 7.2, it is presented y_0 and y_1 *vs* r for $g = 1$ for dimension $D = 1$. Similar plots appear for $D = 2, 3, 6$. Making an analysis of these plots, one can see that in the domain $0 \le r \lesssim 1$, which gives the dominant contribution to the integrals

[10]In which we have only imposed (7.3.27) and (7.2.23) as constraints.

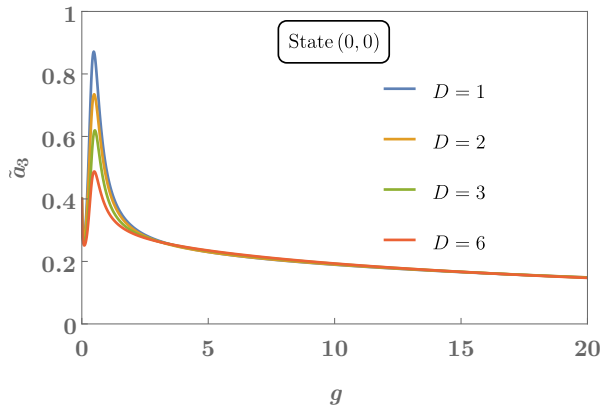

Figure 7.1: Variational parameter $\tilde{a}_3$ for the one-parametric ground state $(0,0)$ Approximant as function of g for $D = 1, 2, 3, 6$. From $g \approx 2.3$ the single parameter $\tilde{a}_3$ becomes approximately D-independent.

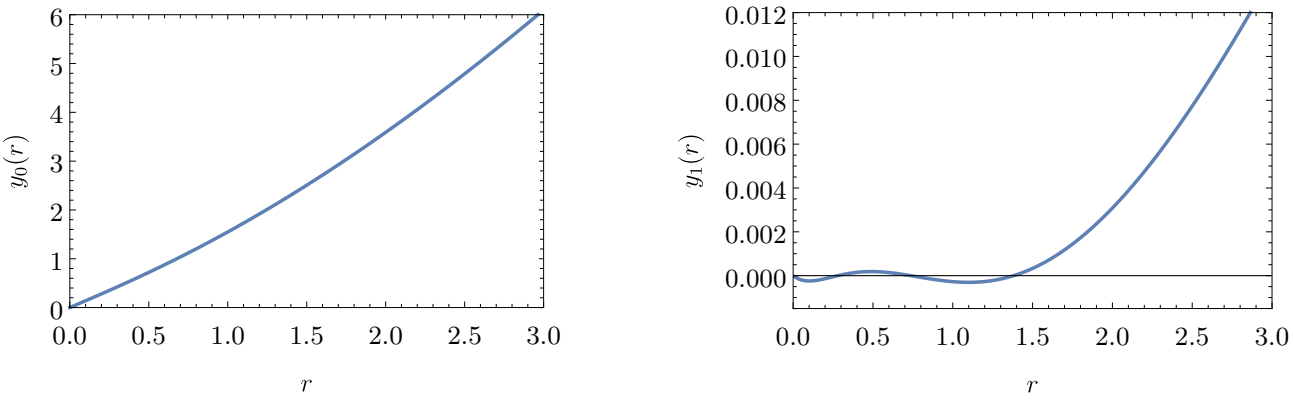

Figure 7.2: Function $y_0 = \partial_r \Phi_t$ (on left) and its first order correction y_1 (on right) at $g = 1$ as a function of r at $D = 1$.

which define the energy corrections, $|y_1|$ is extremely small compared to $|y_0|$, being close to zero. It explains why the energy correction $E_2^{(t)}$ is small being of order $\sim 10^{-7}$, or $\sim 10^{-8}$.

In a similar way, one can show numerically that higher corrections $y_2, y_3, \ldots$ drop down to zero in the domain $0 \le r \lesssim 1$ even faster. This is a clear indication of the convergence of the expansion (1.18) as $n \to \infty$.

At $D > 1$, we checked that the Approximant $\Psi_{1,0}^{(t)}$ also provides an accurate estimate of the position of the radial node of the exact wave function, see (7.2.26). The orthogonality condition described in Section 6.2 provides a simple analytic expression for the zeroth order approximation $r_0^{(0)}$ to r_0. Making a comparison of $r_0^{(0)}$ with numerical estimates which come from the Lagrange-Mesh method with ~ 50 mesh points, we can see the coincidence of r_0 and $r_0^{(0)}$ for at least 5 d.d. at integer dimension D at any coupling constant $g \ge 0$. The results are presented in Table 7.4.

7.2.5 First Terms in the Strong Coupling Expansion

We present the estimates of the first two terms in the strong coupling expansion (5.1.7) for the ground state energy of the cubic oscillator. Assuming for simplicity $2M = \hbar = 1$, this expansion has the form

$$E \;=\; g^{2/5}\left(\tilde{\varepsilon}_0 \;+\; \tilde{\varepsilon}_1 g^{-4/5} \;+\; \tilde{\varepsilon}_2 g^{-8/5} \;+\; \ldots\right) \;. \tag{7.2.30}$$

It is worth mentioning that similar expansion holds for any excited state. This expansion corresponds to PT in powers of $\hat{\lambda}$ for the potential

$$V(w) \;=\; w^3 \;+\; \hat{\lambda}\, w^2 \;, \quad \hat{\lambda} \;=\; g^{-4/5} \;, \tag{7.2.31}$$

defined in $w \in [0, \infty)$. Evidently, it has a finite radius of convergence.

As the first step, we focus on the calculation of $\tilde{\varepsilon}_0$ in (7.2.30), which is the ground state energy in the pure cubic potential $V = w^3$ (the ultra-strong coupling regime). To do it, we use the simplest *physically relevant trial function* (5.1.12),

$$\Psi^{(t)}_{0,0} \;=\; e^{-\frac{2}{5}w^5} \;. \tag{7.2.32}$$

Taking $\Psi^{(t)}_{0,0}$ as zero approximation, we calculate variational energy analytically and then develop the PT procedure described in Section 5.1. In this manner we obtain different PT corrections[11] $\tilde{\varepsilon}_{0,k}\,,\ k = 0, 1, 2, 3, \ldots$ to the exact value of $\tilde{\varepsilon}_0$ and then form the partial sums (5.1.15). The first non-trivial partial sum $(\tilde{\varepsilon}_{0,k} + \tilde{\varepsilon}_{0,1})$ is equal to variational energy. Explicit results, including partial sums up to sixth order, are presented in Table 7.5 for the one-dimensional case. We have to note a slow convergence of the partial sums to the exact result with respect to the increase of the number of perturbative terms in the expansion (5.1.15). For example, the partial sum $\sum_{k=0}^{6} \tilde{\varepsilon}_{0,k}$ with seven terms included allows us to reproduce 7 s.d. of the exact result[12] It is natural to accelerate convergence taking more advanced trial functions as entry.

Table 7.5: Different partial sums (5.1.15) for the leading term $\tilde{\varepsilon}_0$ of the strong coupling expansion (7.2.30) for the one-dimensional cubic anharmonic oscillator in PT with trial function (7.2.32) as zero approximation.

$\tilde{\varepsilon}_{0,0}$	$\sum_{k=0}^{1} \tilde{\varepsilon}_{0,k}$	$\sum_{k=0}^{2} \tilde{\varepsilon}_{0,k}$	$\sum_{k=0}^{3} \tilde{\varepsilon}_{0,k}$	$\sum_{k=0}^{4} \tilde{\varepsilon}_{0,k}$	$\sum_{k=0}^{5} \tilde{\varepsilon}_{0,k}$	$\sum_{k=0}^{6} \tilde{\varepsilon}_{0,k}$	Exact $\tilde{\varepsilon}_0$
0	1.053 006 976	1.021 174 929	1.022 989 568	1.022 956 899	1.022 946 414	1.022 947 763	1.022 947 875

As an alternative to the trial function (7.2.32), let us use the Approximant[13] (7.2.21) in order to calculate the first two terms in the strong coupling expansion (7.2.30), see also (5.1.7). In Table 7.6, we present for different D the leading coefficient of the strong coupling expansion

[11] The calculation of corrections is a numerical process.

[12] By saying *exact*, we mean that the (truncated) displayed d.d. in $\tilde{\varepsilon}_0$ are exact digits.

[13] We fix $g = 1$ as normalization of the free parameters.

$\tilde{\varepsilon}_0$ found in VM, denoted by $\tilde{\varepsilon}_0^{(1)}$, and the second PT correction to it $\hat{\varepsilon}_2$ calculated via the Non-Linearization Procedure. We introduce the partial sum $\tilde{\varepsilon}_0^{(2)} = \tilde{\varepsilon}_0^{(1)} + \hat{\varepsilon}_2$. The final results are verified using the Lagrange-Mesh method with 200 mesh points. One can see that systematically, the correction $\hat{\varepsilon}_2$ is of order $\sim 10^{-7}$. Hence, the first six d. d. in variational energy are correct. It defines the accuracy of variational calculations of $\tilde{\varepsilon}_0$ with the Approximant (7.2.21) as the trial function. One can estimate the order of the third PT correction: for all D studied $\hat{\varepsilon}_3 \sim 10^{-2}\,\hat{\varepsilon}_2$. It indicates an extremely high rate of convergence $\sim 10^{-2}$ in PT. In Table 7.7 we present the first two approximations of the coefficient $\tilde{\varepsilon}_1$ - the expectation value of w^2 - , see (7.2.30).

Table 7.6: Ground state energy $\tilde{\varepsilon}_0$, see (7.2.30), for the potential $W(w) = w^3$ for $D = 1, 2, 3, 6$ found in PT with the Approximant $\Psi_{0,0}^{(t)}$ as the entry: $\tilde{\varepsilon}_0^{(1)}$ is the variational energy, $\hat{\varepsilon}_2$ is the second PT correction and $\tilde{\varepsilon}_0^{(2)} = \tilde{\varepsilon}_0^{(1)} + \hat{\varepsilon}_2$ is corrected variational energy. Eight d.d. in $\tilde{\varepsilon}_0^{(2)}$ confirmed in Lagrange mesh calculation.

$D=1$			$D=2$		
$\tilde{\varepsilon}_0^{(1)}$	$-\hat{\varepsilon}_2$	$\tilde{\varepsilon}_0^{(2)}$	$\tilde{\varepsilon}_0^{(1)}$	$-\hat{\varepsilon}_2$	$\tilde{\varepsilon}_0^{(2)}$
1.022948250	3.75×10^{-7}	1.022 947 875	2.187 461 809	3.09×10^{-7}	2.187 461 499
$D=3$			$D=6$		
$\tilde{\varepsilon}_0^{(1)}$	$-\hat{\varepsilon}_2$	$\tilde{\varepsilon}_0^{(2)}$	$\tilde{\varepsilon}_0^{(1)}$	$-\hat{\varepsilon}_2$	$\tilde{\varepsilon}_0^{(2)}$
3.450 562 918	2.29×10^{-7}	3.450 562 689	7.647 118 254	1.01×10^{-7}	7.647 118 153

Table 7.7: Subdominant (next-to-leading) term $\tilde{\varepsilon}_1$ in the strong coupling expansion (7.2.30) of the ground state energy for the cubic anharmonic radial potential for $D = 1, 2, 3, 6$. The first correction to it $\tilde{\varepsilon}_{1,1}$ as well as the corrected value $\tilde{\varepsilon}_1^{(2)} = \tilde{\varepsilon}_1^{(1)} + \tilde{\varepsilon}_{1,1}$ displayed.

$D=1$			$D=2$		
$\tilde{\varepsilon}_1^{(1)}$	$\tilde{\varepsilon}_{1,1}$	$\tilde{\varepsilon}_1^{(2)}$	$\tilde{\varepsilon}_1^{(1)}$	$\tilde{\varepsilon}_{1,1}$	$\tilde{\varepsilon}_1^{(2)}$
0.410 598 524	6.78×10^{-7}	0.410 599 202	0.766 573 847	5.24×10^{-7}	0.766 574 371
$D=3$			$D=6$		
$\tilde{\varepsilon}_1^{(1)}$	$\tilde{\varepsilon}_{1,1}$	$\tilde{\varepsilon}_1^{(2)}$	$\tilde{\varepsilon}_1^{(1)}$	$\tilde{\varepsilon}_{1,1}$	$\tilde{\varepsilon}_1^{(2)}$
1.092 125 224	2.67×10^{-7}	1.092 125 491	1.967 599 668	1.42×10^{-7}	1.967 599 810

7.3 Quartic Anharmonic Oscillator

The simplest and most popular formally even radial anharmonic oscillator potential is characterized by a quartic anharmonicity

$$V(r) \;=\; r^2 \;+\; g^2\, r^4 \;, \tag{7.3.1}$$

cf. (7.0.1) at $m = 4$. Many properties that the quartic anharmonic radial oscillator exhibits are typical for any even anharmonic potential, $V(r) = V(-r)$. In particular, the polynomial nature of corrections ε_n and $\mathcal{Y}_n(v)$, see (4.1.11) and (4.1.9) is one of such common features.

7.3.1 Perturbation Theory in the Weak Coupling Regime

For the quartic anharmonic oscillator, the perturbative expansions of ε and $\mathcal{Y}(v)$ may be derived from the RB equation (3.3.9),

$$\partial_v \mathcal{Y}(v) \;-\; \mathcal{Y}(v) \left(\mathcal{Y}(v) - \frac{D-1}{v} \right) \;=\; \varepsilon\,(\lambda) \;-\; v^2 \;-\; \lambda^2\, v^4 \quad , \quad \partial_v \equiv \frac{d}{dv} \;, \tag{7.3.2}$$

where v and λ are defined in (3.3.7) and (3.3.10), respectively. These expansions are of the form

$$\varepsilon \;=\; \varepsilon_0 \;+\; \varepsilon_2\, \lambda^2 \;+\; \varepsilon_4\, \lambda^4 \;+\; \ldots \;, \qquad \varepsilon_0 \;=\; D \;, \tag{7.3.3}$$

and

$$\mathcal{Y}(v) \;=\; \mathcal{Y}_0(v) \;+\; \mathcal{Y}_2(v)\, \lambda^2 \;+\; \mathcal{Y}_4(v)\, \lambda^4 \;+\; \ldots \;, \qquad \mathcal{Y}_0(v) \;=\; v \;, \tag{7.3.4}$$

respectively. All odd terms in λ vanish in both expansions, see (4.1.5) and (4.1.6). In general, a large number of corrections can be calculated by linear algebra means. In particular, the first non-vanishing corrections are

$$\varepsilon_2 \;=\; \frac{1}{4}\, D\,(D+2) \quad , \quad \mathcal{Y}_2(v) \;=\; \frac{1}{2}\, v^3 \;+\; \frac{1}{4}\,(D+2)\, v \;. \tag{7.3.5}$$

The next two corrections $\varepsilon_{4,6}$ and $\mathcal{Y}_{4,6}(v)$ are presented in Appendix B. The algebraic procedure of finding PT corrections holds for all even anharmonic potential, $V(r) = V(-r)$. However, it is enough to have one single odd monomial term in the potential to break this property down. In this situation, the calculation of the correction ε_n becomes a numerical procedure, just like it happened for the cubic case. In general, all corrections $\mathcal{Y}_{2n}(v)$ are odd-degree polynomials in v of the form,

$$\mathcal{Y}_{2n}(v) \;=\; v \sum_{k=0}^{n} c_{2k}^{(2n)} v^{2(n-k)} \;, \tag{7.3.6}$$

where any coefficient $c_{2k}^{(2n)}$ is a polynomial in D of degree k,

$$c_{2k}^{(2n)} \;=\; P_k^{(2n)}(D) \quad , \quad c_{2n}^{(2n)} \;=\; \frac{\varepsilon_{2n}}{D} \;. \tag{7.3.7}$$

The energy corrections ε_{2n} are of the form [60]

$$\varepsilon_{2n}(D) \;=\; D\,(D+2)\,R_{n-1}(D)\;, \tag{7.3.8}$$

where $R_{n-1}(D)$ is a polynomial of degree $(n-1)$ in D. In particular, $R_0(D) = \frac{1}{4}$.

From (7.3.8), one can see that any energy correction ε_{2n} vanishes when $D = 0$. In this situation, the formal sum of corrections results in $\varepsilon = 0$, and ultimately in $E = 0$. Thus, the radial Schrödinger equation is reduced to

$$-\,\frac{\hbar^2}{2M}\left(\frac{d^2\Psi(r)}{dr^2}\;-\;\frac{1}{r}\,\frac{d\Psi(r)}{dr}\right)\;+\;(r^2+g^2\,r^4)\,\Psi(r)\;=\;0 \tag{7.3.9}$$

at $D = 0$. This equation defines the *zero mode* of the radial Schrödinger operator at $D = 0$. It can be solved exactly in terms of Airy functions [39],

$$\Psi \;=\; C_1\,\mathrm{Ai}\left(\frac{1+(\lambda v)^2}{\lambda^{4/3}}\right)\;+\;C_2\,\mathrm{Bi}\left(\frac{1+(\lambda v)^2}{\lambda^{4/3}}\right)\;, \tag{7.3.10}$$

see (3.3.7) and (3.3.10) for the definition of λ and v, respectively. However, this linear combination can not be made normalizable[14] by any choice of constants C_1 and C_2. Therefore, it is an indication of the absence of a normalizable zero mode at $D = 0$. Interestingly, at the non-physical dimension $D = -2$, ε_{2n} with $n > 1$ also vanish. Thus, the formal sum of the corrections results is $\varepsilon = -2$, see (7.3.8). In this case, no exact solution for the corresponding radial Schrödinger equation was found.

7.3.2 Generating Functions

For the quartic anharmonic oscillator, the function $\mathcal{Z}(u)$ satisfies the GB equation

$$\lambda^2\,\partial_u\mathcal{Z}(u)\;-\;\mathcal{Z}(u)\left(\mathcal{Z}(u)-\frac{\lambda^2(D-1)}{u}\right)\;=\;\lambda^2\,\varepsilon(\lambda)\;-\;u^2\;-\;u^4\quad,\quad\partial_u\equiv\frac{d}{du}\;, \tag{7.3.11}$$

cf. (3.3.20). The solution of this equation can be written as an expansion in terms of generating functions, namely,

$$\mathcal{Z}(u)\;=\;\mathcal{Z}_0(u)\;+\;\mathcal{Z}_2(u)\,\lambda^2\;+\;\mathcal{Z}_4(u)\,\lambda^4\;+\;\ldots\;, \tag{7.3.12}$$

where each coefficient is of the form

$$\mathcal{Z}_{2k}(u)\;=\;u\sum_{n=k}^{\infty}c_{2k}^{(2n)}u^{2(n-k)}\quad,\quad k\;=\;0,1,\ldots\;. \tag{7.3.13}$$

Here, the expansion of ε in powers of λ is given by (7.3.3). Note that all generating functions $\mathcal{Z}_{2k+1}(u)$, $k = 1, 2, ...$, of odd order λ^{2k+1} are absent in expansion (4.2.1). Interestingly, from the

[14] At $D = 0$, the normalizability of the wave function is guaranteed if $\int_0^\infty \psi^2\,r^{-1}dr < \infty$.

polynomial form of the coefficient $c_{2k}^{(2n)}$ in D, see (7.3.8), one can find the structure of generating function in the variable D, namely

$$\mathcal{Z}_{2k}(u) \;=\; u\sum_{n=0}^{k} f_n^{(k)}(u^2)\,D^n\;, \tag{7.3.14}$$

where $f_n^{(k)}(u^2)$, $n=0,1,...,k$, are real functions. Hence, $\mathcal{Z}_{2k}(u)$ is a polynomial in D of degree k. For instance, this feature can be explicitly noted in the first two terms of the expansion (7.3.12),

$$\mathcal{Z}_0(u) \;=\; u\sqrt{1+u^2}\;, \tag{7.3.15}$$

$$\mathcal{Z}_2(u) \;=\; \frac{u^2+D\left(1+u^2-\sqrt{1+u^2}\right)}{2u(1+u^2)}\;. \tag{7.3.16}$$

Thus,

$$f_0^{(0)}(u^2) \;=\; \sqrt{1+u^2}\,,\qquad f_0^{(2)}(u^2) \;=\; \frac{1}{2(1+u^2)}\,,\qquad f_1^{(2)}(u^2) \;=\; \frac{1+u^2-\sqrt{1+u^2}}{2u^2(1+u^2)}\;. \tag{7.3.17}$$

The asymptotic behavior of the generating functions $\mathcal{Z}_{2k}(u)$, $k=0,1,2,\ldots$, in the expansion (7.3.12) at large u is related to the asymptotic behavior of the function $y(r)$ at large r in a quite interesting manner. It can be easily found that for fixed effective coupling constant λ, the asymptotic expansion of y at large r, written in variable v, see (3.3.7), has the form

$$y \;=\; (2M\hbar^2)^{\frac{1}{4}}\left(\lambda v^2 \;+\; \frac{1}{2\lambda} \;+\; \frac{D+1}{2}v^{-1} \;-\; \frac{4\lambda^2\varepsilon+1}{8\lambda^3}v^{-2} \;+\; \ldots\right)\;,\quad v\to\infty\;. \tag{7.3.18}$$

Note that the first three terms of the expansion are ε-independent, but only the first two are D-independent. On the other hand, the first three terms in the expansion of lowest generating function $(\frac{2M}{g^2})^{1/2}\mathcal{Z}_0(u)$ at large u are

$$\left(\frac{2M}{g^2}\right)^{1/2}\mathcal{Z}_0(u) \;=\; \left(\frac{2M}{g^2}\right)^{1/2}\left(u^2 \;+\; \frac{1}{2} \;-\; \frac{1}{8}u^{-2} \;+\; \ldots\right)\;,\quad u\to\infty\;, \tag{7.3.19}$$

see (7.3.15). To compare the expansions (7.3.18) and (7.3.19), let us replace the classical coordinate u by the quantum one v via $u \;=\; \lambda\, v$, see (3.3.24). Evidently, large v implies large u and vice versa (as long as λ is fixed). Then the expansion (7.3.19) becomes

$$\left(\frac{2M}{g^2}\right)^{1/2}\mathcal{Z}_0(\lambda v) \;=\; (2M\hbar^2)^{\frac{1}{4}}\left(\lambda v^2 \;+\; \frac{1}{2\lambda} \;-\; \frac{1}{8\lambda^3}v^{-2} \;+\; \ldots\right)\;,\quad v\to\infty\;. \tag{7.3.20}$$

It reproduces exactly the first two terms in (7.3.18) but fails to reproduce the term of order $O(v^{-1})$, which is absent. However, the next generating function $(\frac{2M}{g^2})^{1/2}\lambda^2\mathcal{Z}_2(\lambda v)$ at large v-expansion reproduces the term $O(v^{-1})$ exactly in the original expansion (7.3.18),

$$\left(\frac{2M}{g^2}\right)^{1/2}\lambda^2\mathcal{Z}_2(\lambda v) \;=\; (2M\hbar^2)^{\frac{1}{4}}\left(\frac{D+1}{2}v^{-1} \;-\; \frac{D}{2\lambda}v^{-2} \;+\; \ldots\right)\;,\qquad v\to\infty\;. \tag{7.3.21}$$

In turn, it fails to reproduce the term $O(v^{-2})$ correctly. Thus, the expansion of the sum $(\frac{2M}{g^2})^{1/2}(\mathcal{Z}_0(\lambda v) + \lambda^2 \mathcal{Z}_2(\lambda v))$ at large v reproduces exactly the first three ε-independent terms in the expansion (7.3.18). These three terms are responsible of the normalizability of the wave function at large v.

All higher generating functions $\mathcal{Z}_4(\lambda v)$, $\mathcal{Z}_6(\lambda v)\ldots$ contribute at large v to the same term $O(v^{-2})$ as follows

$$\left(\frac{2M}{g^2}\right)^{1/2} \lambda^{2n} \mathcal{Z}_{2n}(\lambda v) \;=\; (2M\hbar^2)^{\frac{1}{4}} \left(-\frac{\varepsilon_{2n-2}\,\lambda^{2n-3}}{2}\, v^{-2} \;+\; \ldots\right), \quad v \to \infty\,,\; n \,>\, 2\,, \tag{7.3.22}$$

where ε_{2n-2} is the energy PT correction of the order $(2n-2)$. As a consequence, no matter how many generating functions we consider in the expansion $(\frac{2M}{g^2})^{1/2}(\mathcal{Z}_0(\lambda v) + \lambda^2 \mathcal{Z}_2(\lambda v) + ...)$, the term of order $O(v^{-2})$ of (7.3.18) can not be reproduced exactly.

7.3.3 The Approximant

The first two[15] generating functions of the phase in the expansion (4.4.1), $G_0(r)$ and $G_2(r)$, are given by

$$G_0(r) \;=\; \frac{(2M)^{1/2}}{g^2}\left(\frac{(1+g^2r^2)^{3/2}}{3}\right), \tag{7.3.23}$$

$$G_2(r) \;=\; \frac{(2M)^{1/2}}{g^2}\left(\frac{1}{4}\log[1+g^2r^2] \;+\; \frac{D}{2}\log\left[1+\sqrt{1+g^2r^2}\right]\right). \tag{7.3.24}$$

These two functions serve as building blocks for the construction of the Approximant. Following the general prescription (6.1.2), we write the Approximant of the ground state in the exponential representation $\Psi^{(t)}_{0,0} = e^{-\frac{1}{\hbar}\Phi_t}$ where

$$\frac{1}{\hbar}\Phi_t(r) \;=\; \frac{\tilde{a}_0 + \tilde{a}_2\, r^2 + \tilde{a}_4\, g^2\, r^4}{\sqrt{1+\tilde{b}_4\, g^2\, r^2}} \;+\; \frac{1}{4}\log\left[1+\tilde{b}_4\, g^2\, r^2\right] \;+\; \frac{D}{2}\log\left[1+\sqrt{1+\tilde{b}_4\, g^2\, r^2}\right], \tag{7.3.25}$$

here $\tilde{a}_{0,2,4}$, and $\tilde{b}_4$ are free parameters. The logarithmic terms, added in (7.3.25), generate a prefactor to the exponential function. These terms are just a certain *minimal* modification of those which occur in the second generating function (7.3.24). As a result, the Approximant of the ground state for arbitrary $D = 1, 2, 3, \ldots$ is given by

[15] The generating functions $G_4(r)$ and $G_6(r)$ are presented explicitly in Appendix B.

$$\Psi^{(t)}_{0,0}(r) = \frac{1}{\left(1+\tilde{b}_4\, g^2\, r^2\right)^{1/4}\left(1+\sqrt{1+\tilde{b}_4\, g^2\, r^2}\right)^{D/2}}\, \exp\left(-\frac{\tilde{a}_0+\tilde{a}_2\, r^2+\tilde{a}_4\, g^2\, r^4}{\sqrt{1+\tilde{b}_4\, g^2\, r^2}}\right)\,. \tag{7.3.26}$$

This is the central formula of this Section devoted to the quartic anharmonicity. We will show that it provides a highly accurate uniform approximation of the exact ground state wave function. We impose the constraint

$$\tilde{b}_4 \;=\; 9\,\tilde{a}_4^2\,, \tag{7.3.27}$$

which allows us to reproduce the dominant term in the expansion (7.3.18) exactly[16]. Hence, it reproduces the exact asymptotic behavior of the phase at large distances. Therefore, the final form of the Approximant contains only 3 free parameters, say $\{\tilde{a}_0, \tilde{a}_2, \tilde{a}_4\}$. Note that by choosing

$$\tilde{a}_0 \;=\; \frac{(2M)^{1/2}}{3g^2}\,, \qquad \tilde{a}_2 \;=\; \frac{(8M)^{1/2}}{3}\,, \qquad \tilde{a}_4 \;=\; \frac{(2M)^{1/2}}{3}\,, \tag{7.3.28}$$

the phase Φ_t reproduces exactly the first two terms in the expansion in generating functions (4.4.1). However, parameters $\tilde{a}_0, \tilde{a}_2, \tilde{a}_4$ in (7.3.28) are not optimal from the point of view of the VM. To construct 3-parametric Approximants for excited states, we follow the prescription presented in the previous Section 6.2. Hence, at $D = 1$ we have

$$\Psi^{(t)}_{n_r,p}(x) = \frac{x^p\, P^{(p)}_{n_x}(x^2)}{\left(1+\tilde{b}_4\, g^2\, x^2\right)^{1/4}\left(1+\sqrt{1+\tilde{b}_4\, g^2\, x^2}\right)^{D/2}}\, \exp\left(-\frac{\tilde{a}_0+\tilde{a}_2\, x^2+\tilde{a}_4\, g^2\, x^4}{\sqrt{1+\tilde{b}_4\, g^2\, x^2}}\right), \tag{7.3.29}$$

while at $D > 1$

$$\Psi^{(t)}_{n_r,\ell}(r) \;=\; \frac{r^\ell\, P^{(\ell)}_{n_r}(r^2)}{\left(1+\tilde{b}_4\, g^2\, r^2\right)^{1/4}\left(1+\sqrt{1+\tilde{b}_4\, g^2\, r^2}\right)^{D/2}}\, \exp\left(-\frac{\tilde{a}_0+\tilde{a}_2\, r^2+\tilde{a}_4\, g^2\, r^4}{\sqrt{1+\tilde{b}_4\, g^2\, r^2}}\right)\,. \tag{7.3.30}$$

Definitions of $P^{(p)}_{n_r}(x^2)$ and $P^{(\ell)}_{n_r}(r^2)$ are presented in (6.2.1) and (6.2.4), explicitly.

[16] In numerical computations we set $\hbar = 1$ and $M = 1/2$.

7.3.4 Numerical Results: Variational Calculations

The calculations of the variational energy for the first low-lying states with quantum numbers (0,0), (0,1), (0,2), (1,0) are presented in Tables 7.8 - 7.11 for different values of D and g^2. For some of those states, the variational energy $E_{var} = E_0^{(t)} + E_1^{(t)}$, the first correction $E_2^{(t)}$ to it, as well as its corrected value $E_{var}+E_2^{(t)}$ are shown. All states are studied in dimension $D = 1, 2, 3, 6$ and coupling constant $g^2 = 0.1, 1, 10$. The variational energy E_{var} is obtained with absolute deviation (from the exact result) in the order $10^{-8} - 10^{-14}$ $(8 - 14$ s.d.). This deviation is found by calculating the second correction $E_2^{(t)}$ (the first correction to the variational energy).

To check the energies obtained in Non-Linearization Procedure, we calculated them numerically in the Lagrange-Mesh method. These numerical calculations show that all digits presented for $E_{var} + E_2^{(t)}$ are exact: we obtain not less than 12 exact d.d. in the Non-Linearization Procedure. This accuracy is confirmed independently by calculating the second correction $E_3^{(t)}$ to variational energy: this correction is $\lesssim 10^{-13}$ for any D and g^2 that we have studied. It indicates a very fast rate of convergence in Non-Linearization Procedure with trial function either (7.3.29) or (7.3.30) taken as zero approximation. In general, the energies grow with an increase of D and/or g^2. At $D > 1$ we can classify the states by radial quantum number n_r and angular momentum ℓ as (n_r, ℓ), we mention the hierarchy of eigenstates which holds for any fixed integer $D > 1$ and g^2: (0,0), (0,1), (0,2), (1,0). There is a considerable number of calculations devoted to estimating the energy of the first low-lying states. Our results, see Tables 7.8 - 7.11, are in complete agreement with [23] and [24] for $D = 1$, and superior considerably of those obtained for different $D > 1$ and g^2, see e.g. [25], [26] and [32]. At $D = 6$ the calculations are carried out for the first time.

The Deviation of the Approximant from the exact (unknown) eigenfunction can be estimated via the Non-Linearization Procedure. For the ground state function, this deviation is extremely small and bounded,

$$\left| \frac{\Psi_{0,0}(r) - \Psi_{0,0}^{(t)}(r)}{\Psi_{0,0}^{(t)}(r)} \right| \lesssim 10^{-6} \tag{7.3.31}$$

in the whole range of $r \in [0, \infty)$ at any D and g^2. Therefore, the Approximant of the ground state is a locally accurate approximation of the exact wave function $\Psi_{0,0}(r)$ once the optimal parameters are chosen. In general, the optimal variational parameters are smooth, slow changing as functions of g^2 without a strong D dependence.

For the ground state (0,0), the plots of the parameters $\tilde{a}_{0,2,3}$ vs g for $D = 1, 2, 3, 6$ are shown in Appendix C, Fig. C.2. In turn, Fig. C.3 shows the plots of the parameters as functions of D for fixed g^2. Similar plots appear for the excited states for different D and g^2. Making an analysis of the parameters $\tilde{a}_{0,2,4}$ *vs* g^2 for different D, one can see the (accidental) appearance of another D-independent constraint on the parameters, namely

$$\tilde{a}_2 \;=\; \frac{1 + 27\,\tilde{a}_4^2}{18\tilde{a}_4}\;. \tag{7.3.32}$$

It corresponds to the fact that the coefficient in front of r - another growing term at $r \to \infty$ in

Table 7.8: Ground state energy for the quartic potential $V(r) = r^2 + g^2\, r^4$ for $D = 1, 2, 3, 6$ and $g^2 = 0.1, 1, 10$, labeled by quantum numbers (0,0) at any D. Variational energy $E_{var} = E_{var}$, the first correction $E_2^{(t)}$ (rounded to 3 s.d.) found with use of $\Psi_{0,0}^{(t)}$, see text, and the corrected energy $E_{var} + E_2^{(t)} = E_{var} + E_2^{(t)}$ shown. $E_{var} + E_2^{(t)}$ coincides with Lagrange Mesh results (see text) in 12 displayed d. d., hence all printed digits are exact.

g^2	$D = 1$			$D = 2$		
	E_{var}	$-E_2^{(t)}$	$E_{var} + E_2^{(t)}$	E_{var}	$-E_2^{(t)}$	$E_{var} + E_2^{(t)}$
0.1	1.065 285 509 544	3.00×10^{-14}	1.065 285 509 544	2.168 597 211 269	5.28×10^{-14}	2.168 597 211 269
1.0	1.392 351 641 563	3.37×10^{-11}	1.392 351 641 530	2.952 050 091 995	3.17×10^{-11}	2.952 050 091 962
10.0	2.449 174 072 588	4.69×10^{-10}	2.449 174 072 118	5.349 352 819 751	3.44×10^{-10}	5.349 352 819 462
g^2	$D = 3$			$D = 6$		
	E_{var}	$-E_2^{(t)}$	$E_{var} + E_2^{(t)}$	E_{var}	$-E_2^{(t)}$	$E_{var} + E_2^{(t)}$
0.1	3.306 872 013 152	2.20×10^{-13}	3.306 872 013 152	6.908 332 111 232	9.80×10^{-14}	6.908 332 111 232
1.0	4.648 812 704 237	2.69×10^{-11}	4.648 812 704 210	10.390 627 295 514	9.68×10^{-12}	10.390 627 295 504
10.0	8.599 003 455 030	2.22×10^{-10}	8.599 003 454 807	19.936 900 374 076	6.48×10^{-11}	19.936 900 374 011

Table 7.9: The first excited state energy for the quartic potential $V(r) = r^2 + g^2\, r^4$ for different D and g^2. Variational energy E_{var}, the first correction $E_2^{(t)}$ found with use of $\Psi_{0,1}^{(t)}$ for $D = 1$ and $\Psi_{0,1}^{(t)}$ for $D > 1$, see (7.3.29) and (7.3.30). The corrected energy $E_{var} + E_2^{(t)} = E_{var} + E_2^{(t)}$ shown, the correction $E_2^{(t)}$ rounded to 3 s.d. All printed digits for $E_{var} + E_2^{(t)}$ are exact.

g^2	$D = 1$			$D = 2$		
	E_{var}	$-E_2^{(t)}$	$E_{var} + E_2^{(t)}$	E_{var}	$-E_2^{(t)}$	$E_{var} + E_2^{(t)}$
0.1	3.306 872 013 236	8.33×10^{-11}	3.306 872 013 153	4.477 600 360 878	1.10×10^{-10}	4.477 600 360 768
1.0	4.648 812 707 206	2.99×10^{-9}	4.648 812 704 212	6.462 906 003 251	3.39×10^{-9}	6.462 905 999 864
10.0	8.599 003 467 556	1.27×10^{-8}	8.599 003 454 810	12.138 224 752 729	1.38×10^{-8}	12.138 224 738 901
g^2	$D = 3$			$D = 6$		
	E_{var}	$-E_2^{(t)}$	$E_{var} + E_2^{(t)}$	E_{var}	$-E_2^{(t)}$	$E_{var} + E_2^{(t)}$
0.1	5.678 682 663 377	1.33×10^{-10}	5.678 682 663 243	9.447 358 518 278	1.80×10^{-10}	9.447 358 518 099
1.0	8.380 342 533 658	3.56×10^{-9}	8.380 342 530 101	14.658 513 816 952	3.39×10^{-9}	14.658 513 813 563
10.0	15.927 096 988 667	1.40×10^{-8}	15.927 096 974 709	28.536 810 849 436	1.21×10^{-8}	28.536 810 837 360

Table 7.10: The second excited state energy for the quartic potential $V(r) = r^2 + g^2\, r^4$ for different D and g^2. Variational energy E_{var} found with use of $\Psi^{(t)}_{1,0}$ for $D = 1$ and $\Psi^{(t)}_{0,2}$ for $D > 1$, see (7.3.29) and (7.3.30). The first correction $E^{(t)}_2$ and the corrected energy $E_{var}+E^{(t)}_2 = E_{var} + E^{(t)}_2$ shown. Correction $E^{(t)}_2$ rounded to 3 s.d. All 12 printed d. d. in $E_{var} + E^{(t)}_2$ are exact.

g^2	$D=1$	$D=2$		
	E_{var}	E_{var}	$-E^{(t)}_2$	$E_{var} + E^{(t)}_2$
0.1	5.747 959 269 942	6.908 332 112 167	9.35×10^{-10}	6.908 332 111 232
1.0	8.655 049 995 062	10.390 627 321 799	2.63×10^{-8}	10.390 627 295 506
10	16.635 921 650 401	19.936 900 479 247	1.05×10^{-7}	19.936 900 374 040

g^2	$D=3$			$D=6$		
	E_{var}	$-E^{(t)}_2$	$E_{var} + E^{(t)}_2$	E_{var}	$-E^{(t)}_2$	$E_{var} + E^{(t)}_2$
0.1	8.165 006 438 494	1.00×10^{-9}	8.165 006 437 493	12.084 471 853 886	1.11×10^{-9}	12.084 471 852 776
1.0	12.485 556 075 670	2.47×10^{-8}	12.485 556 051 000	19.217 523 515 555	1.97×10^{-8}	19.217 523 495 879
10.0	24.145 857 689 623	9.48×10^{-8}	24.145 857 594 824	37.811 402 320 699	6.90×10^{-8}	37.811 402 251 702

Table 7.11: The third excited state energy for the quartic potential $V = r^2+g^2\, r^4$ for different D and g^2. The radial node r_0 calculated in Lagrange-Mesh method with 9 correct d.d. Variational energy E_{var} and its radial node $r^{(0)}_0$ given by underlined digits, both found with $\Psi^{(t)}_{1,0}$, see (7.3.30).

g^2	$D=2$		$D=3$		$D=6$	
	$E^{(1)}_0$	$r^{(0)}_0$	$E^{(1)}_0$	$r^{(0)}_0$	$E^{(1)}_0$	$r^{(0)}_0$
0.1	7.039 707 584	0.918 783 458	8.352 677 825	1.111 521 078	12.415 256 177	1.522 966 591
1.0	10.882 435 576	0.733 724 778	13.156 803 922	0.875 567 486	20.293 829 707	1.166 753 149
10.0	21.175 135 370	0.524 083 057	25.806 276 215	0.621 795 290	40.388 142 970	0.820 068 428

the trial phase (7.3.25) - is reproduced *almost exactly* in accordance to (7.3.18). Not surprisingly, if we demand to fulfill exactly constraint (7.3.32), no deterioration in the accuracy of the energy and wave function occurs. Thus, it can be concluded that the approximate phase (7.3.25), at large r, reproduces (almost) exactly all three growing with r terms: r^3, r, and $\log r$. Eventually, if we require to reproduce all those terms exactly by the Approximant in its final form, it will contain two free parameters $\{\tilde{a}_0, \tilde{a}_4\}$ only. In this case, the parameters $\{\tilde{a}_2, \tilde{b}_4\}$ obey constraints (7.3.32), (7.3.27), respectively.

The first order correction y_1 to the logarithmic derivative of the ground state $y_0 = \partial_r \Phi_t$ is a bounded function at different D and g^2. For example, for $g^2 = 1$ the first correction y_1 has the bound

$$|y_1|_{max} \sim \begin{cases} 0.0101\ , & D = 1 \\ 0.0087\ , & D = 2 \\ 0.0077\ , & D = 3 \\ 0.0060\ , & D = 6 \end{cases} \tag{7.3.33}$$

It is the consequence of the fact that the derivative of Φ_t reproduces exactly the growing terms at large r in the expansion (7.3.18). "Boundness" of y_1, together with the small value of the

maximum, implies that we deal with smartly designed zeroth order-approximation $\Psi^{(t)}_{0,0}$; it leads, in the framework of the Non-Linearization Procedure, to a fast convergent series of the energy and wave function. In Fig. 7.3 y_0 and y_1 *vs* r are presented for $g^2 = 1$ in $D = 1$. It is not a surprise that a similar plot should appear for $D = 2, 3, 6$ (not shown). An analysis of these plots indicates that $|y_1|$ is an extremely small function in comparison with $|y_0|$ in the domain $0 \le r \lesssim 1$ where the dominant contribution to variational integrals occurs, see (1.1). It explains why the energy correction $E^{(t)}_2$ is small being the order of $\sim 10^{-8}$, or $\sim 10^{-11}$. In a similar way one can show numerically that the higher corrections $y_2, y_3, \ldots$, drop down to zero in the domain $0 \le r \lesssim 1$ even faster, indicating the convergence of the expansion (1.18) as $n \to \infty$.

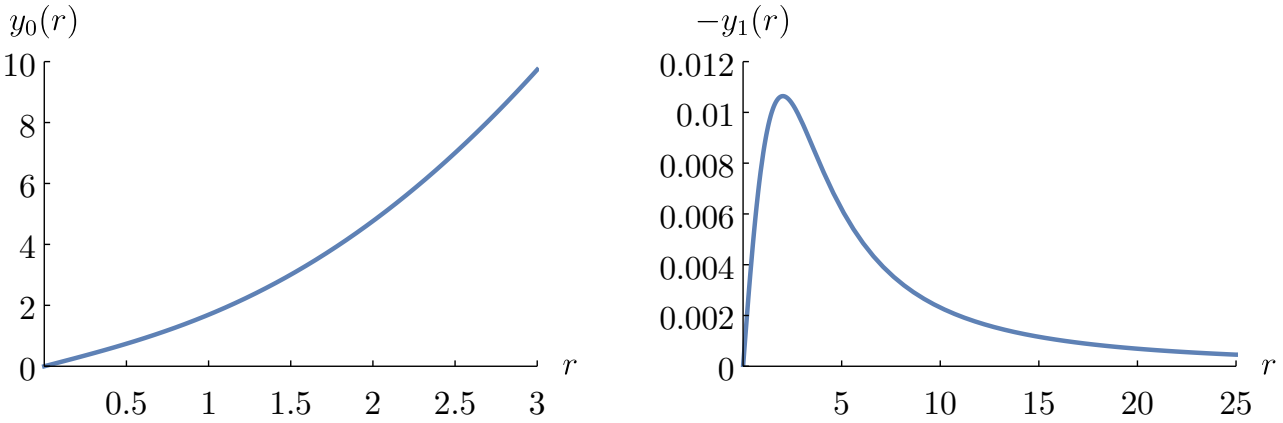

Figure 7.3: Quartic oscillator at $D = 1$: function $y_0 = (\Phi_t)'$ (on left) and its first correction y_1 (on right) *vs* r for $g^2 = 1$.

At $D > 1$ we checked that the Approximant $\Psi^{(t)}_{1,0}$ also provides an accurate estimate of the position of the radial node of the exact wave function, see (7.2.26). The orthogonality condition described in Section 6.2 provides a simple analytic expression for the zeroth order approximation $r^{(0)}_0$ to r_0. Making a comparison of $r^{(0)}_0$ with numerical estimates which come from the Lagrange-Mesh method with 200 mesh points, we can see the coincidence of r_0 and $r^{(0)}_0$ for at least 6 d.d. at integer dimension D at any coupling constant $g^2 \ge 0$. The results are presented in Table 7.11.

7.3.5 First Terms in the Strong Coupling Expansion

In this Section, we will explicitly find the first two terms of the strong coupling expansion (5.1.7) of the ground state energy for the quartic anharmonic oscillator (7.3.1),

$$E \;=\; g^{2/3}(\tilde{\varepsilon}_0 \;+\; \tilde{\varepsilon}_2 g^{-4/3} \;+\; \tilde{\varepsilon}_4 g^{-8/3} \;+\; \ldots)\;, \tag{7.3.34}$$

assuming $2M = \hbar = 1$. In contrast with the weak coupling expansion, the expansion (7.3.34) has a finite radius of convergence. This expansion corresponds to PT in powers of $\hat{\lambda}$ for the potential

$$V(w) \;=\; w^4 \;+\; \hat{\lambda}\, w^2\;, \quad \hat{\lambda} \;=\; g^{-2/3}\;, \tag{7.3.35}$$

in the radial Schrödinger equation defined in $w \in [0, \infty)$. In order to calculate the first two terms $\tilde{\varepsilon}_0$ and $\tilde{\varepsilon}_2$ of the strong coupling expansion (7.3.34), we use the Approximant (7.3.26). In Table 7.12, the leading coefficient $\tilde{\varepsilon}_0$ and the second perturbative correction to it $\hat{\varepsilon}_2$, as well as the corrected value $\tilde{\varepsilon}_0^{(2)} = \tilde{\varepsilon}_0^{(1)} + \hat{\varepsilon}_2$, calculated via the Non-Linearization Procedure, are presented for different D. Numerical results for $\tilde{\varepsilon}_0$, based on the Lagrange-Mesh method and obtained with 12 d.d., indicate that $\tilde{\varepsilon}_0^{(2)} = \tilde{\varepsilon}_0^{(1)} + \hat{\varepsilon}_2$ reproduce not less than 10 d.d. This accuracy is verified independently by calculating the next correction $\hat{\varepsilon}_3$, which results in the order of $\hat{\varepsilon}_3 \sim 10^{-2}\hat{\varepsilon}_2$. In turn, Table 7.13 contains the results of the first two approximations for the coefficient $\tilde{\varepsilon}_2$ in (7.3.34). It should be mentioned that our final results for the coefficient $\tilde{\varepsilon}_0$ reproduce and sometimes exceed the best results available in the literature, see [62], [63], [64]. Hence, we have established some benchmarks. At $D = 6$ the calculations are carried out for the first time.

Table 7.12: Ground state energy $\tilde{\varepsilon}_0$ for the potential $W = w^4$ (see (7.3.35)) for $D = 1, 2, 3, 6$ found in PT based on the Approximant $\Psi_{0,0}^{(t)}$: $\tilde{\varepsilon}_0^{(1)}$ corresponds to the variational energy, $\hat{\varepsilon}_2$ is the second PT correction, $\tilde{\varepsilon}_0^{(2)} = \tilde{\varepsilon}_0^{(1)} + \hat{\varepsilon}_2$ is the corrected variational energy. 10 d.d. in $\tilde{\varepsilon}_0^{(2)}$ confirmed independently in Lagrange-Mesh method.

$D = 1$			$D = 2$		
$\tilde{\varepsilon}_0^{(1)}$	$-\hat{\varepsilon}_2$	$\tilde{\varepsilon}_0^{(2)}$	$\tilde{\varepsilon}_0^{(1)}$	$-\hat{\varepsilon}_2$	$\tilde{\varepsilon}_0^{(2)}$
1.060 362 090 491	7.02×10^{-12}	1.060 362 090 484	2.344 829 072 753	9.27×10^{-12}	2.344 829 072 744
$D = 3$			$D = 6$		
$\tilde{\varepsilon}_0^{(1)}$	$-\hat{\varepsilon}_2$	$\tilde{\varepsilon}_0^{(2)}$	$\tilde{\varepsilon}_0^{(1)}$	$-\hat{\varepsilon}_2$	$\tilde{\varepsilon}_0^{(2)}$
3.799 673 029 810	9.27×10^{-12}	3.799 673 029 801	8.928 082 199 890	4.07×10^{-11}	8.928 082 199 850

Table 7.13: Subdominant coefficient $\tilde{\varepsilon}_2$ in the strong coupling expansion (7.3.34) for the ground state energy for the quartic radial anharmonic potential (7.3.35) for different $D = 1, 2, 3, 6$. The first correction to it $\tilde{\varepsilon}_{2,1}$ as well as the corrected value $\tilde{\varepsilon}_2^{(2)} = \tilde{\varepsilon}_2^{(1)} + \tilde{\varepsilon}_{2,1}$ displayed

$D = 1$			$D = 2$		
$\tilde{\varepsilon}_2^{(1)}$	$\tilde{\varepsilon}_{2,1}$	$\tilde{\varepsilon}_2^{(2)}$	$\tilde{\varepsilon}_2^{(1)}$	$\tilde{\varepsilon}_{2,1}$	$\tilde{\varepsilon}_2^{(2)}$
0.362 022 648 388	3.96×10^{-10}	0.362 022 648 784	0.651 477 773 845	4.38×10^{-10}	0.651 477 774 283
$D = 3$			$D = 6$		
$\tilde{\varepsilon}_2^{(1)}$	$\tilde{\varepsilon}_{2,1}$	$\tilde{\varepsilon}_2^{(2)}$	$\tilde{\varepsilon}_2^{(1)}$	$\tilde{\varepsilon}_{2,1}$	$\tilde{\varepsilon}_2^{(2)}$
0.901 605 894 682	2.03×10^{-9}	0.901 605 896 709	1.526 804 282 772	-3.06×10^{-8}	1.526 804 252 175

7.4 Sextic Anharmonic Oscillator

In this Section, it will be considered the two-term sextic anharmonic radial oscillator potential

$$V(r) \;=\; r^2 \;+\; g^4\, r^6 \;, \tag{7.4.1}$$

see (7.0.1) at $m = 6$.

7.4.1 Perturbation Theory in the Weak Coupling Regime

In the Weak Coupling Regime, the perturbative expansion for ε and $\mathcal{Y}(v)$ can be developed from the RB equation (3.3.9),

$$\partial_v \mathcal{Y}(v) \; - \; \mathcal{Y}(v) \left(\mathcal{Y}(v) - \frac{D-1}{v} \right) \; = \; \varepsilon\,(\lambda) \; - \; v^2 \quad - \; \lambda^4\, v^6 \quad , \quad \partial_v \equiv \frac{d}{dv} \; . \tag{7.4.2}$$

The definition of v and λ is shown in (3.3.7) and (3.3.10), respectively. The perturbation series for ε and $\mathcal{Y}(v)$ are of the form

$$\varepsilon \; = \; \varepsilon_0 \; + \; \varepsilon_4\, \lambda^4 \; + \; \varepsilon_8\, \lambda^8 \; + \; \ldots \quad , \qquad \varepsilon_0 \; = \; D \; , \tag{7.4.3}$$

and

$$\mathcal{Y}(v) \; = \; \mathcal{Y}_0(v) \; + \; \mathcal{Y}_4(v)\, \lambda^4 \; + \; \mathcal{Y}_8(v)\, \lambda^8 \; + \; \ldots \quad , \quad \mathcal{Y}_0(v) \; = \; v \; , \tag{7.4.4}$$

respectively. The terms of order λ^{4n+1} and λ^{4n+2} are absent in both expansions. Since the potential (7.4.1) is even, PT can be constructed by algebraic means due to the polynomial nature of correction $\mathcal{Y}_n(v)$. The first non-vanishing correction is

$$\varepsilon_4 \; = \; \frac{1}{8}\, D\,(D+2)\,(D+4) \quad , \quad \mathcal{Y}_4(v) \; = \; \frac{1}{2}\, v^5 \; + \; \frac{1}{4}(D+4)\, v^3 \; + \; \frac{1}{8}\,(D+2)\,(D+4)\, v \; . \tag{7.4.5}$$

The next two corrections, $\varepsilon_{8,12}$ and $\mathcal{Y}_{8,12}(v)$, are presented in Appendix B. It can be shown that the correction $\mathcal{Y}_{4n}(v)$ has the form of an odd polynomial in v, namely

$$\mathcal{Y}_{4n}(v) \; = \; v \sum_{k=0}^{2n} c_{2k}^{(4n)} v^{2(2n-k)} \; , \tag{7.4.6}$$

with coefficients $c_{2k}^{(4n)}$ being polynomials in D of degree k,

$$c_{2k}^{(4n)} \; = \; P_k^{(4n)}(D) \quad , \qquad c_{4n}^{(4n)} \; = \; \frac{\varepsilon_{4n}}{D} \; , \tag{7.4.7}$$

cf. (7.3.6), (7.3.7). The correction ε_{4n} has the factorization property

$$\varepsilon_{4n}(D) \; = \; D\,(D+2)\,(D+4)\, R_{2n-2}(D) \; , \tag{7.4.8}$$

where $R_{2n-2}(D)$ is a polynomial in D of degree $(2n-2)$, cf. (7.3.8). In particular, $R_0 = \frac{1}{8}$. From (7.4.7), one can see that all corrections ε_{4n} vanish at $D = 0, -2, -4$. Hence, their formal sum results in $\varepsilon = 0, -2, -4$, respectively. In the case $D = 0$, the radial Schrödinger equation takes the form

$$-\, \frac{\hbar^2}{2M} \left(\frac{d^2\Psi(r)}{dr^2} \; - \; \frac{1}{r} \frac{d\Psi(r)}{dr} \right) \; + \; (r^2 \; + \; g^4\, r^6)\, \Psi(r) \; = \; 0 \; , \tag{7.4.9}$$

cf.(7.3.9). Its formal solution is given in terms of the parabolic cylinder functions [65] (also known as Weber functions),

$$\Psi \; = \; C_1\, D_{\nu_-}(\lambda v^2) \; + \; C_2\, D_{\nu_-}\left(i\, \lambda v^2 \right) \; , \qquad \nu_\pm \; = \; -\frac{1}{2} \; \pm \; \frac{1}{4\lambda^2} \; , \tag{7.4.10}$$

where v and λ are defined in (3.3.7) and (3.3.10), respectively. This formal solution has the meaning of the zero mode of the Schrödinger operator at $D = 0$. The function shown in (7.4.10) cannot be made normalizable by any choice of constants C_1 and C_2. Hence, the Schrödinger operator at $D = 0$ for the sextic potential (7.4.1) has no zero mode in the Hilbert space. It complements a similar statement made for quartic potential (7.3.1). One can guess that the zero mode in the Hilbert space at $D = 0$ is absent for the Schrödinger operator with anharmonicity r^{2m}. At $D = -2, -4$, all corrections ε_{4n} vanish. As a result, we formally have $\varepsilon = -2$ and $\varepsilon = -4$, respectively. For both cases, no exact solution has been found for their corresponding radial Schrödinger equations.

7.4.2 Generating Functions

For the sextic anharmonic oscillator, the GB equation is given by

$$\lambda^2 \, \partial_u \mathcal{Z} \; - \; \mathcal{Z} \left(\mathcal{Z} - \frac{\lambda^2 (D-1)}{u} \right) \; = \; \lambda^2 \, \varepsilon(\lambda) \; - \; u^2 - u^6 \quad , \quad \partial_u \equiv \frac{d}{du} \; , \tag{7.4.11}$$

see (3.3.20). The expansion of $\mathcal{Z}(u)$ in terms of generating functions has the form

$$\mathcal{Z}(u) \; = \; \mathcal{Z}_0(u) \; + \; \mathcal{Z}_2(u) \, \lambda^2 \; + \; \mathcal{Z}_4(u) \, \lambda^4 \; + \; \ldots \; . \tag{7.4.12}$$

In turn, the expansion of the energy reads

$$\varepsilon \; = \; \varepsilon_0 \; + \; \varepsilon_4 \, \lambda^4 \; + \; \varepsilon_8 \, \lambda^8 \; + \; \ldots \quad , \qquad \varepsilon_0 \; = \; D \; , \tag{7.4.13}$$

see (7.4.3). Interestingly, (7.4.12) has the same structure as the expansion for the quartic anharmonic case: all generating functions $\mathcal{Z}_{2k+1}(u)$, $k = 1, 2, ...$ of odd orders λ^{2k+1} are absent in expansion, cf. (7.3.12). It contrasts with the expansion of $\mathcal{Y}(v)$ and $\varepsilon(\lambda)$ in which the powers λ^{4n} are present only. In fact, for any even radial anharmonic potential, $V(r) = V(-r)$, the function $\mathcal{Z}(u)$ is written in terms of generating functions as an expansion in powers of λ^2. Further properties of the generating function for the sextic anharmonic oscillator can be established. For example, there are two different families of generating functions,

$$\mathcal{Z}_{4k}(u) \; = \; u \sum_{n=k}^{\infty} c_{4k}^{(4n)} u^{4(n-k)} \; , \tag{7.4.14}$$

and

$$\mathcal{Z}_{4k+2}(u) \; = \; u \sum_{n=k+1}^{\infty} c_{4k+2}^{(4n)} u^{4(n-k)-2} \; . \tag{7.4.15}$$

Those families occur in correspondence to $\varepsilon_{4k+2} = 0$ and $\varepsilon_{4k} \neq 0$, respectively. Following (7.4.6) and (7.4.7), it is easy to see that both families of generating functions are of the form $\mathcal{Z}_{2k}(u)$,

$$\mathcal{Z}_{2k}(u) \; = \; u \sum_{n=0}^{k} f_n^{(k)}(u^2) \, D^n \; , \tag{7.4.16}$$

where $f_n^{(p)}(u^2)$ are some real functions. It implies that $\mathcal{Z}_{2k}(u)$ is a polynomial in D of degree k. For example, the first two terms in the expansion (7.4.12) are

$$\mathcal{Z}_0(u) \;=\; u\,\sqrt{1+u^4}\;, \tag{7.4.17}$$

$$\mathcal{Z}_2(u) \;=\; \frac{2u^4+D\left(1+u^4-\sqrt{1+u^4}\right)}{2u\,(1+u^4)}\;. \tag{7.4.18}$$

From these expressions, we can conclude immediately that

$$f_0^{(0)}(u^2) \;=\; \sqrt{1+u^4}\;, \qquad f_0^{(2)}(u^2) \;=\; \frac{u^2}{(1+u^4)}\;, \qquad f_1^{(2)}(u^2) \;=\; \frac{1+u^4-\sqrt{1+u^4}}{2u^2(1+u^4)}\;. \tag{7.4.19}$$

The asymptotic behavior at large u of $\mathcal{Z}_{2p}(u)$ is related to the expansion of y at large r. For the sextic anharmonic oscillator, the expansion of y at large r and fixed effective coupling λ is rewritten conveniently in variable v, see (3.3.7),

$$y \;=\; (2M\hbar^2)^{\frac{1}{4}}\left(\lambda^2 v^3 \;+\; \frac{(D+2)\lambda^2+1}{2\lambda^2}v^{-1} - \;\frac{\varepsilon}{2\lambda^2}v^{-3} \;+\; \ldots\right)\;, \qquad v\to\infty\;. \tag{7.4.20}$$

The first two terms of this expansion are ε-independent, but only the first one is D-independent. Following an analogous procedure to that used for the cubic and quartic oscillator, we can transform the expansion of $\mathcal{Z}_{2k}(u)$ at large u into an expansion at large v via the connection between the classical and quantum coordinate shown in (3.3.24). The first two terms in (7.4.12) expanded at large v read

$$\left(\frac{2M}{g^2}\right)^{1/2}\mathcal{Z}_0(\lambda v) \;=\; (2M\hbar^2)^{\frac{1}{4}}\left(\lambda^2 v^3 \;+\; \frac{1}{2\lambda^2}v^{-1} \;-\; \frac{1}{8\lambda^6}v^{-5} \;+\; \ldots\right)\;, \qquad v\to\infty\;, \tag{7.4.21}$$

and

$$\left(\frac{2M}{g^2}\right)^{1/2}\lambda^2\mathcal{Z}_2(\lambda v) \;=\; (2M\hbar^2)^{\frac{1}{4}}\left(\frac{D+2}{2}v^{-1} \;-\; \frac{D}{2\lambda^2}v^{-3} \;-\; \frac{1}{\lambda^4}v^{-5} \;+\; \ldots\right)\;, \qquad v\to\infty\;, \tag{7.4.22}$$

see (7.4.17) and(7.4.18). The sum $(\frac{2M}{g^2})^{1/2}(\mathcal{Z}_0(\lambda v)+\lambda^2\mathcal{Z}_2(\lambda v))$ at large v reproduces exactly the first two terms in the expansion (7.4.20). However, higher generating functions, $\mathcal{Z}_4(\lambda v)$, $\mathcal{Z}_6(\lambda v), ...$ contribute to the same order $O(v^{-3})$ at large v,

$$\left(\frac{2M}{g^2}\right)^{1/2}\lambda^{2k}\mathcal{Z}_{2k}(\lambda v) \;=\; (2M\hbar^2)^{\frac{1}{4}}\left(-\frac{\varepsilon_{4k-4}\lambda^{4k-6}}{2}v^{-3} \;+\; \ldots\right)\;, \quad v\to\infty\;. \tag{7.4.23}$$

Here ε_{4k-4} denotes the energy correction of order λ^{4k-4}. Therefore, it does not matter how many generating functions are considered in the expansion $(\frac{2M}{g^2})^{1/2}(\mathcal{Z}_0(\lambda v)+\lambda^2\mathcal{Z}_2(\lambda v)+...)$ re-expanded at large v, the ε-dependent coefficient in front of the term of order $O(v^{-3})$ will never be reproduced exactly. A similar situation occurred for the cubic and quartic cases.

7.4.3 The Approximant

The first two[17] generating functions of the phase, $G_0(r)$ and $G_2(r)$, are given by

$$G_0(r) \;=\; \frac{(2M)^{1/2}}{g^2}\left(\frac{r^2}{4}\sqrt{1+g^4r^4} \;+\; \log\left[g^2r^2+\sqrt{1+g^4r^4}\right]\right)\;, \tag{7.4.24}$$

and

$$G_2(r) \;=\; \frac{(2M)^{1/2}}{g^2}\left(\frac{1}{4}\log\left[1+g^4r^4\right] \;+\; \frac{D}{4}\log\left[1+\sqrt{1+g^4r^4}\right]\right)\;. \tag{7.4.25}$$

These two functions serve as building blocks for the construction of the Approximant. Following the general prescription (6.1.2), we write the Approximant of the ground state in the exponential representation $\Psi^{(t)}_{0,0} = e^{-\frac{1}{\hbar}\Phi_t}$ where

$$\begin{aligned}\frac{1}{\hbar}\Phi_t(r) = {}& \frac{\tilde a_0+\tilde a_2\,r^2+\tilde a_4\,g^2\,r^4+\tilde a_6\,g^4\,r^6}{\sqrt{1+\tilde b_4\,g^2\,r^2+\tilde b_6\,g^4\,r^4}} + \frac{1}{4g^2}\,\log\left[\tilde c_2\,g^2\,r^2+\sqrt{1+\tilde b_4\,g^2\,r^2+\tilde b_6\,g^4\,r^4}\right]\\ & + \frac{1}{4}\log\left[1+\tilde b_4\,g^2\,r^2+\tilde b_6\,g^4r^4\right] + \frac{D}{4}\log\left[1+\sqrt{1+\tilde b_4\,g^2\,r^2+\tilde b_6g^4r^4}\right]\;. \end{aligned}\tag{7.4.26}$$

At this stage $\tilde a_{0,2,4,6}$, $\tilde b_{4,6}$, and $\tilde c_2$ are 7 free parameters. The logarithmic terms added in (7.4.26) generate prefactor to the exponential function, Those terms are a certain *minimal* modification of those that occur in the first two generating functions (7.3.24) and (7.4.25). As a result, the Approximant of the ground state for arbitrary $D = 1, 2, 3, \ldots$ is given by

$$\begin{aligned}\Psi^{(t)}_{0,0}(r) = {}& \frac{1}{\left(1+\tilde b_4\,g^2\,r^2+\tilde b_6\,g^4r^4\right)^{1/4}\left(1+\sqrt{1+\tilde b_4\,g^2\,r^2+\tilde b_6g^4\,r^4}\right)^{D/4}}\times\\ & \frac{1}{\left(\tilde c_2g^2r^2+\sqrt{1+\tilde b_4\,g^2\,r^2+\;\tilde b_6\,g^4\,r^4}\right)^{1/4g^2}}\exp\left(-\frac{\tilde a_0+\tilde a_2\,r^2+\tilde a_4\,g^2\,r^4+\tilde a_6\,g^4\,r^6}{\sqrt{1+\tilde b_4\,g^2\,r^2+\tilde b_6\,g^4\,r^4}}\right).\end{aligned}\tag{7.4.27}$$

This is the central formula of this Section devoted to the sextic anharmonicity. Once the optimal parameters coming from the VM are chosen, we will show that it provides a highly accurate and uniform approximation for the exact ground state eigenfunction. We impose the constraint

$$\tilde b_6 \;=\; 16\,\tilde a_6^2 \tag{7.4.28}$$

[17]The generating functions $G_4(r)$ and $G_6(r)$ are presented explicitly in Appendix B.

which allows us to reproduce the dominant term in the expansion (7.4.20) exactly[18]. Hence, it reproduces the exact dominant asymptotic behavior of the phase at large distances. To construct 5-parametric Approximants for excited states, we follow the prescription presented in Section 6.2. Hence, at $D = 1$ we have

$$\Psi^{(t)}_{n_r,p}(x) = \frac{x^p P^{(p)}_{n_x}(x^2)}{\left(1+\tilde{b}_4\, g^2\, x^2+\tilde{b}_6\, g^4 x^4\right)^{1/4}\left(1+\sqrt{1+\tilde{b}_4\, g^2\, x^2+\tilde{b}_6 g^4\, x^4}\right)^{D/4}}\times$$
$$\frac{1}{\left(\tilde{c}_2 g^2 x^2+\sqrt{1+\tilde{b}_4\, g^2\, x^2+\ \tilde{b}_6\, g^4\, x^4}\right)^{1/4g^2}}\exp\left(-\frac{\tilde{a}_0+\tilde{a}_2\, x^2+\tilde{a}_4\, g^2\, x^4+\tilde{a}_6\, g^4\, x^6}{\sqrt{1+\tilde{b}_4\, g^2\, x^2+\tilde{b}_6\, g^4\, x^4}}\right). \tag{7.4.29}$$

while at $D > 1$

$$\Psi^{(t)}_{n_r,\ell}(r) = \frac{r^\ell\, P^{(\ell)}_{n_r}(r^2)}{\left(1+\tilde{b}_4\, g^2\, r^2+\tilde{b}_6\, g^4 r^4\right)^{1/4}\left(1+\sqrt{1+\tilde{b}_4\, g^2\, r^2+\tilde{b}_6 g^4\, r^4}\right)^{D/4}}\times$$
$$\frac{1}{\left(\tilde{c}_2 g^2 r^2+\sqrt{1+\tilde{b}_4\, g^2\, r^2+\ \tilde{b}_6\, g^4\, r^4}\right)^{1/4g^2}}\exp\left(-\frac{\tilde{a}_0+\tilde{a}_2\, r^2+\tilde{a}_4\, g^2\, r^4+\tilde{a}_6\, g^4\, r^6}{\sqrt{1+\tilde{b}_4\, g^2\, r^2+\tilde{b}_6\, g^4\, r^4}}\right). \tag{7.4.30}$$

Definitions of $P^{(p)}_{n_r}(x^2)$ and $P^{(\ell)}_{n_r}(r^2)$ are presented in (6.2.1) and (6.2.4), explicitly.

7.4.4 Numerical Results: Variational Calculations

The calculations of the variational energy for the first low-lying states with quantum numbers (0,0), (0,1), (0,2), (1,0) are presented in Tables 7.14 - 7.17 for different values of D and g^4. For some states, the variational energy $E_{var} = E^{(t)}_0 + E^{(t)}_1$, the first correction $E^{(t)}_2$, and the corrected value $E_{var} + E^{(t)}_2$ are shown. All states are studied in dimension $D = 1, 2, 3, 6$ and coupling constant $g^4 = 0.1, 1, 10$. For all cases, the variational energy E_{var} is obtained with absolute

[18] In numerical computations we set $\hbar = 1$ and $M = 1/2$.

deviation (from the exact result) in the order $10^{-9} - 10^{-12}$ $(9 - 12$ s.d.). This deviation is found by calculating the second correction $E_2^{(t)}$ (the first correction to the variational energy).

To check the energies obtained in Non-Linearization Procedure, we calculated them numerically in the Lagrange-Mesh method. These numerical calculations show that all digits presented for $E_{var} + E_2^{(t)}$ are exact: we obtain not less than 13 d.d. correctly in the Non-Linearization Procedure. In general, the energies grow with an increase of D and/or g^4. At $D > 1$, we classify the states by radial quantum number n_r and angular momentum ℓ as (n_r, ℓ); we mention the hierarchy of eigenstates which holds for any fixed integer $D > 1$ and g: (0,0), (0,1), (0,2), (1,0). This hierarchy is the same that we obtained for the cubic and quartic anharmonic oscillators.

In contrast with the quartic oscillator case, the available literature with estimates of the energy of the low-lying states for the sextic radial anharmonic oscillator is very limited. Most of the calculations are made for the one-dimensional case. In general, our results reproduce all known numerical ones that can be found for $D = 1$, while for $D = 2, 3$, we sometimes exceeded their accuracy, see e.g. [25], [26], [66], and [67]. At $D = 6$, the calculations are carried out for the first time.

The relative deviation of $\Psi_{0,0}^{(t)}$ from the exact (unknown) ground state eigenfunction $\Psi_{0,0}$ is estimated with the Non-Linearization Procedure. The deviation is bounded and very small,

$$\left| \frac{\Psi_{0,0}(r) - \Psi_{0,0}^{(t)}(r)}{\Psi_{0,0}^{(t)}(r)} \right| \lesssim 10^{-6} \ , \tag{7.4.31}$$

in the whole range of $r \in [0, \infty)$ at any integer D and at any coupling constant g^4 that we considered. Thus, our Approximant leads to a locally accurate approximation of the exact wave function once optimal parameters are chosen. In general, optimal variational parameters are smooth, slow changing as functions of g^4 without strong D dependence. The plots of the optimal parameters for the ground state (0,0) $a_{0,2,3}$ vs g for $D = 1, 2, 3, 6$ are shown in Fig. C.4 in Appendix C. In turn, Fig. C.5 presents the plots of the parameters as functions of D for fixed g^4. Similar plots occur for excited states for different D and g^4. Making an analysis of those plots, one can check that they obey (with high accuracy) another constraint,

$$\tilde{b}_4 \ \approx \ 32\, \tilde{a}_6\, \tilde{a}_4 \ . \tag{7.4.32}$$

This constraint guarantees the exact reproduction of the first two terms in the expansion (7.4.20). If we demand to fulfill exactly constraint (7.4.32), no deterioration in the accuracy of the energy and wave function occurs. Thus, the Approximants either (7.4.29) or (7.4.30) contains ultimately 5 free parameters, namely $\{\tilde{a}_0, \tilde{a}_2, \tilde{a}_4, \tilde{a}_6, \tilde{c}_2\}$.

Now we focus on the ground state. For all D and g^4, the correction $|y_1|$ to $y_0 = \partial_r \Phi_t$ is a very small and bounded function in $0 \lesssim r \lesssim 1.7$. In this domain, the dominant contribution of integrals - required by the variational method - occurs. For example, for $g^4 = 1$ and $D = 1, 2, 3, 6$

Table 7.14: Ground state energy for the sextic potential $V(r) = r^2 + g^4\, r^6$ for $D = 1, 2, 3, 6$ and $g^4 = 0.1, 1, 10$, labeled by quantum numbers (0,0) at any D. Variational energy $E_{var} = E_{var}$, the first correction $E_2^{(t)}$ (rounded to three s.d.) found with use of $\Psi_{0,0}^{(t)}$, see text, the corrected energy $E_{var} + E_2^{(t)} = E_{var} + E_2^{(t)}$ shown. $E_{var} + E_2^{(t)}$ coincides with Lagrange Mesh results (see text) in 12 displayed d. d., hence all printed digits are exact.

g^4	$D=1$			$D=2$		
	E_{var}	$-E_2^{(t)}$	$E_{var}+E_2^{(t)}$	E_{var}	$-E_2^{(t)}$	$E_{var}+E_2^{(t)}$
0.1	1.109 087 078 465	1.20×10^{-13}	1.109 087 078 465	2.307 218 600 932	7.04×10^{-13}	2.307 218 600 931
1.0	1.435 624 619 003	3.22×10^{-13}	1.435 624 619 003	3.121 935 474 246	9.81×10^{-13}	3.121 935 474 246
10.0	2.205 723 269 598	3.22×10^{-12}	2.205 723 269 595	4.936 774 524 584	1.72×10^{-12}	4.936 774 524 582
g^4	$D=3$			$D=6$		
	E_{var}	$-E_2^{(t)}$	$E_{var}+E_2^{(t)}$	E_{var}	$-E_2^{(t)}$	$E_{var}+E_2^{(t)}$
0.1	3.596 036 921 222	1.76×10^{-12}	3.596 036 921 220	7.987 905 269 800	7.11×10^{-13}	7.987 905 269 799
1.0	5.033 395 937 721	5.21×10^{-12}	5.033 395 937 720	11.937 202 695 862	9.62×10^{-13}	11.937 202 695 862
10.0	8.114 843 118 826	7.60×10^{-12}	8.114 843 118 819	19.880 256 604 739	3.12×10^{-12}	19.880 256 604 736

Table 7.15: The first excited state energy for the sextic potential $V(r) = r^2 + g^4\, r^6$ for different D and g^4. Variational energy E_{var}, the first correction $E_2^{(t)}$ found with use of $\Psi_{0,1}^{(t)}$ for $D = 1$ and $\Psi_{0,1}^{(t)}$ for $D > 1$, see (7.4.29) and (7.4.30). The corrected energy $E_{var} + E_2^{(t)} = E_{var} + E_2^{(t)}$ shown, the correction $E_2^{(t)}$ rounded to 3 s.d. All printed digits for $E_{var} + E_2^{(t)}$ are exact.

g^4	$D=1$			$D=2$		
	E_{var}	$-E_2^{(t)}$	$E_{var}+E_2^{(t)}$	E_{var}	$-E_2^{(t)}$	$E_{var}+E_2^{(t)}$
0.1	3.596 036 921 295	7.50×10^{-11}	3.596 036 921 220	4.974 197 493 807	9.01×10^{-11}	4.974 197 493 717
1.0	5.033 395 937 795	7.52×10^{-11}	5.033 395 937 720	7.149 928 601 496	5.84×10^{-11}	7.149 928 601 438
10.0	8.114 843 118 966	1.48×10^{-10}	8.114 843 118 818	11.688 236 0345 77	1.81×10^{-10}	11.688 236 034 396
g^4	$D=3$			$D=6$		
	E_{var}	$-E_2^{(t)}$	$E_{var}+E_2^{(t)}$	E_{var}	$-E_2^{(t)}$	$E_{var}+E_2^{(t)}$
0.1	6.439 143 322 388	6.64×10^{-11}	6.439 143 322 321	11.324 899 788 818	8.15×10^{-10}	11.324 899 788 004
1.0	9.455 535 276 950	1.09×10^{-10}	9.455 535 276 841	17.387 207 808 723	1.26×10^{-9}	17.387 207 807 460
10.0	15.619 579 279 334	5.05×10^{-10}	15.619 579 278 830	29.302 506 554 618	1.22×10^{-9}	29.302 506 553 402

Table 7.16: The second excited state energy for the sextic potential $V(r) = r^2 + g^4\, r^6$ for different D and g^4. Variational energy E_{var} found with use of $\Psi^{(t)}_{1,0}$ for $D = 1$ and $\Psi^{(t)}_{0,2}$ for $D > 1$, see (7.4.29) and (7.4.30). The first correction $E^{(t)}_2$ and the corrected energy $E_{var}+E^{(t)}_2 = E_{var} + E^{(t)}_2$ shown. Correction $E^{(t)}_2$ rounded to 3 s.d. All 12 printed d. d. in $E_{var} + E^{(t)}_2$ are exact.

g^4	$D=1$	$D=2$		
	E_{var}	E_{var}	$-E^{(t)}_2$	$E_{var} + E^{(t)}_2$
0.1	6.644 391 710 782	7.987 905 270 111	3.12×10^{-10}	7.987 905 269 799
1.0	9.966 622 004 356	11.937 202 696 127	2.66×10^{-10}	11.937 202 695 862
10.0	16.641 218 168 076	19.880 256 605 756	1.02×10^{-9}	19.880 256 604 742

g^4	$D=3$			$D=6$		
	E_{var}	$-E^{(t)}_2$	$E_{var} + E^{(t)}_2$	E_{var}	$-E^{(t)}_2$	$E_{var} + E^{(t)}_2$
0.1	9.617 462 285 440	1.50×10^{-10}	9.617 462 285 290	14.962 630 328 506	1.60×10^{-10}	14.962 630 328 346
1.0	14.584 132 948 883	3.15×10^{-9}	14.584 132 945 729	23.431 551 835 405	2.19×10^{-9}	23.431 551 833 215
10.0	24.447 468 037 325	5.42×10^{-9}	24.447 468 031 906	39.815 551 142 800	7.05×10^{-9}	39.815 551 135 750

Table 7.17: The third excited state energy for the sextic potential $V = r^2 + g^4\, r^6$ for different D and g^4. The radial node r_0 calculated in Lagrange-Mesh method with 9 correct d.d. Variational energy E_{var} and its radial node $r^{(0)}_0$ given by underlined digits, both found with $\Psi^{(t)}_{1,0}$, see (7.4.30).

g^4	$D=2$		$D=3$		$D=6$	
	E_{var}	r_0	E_{var}	r_0	E_{var}	r_0
0.1	8.402 580 462	0.837 310 052	10.237 873 721	0.995 787 872	16.154 260 610	1.308 543 484
1.0	12.914 938 793	0.671 821 606	15.989 440 787	0.790 364 964	25.938 441 037	1.019 166 200
10.0	21.792 578 251	0.515 914 526	27.155 085 604	0.604 322 682	44.521 781 513	0.773 860 964

the first correction y_1 has the upper bound

$$|y_1|_{max} \sim \begin{cases} 0.0078\ , & D = 1 \\ 0.0065\ , & D = 2 \\ 0.0048\ , & D = 3 \\ 0.0031\ , & D = 6 \end{cases} \tag{7.4.33}$$

It is the consequence of the fact that, by construction, the derivative $y_0 = \partial_r \Phi_t$ reproduces the growing terms in the expansion (7.4.20). It implies that we deal with a smartly designed zeroth order-approximation $\Psi^{(t)}_{0,0}$ which leads (in the framework of the Non-Linearization Procedure) to a fast convergent series for the energy and wave function. In Fig. 7.4, y_0 and y_1 *vs* r are presented for $g^4 = 1$ in $D = 1$. We emphasize that all curves in these figures are slow-changing *vs* D. Similar plots appear for $D = 2, 3, 6$ (not shown) as well as for other values of $g^4 > 0$. An analysis of these plots indicates that $(-y_1)^2$ is an extremely small function in comparison with y_0 in the domain $0 \le r \lesssim 1.7$, thus, in the domain which provides the dominant contribution

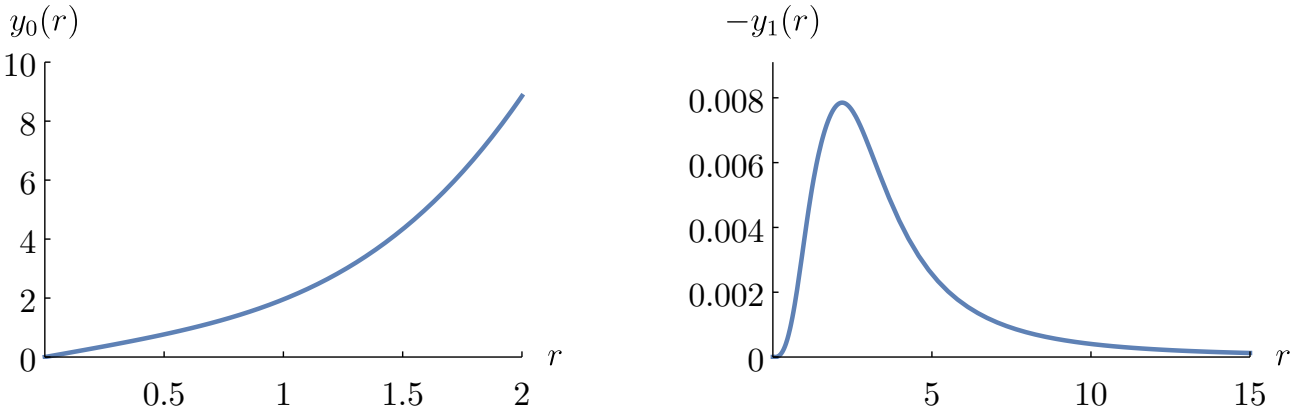

Figure 7.4: Sextic oscillator at $D = 1$: function $y_0 = (\Phi_t)'$ (on left) and its first correction y_1 (on right) *vs* r for $g^4 = 1$.

in variational integrals. It is the real reason why the energy correction $E_2^{(t)}$ is extremely small being of order $\sim 10^{-8}$, or sometimes even smaller, $\sim 10^{-10}$. A similar situation occurs for the phase (and its derivative) of the Approximants for the excited states.

At $D > 1$, it was checked that the Approximant provides an estimate of the radial node position of the wave function $\Psi_{1,0}^{(t)}$ by imposing the orthogonality constraint to the Approximant of the ground state. For sextic anharmonic potential, the zeroth order approximation $r_0^{(0)}$ gives not less than 7 d.d. of accuracy. The first order correction $r_0^{(1)}$ gives a contribution to the 6 d.d. Variational results are presented in Table 7.17. They are compared with ones obtained in Lagrange-Mesh method with 200 mesh points. It can be noted that the radial node r_0 grows with an increase of D at fixed g^4, but decreases with the increase of g^4 at fixed D.

7.4.5 First Terms in the Strong Coupling Expansion

In this Section, we calculate the first two terms in the strong coupling expansion (5.1.7). For the sextic anharmonic oscillator potential (7.4.1) this (convergent) expansion has the form

$$\varepsilon \;=\; g(\tilde{\varepsilon}_0 \;+\; \tilde{\varepsilon}_6\, g^{-3} \;+\; \tilde{\varepsilon}_{12}\, g^{-6} \;+\; \ldots)\;. \tag{7.4.34}$$

We have assumed that $2M = \hbar = 1$. Evidently, this expansion corresponds to PT in powers of $\hat{\lambda}$ for the potential

$$V(w) \;=\; w^6 \;+\; \hat{\lambda}\, w^2\;, \quad \hat{\lambda} \;=\; g^{-3} \tag{7.4.35}$$

in the Schrödinger equation defined in $w \in [0, \infty)$.

We use the Approximant (7.4.27) and develop the perturbation procedure already described in Chapter 5 to calculate $\tilde{\varepsilon}_0$ and $\tilde{\varepsilon}_6$. In Table 7.18, we present for different D the variational estimate for $\tilde{\varepsilon}_0$ (denoted by $\tilde{\varepsilon}_0^{(1)}$), the first correction to it $\hat{\varepsilon}_2$, and the corrected value $\tilde{\varepsilon}_0^{(2)} = \tilde{\varepsilon}_0^{(1)} + \hat{\varepsilon}_2$ calculated via the Non-Linearization Procedure. Using the Lagrange-Mesh method it was verified that $\tilde{\varepsilon}_0^{(2)}$ provides not less than 12 exact d.d. at every D considered. Hence,

the first 10 d.d. in variational energy $\tilde{\varepsilon}_0^{(1)}$ displayed in Table 7.18 are exact. In this case, the $\hat{\varepsilon}_3 \sim 10^{-2}\hat{\varepsilon}_2$, it indicates a high rate of convergence in PT. Finally, in Table 7.19, we present the first two approximations of the coefficient $\tilde{\varepsilon}_6$ - the expectation value of w^2 - , see (7.4.34). Comparing our results for $\tilde{\varepsilon}_0$ and $\tilde{\varepsilon}_6$ with those available in the literature, see e.g. [25] and [66], one can see that we usually reproduce, although often exceed them.

Table 7.18: Ground state $(0,0)$ energy $\tilde{\varepsilon}_0$ for the potential $W = r^6$ at $D = 1, 2, 3, 6$ found in PT based on the Approximant $\Psi^{(t)}_{(0,0)}$: $\tilde{\varepsilon}_0^{(1)}$ corresponds to the variational energy, $\hat{\varepsilon}_2$ is the second PT correction, $\tilde{\varepsilon}_0^{(2)} = \tilde{\varepsilon}_0^{(1)} + \hat{\varepsilon}_2$ is the corrected variational energy. 10 d.d. in $\tilde{\varepsilon}_0^{(2)}$ confirmed independently in Lagrange-Mesh method, see text.

$D=1$			$D=2$		
$\tilde{\varepsilon}_0^{(1)}$	$-\hat{\varepsilon}_2$	$\tilde{\varepsilon}_0^{(2)}$	$\tilde{\varepsilon}_0^{(1)}$	$-\hat{\varepsilon}_2$	$\tilde{\varepsilon}_0^{(2)}$
1.144 802 453 800	3.21×10^{-12}	1.144 802 453 797	2.609 388 463 259	5.72×10^{-12}	2.609 388 463 253
$D=3$			$D=6$		
$\tilde{\varepsilon}_0^{(1)}$	$-\hat{\varepsilon}_2$	$\tilde{\varepsilon}_0^{(2)}$	$\tilde{\varepsilon}_0^{(1)}$	$-\hat{\varepsilon}_2$	$\tilde{\varepsilon}_0^{(2)}$
4.338 598 711 518	4.73×10^{-12}	4.338 598 711 513	10.821 985 609 895	7.21×10^{-12}	10.821 985 609 888

Table 7.19: Subdominant coefficient $\tilde{\varepsilon}_6$ in the strong coupling expansion (7.4.34) of the ground state $(0,0)$ energy for the sextic radial anharmonic potential (7.4.1) for $D = 1, 2, 3, 6$. The first correction to it $\tilde{\varepsilon}_{6,1}$ as well as the corrected value $\tilde{\varepsilon}_6^{(2)} = \tilde{\varepsilon}_6^{(1)} + \tilde{\varepsilon}_{6,1}$ displayed

$D=1$			$D=2$		
$\tilde{\varepsilon}_6^{(1)}$	$-\tilde{\varepsilon}_{6,1}$	$\tilde{\varepsilon}_6^{(2)}$	$\tilde{\varepsilon}_6^{(1)}$	$-\tilde{\varepsilon}_{6,1}$	$\tilde{\varepsilon}_6^{(2)}$
0.307 920 304 114	3.83×10^{-10}	0.307 920 303 731	0.534 591 069 789	2.85×10^{-10}	0.534 591 069 504
$D=3$			$D=6$		
$\tilde{\varepsilon}_6^{(1)}$	$-\tilde{\varepsilon}_{6,1}$	$\tilde{\varepsilon}_6^{(2)}$	$\tilde{\varepsilon}_6^{(1)}$	-$\tilde{\varepsilon}_{6,1}$	$\tilde{\varepsilon}_6^{(2)}$
0.718 220 134 970	1.55×10^{-9}	0.718 220 133 425	1.137 762 108 070	2.68×10^{-10}	1.137 762 107 802

Chapter 8

Conclusions

It has been developed a formalism to study the bound states of the quantum radial polynomial anharmonic potential

$$V(r) \;=\; \frac{1}{g^2}\sum_{k=2}^{m} a_k\, g^k\, r^k \;, \qquad m \geq 2 \;.$$

For this potential, our primary goal was to construct a *locally accurate* approximate solution of the D-dimensional radial Schrödinger equation. In this context, the key question was: how to design an appropriate approximation leading to locally accurate solutions and also to accurate estimates for the energies? Our answer is based on the available analytical information about the (unknown) exact ground state wave function.

General Overview

There are two parameterizations of the configuration space to study the radial anharmonic oscillator:

(i) *Quantum* coordinate v-space, $v \propto r/\sqrt{\hbar}$. In this case, the anharmonic potential is a finite-degree perturbation in variable v of the harmonic oscillator through the effective coupling constant $\lambda \propto \sqrt{\hbar}\, g$. The *dynamics* of the wave function, taken in the exponential representation $\Psi = e^{-\Phi}$, is defined by the derivative of the *phase* $y(r) = \partial_r \Phi$. Written in the quantum variable v, the unknown function $y(r)$ satisfies a non-linear $\hbar$-independent differential equation: the so-called Riccati-Bloch (RB) equation. Relevant analytical information can be extracted by studying this equation. One can construct the asymptotic series of $y(r)$ at small and large r. To solve the RB equation, Perturbation Theory (PT) for the energy and the wave function can be developed in the weak and strong coupling regimes. For both cases, the construction of PT is nothing but an application of the Non-Linearization Procedure developed a long time ago. For the general anharmonic potential,

the construction of PT is a non-algebraic procedure. However, for even anharmonic potentials, $V(r) = V(-r)$, the Non-Linearization Procedure in the weak coupling regime is purely algebraic at any dimension D.

(*ii*) *Classical* coordinate u-space, with $u = gr$. Here, the potential is a finite degree polynomial in u. The coupling constant appears in front of the potential as the factor $1/g^2$. In this space, the dynamics of $y(r) = \partial_r \Phi$ is governed by the Generalized Bloch (GB) equation: a new non-linear $\hbar$-independent differential equation different from the RB one. Just as it occurred with the RB equation, we can obtain analytical information from the GB one as well. In particular, the same asymptotic series for small and large r described in (*i*) can be constructed from the GB equation. When PT is developed for the GB equation in the weak coupling regime, we checked that it generates the *true* type of semi-classical expansion (in the non-classical domain, beyond the turning point) for the phase. The main difference between the *standard* WKB expansion and the present new one is based on the fact that in the true expansion the energy does have an explicit dependence on the Planck constant $\hbar$. On the other hand, when PT is developed for the strong coupling regime, we found an interesting connection between the expansion for large g and that for small r: both expansions describe the same domain in r.

Both spaces are related through a simple expression: $u = \lambda\, v$. Furthermore, it turned out that there is a remarkable connection between them in the weak coupling regime. This non-trivial connection can be summarized as follows: perturbative corrections calculated for the GB equation are generating functions of those corrections calculated on the basis of the RB equation.

All the information collected from (*i*) and (*ii*), such as asymptotic series and PT in weak and strong regimes, was used to design a general prescription to construct a locally accurate approximation of the ground state wave function at any D: *the Approximant* $\Psi^{(t)}_{0,0}(r)$. When the exponential representation is assumed for the Approximant,

$$\Psi^{(t)}_{0,0}(r) = e^{-\frac{1}{\hbar}\Phi_t(r)} \ ,$$

we may focus on finding approximately Φ_t. One key result of this Thesis is a compact expression for the phase

$$\frac{1}{\hbar}\Phi_t(r) \ = \ \frac{\tilde{a}_0 \ + \ \tilde{a}_1\, g\, r + \frac{1}{g^2} V(r\,;\tilde{a}_2,\ldots,\tilde{a}_m)}{\sqrt{\frac{1}{g^2\, r^2} V(r\,;\,\tilde{b}_2,\ldots,\tilde{b}_m)}} \ + \ \text{Logarithmic Terms}\,(r\,;\,\{\tilde{c}\})\,.$$

It contains a finite number of parameters, $\{\tilde{a}, \tilde{b}, \tilde{c}\}$. At the weak and strong coupling regimes, it interpolates the asymptotic series of the phase at small and large distances. Furthermore,

we showed that this formula contains the analytical information obtained from (i) and (ii) if appropriate constraints are imposed on free parameters. Interestingly, those constraints came from the asymptotic series at large r. Let us emphasize that the potential $V(r)$ appeared as a building block of the approximate phase. The recipe to insert logarithmic terms in $\Phi_t(r)$ was also established: they should mimic the logarithmic terms of the first two generating functions for the phase: $G_0(r)$ and $G_2(r)$. Imposing orthogonality constraints, the prescription may be used to design Approximants of excited states.

Some of these parameters were fixed requiring Φ_t to reproduce the coefficients of all growing terms in the expansion of the exact phase at large distances. The remaining parameters are considered as variational. In this way, the Approximant is taken as a trial function in the VM. The Approximant is not only suitable to estimate (with high accuracy) the energy of the first low-lying states for finite values of g, but also, due to its features, it can be used to construct the strong coupling expansion. Through the connection of PT with the variational energy, the (relative) deviation between the Approximant and the exact (unknown) wave function may be estimated. A similar situation occurs with the variational energy: we can determine its deviation from the exact result. Results for three particular anharmonic oscillators are summarized below.

Two-Term Potentials

We applied the formalism summarized above for the anharmonic potential

$$V(r) \;=\; r^2 \;+\; g^{m-2} r^m \;,$$

where $m = 3, 4, 6$ (cubic, quartic, and sextic). In this Section, we present the conclusions associated with each anharmonicity.

Cubic

The key expression for the approximate phase of the Approximant is

$$\frac{1}{\hbar}\Phi_t(r) \;=\; \frac{\tilde{a}_0 + \tilde{a}_1\, g r + \tilde{a}_2\, r^2 + \tilde{a}_3\, g\, r^3}{\sqrt{1+\tilde{b}_1\, g\, r}} \;+\; \frac{1}{4}\,\log[1+\tilde{b}_1\, g\, r] \;+\; D\log\left[1+\sqrt{1+\tilde{b}_1\, g\, r}\right] \;,$$

where $\{\tilde{a}_0, \tilde{a}_1, \tilde{a}_2, \tilde{a}_3, \tilde{b}_1\}$ are parameters. If the constraints

$$\tilde{b}_1 = \frac{25}{4}\tilde{a}_3^2 \;, \qquad \tilde{a}_2 \;=\; \frac{125\,\tilde{a}_3^2 + 12}{150\tilde{a}_3} \;, \qquad -g^2\tilde{a}_1 \;=\; \frac{9375\, a_3^4 \;-\; 1000\, a_3^2 \;+\; 48}{15000\, a_3^3} \;,$$

are imposed, Φ_t reproduces all growing terms of the exact phase at large distances. Furthermore, the constraint

$$\tilde{a}_0 \;=\; \frac{2\tilde{a}_1}{\tilde{b}_3} \;+\; \frac{D+1}{2}$$

is imposed to have vanishing $\partial_r \Phi_t$ at $r = 0$. As a result, Φ_t depends only on 1 free parameter. Taking $\Psi^{(t)}_{0,0}$ as trial function, the single parameter can be chosen as optimal in the VM. Thus, the variational energy of the ground state is obtained with absolute accuracy $\sim 10^{-5}$ (4- 5 s.d.) for $D = 1, 2, 3, 6$ and $g = 0.1, 1.0, 10.0$. This is confirmed by the calculation of the first correction $E^{(t)}_2$ to the variational energy E_{var}, which is always of the order $\sim 10^{-6}$, while the rate of convergence of the energy in Non-Linearization Procedure is $\left|\frac{E^{(t)}_3}{E^{(t)}_2}\right| \sim 10^{-4}$. The relative deviation of $\Psi^{(t)}_{0,0}(r)$ from the exact wave function is bounded and small, it does not exceed $\sim 10^{-2}$ for any value of r. Hence, the Approximant leads to a locally accurate approximation to the exact ground state wave function. Results of this accuracy were obtained for the low-lying states: $(0,0), (0,1), (0,2), (1,0)$. Undoubtedly, a similar accuracy would be reached for other dimensions D and coupling constants g. For those states, the optimal parameters are smooth, slow-changing functions of g and D. These results represent the first accurate calculations of the energy of the low-lying states for the D-dimensional cubic anharmonic oscillator. Hence, these results may serve as a benchmark for other calculations. To the best of the knowledge of the author, there are not many examples in the literature in which a one-parametric Approximant (trial function) leads to such accuracies for the energy and wave functions.

Quartic

For this anharmonicity, the prescription generates an approximate phase of the form

$$\frac{1}{\hbar}\Phi_t(r) \;=\; \frac{\tilde{a}_0 + \tilde{a}_2\, r^2 + \tilde{a}_4\, g^2\, r^4}{\sqrt{1 + \tilde{b}_4\, g^2\, r^2}} \;+\; \frac{1}{4}\log\left[1 + \tilde{b}_4\, g^2\, r^2\right] \;+\; \frac{D}{2}\log\left[1 + \sqrt{1 + \tilde{b}_4\, g^2\, r^2}\right] \;,$$

where $\{\tilde{a}_0, \tilde{a}_2, \tilde{a}_4, \tilde{b}_4\}$ are parameters, which are constrained

$$\tilde{b}_4 \;=\; 9\,\tilde{a}_4^2 \;, \qquad \tilde{a}_2 \;=\; \frac{1 + 27\,\tilde{a}_4^2}{18\tilde{a}_4} \;.$$

These constraints guarantee that Φ_t reproduces exactly all two growing terms of the exact phase at large distances. The remaining 2 free parameters are chosen to be optimal in the VM with $\Psi^{(t)}_{0,0}(r)$ as trial function. The variational energy of the ground state is obtained with absolute accuracy $\sim 10^{-8}$ (8 - 9 s.d.) for $D = 1, 2, 3, 6$ and $g = 0.1, 1.0, 10.0$. This is confirmed by the first correction $E^{(t)}_2$, which is always of the order $\sim 10^{-8}$. The rate of convergence of the

energy in the Non-Linearization Procedure is $\left|\frac{E_3^{(t)}}{E_2^{(t)}}\right| \sim 10^{-4}$. The relative deviation of $\Psi_{0,0}^{(t)}(r)$ from the exact wave function is bounded and very small, it does not exceed $\sim 10^{-6}$. Hence, the Approximant led to a locally accurate approximation to the exact wave function. Results of similar accuracy were obtained for the low-lying states: $(0,0),(0,1),(0,2),(1,0)$. Clearly, the same accuracy would be reached for other dimensions and coupling constants. For those states, the optimal parameters are smooth and slow-changing functions of g and D. The variational estimates energy have confirmed, and some times exceeded, the results found in the literature.

Sextic

According to the prescription, the approximate phase of the sextic case is given by

$$\frac{1}{\hbar}\Phi_t(r) = \frac{\tilde{a}_0 + \tilde{a}_2\, r^2 + \tilde{a}_4\, g^2\, r^4 + \tilde{a}_6\, g^4\, r^6}{\sqrt{1 + \tilde{b}_4\, g^2\, r^2 + \tilde{b}_6\, g^4\, r^4}} + \frac{1}{4g^2}\,\log\left[\tilde{c}_2\, g^2\, r^2 + \sqrt{1 + \tilde{b}_4\, g^2\, r^2 + \tilde{b}_6\, g^4\, r^4}\right] + \frac{1}{4}\log\left[1 + \tilde{b}_4\, g^2\, r^2 + \tilde{b}_6\, g^4 r^4\right] + \frac{D}{4}\log\left[1 + \sqrt{1 + \tilde{b}_4\, g^2\, r^2 + \tilde{b}_6 g^4 r^4}\right] \ ,$$

where $\{\tilde{a}_0, \tilde{a}_2, \tilde{a}_4, \tilde{a}_6, \tilde{b}_2, \tilde{b}_4\}$ are parameters. which are constrained

$$\tilde{b}_6 \ = \ 16\,\tilde{a}_6^2 \ , \qquad \tilde{b}_4 \ = \ 32\,\tilde{a}_6\,\tilde{a}_4 \ .$$

These constraints reduced the number of parameters to 4; they guarantee that Φ_t reproduces exactly all growing terms of the exact phase at large distances. The remaining 4 free parameters are chosen to be optimal in the VM with $\Psi_{0,0}^{(t)}(r)$ as trial function. The variational energy coincides with the exact one with not less than 8 s.d. for the states $(0,0),(0,1),(0,2),(1,0)$ for $D = 1,2,3,6$ and $g^4 = 0.1, 1.0, 10.0$. However, there are no doubts that it will be the same for any integer D and $g^4 > 0$. For those states, the optimal parameters are smooth slow-changing as functions of g and D. The rate of convergence of energy in the Non-Linearization Procedure remains $\left|\frac{E_3^{(t)}}{E_2^{(t)}}\right| \sim 10^{-4}$. The relative deviation of $\Psi_{0,0}^{(t)}(r)$ from the exact eigenfunction is a bounded function and very small, it does not exceed $\sim 10^{-6}$. Hence, the Approximant led to a locally accurate approximation of the exact wave function. Results of similar accuracy were obtained for the first low-lying states. The variational estimates of the energy have confirmed, and some times exceeded, the results found in the literature.

Final Remarks

The reproduction of the growing terms at large distances of the phase reduces the number of parameters that the Approximant contains. Hence, the *dimensionality* of the space of parameters is reduced. If the remaining free parameters are chosen to be optimal in the VM, highly accurate estimates of the energy will occur. In addition, the Approximant will become a locally accurate approximation of the exact wave function.

We noticed that the hierarchy of the energies of the first four low-lying states of the cubic, quartic, and sextic anharmonic oscillators is the same: $(0,0), (0,1), (0,2), (1,0)$ in arbitrary $D > 1$ and non-vanishing coupling constant g. See Fig 8.1.

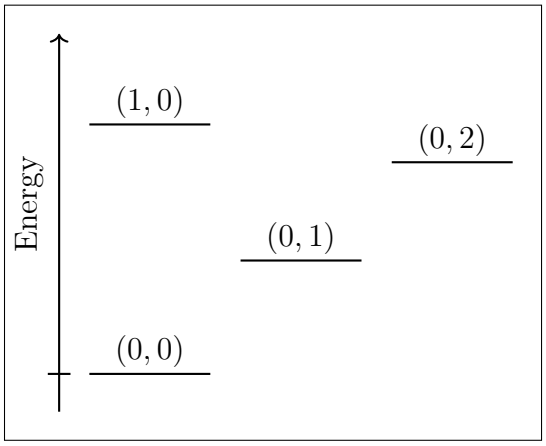

Figure 8.1: Schematic energy diagram for the first four bound states (n_r, ℓ) for the potential $V(r) = r^2 + g^{m-2} r^m$, $m = 3, 4, 6$, at $g > 0$ in arbitrary dimension D.

The first two terms in the strong coupling expansion were estimated with not less than 9 d.d. for the cubic, quartic, and sextic anharmonic oscillator. For the cubic potential, the first two terms were calculated for the first time. For quartic and sextic, our estimates reproduced the benchmarks known in the literature at $D = 1, 2, 3$. In $D = 6$, we established the benchmark.

It is clear that the formalism presented in this Part can be used to study some other systems in quantum mechanics. For example, a similar formalism was used in the past to study the low-lying states of the Yukawa potential leading to highly accurate results, see [47].

Part II

Hydrogen Atom in Constant Magnetic Field

Chapter 9

Introduction

The hydrogen atom is the simplest atomic system in Nature. It contains a positively charged proton and a negatively charged electron bound to the nucleus via the Coulomb force. Due to the separation of variables in spherical coordinates (and in some other systems of coordinates), the Schrödinger equation associated with this system was solved exactly in the seminal paper of modern quantum mechanics [13]. It is not an exaggeration to say that it laid the groundwork for subsequent studies of more complex atoms and molecules. In a non-relativistic consideration, when the hydrogen atom is placed in a constant uniform magnetic field, separation of variables no longer occurs for the Schrödinger equation, and it becomes non-solvable. The impossibility of obtaining exact solutions makes necessary the use of approximate methods to find the spectrum of the system. This feature makes the hydrogen atom in a constant uniform magnetic field an appropriate system to study using the formalism presented in Part I.

9.1 Motivation

The study of the atomic properties in the presence of a magnetic field dates back to a series of experiments carried out by Zeeman around 1896. In those experiments, he noticed the splitting of the spectral lines of sodium when their source is placed under the influence of a magnetic field.[1]

Early atomic models were incapable of describing adequately such phenomena. It was not until the theory of quantum mechanics was established (1926) that a satisfactory theoretical description occurred. Due to the *success* of this new theory, it was intermediately clear that a study in this quantum mechanical framework could explain in full detail the splitting observed by Zeeman. It was Schrödinger who presented the first results of quantum nature for the

[1] It is necessary to mention that around that time, the notions of proton and electron were absent. The electron would be experimentally detected one year later, while the proton 15 years later.

splitting of the spectral lines of atoms with one electron of valence[2] [68]. The splitting of a given spectral line into components in the presence of a small magnetic field became known as (linear) Zeeman effect. In stronger fields, the resulting splitting was called Paschen-Back effect [69]. At ultra-strong fields, the splitting was known as Quadratic Zeeman effect. Each regime was treated mainly in divergent perturbation theory (PT) and some other approximate methods such as the adiabatic approximation and the Variational Method. Early attempts to explore atomic systems in a magnetic field are summarized in the review paper by Garstang [70]. Some of those early attempts were motivated by astrophysics discoveries. This motivation dates from the discovery by Hale in 1908 of magnetic fields in sunspots from the Zeeman splitting of their spectral lines. Some other works were motivated by plasma and semiconductor physics, where the effects of a large magnetic field can be present. In recent decades, the interest has been renewed due to the discovery of white dwarfs and neutron stars. Their atmospheres, rich in hydrogen, experience the strongest magnetic fields γ that can be found in Nature until today. For example, a neutron star may have magnetic fields in the range $10^{12} - 10^{13}$ G, while magnetars in the range $10^{13} - 10^{15}$ G.

Due to its simplicity, in comparison with other atoms, the hydrogen one has played a fundamental role in the understanding of the behavior of more complex atoms in magnetic fields. In fact, the hydrogen atom is the most studied *Coulombic* system in weak, intermediate, and strong magnetic fields. In the non-relativist consideration, there is a large number of works devoted to finding its spectrum approximately as a function of the magnetic field. Most of them are devoted to study the energy levels, but no other relevant quantities like the quadrupole moment or even the wave function.

9.2 Present Work

The purpose of Part II is to extend and apply the formalism presented in Part I to one of the most relevant atomic systems in the presence of a constant uniform magnetic field: a hydrogen atom. Our ultimate goal is to design an adequate approximation of the ground state wave function following the *spirit* of Part I. However, it should be noted that the Schrödinger equation associated with the hydrogen atom in a magnetic field is *effectively* a two-dimensional partial differential equation. It contrasts with the Schrödinger equation that corresponds to the D-dimensional radial anharmonic oscillator, which was *effectively* one-dimensional due to the separation of angular variables from the radial one. Despite this significant *difference*, as well as of the obvious ones (potentials with different physical and analytical natures), we will show that the formalism can be applied with success. In particular, the Riccati-Bloch and Generalized Bloch equations can be derived to calculate PT in the weak coupling regime and study asymptotic series. All the analytical information is collected to construct *The Approximant*: a locally accurate and uniform approximation of the wave function of the ground state.

This Part may be read independently on the previous one, it is self-contained. However,

[2] Just like the sodium atoms considered experimentally by Zeeman.

sometimes we will make some analogies between the results presented here and those of Part I.

Chapter 10

Generalities

The Hamiltonian

$$\hat{H} \;=\; \frac{1}{2\,m_e}\left(\hat{\mathbf{p}} \,+\, \frac{e}{c}\mathbf{A}\right)^2 \;-\; \frac{e^2}{r} \quad , \qquad r=\sqrt{x^2+y^2+z^2}\;, \tag{10.0.1}$$

may describe a hydrogen atom in the presence of a constant magnetic field $\mathbf{B}=\gamma\,\hat{\mathbf{z}}$. In (10.0.1), the mass of the proton is assumed to be infinite, $m_p=\infty$. Here m_e and $-e$ are the mass and charge of the electron, respectively, e corresponds to the charge of the infinitely massive proton located at the origin of coordinates, and c is the speed of light. Besides, $\hat{\mathbf{p}} \,=\, -i\hbar\nabla$ is the momentum operator of the electron, r is its distance to the origin. See Fig. 10.1 for the geometrical setting.

It is straightforward to show that (10.0.1) is equivalent to

$$\hat{H} \;=\; \frac{1}{2m_e}\hat{\mathbf{p}}^2 \;+\; \frac{1}{m_e c}\hat{\mathbf{p}}\cdot\mathbf{A} \;+\; \frac{1}{m_e c}\mathbf{A}\cdot\hat{\mathbf{p}} + \;\frac{e^2}{2m_e c^2}\mathbf{A}^2 \;-\; \frac{e^2}{r} \tag{10.0.2}$$

From now on, the symmetric gauge

$$\mathbf{A} \;=\frac{1}{2}\mathbf{B}\times\mathbf{r}\;, \qquad \mathbf{B}=\gamma\,\hat{\mathbf{z}}\;, \tag{10.0.3}$$

is assumed[1], it implies that the Hamiltonian (10.0.2) takes the form

$$\hat{H} \;=\; -\frac{\hbar^2}{2m_e}\Delta \;+\; \frac{|e|\gamma}{2m_e c}\hat{L}_z + \;\; V\;, \qquad \Delta \;=\; \partial_x^2 \;+\; \partial_y^2 \;+\; \partial_z^2\;. \tag{10.0.4}$$

Here, we defined the potential

$$V \;=\; -\frac{e^2}{r} \;+\; \frac{e^2\gamma^2}{8m_e c^2}\,\rho^2\;, \qquad \rho=\sqrt{x^2+y^2}\;, \tag{10.0.5}$$

[1]This choice of the vector potential leads to a constant magnetic field directed along the z-axis. The magnitude of this magnetic field is γ, measured in Gauss/Teslas.

depends on r and ρ only, $\hat{L}_z$ is the projection of the momentum operator on the direction of magnetic field,

$$\hat{L}_z \;=\; -i\hbar\,(x\,\partial_y \;-\; y\,\partial_x)\;, \tag{10.0.6}$$

which is conserved. The Schrödinger equation associated to (10.0.4) is

$$\hat{H}\psi \;=\; E\psi\;, \tag{10.0.7}$$

with boundary conditions imposed in such a way that the wave function is normalizable

$$\int \psi^2\,dV \;<\infty\;. \tag{10.0.8}$$

The dependence of the potential on variables ρ and r hints that it is convenient to write the Schrödinger equation (10.0.7) in the non-orthogonal system of coordinates (ρ, r, φ), see Fig. 10.1. In these coordinates it reads[2]

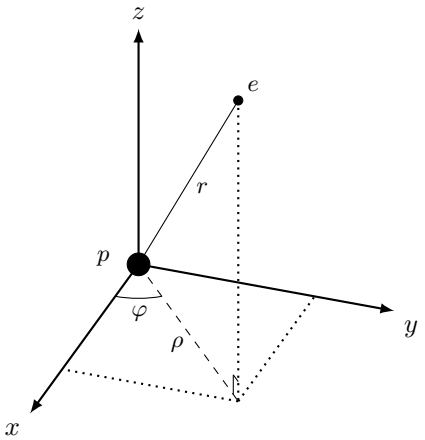

Figure 10.1: System of coordinates (ρ, r, φ) at half-space $z \geq 0$. The infinitely heavy proton (p) is located at the origin.

$$-\frac{\hbar^2}{2m_e}\left[\partial_\rho^2 \;+\; \frac{2\rho}{r}\partial_{\rho r} \;+\; \partial_r^2 \;+\; \frac{1}{\rho}\partial_\rho \;+\; \frac{2}{r}\partial_r \;+\; \frac{1}{\rho^2}\partial_\varphi^2\right]\psi \;-\; \frac{i|e|\hbar\gamma}{2m_e c}\partial_\varphi\psi$$
$$+\;\left[\,-\frac{e^2}{r} \;+\; \frac{\gamma^2 e^2}{8m_e c^2}\rho^2\right]\psi = \;E\,\psi\;. \tag{10.0.9}$$

In Appendix E we present some relevant expressions involving differential operators written in this system of coordinates. Needless to say, equation (10.0.9) is non-solvable for $\gamma \neq 0$: energy and wave function can be found only in approximate form.

[2]Note that in this coordinates $\hat{L}_z = -i\hbar\,\partial_\varphi$.

Due to cylindrical symmetry of the system, any wave function is characterized by two quantum numbers: the magnetic quantum number m (eigenvalue of $\hat{L}_z$) and the parity $\nu = \pm 1$ with respect to a reflection $z \to -z$. It suggests considering the representation

$$\psi(\rho, r, \varphi) \;=\; z^p \rho^{|m|} \Psi(\rho, r)\, e^{im\varphi} \;, \qquad m \;=\; 0, \pm 1, \pm 2, \ldots \;, \qquad p = \pm 1 \tag{10.0.10}$$

for the states with definite parity, hence $\nu = (-1)^p$. Here $z = \sqrt{r^2 - \rho^2}$, see Fig. 10.1. The function $\Psi(\rho, r)$ satisfies the equation

$$-\frac{\hbar^2}{2m_e}\left[\partial_\rho^2 \;+\; \frac{2\rho}{r}\partial_{\rho r} \;+\; \partial_r^2 \;+\; \frac{2|m|+1}{\rho}\partial_\rho \;+\; \frac{2(|m|+p+1)}{r}\partial_r\right]\Psi$$
$$+\;\left[-\frac{e^2}{r} \;+\; \frac{\gamma^2 e^2}{8m_e c^2}\rho^2\right]\Psi \;=\; \mathcal{E}_{m,p}\,\Psi \;, \tag{10.0.11}$$

where

$$\mathcal{E}_{m,p} \;=\; E_{m,p} \;-\; \frac{|e|\hbar\gamma\, m}{2m_e c} \tag{10.0.12}$$

is the energy with the linear Zeeman term subtracted. Note that the quantum number m now plays the role of a parameter. From equation (10.0.11) one can explicitly see that $\mathcal{E}_{m,p}$ should be an even function with respect to the magnetic quantum number m,

$$\mathcal{E}_{m,p} \;=\; \mathcal{E}_{-m,p} \;, \tag{10.0.13}$$

for any possible value of p. Therefore

$$E_{m,p} \;=\; E_{-m,p} \;+\; \frac{|e|\hbar\gamma\, m}{m_e c} \;. \tag{10.0.14}$$

Some general properties of the spectrum of the Schrödinger equation, such as the appearance quasi-crossings and crossings of energy levels, its structure as well as analytical information, can be found in the literature, see [70].

10.1 The Ground State: Riccati Equation:

The present study focuses on the ground state, which corresponds to quantum numbers $m = 0$ and $\nu = +$. Thus, its wave function depends only on variables (ρ, r). At $\gamma = 0$, it corresponds to the $1s_0$ state of the hydrogen atom. From now on, we present the (nodeless) ground wave function and its energy dropping the labels of quantum numbers, presenting them as Ψ and $\mathcal{E}$, respectively. It is usual to denote these states as $1s_0$ even for $\gamma \neq 0$. Following (10.0.11), the equation that determines Ψ and $\mathcal{E}$ reads

$$-\frac{\hbar^2}{2m_e}\left[\partial_\rho^2 \;+\; \frac{2\rho}{r}\partial_{\rho r} \;+\; \partial_r^2 \;+\; \frac{1}{\rho}\partial_\rho \;+\; \frac{2}{r}\partial_r\right]\Psi \;+\; \left[-\frac{e^2}{r} \;+\; \frac{\gamma^2 e^2}{8m_e c^2}\rho^2\right]\Psi = \;\mathcal{E}\,\Psi \;. \tag{10.1.1}$$

We now study the function $\Psi(\rho, r)$ when it is written in the exponential representation, namely

$$\Psi(\rho, r) \;=\; e^{-\Phi(\rho, r)} \;. \tag{10.1.2}$$

One can show that the *phase* $\Phi(\rho, r)$ satisfies a non-linear partial differential equation of second order,

$$\partial_\rho^2\Phi \ + \ \frac{2\rho}{r}\partial_{\rho r}\Phi \ + \ \partial_r^2\Phi \ + \ \frac{1}{\rho}\partial_\rho\Phi \ + \ \frac{2}{r}\partial_r\Phi \ - \ (\partial_\rho\Phi)^2 \ - \ \frac{2\rho}{r}(\partial_\rho\Phi)(\partial_r\Phi) \ - \ (\partial_r\Phi)^2$$
$$= \ \frac{2m_e}{\hbar^2}\left[\mathcal{E} \ + \ \frac{e^2}{r} \ - \ \frac{\gamma^2 e^2}{8m_e c^2}\rho^2\right] \ . \quad (10.1.3)$$

This equation is defined in the domain $0 \leq \rho \leq r$ and $0 \leq r < \infty$, see Fig. 10.2.

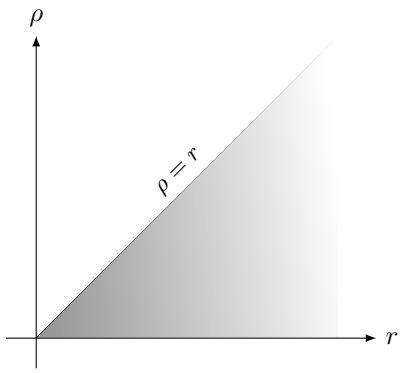

Figure 10.2: Infinite wedge domain (shaded in gray) of the equation (10.1.3) in (ρ, r) space.

Note that (10.1.3) can be regarded as a generalization for two dimensions of the well-known one-dimensional Riccati equation, cf. (3.3.4). It is worth mentioning that (10.1.3) is the key equation of the present Chapter. Naturally, this equation can be solved exactly at $\gamma = 0$; it will generate the $1s_0$ orbital. For $\gamma \neq 0$ it becomes non-solvable: its solution has to be found in approximate form. We have already met in the past this situation for the D-dimensional radial anharmonic oscillator. In the next Sections, we will show that the Riccati-Bloch and Generalized Bloch equations may be found from equation (10.1.3).

10.2 Riccati-Bloch Equation

Let us define the dimensionless variables

$$s \ = \ \frac{\rho}{r_0} \ , \qquad t \ = \ \frac{r}{r_0} \ , \quad (10.2.1)$$

where

$$r_0 = \frac{\hbar^2}{m_e e^2} \ \simeq \ 5.29 \times 10^{-9}\text{cm} \quad (10.2.2)$$

is the Bohr radius. In these new variables (10.2.1), the Riccati equation (10.1.3) appears without explicit dependence on c, e, $\hbar$, and m_e, namely

$$\partial_s^2\Phi + \frac{2s}{t}\partial_{st}\Phi + \partial_t^2\Phi + \frac{1}{s}\partial_s\Phi + \frac{2}{t}\partial_t\Phi - (\partial_s\Phi)^2 - \frac{2s}{t}(\partial_s\Phi)(\partial_t\Phi) - (\partial_t\Phi)^2 = \varepsilon + \frac{2}{t} - \frac{\lambda^2 s^2}{4}\,, \tag{10.2.3}$$

where

$$\varepsilon = \frac{\mathcal{E}}{\mathcal{E}_0}\,, \qquad \mathcal{E}_0 = \frac{m_e e^4}{2\hbar^2} \tag{10.2.4}$$

and

$$\lambda = \frac{\gamma}{\gamma_0}\,, \qquad \gamma_0 = \frac{c|e|^3 m_e^2}{\hbar^3}\,. \tag{10.2.5}$$

Note that $\mathcal{E}_0$ is the Rydberg constant while γ_0 is the atomic unit of magnetic field, respectively;

$$\mathcal{E}_0 \approx 2.18\times 10^{-18}\mathrm{J} = 13.6\,\mathrm{eV}\,, \tag{10.2.6}$$

$$\gamma_0 \approx 2.35\times 10^{5}\,\mathrm{T} = 2.35\times 10^{9}\,\mathrm{G}\,. \tag{10.2.7}$$

Expressions (10.2.6) and (10.2.7) suggest that λ is the *effective* magnetic field measured in atomic units γ_0, which occurs instead of γ, while ε plays the role of energy measured in Rydbergs (Ry).

Equation (10.2.3) is nothing but the dimensionless version of the Riccati equation, and we call it *Riccati-Bloch (RB) equation*. Both equations coincide when we set $\hbar = 1$, $m_e = 1$ and $e = -1$. The RB equation governs the dynamics via the phase Φ in the (s,t)-space. Note that (10.2.3) is analogous to equation (3.3.9).

10.3 Generalized Bloch Equation

Let us introduce in (10.1.3) different dimensionless variables

$$u = \frac{\rho}{\rho_0}\,, \qquad v = \frac{r}{r_0}\,, \tag{10.3.1}$$

where

$$\rho_0 = \frac{m_e c|e|}{\hbar\gamma}\,. \tag{10.3.2}$$

Note that ρ_0 has explicit dependence on γ, while v coincides with t, see (10.2.1) and (10.3.1). Introducing (10.3.1) into the Riccati equation (10.1.3), we obtain a two-dimensional *Generalized Bloch (GB) equation*

$$\lambda^2\,\partial_u^2\Phi + \frac{2u}{v}\partial_{uv}\Phi + \partial_v^2\Phi + \frac{\lambda^2}{u}\partial_u\Phi + \frac{2}{v}\partial_v\Phi - \lambda^2(\partial_u\Phi)^2 - \frac{2u}{v}(\partial_u\Phi)(\partial_v\Phi) - (\partial_v\Phi)^2 = \varepsilon + \frac{2}{v} - \frac{u^2}{4}\,. \tag{10.3.3}$$

cf. (3.3.20), see [44,45]. Note that the potential in the right hand side does not have any explicit dependence on the parameters of the problem. The definitions of ε and λ are given in (10.2.4) and (10.2.5), respectively. Just as it occurred for the RB equation, all variables/quantities involved in (10.3.3) are dimensionless. Let us note that the variables u and s are remarkable easy related

$$u \;=\; \lambda\, s \;, \tag{10.3.4}$$

see (10.2.1), (10.2.5) and (10.3.1). This relation looks very similar to the one which occurred for the anharmonic oscillator between the classical coordinate and the quantum one, see (3.3.24).

Chapter 11

Weak Coupling Regime

11.1 Riccati Bloch Equation

Just like we did for the D-dimensional radial anharmonic oscillator, we can use PT assuming a weak coupling regime to solve the RB equation (10.2.3),

$$\Phi(s,t) \;=\; \sum_{n=0}^{\infty} \lambda^{2n} \Phi_n(s,t) \;, \qquad\qquad \varepsilon \;=\; \sum_{n=0}^{\infty} \lambda^{2n} \varepsilon_n \;. \tag{11.1.1}$$

The zeroth order correction is

$$\Phi_0(s,t) \;=\; t \;, \qquad\qquad \varepsilon_0 \;=\; -1 \;, \tag{11.1.2}$$

it corresponds to the exact phase and energy of ground state ($1s_0$) of the hydrogen atom at $\gamma = 0$, respectively. It must be emphasized that if we set $c = 1$, $m_e = 1$ and $e = 1$, then the effective coupling constant results in $\lambda = \gamma\hbar^3$. It implies that the PT developed for the ε in powers of γ coincides with the semi-classical expansion in powers of $\hbar^3$.[1]

For $n > 0$, one can show that corrections Φ_n and ε_n are determined by a linear partial differential equation,

$$\partial_{ss}\Phi_n \;+\; \frac{2s}{t}\partial_{st}\Phi_n \;+\; \partial_{tt}\Phi_n \;+\; \left(\frac{1}{s} - \frac{2s}{t}\right)\partial_s\Phi_n \;+\; \left(\frac{2}{t} - 1\right)\partial_t\Phi_n \;=\; \varepsilon_n \;-\; Q_n \;, \tag{11.1.3}$$

where

$$Q_n \;=\; -\sum_{k=1}^{n-1} \Big[\partial_s\Phi_k\partial_s\Phi_{n-k} \;+\; \partial_t\Phi_k\partial_t\Phi_{n-k} \;+\; \frac{s}{t}\left(\partial_s\Phi_k\partial_t\Phi_{n-k} \;+\; \partial_t\Phi_k\partial_s\Phi_{n-k}\right)\Big] \tag{11.1.4}$$

[1] We already showed in the previous Part that a similar situation occurs for the radial anharmonic potential. In that case, the semi-classical expansion of the energy is in powers of $\hbar^{1/2}$.

is constructed from the previous $(n-1)$ corrections. The explicit analytical solution can be found for equation (11.1.3), for example, the first order correction is

$$\Phi_1(s,t) \;=\; \frac{1}{24}s^2t \;+\; \frac{1}{16}s^2 \;+\frac{1}{24}t^2 \;, \qquad \varepsilon_1 \;=\; \frac{1}{2} \;. \tag{11.1.5}$$

In general, the nth correction Φ_n is a polynomial in variables (s,t) with the following structure

$$\Phi_n(s,t) \;=\; \sum_{j=0}^{n-1}\sum_{k=j}^{n}\left(a_{j,k}^{(n)}\,t \;+\; b_{j,k}^{(n)}\right)s^{2(n-k)}t^{2(k-j)} \;, \qquad a_{0,n}^{(n)} \;=\; 0 \;. \tag{11.1.6}$$

For all order n, the coefficients $a_{j,k}^{(n)}$ and $b_{j,k}^{(n)}$ are rational real numbers. Interestingly, the equation

$$\varepsilon_n \;=\; 4\,b_{n-1,n-1}^{(n)} \;+\; 6\,b_{n-1,n}^{(n)} \tag{11.1.7}$$

holds for any $n>1$. Hence the correction ε_n is also a rational number. Several corrections can be easily constructed in this framework as a consequence of the polynomial nature of the corrections Φ_n. They are determined by solving algebraic linear equations via elementary algebra. Hence, the realization of PT is ultimately an algebraic procedure. As a consequence, many terms in expansions (11.1.1) can be calculated explicitly. In Appendix F, we present the first corrections of the Φ for $n=2,3,4$. In turn, we present some corrections up to 100th order for the energy ε; see Tables F.1 and F.2. It must be emphasized that it is the first time that the coefficient ε_{100} has been calculated exactly. The corrections were computed using *Mathematica* with absolute accuracy (in the form of rational numbers). The code designed for this purpose is very compact: only 15 lines of commands are needed. The code is presented in explicit form in Appendix F. The calculation of the first 50 corrections does not take more than one hour of computations in a common laptop. To arrive up to order 100, it was necessary to leave the laptop working for about two weeks.

Despite the simplicity of the calculation of PT corrections, it should be mentioned that, according to the Dyson instability argument [50], both series (11.1.1) should be divergent. This can be seen from the asymptotic behavior of ε_n for large n [71],

$$\varepsilon_n \;=\; 64\,\frac{(-1)^{n+1}}{\pi^{\frac{5}{2}+2n}}\,\Gamma\left(2n+\frac{3}{2}\right)\left((1 \;+\; O(n^{-1})\right) \;, \quad n\to\infty \;. \tag{11.1.8}$$

Following this formula, it is clear that the PT for ε is Borel-summable[2]. However, the Padé-Borel procedure does not provide accurate results, even taking into account the first hundred coefficients ε_n, see below. A similar situation occurs with conformal mapping [73].

From equations (11.1.8) and (11.1.7), we note that the coefficients $b_{n-1,n-1}^{(n)}$ and $b_{n-1,n}^{(n)}$ also grow factorially at large n. It is worth mentioning that the perturbative approach used to solve the Riccati-Bloch equation is nothing but an example of the application of the so-called Non-Linearization Procedure [8] (sometimes referred as logarithmic PT). In the previous Part, it was used to solve the one-dimensional version of the RB equation. Here we have shown that it can also be applied *successfully* to two-dimensional problems. A general description of this method can be found in [8].

[2]See [72] for a detailed description of this method.

11.1.1 Behavior of the Phase Φ at Small Distances

For one-dimensional spectral problems, the exponential representation is convenient to study the asymptotic behavior of the phase at some particular limits. For the D-dimensional radial anharmonic oscillator, we showed that both RB and GB equations are suitable to construct asymptotic series of the phase. This situation changes *dramatically* for the hydrogen atom in a constant magnetic field. In this case, the phase is determined by a non-linear partial (RB or GB) differential equation in two variables; it complexifies the construction of asymptotic series. Interestingly, from the structure of corrections Φ_n, we can overcome this difficulty. The structure of the Taylor series of the phase Φ at small s and t can be obtained from the polynomial form of the correction Φ_n, see (11.1.6). Collecting the same powers in s and t, coming from different corrections Φ_n, their formal sums will result in the asymptotic expansion at small (s,t), namely

$$\Phi(s,t) \;=\; t \;+\; \sigma_1(\lambda^2)\,s^2 \;+\; \sigma_2(\lambda^2)\,t^2 \;+\; \sigma_3(\lambda^2)\,s^2 t \;+\; \ldots\;, \quad (s,t)\to 0\;. \tag{11.1.9}$$

The functions σ_1, σ_2 and σ_3 are given (formally) by

$$\sigma_1(\lambda^2) \;=\; \sum_{n=1}^{\infty} b^{(n)}_{n-1,n-1}\lambda^{2n}\;, \qquad \sigma_2(\lambda^2) = \sum_{n=1}^{\infty} b^{(n)}_{n-1,n}\lambda^{2n}\;, \qquad \sigma_3 = \sum_{n=1}^{\infty} a^{(n)}_{n,n-1}\lambda^{2n}\;. \tag{11.1.10}$$

From equation (11.1.7), it is clear that

$$\varepsilon(\lambda^2) \;=\; -1 \;+\; 4\,\sigma_1(\lambda^2) \;+\; 6\,\sigma_2(\lambda^2)\;. \tag{11.1.11}$$

From Taylor series (11.1.9), once variables ρ and r are restored, one can immediately conclude that the presence of a magnetic field does not break the *cusp condition* for the exact wave function

$$C \equiv \;\frac{\langle\psi\,|\,\delta(\vec{r})\frac{\partial}{\partial r}\,|\,\psi\rangle}{\langle\psi\,|\,\delta(\vec{r})\,|\,\psi\rangle} \;=\; -\frac{1}{r_0}\;. \tag{11.1.12}$$

In atomic physics, the parameter C is known as the *cusp parameter* [6]. For non-solvable systems which consist of electrons and (infinitely massive) positive charges, it is usually used to *measure* the local quality of the approximate wave function near the Coulomb singularities.

11.2 Generalized Bloch Equation

To solve the GB equation, we can develop PT in powers of λ^2,

$$\Phi(u,v) \;=\; \sum_{n=0}^{\infty}\lambda^{2n}\phi_n(u,v)\;, \qquad\qquad \varepsilon \;=\; \sum_{n=0}^{\infty}\lambda^{2n}\varepsilon_n\;. \tag{11.2.1}$$

The expansion for ε coincides with the one presented in (11.2.1). The zeroth order correction $\phi_0(u,v)$ is determined by the non-linear partial differential equation

$$\frac{2u}{v}\partial_{uv}\phi_0 \;+\; \partial_v^2\phi_0 \;+\; \frac{2}{v}\partial_v\phi_0 \;-\frac{2u}{v}(\partial_u\phi_0)(\partial_v\phi_0) \;-\; (\partial_v\phi_0)^2 \;=\; \varepsilon_0 \;+\; \frac{2}{v} \;-\; \frac{u^2}{4}\;. \tag{11.2.2}$$

Its explicit solution in closed analytical form is given by

$$\phi_0(u,v) \;=\; A_0^{(0)}(u)\,v \;+\; B_0^{(0)}(u) \tag{11.2.3}$$

where

$$A_0^{(0)}(u) \;=\; \sqrt{1+\frac{u^2}{12}}\,, \qquad B_0^{(0)}(u) \;=\; \frac{1}{2}\log\left(1+\frac{u^2}{12}\right) \;+\; \log\left(1+\sqrt{1+\frac{u^2}{12}}\right)\,. \tag{11.2.4}$$

The correction $\phi_n(u,v)$ with $n \geq 1$ obeys a linear partial differential equation, namely

$$\frac{2u}{v}\partial_{u,v}\phi_n \;+\; \partial_v^2\phi_n \;+\; \frac{2}{v}\partial_v\phi_n \;-\; \frac{2u}{v}\left(\partial_u\phi_0\,\partial_v\phi_n \;+\; \partial_u\phi_n\,\partial_v\phi_0\right) \;-\; 2(\partial_v\phi_n\,\partial_v\phi_0) \;=\; \varepsilon_n \;-\; q_n \tag{11.2.5}$$

where

$$\begin{aligned} q_n \;&= \partial_u^2\phi_{n-1} \;+\; \left(\frac{1}{u}-\partial_u\phi_0\right)\partial_u\phi_{n-1} \\ &\quad -\sum_{k=1}^{n-1}\left\{\partial_u\phi_{n-k-1}\partial_u\phi_k \;+\; \frac{2u}{v}\partial_u\phi_{n-k-1}\partial_v\phi_k \;+\; \partial_v\phi_{n-k-1}\partial_v\phi_k\right\}\,. \end{aligned} \tag{11.2.6}$$

It can be shown that all correction $\phi_n(u,v)$ is a polynomial in v with u-dependent coefficients,

$$\phi_n(u,v) \;=\; \sum_{k=0}^{n}\left\{A_k^{(n)}(u)\,v \;+\; B_k^{(n)}(u)\right\}v^{2(n-k)}\,. \tag{11.2.7}$$

In general terms, the functions $A_k^{(n)}(u)$ and $B_k^{(n)}(u)$ are determined by solving (ordinary) linear differential equations of first degree. To write the first order correction (and next ones), it is convenient to introduce the variable

$$w(u) \;=\; \sqrt{1+\frac{u^2}{12}}\,. \tag{11.2.8}$$

Thus,

$$\phi_1(u,v) \;=\; A_0^{(1)}(u)\,v^3 \;+\; B_0^{(1)}(u)\,v^2 \;+\; A_1^{(1)}(u)\,v \;+\; B_1^{(1)}(u) \tag{11.2.9}$$

where

$$A_0^{(1)} \;=\; -\frac{(w-1)(w+1)}{120\,w^3}\,, \tag{11.2.10}$$

$$B_0^{(1)} \;=\; -\frac{6w^3-w^2-9w-6}{120\,(w+1)\,w^4}\,, \tag{11.2.11}$$

$$A_1^{(1)} \;=\; -\frac{(w-1)\,(30w^4+52w^3+54w^2+42w+15)}{120\,(w+1)\,w^5}\,, \tag{11.2.12}$$

$$B_1^{(1)} \;=\; -\frac{(w-1)\,(9w^6+18w^5+38w^4+46w^3+42w^2+30w+10)}{80\,(w+1)\,w^6}\,. \tag{11.2.13}$$

The next corrections $\phi_2, \phi_3, ...$, can also be calculated explicitly. However, we omit to present them since they involve cumbersome expressions. As we discuss in the next Section, some interesting properties of functions $A_k^{(n)}(u)$ and $B_k^{(n)}(u)$ are related to their asymptotic behavior[3] at large u and v.

11.2.1 Asymptotic Behavior of Φ at Large Distances

Using the corrections in PT obtained from the generalized Bloch equation, the asymptotic series can be calculated in some particular directions in the domain (s,t).

Let us consider the line

$$s \;=\; \alpha\, t \tag{11.2.14}$$

where $\alpha \in (0,1]$ is a parameter. One can see that along this line (keeping the value of α fixed), the dominant asymptotic behavior of the nth correction to the phase

$$\phi_n(u,v) \;=\; \phi_n(\lambda s,t)_{s=\alpha t} \tag{11.2.15}$$

at large t comes from the term $A_0^{(n)}(\lambda(\alpha t))t^{2n+1}$, see (11.2.7). Concisely,

$$\phi_n(\lambda\, s,t)_{s=\alpha t} \;\sim\; \frac{\mathcal{A}_n}{(\alpha\lambda)^{2n-1}}\, t^2 \;+\; O\left(t^0\right)\;, \qquad t\to\infty\;, \qquad n \;=\; 0,1,2,...\;, \tag{11.2.16}$$

where $\mathcal{A}_n$ is a coefficient. The first three coefficients are

$$\mathcal{A}_0 \;=\; \frac{1}{2\sqrt{3}}\;, \qquad \mathcal{A}_1 \;=\; -\frac{1}{20\sqrt{3}}\;, \qquad \mathcal{A}_2 \;=\; -\frac{23}{2800\sqrt{3}}\;. \tag{11.2.17}$$

From (11.2.16), one can note that the behavior of $\phi(\lambda\, s,t)_{s=\alpha t}$ is given by

$$\phi(\lambda\, s,t)_{s=\alpha t} \;=\; \lambda\left(\alpha\sum_{n=0}^{\infty}\mathcal{A}_n\alpha^{-2n}\right)t^2 \;+\; 2\log(t) \;+\; \ldots\;, \qquad t\;\to\;\infty\;. \tag{11.2.18}$$

The logarithmic (subdominant) term comes from the function $B_0^{(0)}(u)$ displayed in (11.2.4). In order to determine the sum in (11.2.18), we can define the generating function

$$\mathcal{A}(\alpha) \;=\; \alpha\sum_{n=0}^{\infty}\mathcal{A}_k\alpha^{-2n}\;. \tag{11.2.19}$$

One can check that it satisfies a non-linear differential equation, namely

$$(1-\alpha^2)\,(\mathcal{A}')^2 \;+\; 4\,\mathcal{A}^2 \;-\; \frac{1}{4}\,\alpha^2 \;=\; 0\;, \qquad \mathcal{A}(1) \;=\; \frac{1}{4}\;. \tag{11.2.20}$$

[3]At this stage, one can suspect that corrections ϕ_n play the role of generating functions, just like $G_n(r)$ did in the case of the radial anharmonic oscillator, see (4.4.2). Let us remind that, based on the functions $G_n(r)$, one can construct the asymptotic expansion of the phase at large distances.

The exact solution to this equation is given by

$$\mathcal{A}(\alpha) \;=\; \frac{1}{4}\,\alpha^2 \;. \tag{11.2.21}$$

Hence, the behavior of the phase (11.2.15) at $t \to \infty$ results in

$$\Phi(\lambda\, s, t)_{s=\alpha t} \;=\; \frac{1}{4}\,\alpha^2\,\lambda\, t^2 \;+\; 2\log(t) \;+\; O(t^0)\;, \qquad t \to \infty\;. \tag{11.2.22}$$

Some other relevant limits in different directions can also be studied. For example, if s is fixed, say $s = s_0$, the asymptotic expansion at large t is of the form

$$\Phi(s_0, t) \;=\; C_0(s_0, \lambda)\, t \;+\; C_1(s_0, \lambda)\log(t) \;+\; O(t^0)\;, \qquad t \to \infty\;. \tag{11.2.23}$$

Here C_1 and C_2 are some unknown functions, except at $\lambda = 0$.

As we have seen, the perturbative solution of the GB equation in powers of λ^2 can provide information about the behavior of the exact phase at large distances. In contrast with the solution of the GB equation of the radial anharmonic oscillator, further manipulations[4] in corrections ϕ_n are needed to obtain the asymptotic behavior of the phase.

11.3 Connection between RB and GB Equations

We have constructed two different representations for the phase Φ of the ground state wave function. From one side

$$\Phi \;=\; \sum_{n=0}^{\infty} \lambda^{2n} \Phi_n(s,t)\;, \qquad s \;=\; \frac{\rho}{r_0}\;, \quad t \;=\; \frac{r}{r_0}\;, \tag{11.3.1}$$

and from the other

$$\Phi \;=\; \sum_{n=0}^{\infty} \lambda^{2n} \phi_n(u,v)\;, \qquad u \;=\; \frac{\rho}{\rho_0}\;, \quad v \;=\; \frac{r}{r_0}\;. \tag{11.3.2}$$

The definitions of r_0 and ρ_0 appear in (10.2.2) and (10.3.2), respectively. Due to uniqueness of the phase Φ, it is clear that there must be a connection between corrections $\Phi_n(s,t)$ and $\phi_n(u,v)$. In order to establish it, we use the polynomial structure of corrections (11.1.6) in (11.3.1), thus

$$\Phi \;=\; \sum_{n=0}^{\infty} \lambda^{2n} \sum_{j=0}^{n} \sum_{k=j}^{n} \left(a_{j,k}^{(n)}\, t \;+\; b_{j,k}^{(n)} \right) s^{2(n-k)} t^{2(k-j)}\;. \tag{11.3.3}$$

[4] In the case of the D-dimensional anharmonic oscillator, it was enough to expand the first functions $G_n(r)$ at large distances to obtain the asymptotic behavior of the phase.

Changing the order of summation and using the relation (10.3.4) between variables s and u, it can be shown that (11.3.3) is equivalent to

$$\Phi \;=\; \sum_{n=0}^{\infty} \lambda^{2n} \sum_{k=0}^{n} \sum_{j=n}^{\infty} \left(a_{k,n}^{(j)}\, v \;+\; b_{k,n}^{(j)} \right) u^{2(j-n)} v^{2(n-k)} \;. \tag{11.3.4}$$

Comparing expansions (11.3.2) and (11.3.4), we conclude that

$$\phi_n(u,v) \;=\; \sum_{k=0}^{n} \sum_{j=n}^{\infty} \left(a_{k,n}^{(j)}\, v \;+\; b_{k,n}^{(j)} \right) u^{2(j-n)} v^{2(n-k)} \tag{11.3.5}$$

due to the uniqueness of the Taylor series. After further manipulations, (11.3.5) is expressed as follows

$$\phi_n(u,v) \;=\; \sum_{k=0}^{n} v^{2(n-k)} \sum_{j=0}^{\infty} \left(a_{k,n}^{(n+j)}\, v \;+\; b_{k,n}^{(n+j)} \right) u^{2j} \;. \tag{11.3.6}$$

Comparing (11.2.7) and (11.3.6), we explicitly find that

$$A_k^{(n)}(u) \;=\; \sum_{j=0}^{\infty} a_{k,n}^{(n+j)} u^{2j} \;, \tag{11.3.7}$$

and

$$B_k^{(n)}(u) \;=\; \sum_{j=0}^{\infty} b_{k,n}^{(n+j)} u^{2j} \;. \tag{11.3.8}$$

Therefore, the meaning of the connection between the GB and RB equations is the following: the *coefficient* functions $A_k^{(n)}(u)$ and $B_k^{(n)}(u)$ are nothing but generating functions of the coefficients $a_{j,k}^{(n)}$ and $b_{j,k}^{(n)}$, respectively. [5]

[5] A similar statement was formulated for the D-dimensional radial anharmonic oscillator, see Chapter 2, Section 4.3.

Chapter 12

The Approximant

The analytical information about the phase, obtained from the RB and GB equations, Taylor and asymptotic series, is now used to design the *Approximant*: an approximation of the exact (unknown) ground state wave function denoted by $\psi^{(t)}$. To do so, we follow (as long as possible) the prescription proposed and applied in the previous Part, where it was successful in constructing the Approximant of some particular cases of the D-dimensional radial polynomial anharmonic oscillator.

First, we assume the exponential representation for the Approximant in coordinates (ρ, r),

$$\psi^{(t)}(\rho, r) \;=\; e^{-\Phi_t(\rho,r)} \;. \tag{12.0.1}$$

Therefore, we can focus only on the construction of $\Phi_t(\rho, r)$. According to the prescription, the approximate phase has to interpolate the expansions of small and large distances, i.e., the expansions (11.1.9), (11.2.22), and (11.2.23). Following the reflection symmetry of the system $\rho \to -\rho$ for fixed r, $\Phi_t(\rho, r)$ should be a function of ρ^2. One of the simplest interpolations, which accomplishes the prescription given above, is of the form

$$\Phi_t(\rho, r) \;=\; \frac{\alpha_0 + \alpha_1\, r + \;\alpha_3\, r^2 + a_3\, \gamma\, \rho^2 + \alpha_4\, \gamma\, \rho^2\, r}{\sqrt{1 + \beta_1\, r + \beta_2\, r^2 + \beta_3\, \rho^2}} \;+\; \log(1 + \beta_1\, r + \beta_3\, r^2 + \beta_4\, \rho^2) \tag{12.0.2}$$

where $\{\alpha_0, \alpha_1, \alpha_2, \alpha_3, \alpha_4, \beta_1, \beta_3, \beta_4\}$ are 8 free real parameters that later will be fixed via the VM. Note that this formula is analogous to (6.1.2).

The appearance of a square root in the denominator is motivated by the generating function ϕ_0, see (11.2.3). The logarithmic term is included to mimic the appearance of logarithmic terms in the exact wave function, see (11.2.4). It will generate a prefactor in the approximate wave function, which ultimately is given by

$$\psi^{(t)}_{1s_0}(\rho, r) \;=\; \frac{1}{1+\beta_1\, r+\beta_2\, r^2+\beta_3\, \rho^2}\, \exp\left(-\frac{\alpha_0+\alpha_1\, r+\;\alpha_2\, r^2+\alpha_3\, \gamma\, \rho^2+\alpha_4\, \gamma\, \rho^2\, r}{\sqrt{1+\beta_1\, r+\beta_2\, r^2+\beta_3\, \rho^2}}\right). \tag{12.0.3}$$

This is the expression of the trial function that is going to be used in numerical calculations. We have labeled this Approximant with $1s_0$, indicating the usual notation for the ground state hydrogen atom in the absence of a magnetic field.

As was discussed in Chapter 1, the variational method allows us to fix the value of the free parameters. We take the Approximant (12.0.3) and compute its associated variational energy E_{var}: the parameter-dependent expectation value of the Hamiltonian (10.0.4). The variational principle guarantees that the variational energy is an upper bound of the exact energy, $E_{var} \geq E_{exact}$. Then, we minimize with respect to the free parameters to obtain their optimal configuration that provides the lowest upper bound.

12.1 Results

12.1.1 Energy

From now on we set $c = \hbar = e = m_e = 1$ in numerical computations, see (10.2.4). It is not a surprise that a numerical integration and minimization are needed to calculate and minimize the variational energy associated with (12.0.3). A code in FORTRAN 77 was written for this purpose. It uses the integration routine D01FCF from NAG-LIB as well as the minimization routine MINUIT of CERN-LIB. Further details of the computational code can be found in [54], [55], and [56]. Variational estimates of the energy are presented in Table 12.1 for some representative magnetic fields in the range $\gamma \in [0.01, 10\,000]$ a.u.

Plots of optimal variational parameters as functions of $\log(1+\gamma^2)$ are shown in Appendix I, see Fig. C.1. In general terms, they are smooth changing parameters in the whole domain of magnetic fields studied.

Our variational calculations are compared with some benchmarks coming from literature. However, for some magnetic fields, no estimate of the energy was found. Hence, to analyze the accuracy of our results, we carried out some numerical calculations via the Lagrange-Mesh method in the formulation presented in [58] using spherical coordinates $\{r, \theta, \varphi\}$. The complete description and application of this method to the present system - hydrogen atom in a constant magnetic field - was already presented, see Section 2.5 in [75]. We implemented the Lagrange-Mesh method in a notebook of *Mathematica*. For the whole range of magnetic fields studied, the mesh was kept unchanged, it consisted of $N_r = 80$ radial functions and

Table 12.1: Energy E and quadrupole moment Q_{zz} of the ground state $1s_0$ of the hydrogen atom in constant magnetic field calculated in Variational Method (results without superscript) for $\gamma \in [0.01, 10\,000]$ with trial function (12.0.3). Benchmarks are included. Energy presented in Ry.

γ	E	$-Q_{zz}$	γ	E	$-Q_{zz}$
0.01	-0.999 950 005 51	0.000 248	5.0	2.239 209	0.506 493
	-0.999 950 005 52[a,e]	0.000 249[e]		2.239 202[a,e]	0.506 331[e]
0.1	-0.995 052 960 5	0.023 270	10.0	6.504 427	0.445 22
	-0.995 052 960 8[a,e]	0.023 2712[e]		6.504 405[a,d]	0.445 09[d]
0.5	-0.894 421 065	0.256 143	100.0	92.420 7	0.217 5
	-0.894 421 075[a,e]	0.256 156 21[e]		92.420 3[a,d]	0.216 8[d]
1.0	-0.662 337 66	0.417 618	500.0	487.487	0.125 1
	-0.662 337 79[a,d]	0.417 654[d]		487.485[a,e]	0.123 8[e]
2.0	-0.044 426 7	0.511 354	1 000.0	984.678	0.099 4
	-0.044 427 8[a,e]	0.511 432[e]		984.675[a,d]	0.098 2[d]
γ_0	0.000 001	0.513 561	10 000.0	9 971.74	0.049 3
	0.000 000[e]	0.513 537[e]		9 971.72[e,f]	0.047 9[e]

$\gamma_0 = 2.065\,211\,858$, see (12.1.2).
[a] Power series [74], [d] Lagrange Mesh [75], [e] Lagrange Mesh (present work), [f] Basis of Splines [76].

$N_u = 200$ angular ones[1]. Hence the approximate ground state function is an expansion in terms of $80 \times 200 = 16\,000$ functions. With this enormous mesh, we reproduced the results obtained for all magnetic fields studied in [75]: 1, 10, 100, and 1 000 a.u. It seems that the maximum accuracy in energy - 19 exact s. d. - is obtained for magnetic fields $\gamma \lesssim 1$ a.u. In general terms, for $\gamma \lesssim 1\,000$ a.u. the method reaches in energy an accuracy of not less than 10 exact s. d. The accuracy decays dramatically once we study fields beyond $\gamma \approx 1\,000$ a.u.

For example, it reaches only 6 exact digits at $\gamma = 10\,000$ a.u. Using this method, we have confirmed and extended the results shown in [75].

Making a comparison between our results with benchmarks, we concluded the relative deviation of the variational estimate of the energy to the exact one is very *small* in the whole domain of considered magnetic fields,

$$\left| \frac{E_{var} - E_{exact}}{E_{exact}} \right| \lesssim 10^{-6} , \qquad \gamma \in [0.01, 10\,000] . \tag{12.1.1}$$

To the best of the author's knowledge, there is no other variational calculation with a compact

[1] $u = \cos\theta$.

trial function that provides such an accurate estimate of the energy. This may be seen from Table 12.2, where we show a collection of estimates of the ground state energy at $\gamma = 1$ a.u. In this Table, we have introduced the result obtained from the Padé-Borel summation applied to the first 100 coefficients in the perturbation expansion (11.1.1) of ε. This result provides 11 exact s.d. for the energy at $\gamma \leq 1$a.u. However, the accuracy of the energy calculated by this procedure decays dramatically for $\gamma \gtrsim 2$ a.u.

Table 12.2: The ground state energy E_{1s_0} in Ry of the hydrogen atom in constant magnetic field $\gamma = 1$. The results ranked by accuracy. Infinite massive proton assumed.

Reference	E_{1s_0}	Method
[77] Wallis & Bowlden, 1958	-0.346	Variational Method
[78] Yafet et al., 1956	-0.523	Variational Method
[79] Galindo & Pascual, 1976	-0.690	Rational Approximants
[80] Turbiner, 1984	-0.61	Variational Method
[81] Potekhin & Turbiner, 2001	-0.63	Adiabatic Approximation
[82] Kobori & Ohyama, 1997	-0.654	Variational Method
[83] Pokatilov & Rusanov, 1969	-0.659 1	Variational Method
[84] Larsen, 1968	-0.661	Variational Method
[85] Lee et al., 1973	-0.661 6	Variational Method
[86] Makado & McGill, 1986	-0.662 2	Variational Method
[87] Cabib et al., 1971	-0.662 4	Variational Method
[88] Arteca et al., 1983	-0.662 7	Regularization of PT
[89] Chen & Goldman, 1992	-0.662 35	Expansion of the Wavefunction
[90] Praddaude, 1972	-0.662 33	Power Series
[81] Potekhin & Turbiner, 2001	-0.662 332	Variational Method
[91] Vieyra & Olivares, 2008	-0.662 332	Variational Method
[92] Rösner et al., 1984	-0.662 338	Multi-Configuration Hartree-Fock
[93] Ivanov, 1988	-0.662 337 4	Finite Difference Method
Present Work, 2020	**-0.662 337 7**	**Variational Method**
[94] Xi et al., 1992	-0.662 337 78	Spline-basis
[76] Wang & Hsue, 1995	-0.662 337 79	Spline-basis
[73] Le Guillou & Zinn-Justin, 1983	-0.662 337 79	Borel-Leroy Summation
[95] Wunner & Ruder, 1982	-0.662 337 79	Expansion of the Wavefunction
[96] Fonte et al., 1990	-0.662 337 793	Variational Rayleigh-Ritz
Present Work, 2020	**-0.662 337 793 46**	**Padé-Borel Summation**
[97] Stubbins et al., 2004	-0.662 337 793 466	Variational Rayleigh-Ritz
[74] Kravchenko et al., 1996	-0.662 337 793 466	Method of Moments
[75] Baye et al., 2008	-0.662 337 793 466 315 9	Lagrange Mesh
Present Work, 2020	**-0.662 337 793 466 316 071 2**	**Lagrange Mesh**
[97] Stubbins et al., 2004	-0.662 337 793 466 316 071 220 596 ...	Multiconfiguration
[98] Nakashima & Nakatsuji, 2010	-0.662 337 793 466 316 071 220 596 ...	Free Complement

We also paid attention to the *critical magnetic field* γ_0, for which the ground state energy

vanishes[2],

$$E(\gamma_0) \;=\; 0 \;. \tag{12.1.2}$$

The value of γ_0 in the Lagrange-Mesh method, results in

$$\gamma_0 \;=\; 2.065\,211\,858\,\text{a.u.}\;, \tag{12.1.3}$$

with $E \;\sim\; 10^{-10}$Ry. For this magnetic field, the variational trial function (12.0.3) provides $E \;\sim\; 10^{-6}$Ry.

The local deviation between the Approximant and the exact wave function can be estimated by studying the vicinity of the Coulomb singularity[3] via the cusp parameter (11.1.12). A straightforward calculation shows that the cusp parameter $C^{(t)}$, derived from to the Approximant (12.0.3), is given by a simple formula

$$C^{(t)} \;=\; \alpha_1 \;+\; \left(1 - \frac{\alpha_0}{2}\right)\beta_1\;, \tag{12.1.4}$$

see (11.1.12). The results for $C^{(t)}$ are presented in Table 12.3. It can be seen that $C^{(t)}$, calculated with optimal parameters as entry, satisfies the cusp condition accurately for $\gamma \lesssim 500$ a.u. with an error of $\lesssim 16\%$. For the largest magnetic field studied, $\gamma = 10\,000$ a.u. the deviation increases up to 70%. The cusp parameter C was also estimated in the Lagrange Mesh Method. In general, this calculation provides a parameter C with not less than 6 exact s. d. in the whole range of magnetic fields considered.

Table 12.3: Estimate of the cusp parameter for the ground state $1s_0$ coming from the Approximant (12.0.3). Only s. d. presented. Atomic units used.

γ	$C^{(t)}$	γ	$C^{(t)}$
0.01	1.000 002	5.0	0.997
0.1	0.999 97	10.0	1.002
0.5	0.999 7	100.0	1.065
1.0	0.999 3	500.0	1.159
2.0	0.996 5	1 000.0	1.23
γ_0	0.996 7	10 000.0	1.7

12.1.2 Quadrupole Moment

It is well-known that the hydrogen atom in its ground state acquires a quadrupole moment at $\gamma > 0$, see [81]. Based on the cylindrical symmetry of the system, it can be easily shown that

[2]Note that γ_0 defines a normalizable zero mode of the Hamiltonian (10.0.4).
[3]Located at $r = 0$, see (10.0.5).

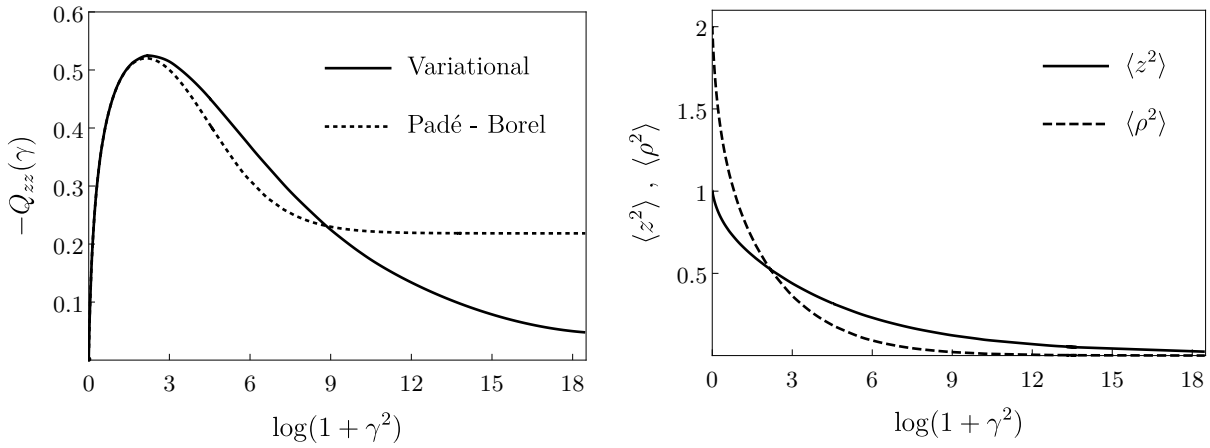

Figure 12.1: Left: Plot of the absolute value of the quadrupole moment $(-Q_{zz})$ in (a.u)^2 as a function $\log(1+\gamma^2)$. Variational estimate (see 12.0.3) of the quadrupole moment as well as the one coming from Padé-Borel summation presented. In the Lagrange-Mesh method, the minimum of the quadrupole moment $-Q_{zz} = 0.524\,52$ (a.u)^2 is reached at $\gamma \cong 2.968\,69$a.u. Right: Expectation values $\langle z^2\rangle$ and $\langle \rho^2\rangle$ calculated by means of Approximant (12.0.3) as functions of $\log(1+\gamma^2)$. The intersection of the curves occurs at $\gamma \approx 2.806$a.u.; at this magnetic field $\langle z^2\rangle = \langle \rho^2\rangle \approx 0.524$. For $\gamma \gtrsim 700$a.u. the value of $\langle z^2\rangle$ is at least two orders of magnitude larger than $\langle \rho^2\rangle$. Atomic units used.

the quadrupole moment tensor is diagonal and only contains one single independent element, say

$$Q_{zz} = \langle \rho^2 \rangle \; - \; 2\,\langle z^2 \rangle \; . \tag{12.1.5}$$

Once optimal parameters are found for the Approximant (12.0.3), the Q_{zz} component can be estimated for different values of γ using the square of the Approximant as a compact analytical expression for the electronic charge distribution. Plots of Q_{zz} and expectations values, $\langle z^2\rangle$ and $\langle \rho^2\rangle$, as functions of γ are presented in Fig. 12.1. The numerical results are shown in Table 12.1. In the literature, there are not many accurate benchmarks for Q_{zz}. Hence, in order to estimate the deviation of Q_{zz} (calculated via the Approximant (12.0.3)) with respect to the *exact* value, we use the Lagrange-mesh method to obtain highly accurate estimates of Q_{zz} that can be regarded as the exact values, see Table 12.1. These estimates indicate that for *small* magnetic fields $\gamma \lesssim 2$, we reproduce not less than 4 exact s.d. In turn, for $\gamma \gtrsim 2$ we reproduce exactly 2-3 s.d.

In addition to those calculations, the quadrupole moment is estimated using the PT calculated for Φ_n, see (11.1.1). In this manner, we can construct the expansion of the quadrupole moment in powers of γ^2,

$$Q_{zz}(\gamma) = \sum_{n=0}^{\infty} Q_{zz}^{(n)} \gamma^{2n} \; . \tag{12.1.6}$$

Up to $O(\gamma^8)$ this expansion[4] looks like

$$Q_{zz}(\gamma) \;=\; -\frac{5}{2}\gamma^2 \;+\; \frac{615}{32}\gamma^4 \;-\; \frac{2564987}{11520}\gamma^6 \;+\; \frac{19550772149}{5529600}\gamma^8 \;+\; \ldots \;. \tag{12.1.7}$$

Due to the polynomial nature of corrections Φ_n with rational coefficients, see (11.1.6), corrections $Q_{zz}^{(n)}$ in the expansion (12.1.6) will be rational numbers as well. The calculation of the first $Q_{zz}^{(n)}$ indicates that series (12.1.6) are alternating with very fast growing coefficients as n grows. It is an indication that (12.1.6) could be a divergent series. The largest coefficient that we calculated was $Q_{zz}^{(26)}$ whose (rounded) value is

$$Q_{zz}^{(26)} \;=\; -8.188 \times 10^{47} \;. \tag{12.1.8}$$

Making a comparison of the first 26 coefficients $Q_{zz}^{(n)}$ in the expansion (12.1.6) with those ε_n in (11.1.1), one can notice that the series for the quadrupole moment diverges faster than for the energy. With a motivation coming from the results obtained for the energy, we tested the applicability of the Padé-Borel summation to the first 26 terms of the series (12.1.6), assuming the same growth of $Q_{zz}^{(n)}$ as in (11.1.8) for ε_n. In general, the Padé-Borel summation provides accurate results for $\gamma \lesssim 2$ a.u: it confirms not less than 3 correct s. d. of Q_{zz} calculated either by means of the Approximant or the Lagrange-Mesh method. The accuracy of the Padé-Borel summation decays dramatically for magnetic fields larger than $\gamma = 2$ a.u. The plot of the Q_{zz} as a function of γ, calculated in this scheme, is presented in Fig. 12.1.

[4]First ten coefficients are presented explicitly in Appendix, see F.3.

Chapter 13

Conclusions

Following the formalism presented for the D-dimensional radial anharmonic oscillator in Part I, a compact wave function *Approximant* for the ground state of a hydrogen atom in a constant magnetic field was constructed. PT, asymptotic expansions at small and large distances, the choice of coordinates (ρ, r) to work with, as well as the RB and GB[1] equations, were basic ingredients to construct the Approximant. The main result of the study is summarized in the following expression for the Approximant

$$\psi^{(t)}_{1s_0}(\rho, r) \;=\; \frac{1}{1+\beta_1\, r+\beta_2\, r^2+\beta_3\, \rho^2}\, \exp\left(-\frac{\alpha_0+\alpha_1\, r+\;\alpha_2\, r^2+\alpha_3\, \gamma\, \rho^2+\alpha_4\, \gamma\, \rho^2\, r}{\sqrt{1+\beta_1\, r+\beta_2\, r^2+\beta_3\, \rho^2}}\right)\,,$$

where $\{\alpha_0, \alpha_1, \alpha_2, \alpha_3, \alpha_4, \beta_1, \beta_3, \beta_4\}$ are 8 free parameters. To fix their value, the Variational Method using the Approximant $\psi^{(t)}_{1s_0}$ as trial function was employed. It led to a variational estimate of the ground state energy with a very small relative deviation, of order $\sim 10^{-6}$ in the whole studied range of magnetic fields $\gamma \in [0.01, 10\,000]$ a.u. These results reproduced with high accuracy the benchmark energies (some of them are established by this work in the Lagrange-Mesh method).

As an additional calculation, the quadrupole moment was computed for the same range using the square of the Approximant as a compact expression of the electronic density. Results coincide with benchmarks (coming from the Lagrange-Mesh method) in not less than 3 s. d. for $\gamma \lesssim 100$ a.u. It was explicitly demonstrated that the cusp condition of the exact hydrogen atom holds even in the presence of a constant magnetic field. Our Approximant provides a cusp parameter with a very small deviation from the exact value. For the weak and intermediate magnetic fields $\gamma \lesssim 500$ a.u., its relative deviation is about 15%.

Due to the success of the Approximant when describing the ground state, it is clear that it can be modified to study excited states. Multiplying the Approximant by a suitable polynomial,

[1] Which leads to the *true* semi-classical expansion.

some particular families of excited states can be studied, just like it was done in [91]. For example,

$$z\,\psi^{(t)}_{1s_0}(\rho, r)$$

where $z = \sqrt{r^2 - \rho^2}$, is a suitable Approximant to describe the excited state $2p_0$. However, it should be mentioned that the general structure of the nodal surfaces, in the form of a prefactor, is still unknown.

Due to the algebraic nature of PT in the framework of the Non-Linearization Procedure, the first 100 energy corrections (in powers of the *effective magnetic field*) with absolute accuracy were obtained: corrections are presented for the first time as rational numbers. Using these corrections, it was *summed* up the (divergent) PT for the energy via the Padé-Borel summation technique. It led to highly accurate results (not less than 11 s.d.) for *small* magnetic field $\gamma \lesssim 1$ a.u.

Further Studies

- PT can be constructed in the framework of the Non-Linearization Procedure to estimate the accuracy of the variational energy and wave function. In this context, the Approximant plays the role of the unperturbed wave function. This approach was successfully applied to the D-dimensional radial anharmonic oscillator: corrections in PT of the variational energy were computed. As a result, its deviation with respect to the exact value was estimated, see Eq. (7.2.27). One could try to follow the same procedure for the hydrogen atom in a magnetic field by considering corrections to the approximate phase and the energy,

$$\Phi_{exact} \;=\; \Phi^{(0)}_t \;+\; \Phi^{(1)}_t \;+\; \Phi^{(2)}_t \;+\; \ldots\;, \qquad E_{exact} \;=\; E_{var} \;+\; E^{(t)}_2 \;+\; E^{(t)}_3 \;+\; \ldots$$

  where $\Phi^{(0)}_t \equiv \Phi_t$, see Eq. (12.0.2). In the Non-Linearization procedure, it can be easily shown that the first order correction to the phase, denoted by $\Phi^{(1)}_t$, obeys a two-dimensional linear partial differential equation (PDE), namely

$$\Delta\Phi^{(1)}_t \;-\; 2\,\nabla\Phi^{(0)}_t \cdot \nabla\Phi^{(1)}_t = \; E_{var} \;- V^{(1)}\;.$$

  Here we have denoted $V^{(1)} = V - V_0$, where

$$V \;=\; -\frac{1}{r} \;+\; \frac{\gamma^2}{8}\,\rho^2\;, \qquad V_0 \;\equiv\; \frac{\Delta\Psi^{(t)}}{\Psi^{(t)}}\;.$$

  If the solution for $\nabla\Phi^{(1)}_t$ is found, one could calculate the first correction to E_{var} using that

$$E^{(t)}_2 \;=\; -\frac{\displaystyle\int \left(\nabla\Phi^{(1)}_t\right)^2 \psi^{(t)}\psi^{(t)}\,dV}{\displaystyle\int \psi^{(t)}\psi^{(t)}\,dV}\;,$$

  see [8]. If $V^{(1)}$ is subdominant in comparison to V, i.e. the ratio of $V^{(1)}$ to V is bounded at large distances, then PT developed in the Non-Linearization Procedure will be convergent.

- We did not take into account the information coming from the strong coupling regime ($\gamma \to \infty$) in the design of the Approximant. For the ground state energy, the first two terms of the strong coupling expansion are well-known,

$$E \;=\; \gamma \;-\; \log^2 \gamma \;+\; \ldots \;,$$

see [99]. It would be interesting to use this expansion in the RB and GB equations and study the strong coupling regime for the phase. This piece of missing information could lead to an improvement of the Approximant.[2]

- In this work, an infinitely massive and static proton was assumed. In the Schrödinger equation, finite mass effects can be incorporated making a pseudoseparation of variables of the center of mass and the relative coordinates, see [100] for details. Naturally, taking into account the finite mass of the proton, the spectrum of the hydrogen atom in a constant magnetic field will be modified. It turns out that when the (finitely) massive proton is fixed in the space (hydrogen atom at rest), the Schrödinger equation that describes this situation looks very similar to Eq. (10.0.1). The only difference is that the reduced mass of the hydrogen atom replaces the electron mass m_e in Eq. (10.0.1), see [101]. As a consequence, the Approximant that we have presented in this Part is also appropriate to describe the ground state of the finite massive static hydrogen atom in a constant magnetic field, see [11]. The study of finite mass effects was beyond of the purpose of the present Thesis, it will be done elsewhere.

[2]For example, an extra parameter, say q, may be inserted in the form of a degree of the prefactor of the Approximant. In this manner

$$\psi^{(t)}_{1s_0}(\rho, r) \;=\; \frac{1}{(1+\beta_1\, r+\beta_2\, r^2+\beta_3\, \rho^2)^q}\, \exp\left(-\frac{\alpha_0+\alpha_1\, r+\,\alpha_2\, r^2+\alpha_3\, \gamma\, \rho^2+\alpha_4\, \gamma\, \rho^2\, r}{\sqrt{1+\beta_1\, r+\beta_2\, r^2+\beta_3\, \rho^2}}\right) \;.$$

The insertion of this extra parameter surely will lead to higher accuracy for both the energy and the cusp parameter.

General Conclusions

- Part I

  For the cubic, quartic, and sextic radial anharmonic oscillator potentials, whose corresponding Schrödinger equations do not allow finding exact solutions, highly accurate approximate eigenfunctions of the low-lying states are written for arbitrary coupling constant and space dimension. Associated energies lead to unprecedented relative accuracies of (at least) order $\lesssim 10^{-5}$ for any coupling constant in any dimension. These energies are in complete agreement with the highly accurate results of the Lagrange-Mesh calculations, performed in the present thesis. Those results can be generalized for the radial anharmonic oscillator with arbitrary anharmonicity. It manifests a solution of the spectral problem of the radial anharmonic oscillator.

- Part II

  A locally accurate ground state wave function (the Approximant) for the hydrogen atom subjected to a constant uniform magnetic field is found. This approximate function leads to high accuracy for the ground state energy (with relative accuracy $\lesssim 10^{-5}$), as well as for the quadrupole moment. In the whole domain of accessible magnetic fields in Nature, the obtained energies are in complete agreement with the highly accurate ones provided by the Lagrange-Mesh method and the Padé-Borel summation[3]. In a non-relativistic consideration with a static proton, the Approximant can be regarded as the solution of the Schrödinger equation, which does not admit exact solutions.

[3]The domain of applicability of the Padé-Borel sum occurs for weak and intermediate fields.

Appendices

Appendix A

The WKB (Semi-Classical) Approximation

We present an extension of the WKB method that can be found in elementary books on quantum mechanics, e.g. [1, 2]. In particular, we focus the discussion on the radial Schrödinger equation in arbitrary dimension $D = 1, 2, ...$, which describes an S-state[1] of an arbitrary radial potential

$$-\frac{\hbar^2}{2M}\left(\partial_r^2 \;+\; \frac{D-1}{r}\,\partial_r\right)\Psi \;+\; V(r)\Psi \;=\; E\,\Psi\;. \tag{A.0.1}$$

If we assume that the potential fulfills

(*i*) $V(r) \geq 0$

(*ii*) $V(0) = 0$

(*iii*) $V(r \to \infty) \to +\infty$

we can guarantee the existence of bound states. We adopt the exponential representation for the wave function to find them,

$$\Psi(r) \;=\; e^{iS(r)/\hbar}\;. \tag{A.0.2}$$

The reason why we include $\hbar$ explicitly will be clear at the end of this Appendix. For now, it is clear that the physical units of S are those of $\hbar$, i.e. units of action. In this representation (A.0.1) becomes a Riccati-type equation

$$i\hbar\,S''(r) - S'(r)\left(S'(r) - \frac{i\hbar\,(D-1)}{r}\right) \;= 2M(V(r) - E) \tag{A.0.3}$$

cf. (3.3.4). For our purposes, it is enough to study this equation in the so-called non-classical domain in r (which is characterized by the inequality $V(r) > E$) beyond the largest turning

[1] Characterized by zero angular momentum $\ell = 0$.

point. To solve (A.0.3) in PT we consider the expansion

$$S(r) \;=\; \sum_{n=0}^{\infty} S_n(r)\hbar^n \tag{A.0.4}$$

keeping E fixed. It is straight forward to show that equations

$$S_0' \;=\; \pm i\sqrt{2M(V-E)}\;, \tag{A.0.5}$$

and

$$S_1' \;=\; \frac{i(D-1)}{2r} \;+\; \frac{i}{2}\frac{S_0''}{S_0} \tag{A.0.6}$$

determine the first 2 corrections. In general, S_n' is given by the expression

$$S_n' \;=\; \frac{iS_{n-1}'' + \frac{i(D-1)}{2r}S_{n-1}' - \sum_{k=1}^{n-1} S_k' S_{n-k}'}{2S_0'}\;, \tag{A.0.7}$$

as we can see, the calculation of S_n' is an algebraic procedure. To guarantee the normalizability of the wave function (A.0.2) we need to take the positive sign in (A.0.5). Thus, it will decay exponentially at large distances. Taking this into account, it is clear that the wave function is of the form

$$\Psi(r) \;=\; \frac{1}{r^{\frac{D-1}{2}}(2M(V(r)-E)^{1/4})}\exp\left(-\frac{1}{\hbar}\int^r \sqrt{2M(V(r)-E)}\,dr \;+\; O(\hbar)\right)\;, \tag{A.0.8}$$

as long as $r \to \infty$. Some remarks should be pointed out:

(i) Contrary to the function $S(r)$, the energy E is considered fixed as a function of $\hbar$. Of course, this is not always true. For most of the potentials, the energy E should be $\hbar$-dependent.

(ii) The integrand that occurs in (A.0.8) has a physical meaning, it is (almost) the classical action presented in the form $\sim \int p\,dq$.

Further properties and results can be obtained from the WKB approximation. To do so, it is necessary to study the behavior of the wave function in the classical domain(s) and then match the solutions for each region (the non-classical and classical one). Some of those results are well known, for example, the celebrated Bohr-Sommerfeld from early quantum mechanics. A review of those properties is found in [1].

Appendix B

First PT Corrections and Generating Functions

B.1 Cubic Case

The expansions in powers of v for the first three corrections $\mathcal{Y}_n(v), n = 1, 2, 3$ for the cubic anharmonic oscillator potential (7.2.1), see (4.1.15) and (4.1.18) are presented.

- At $v \to 0$

$$\begin{aligned}
\mathcal{Y}_1(v) &= \epsilon_1 v + \frac{2\,\epsilon_1}{D+2}v^3 - \frac{1}{D+3}v^4 + \frac{\epsilon_1}{(D+2)(D+4)}v^5 + \dots , \\
\mathcal{Y}_2(v) &= \epsilon_2\, v + \frac{\epsilon_1^2 + 2\,\epsilon_2}{D+2}v^3 + \frac{6\,\epsilon_1^2 + 4\,\epsilon_2}{(D+2)(D+4)}v^5 - \frac{2\,\epsilon_1}{(D+3)(D+5)}v^6 + \dots , \\
\mathcal{Y}_3(v) &= \epsilon_3\, v + \frac{2(\epsilon_1\,\epsilon_2 + \epsilon_3)}{D+2}v^3 + \frac{2(\epsilon_1^3 + 6\,\epsilon_1\,\epsilon_2 + 2\,\epsilon_3)}{(D+2)(D+4)}v^5 - \frac{2\,\epsilon_2}{(D+3)(D+5)}v^6 + \dots .
\end{aligned} \tag{B.1.1}$$

  In these formulas we have denoted $\epsilon_n = \dfrac{\varepsilon_n}{D}$.

- At $v \to \infty$

$$\begin{aligned}
\mathcal{Y}_1(v) &= \frac{1}{2}v^2 + \frac{1}{4}(D+1) - \frac{\varepsilon_1}{2}v^{-1} + \frac{1}{8}(D^2-1)v^{-2} + \dots , \\
\mathcal{Y}_2(v) &= -\frac{1}{8}v^3 - \frac{1}{16}(3D+4)v + \frac{\varepsilon_1}{4} - \frac{1}{32}(6D^2 + 6D + 16\,\varepsilon_2 - 1)v^{-1} \\
&\quad + \frac{1}{8}(3D-2)\,\varepsilon_1 v^{-2} + \dots , \\
\mathcal{Y}_3(v) &= \frac{1}{16}v^4 + \frac{1}{32}(5D+8)v^2 - \frac{3\,\varepsilon_1}{16}v + \frac{1}{64}(15D^2 + 26D + 16\,\varepsilon_2 + 10) \\
&\quad - \frac{1}{32}(15D\,\varepsilon_1 + 16\,\varepsilon_3)v^{-1} + \dots .
\end{aligned} \tag{B.1.2}$$

A straightforward application of the formulas (4.2.3) and (4.4.2) allows us to calculate the

generating functions. In particular, G_3 and G_4 are given by

$$\begin{aligned} G_3 &= -\frac{(2M)^{1/2}}{g^2}\left(\frac{\varepsilon_1}{2}\log\left[\frac{w-1}{w+1}\right]\right) , \\ G_4 &= -\frac{(2M)^{1/2}}{g^2}\left(\frac{5+(5+12D)w+(1-6D(D+1))(w+1)w^2\,(3w^2-2)}{48(w-1)(w+1)^2w^3}\right. \\ &\quad \left.\frac{(1-16\,\varepsilon_2-6D(D+1))}{32}\log\left[\frac{w-1}{w+1}\right]\right) , \end{aligned} \tag{B.1.3}$$

where $w=(1+gr)^{1/2}$. Explicit formulas for the first corrections ε_n in PT at $D=1$ have been presented in (7.2.5).

B.2 Quartic Case

We present the corrections $\varepsilon_{4,6}$ and $\mathcal{Y}_{4,6}$ in explicit form for the quartic anharmonic potential (7.3.1) in the expansion (7.3.6) and (7.3.7),

$$\begin{aligned} \epsilon_2 &= \frac{1}{4}(D+2) , \\ \epsilon_4 &= -\frac{1}{16}(D+2)(2D+5) , \\ \epsilon_6 &= \frac{1}{64}(D+2)(8D^2+43D+60) , \end{aligned} \tag{B.2.1}$$

$$\begin{aligned} \mathcal{Y}_2(v) &= \frac{1}{2}v^3 \;+\; \epsilon_2 v\,, \\ \mathcal{Y}_4(v) &= -\frac{1}{8}v^5 \;-\; \frac{1}{16}(3D+8)v^3 \;+\; \epsilon_4 v\ , \\ \mathcal{Y}_6(v) &= \frac{1}{16}v^7 \;+\; \frac{1}{32}(5D+16)v^5 \;+\; \frac{1}{16}(3D^2+17D+25)v^3 \;+\; \epsilon_6 v\ , \end{aligned} \tag{B.2.2}$$

with $\epsilon_{2n}=\dfrac{\varepsilon_{2n}}{D}$.

We also present two generating functions for the phase, see expansion (4.4.1),

$$G_4 = \frac{5}{24g^2w^3} \;+\; \frac{D\,(1+w+w^2)}{4g^2(w+1)w^2} \;+\; \frac{D^2}{8g^2w}\ ,$$

$$\begin{aligned} G_6 &= -\frac{5}{16g^2w^6} \;-\; \frac{D\,(15+30w+20w^2+16w^3+20w^4+30w^5+15w^6)}{48g^2(w+1)^2w^5} \\ &\quad -\frac{D^2\,(4+8w+8w^2+12w^3+18w^4+9w^5)}{32g^2(w+1)^2w^4} \;-\; \frac{D^3\,(1+3w^2)}{48g^2w^3}\ , \end{aligned} \tag{B.2.3}$$

where $w = \sqrt{1+g^2v^2}$. Two remarks in a row: (i) in the variable w all generating functions are rational functions, (ii) the polynomial structure in variable D of generating functions becomes evident.

B.3 Sextic Case

We present explicitly the first corrections $\varepsilon_{8,12}$ and $\mathcal{Y}_{8,12}$ for the sextic anharmonic oscillator (7.4.1). See (7.4.3) and (7.4.4).

$$\begin{aligned}
\epsilon_4 &= \frac{1}{8}(D+2)(D+4)\ , \\
\epsilon_8 &= -\frac{1}{128}(D+2)(D+4)(9D^2+72D+152)\ , \\
\epsilon_{12} &= \frac{1}{1024}(D+2)(D+4)(81D^4+1404D^3+9624D^2+31152D+40384)\ .
\end{aligned} \tag{B.3.1}$$

$$\mathcal{Y}_4(v) = \frac{1}{2}v^5 + \frac{1}{4}(D+4)v^3 + \epsilon_4 v\ ,$$

$$\begin{aligned}
\mathcal{Y}_8(v) &= -\frac{1}{8}v^9 - \frac{1}{16}(3D+16)v^7 - \frac{1}{16}(3D^2+27D+64)v^5 \\
&\quad - \frac{1}{32}(4D^3+49D^2+204D+288)v^3 + \epsilon_8 v\ ,
\end{aligned}$$

$$\begin{aligned}
\mathcal{Y}_{12}(v) &= \frac{1}{16}v^{13} + \frac{1}{32}(5D+32)v^{11} + \frac{5}{64}(3D^2+34D+104)v^9 \\
&\quad + \frac{1}{32}(8D^3+125D^2+688D+1344)v^7 \\
&\quad + \frac{1}{256}(55D^4+1038D^3+7708D^2+26784D+36800)v^5 \\
&\quad + \frac{1}{256}(36D^5+783D^4+7040D^3+32768D^2+78912D+78336)v^3 \\
&\quad + \epsilon_{12}v,
\end{aligned} \tag{B.3.2}$$

where it has been defined $\epsilon_{4n} = \frac{\varepsilon_{4n}}{D}$.

Now we present explicitly two generating functions G_4, G_6 in the expansion (4.4.1),

$$\begin{aligned}
G_4 &= \frac{r^2\,(5+w^2)}{12w^3} + \frac{Dr^2\,(1+w+w^2)}{4w^2(w+1)} + \frac{D^2r^2}{16w}\ , \\
G_6 &= \frac{5-3w^2}{4g^2w^6} + \frac{D\,(15+15w-4w^2+2w^3+6w^4+6w^5)}{24g^2(w+1)w^5} + \frac{D^2\,(2+2w+w^2+3w^3+3w^4)}{16g^2(w+1)w^4} \\
&\quad + \frac{D^3\,(1+3w^2)}{96g^2w^3}\ ,
\end{aligned} \tag{B.3.3}$$

where $w = \sqrt{1 + g^4 r^4}$. Two remarks: *i*) in the variable w, generating functions are rewritten as rational ones; *ii*) The polynomial structure in variable D of these generating functions is evident.

Appendix C

Plots of Variational Parameters: Anharmonic Oscillator

In this Appendix, we present the plots of the optimal parameters in the Variational Method for the Approximants of the ground state of the cubic, quartic, and sextic anharmonic oscillator. The number of equation of each Approximant is indicated in the title of each Section.

C.1 Cubic: (7.2.24)

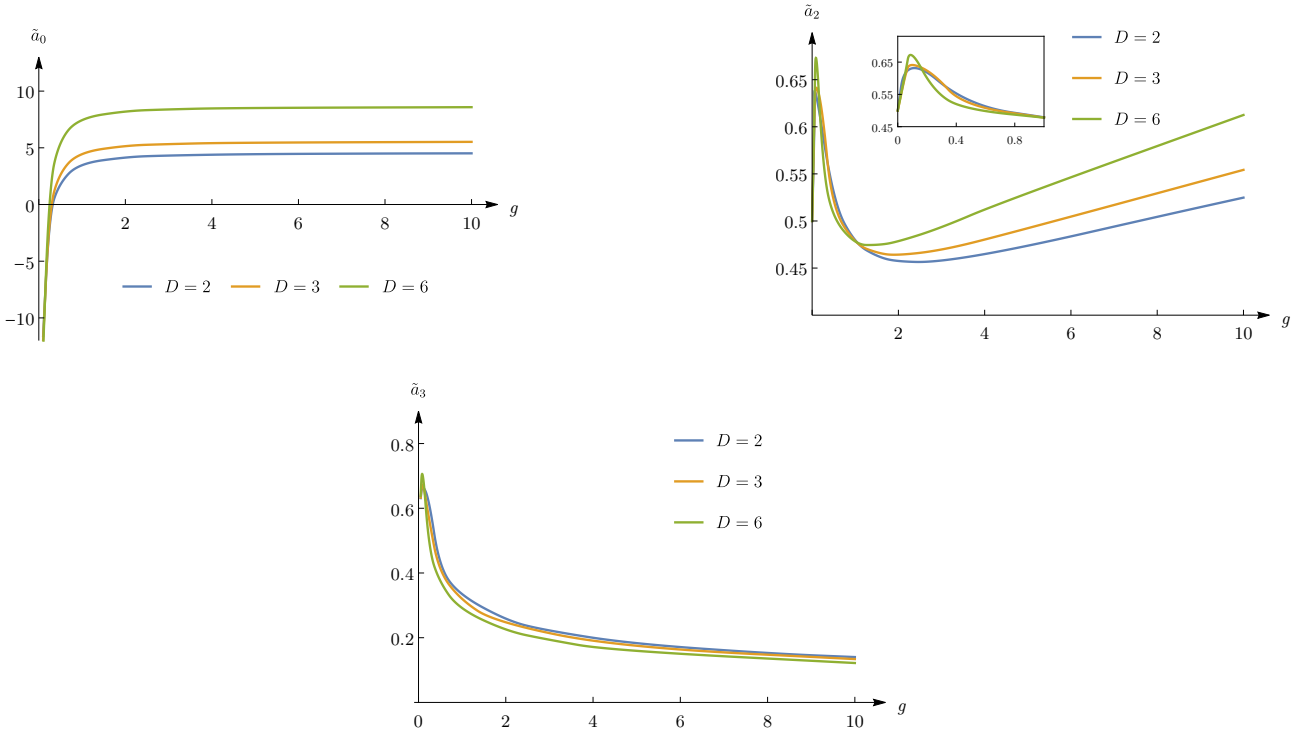

Figure C.1: Variational parameters $\tilde{a}_0$, $\tilde{a}_2$ and $\tilde{a}_3$ of the ground state as functions of g for $D = 2, 3, 6$.

C.2 Quartic: (7.3.26)

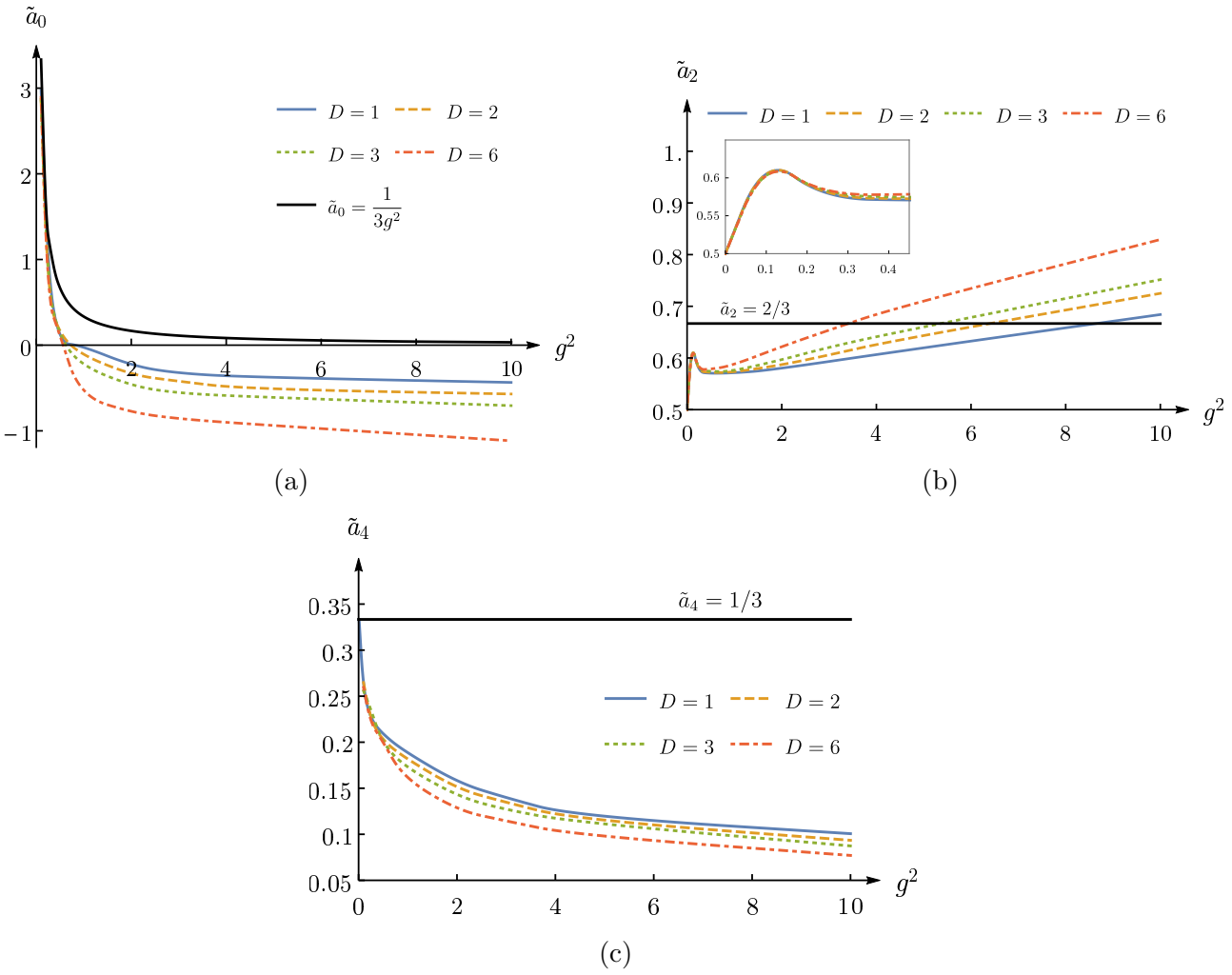

Figure C.2: Ground state: Variational parameters $\tilde{a}_0$ (a), $\tilde{a}_2$ (b) and $\tilde{a}_4$ (c) *vs* the coupling constant g for $D = 1, 2, 3, 6$. Parameters (7.3.28), which allow us to reproduce the first two terms G_0, G_2 in the expansion (4.4.1) shown by solid (black) line which is horizontal for $\tilde{a}_2$ (b) and $\tilde{a}_4$ (c).

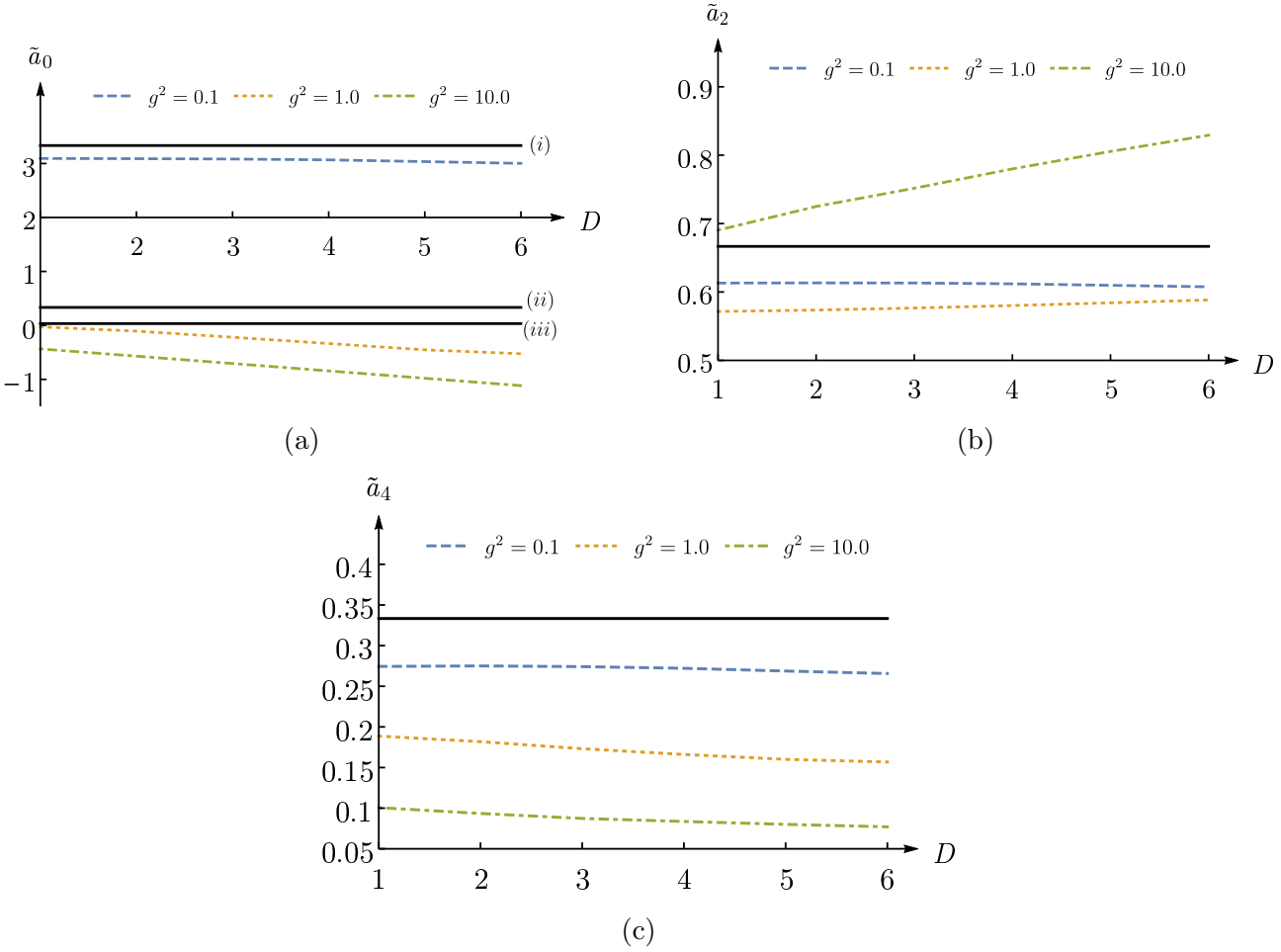

Figure C.3: Variational parameters $\tilde{a}_0$(a), $\tilde{a}_2$(b), $\tilde{a}_4$(c) *vs* D for fixed $g^2 = 0.1, 1, 10$. D-independent parameters (7.3.28), which allow us to reproduce the first two terms G_0, G_2 in the expansion (4.4.2), shown by solid (black) horizontal lines, see (7.3.28). In (a) the horizontal lines correspond to $\tilde{a}_0 = \frac{1}{3g^2}$ at $g^2 = 0.1(i), 1(ii), 10(iii)$.

C.3 Sextic: (7.4.27)

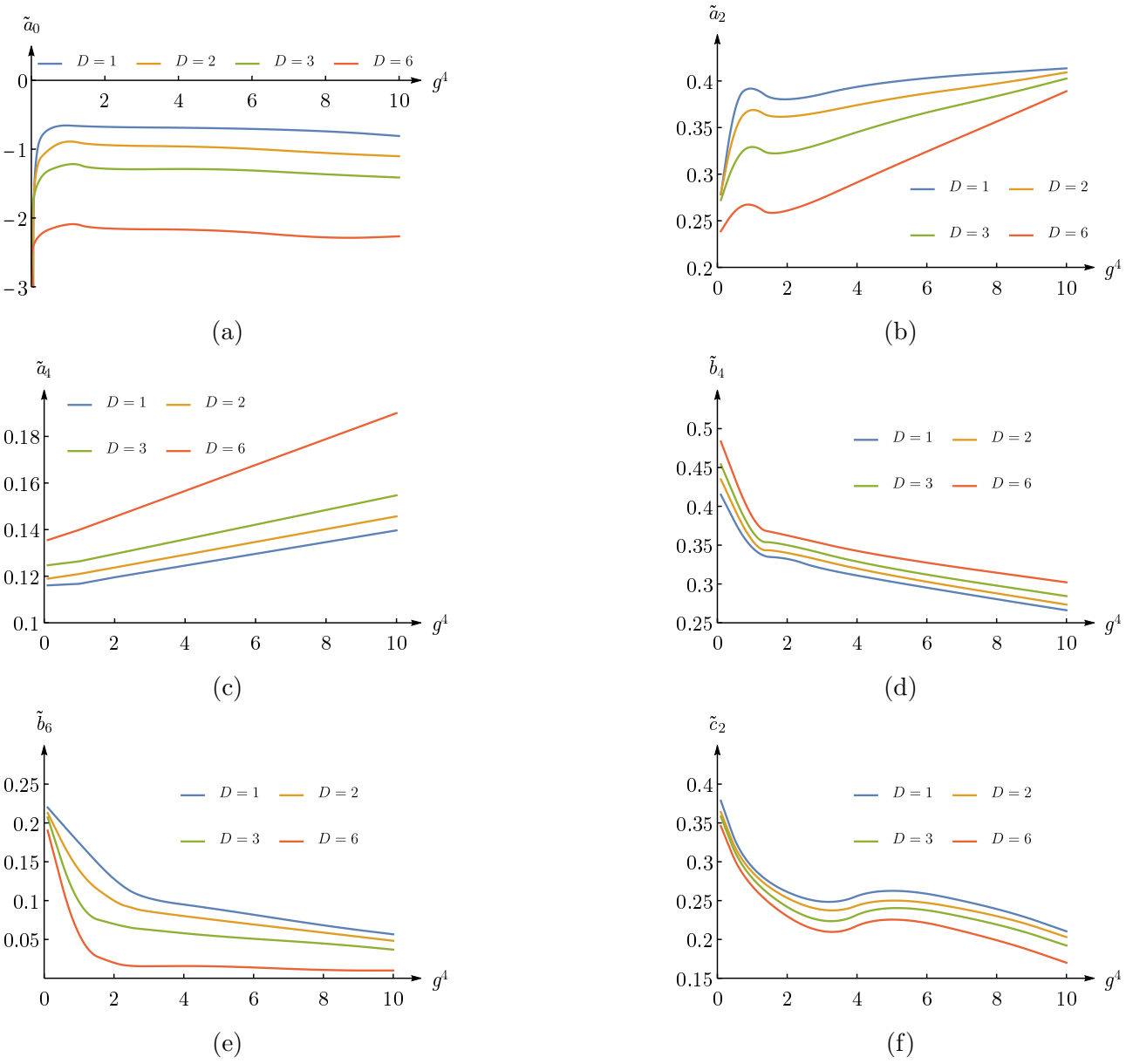

Figure C.4: Ground state $(0,0)$: Variational parameters $\tilde{a}_0$ (a), $\tilde{a}_2$ (b), $\tilde{a}_4$ (c), $\tilde{b}_4$ (d), $\tilde{b}_6$ (e), $\tilde{c}_2$ (f) *vs* the coupling constant g^4 in domain $g^4 \in [0, 10]$ for $D = 1, 2, 3, 6$.

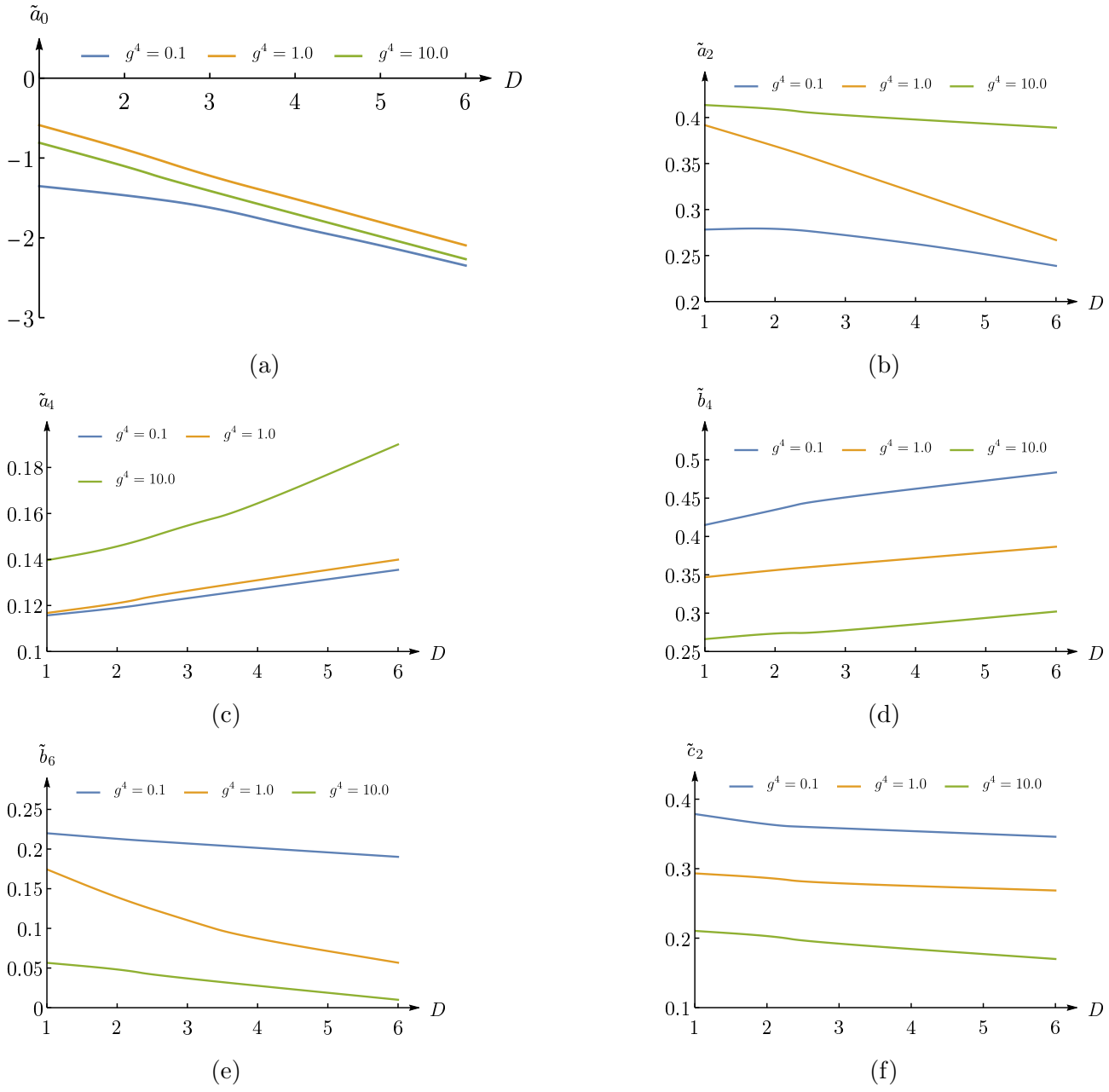

Figure C.5: Ground state $(0, 0)$: Variational parameters $\tilde{a}_0$ (a), $\tilde{a}_2$ (b), $\tilde{a}_4$ (c), $\tilde{b}_4$ (d), $\tilde{b}_6$ (e), $\tilde{c}_2$ (f) *vs* dimension D for $g^4 = 0.1, 1.0, 10.0$.

Appendix D

General Aspects of the Two-Term Radial Anharmonic Oscillator

Let us consider the general two-term radial anharmonic oscillator potential,

$$V(r) \;=\; r^2 \;+\; g^{m-2}r^m \;, \quad m \;>\; 2 \;. \tag{D.0.1}$$

cf. (3.2.1), where $a_2 = a_m = 1$ and $a_3, a_4, ..., a_{m-1} = 0$. Expansion of ε in powers of λ has the form

$$\varepsilon(\lambda) \;=\; \varepsilon_0 \;+\; \lambda^{m-2}\varepsilon_{m-2} \;+\; \lambda^{2(m-2)}\varepsilon_{2(m-2)} \;+\; ... \;, \tag{D.0.2}$$

see (4.1.5). Not surprisingly, for even potentials ($m = 2p$, $p = 1, 2, ...$) the PT coefficients $\varepsilon_{2n(p-1)}$, $n = 1, 2, ...$, are polynomials in D factorized as follows

$$\varepsilon_{2n(p-1)}(D) \;=\; D(D+2)(D+4)\ldots(D+2p-2)R_{(n-1)(p-1)}(D) \tag{D.0.3}$$

where $R_{(n-1)(p-1)}(D)$ is a polynomial in D of degree $(n-1)(p-1)$, see [29]. We emphasize that, in the framework of the Non-Linearization Procedure, any PT coefficient $\varepsilon_{2n(p-1)}(D)$ is calculated by linear algebra means. Series (D.0.2) is divergent due to a Dyson instability argument. It is evident that for larger D and m, the index of divergence is larger, see e.g. [93].

For potential (D.0.1) generating functions $G_0(r)$ and $G_2(r)$ can be written in closed form,

$$\frac{G_0(r)}{(2M)^{1/2}} \;=\; \frac{2}{m+2}r^2\left\{\sqrt{1+(gr)^{m-2}} + \frac{m-2}{4}\,{}_2F_1\left(\frac{1}{2}, \frac{2}{m-2}; \frac{m}{m-2}; -(gr)^{m-2}\right)\right\} \;, \tag{D.0.4}$$

$$\frac{g^2\,G_2(r)}{(2M)^{1/2}} \;=\; \frac{1}{4}\,\log\left[1+(gr)^{m-2}\right] \;+\; \frac{D}{m+2}\,\log\left[1+\sqrt{1+(gr)^{m-2}}\right] \;, \tag{D.0.5}$$

where ${}_2F_1$ is the hypergeometric function.

Appendix E

System of Coordinates $\{\rho, r, \varphi\}$

A general description of the non-orthogonal system of coordinates $\{\rho, r, \varphi\}$ is presented in this Appendix. Here we show some relevant expressions for the differentiation of a given function.

E.1 Definition

The system of coordinates $\{\rho, r, \varphi\}$, shown schematically in Fig. 10.1, is defined by the change of variables

$$\rho = \sqrt{x^2 + y^2} \tag{E.1.1}$$

$$r = \sqrt{x^2 + y^2 + z^2} \tag{E.1.2}$$

$$\varphi = \begin{cases} \arctan\left(\dfrac{y}{x}\right) & x > 0 \ , \ y > 0 \\ 2\pi + \arctan\left(\dfrac{y}{x}\right) & x > 0, \, y < 0 \\ \dfrac{\pi}{2}\mathrm{sgn}(y) & x = 0 \\ \pi + \arctan\left(\dfrac{y}{x}\right) & x < 0 \end{cases} \tag{E.1.3}$$

where $\{x, y, z\}$ denote Cartesian coordinates. The new system of coordinates is defined in the domain

$$0 \leq \rho \leq r \ , \qquad 0 \leq r < \infty \ , \qquad 0 \leq \varphi \leq 2\pi \ . \tag{E.1.4}$$

The change of variables presented in (E.1.1), (E.1.2) and (E.1.3) is unambiguously defined for the half-space $z \geq 0$.

Conversely, the Cartesian coordinates may be retrieved from (E.1.1), (E.1.2) and (E.1.3),

$$x \;=\; \rho\cos\varphi\;, \tag{E.1.5}$$

$$y \;=\; \rho\sin\varphi\;, \tag{E.1.6}$$

$$z \;=\; \sqrt{r^2-\rho^2}\;. \tag{E.1.7}$$

E.2 Differentiation

The Non-Linearization Procedure requires some expressions that involve differential operators; we present them below. The basic expressions come from the partial derivatives, for which a straightforward calculation via the chain rule indicates that

$$\partial_x \;=\; \cos\varphi\,\partial_\rho \;+\; \frac{\rho\cos\varphi}{r}\partial_r \;-\; \frac{\sin\varphi}{\rho}\partial_\varphi\;, \tag{E.2.1}$$

$$\partial_y \;=\; \sin\varphi\,\partial_\rho \;+\; \frac{\rho\sin\varphi}{r}\partial_r \;+\; \frac{\cos\varphi}{\rho}\partial_\varphi\;, \tag{E.2.2}$$

$$\partial_z \;=\; \frac{\sqrt{r^2-\rho^2}}{r}\partial_r\;. \tag{E.2.3}$$

Using these expressions, one can easily check that the Laplacian operator ∇^2 takes the form

$$\nabla^2 \;=\; \partial_\rho^2 \;+\; \frac{2\rho}{r}\partial_{\rho r} \;+\; \partial_r^2 \;+\; \frac{1}{\rho}\partial_\rho \;+\; \frac{2}{r}\partial_r \;+\; \frac{1}{\rho^2}\partial_\phi^2\;. \tag{E.2.4}$$

Another relevant quantity comes from the dot product of two gradients. Let us consider functions f and g written in variables (ρ, r, φ), explicitly

$$f \;=\; f(\rho, r, \varphi)\;, \qquad g \;=\; g(\rho, r, \varphi)\;. \tag{E.2.5}$$

A direct calculation using (E.2.1), (E.2.2), and (E.2.3), leads to

$$\nabla f\cdot\nabla g \;=\; \partial_\rho f\,\partial_\rho g \;+\; \partial_r\, f\partial_r g \;+\; \frac{\rho}{r}\left(\partial_r f\,\partial_\rho g \;+\; \partial_\rho f\,\partial_r g\right) \;+\; \frac{1}{\rho^2}\partial_\phi f\,\partial_\phi g\;. \tag{E.2.6}$$

Appendix F

Perturbation Theory for Hydrogen Atom in Constant Magnetic Field

F.1 Computational Code: Non-Linearization Procedure

Below it is presented in explicit form the Mathematica Notebook which realizes the Non-Linearization procedure for the hydrogen atom in presence of a uniform and constant magnetic field. The program is optimized to run it directly from the terminal/console.

```
(*This program calculates PT series of the enery and phase \
of hydrogen atom in magnetic field in its the ground state \
using the Non-Linerization procedure in variables (rho=s,r) *)


(* Load Module:  module load Mathematica/11.2 *)

(* Usage: math -noprompt -run < file.txt *)


(*-------------------------------------------------------*)
     (* Autor: Juan Carlos de Valle 2019(revisited)   *)
(*-------------------------------------------------------*)


(*-------------------------------------------------------*)

(*  Order (Input Data)  *)
m = 100;

(*-------------------------------------------------------*)

(* Initial Data *)
f[0] = r;

(*-------------------------------------------------------*)

(* Constraint *)

Do[
Subscript[Overscript[a, n], 0, 2*n + 1] = 0,
{n, 1, m}
];

(*-------------------------------------------------------*)

(*    ********************************************    *)
(*                    MAIN PROGRAM                     *)
(*    ********************************************    *)
(* Definitions *)
```

```
f[n_] :=
Expand[Sum[(Subscript[Overscript[A, n], k, j]*r \
+ Subscript[Overscript[B, n], k, j])*s^(2*(n - k))*r^(2*\
(k - j)),
{j, 0, n - 1}, {k, j, n}]];

Subscript[E, 0] = -1^2;

Q[1] := (1/4)*s^2;

Q[n_] :=
-Expand[Sum[D[f[k], s]*D[f[n - k], s] +
D[f[k], r]*D[f[n - k], r] + (s/r)*(D[f[k], s]*D[\
f[n - k], r] +
D[f[k], r]*D[f[n - k], s]), {k, 1, n - 1}]];

eq[n_] :=
Expand[D[f[n], s, s] + ((2*s)/r)*D[f[n], s, r] \
+
D[f[n], r, r] + (1/s - (2*s)/r)*D[f[n], s] +
2*(1/r - 1)*D[f[n], r] - Subscript[E, n] + Q[n]\
];


(*-------------------------------------------------------*)
(*                          OUTPUT                       *)
(*-------------------------------------------------------*)

Energy={};

(* Solving Algebraic Equations *)

Do[
sol = SolveAlways[eq[i] == 0, {r, s}];
Apply[Set, sol[[1]], {1}];
PrintTemporary[i];
AppendTo[Energy,{i,Subscript[E, i]}];
Export["Coefficients.dat", Energy],
{i, 1, m}
];
```

F.2 Corrections in Perturbation Theory

We present explicitly the first corrections ϕ_n, $n = 2, 3, 4$ in the expansion (11.1.1). Additionally, in Tables F.1 - F.2 high order corrections ε_n are shown. Finally, the first 10 coefficients in the expansion of the quadrupole moment, see (12.1.6), are displayed in Table F.3.

$$\begin{aligned}
-\phi_2(s,t) \;=\;& \frac{1}{1152}s^4t + \frac{1}{1440}s^2t^3 \\
&+ \frac{11}{4608}s^4 + \frac{13}{1440}s^2t^2 + \frac{1}{2880}t^4 \\
&+ \frac{193}{5760}s^2t + \frac{1}{120}t^3 \\
&+ \frac{193}{3840}s^2 + \frac{337}{5760}t^2
\end{aligned} \tag{F.2.1}$$

$$\begin{aligned}
\phi_3(s,t) \;=\;& \frac{1}{27648}s^6t + \frac{1}{11520}s^4t^3 + \frac{1}{60480}s^2t^5 \\
&+ \frac{7}{55296}s^6 + \frac{163}{138240}s^4t^2 + \frac{131}{241920}s^2t^4 + \frac{1}{181440}t^6 \\
&+ \frac{61}{11520}s^4t + \frac{8063}{1209600}s^2t^3 + \frac{53}{201600}t^5 \\
&+ \frac{803}{92160}s^4 + \frac{33311}{806400}s^2t^2 + \frac{2927}{604800}t^4 \\
&+ \frac{90877}{691200}s^2t + \frac{2027}{43200}t^3 \\
&+ \frac{90877}{460800}s^2 + \frac{188173}{691200}t^2
\end{aligned} \tag{F.2.2}$$

$$\begin{aligned}
-\phi_4(s,t) \;=\;& \frac{5}{2654208}s^8t + \frac{}{110592}s^6t^3 + \frac{163}{29030400}s^4t^5 + \frac{1}{2419200}s^2t^7 \\
&+ \frac{163}{21233664}s^8 + \frac{293}{2211840}s^6t^2 + \frac{9833}{58060800}s^4t^4 + \frac{727}{29030400}s^2t^6 + \frac{1}{9676800}t^8 \\
&+ \frac{8819}{13271040}s^6t + \frac{1663979}{812851200}s^4t^3 + \frac{24733}{40642560}s^2t^5 + \frac{167}{20321280}t^7 \\
&+ \frac{10577}{8847360}s^6 + \frac{13945163}{1083801600}s^4t^2 + \frac{22721}{2822400}s^2t^4 + \frac{5989}{22579200}t^6 \\
&+ \frac{27927329}{650280960}s^4t + \frac{29335139}{451584000}s^2t^3 + \frac{4828099}{1016064000}t^5 \\
&+ \frac{816005783}{13005619200}s^4 + \frac{1349713153}{4064256000}s^2t^2 + \frac{146213807}{2709504000}t^4 \\
&+ \frac{16222576613s^2t}{16257024000} + \frac{141801871t^3}{338688000} \\
&+ \frac{16222576613s^2}{10838016000} + \frac{36642046037t^2}{16257024000}
\end{aligned} \tag{F.2.3}$$

Table F.1: First ten coefficients ε_n (in rational form) of the series expansion for ε calculated in the Non-Linearization Procedure, see (11.1.1).

n	$(-1)^{n+1}\varepsilon_n$
0	1
1	1/2
2	53/96
3	5581/2304
4	21577397/1105920
5	31283298283/132710400
6	13867513160861/3538944000
7	5337333446078164463/62426972160000
8	995860667291594211123017/419509252915200000
9	866294634238659755927420474 23/1057163317346304000000
10	612787354461355179309164710303303 3/17760343731417907200000000

Table F.2: Coefficients ε_{10n}, $n = 1, 2, ..., 10$, of the series expansion for ε calculated in Non-Linearization Procedure, see (11.1.1). Coefficients rounded to 3 displayed d. d.

n	$-\varepsilon_{10n}$	n	$-\varepsilon_{10n}$
1	3.450×10^{9}	6	5.655×10^{140}
2	2.160×10^{29}	7	1.410×10^{173}
3	3.215×10^{53}	8	6.046×10^{206}
4	3.720×10^{80}	9	3.127×10^{241}
5	6.263×10^{109}	10	1.479×10^{277}

Table F.3: First ten coefficients $Q_{zz}^{(n)}$ of the series expansion in powers of γ^2 for Q_{zz}, see (12.1.6).

n	$(-1)^{n+1}Q_{zz}^{(n)}$
0	0
1	5/2
2	615/32
3	2564987/11520
4	19550772149/5529600
5	16195465214963/221184000
6	1664517172621593361/867041280000
7	3895122983853951241069/62426972160000
8	1209539248687613274458923081 3/4894274617344000000
9	434873002319633844492060165542746 7/37000716107120640000000
10	64695530270244255306557973308680286 4719/976818905227984896000000000

Appendix G

Computational Code: Hydrogen Atom in Magnetic Field

In this Appendix, the computational Hinb.f which performs the variational method using (12.0.3) as the trial function is explicitly shown. It uses the integration routine D01FCF from NAG-LIB as well as the minimization routine MINUIT of CERN-LIB. The input is data (such as magnetic field, domain of integrations, etc.) is written in *data sheet* as shown below.

```
Magnetic field (in units of B_0):    H    (change of vars in rho)
2.35D0
Number of regions in rho (nrho)  nrho+1 limits  (NUM / DEN)
2 2
Limits for rho NUM   (according to Number of Regions)
0.0  1.24  7.86
Limits for rho DEN
0.0  1.24  7.86
Number of regions in z  (nz)  nz+1 limits  (NUM / DEN)
3 3
Limits for z  (NUM)  (according to Number of Regions)
0.0D0 0.78   2.85    15.4
Limits for z  (DEN)
0.0D0 0.78   2.85    15.4
Default Acc. NUM/DEN,  Factor, Flag for corr., acc. for corr, screen=1/file=0
1.D-10    1.D-10        1.0D0         1           1.0D-02           1

SET TITLE
'Variational␣Energy␣for␣H␣in␣a␣magnetic␣field'
PARAMETERS
1  'a0=' 2.2425240         0.1     2.0    3.99
2  'a1=' 1.0104802         0.1     0.9    1.2
3  'a2='-0.2722381         0.01   -0.43   0.51
4  'a3=' 0.0411529         0.01    0.0    0.4
5  'a4=' 0.0545618         0.01   -0.1    0.2
6  'a5=' 0.0369813         0.01    0.0    0.057
7  'b1=' 0.0268046         0.01    0.0    0.03
8  'b2=' 0.0466748         0.01    0.0    0.1
9  'b3=' 0.0000000         0.01    0.00   0.06
10 'b4=' 0.0223345         0.01    0.0    0.8
11 'c␣=' 0.0833333         0.00    0.0    0.24
12 'd␣=' 2.0000000         0.0     0.9    2.8

set strategy 2
minimize
minimize 2000
stop
```

The main body of the program is presented in explicit form in the following pages.

```
c   Program HinB.f
c
c   Compile as: gfortran -o HinB.e HinB.f
c
c   or use g77 instead of gfortran
c
c   ***************************************************************
c                  H in a magnetic field
c                Juan Carlos del Valle
c              New Ansatz with w-variable
c
c   Bo = 2.35 x 10^9 G (ATOMIC UNIT OF MAGNETIC FIELD)
c
c   ***************************************************************
c
c   USAGE:  ./HinB.e < file.dat > file.out&
c
c
c   --- Using MINUIT from CERN-lib and
c
c   --- D01FCF INTEGRATION SUBROUTINE  NAG-lib
c
c
      PROGRAM MAIN
      IMPLICIT DOUBLE PRECISION (A-H,O-Z)
      COMMON / NINPUT3 / nrhoN, nrhoD, nzN, nzD, icorr
      COMMON / XINPUT2 / xB, EPSin, EPSid,  FCT, EPSC
      COMMON / XINPUT1 / RLN(5), RLD(5), ZLN(10), ZLD(10), EPNUM(20)
     $, EPDEN(20)
      COMMON / MONITOR / ebest, icall, icallb
      EXTERNAL FCN, futil
      icall  = 0
      icallb = 0
      ebest  = 1.D10
c
      read(5,*)     ! Magnetic Field strenght
      read(5,*)Bx   ! -> xB (in proper units)
      read(5,*)
      read(5,*)nrhoN, nrhoD  ! Number of regions in rho (NUM / DEN)
      read(5,*)
      read(5,*)(RLN(ir), ir=1,nrhoN+1)  ! rho Num limits
      read(5,*)
      read(5,*)(RLD(ir), ir=1,nrhoD+1)  ! rho Den limits
      read(5,*)
      read(5,*)nzN, nzD                 ! Number of regions in z (NUM / DEN)
      read(5,*)
      read(5,*)(ZLN(ir), ir=1,nzN+1)    ! z Num limits
      read(5,*)
      read(5,*)(ZLD(ir), ir=1,nzD+1)    ! z Den limits
      read(5,*)
      read(5,*)EPSin, EPSid, FCT, icorr, epsc, nscreen
c
      units=2.35D0      ! Our units (Proper definition of Ry)
      xB=Bx/units       ! Units conversion for B
c                       ! B in units of Bo=1/2.35
c                       ! See common DATOS
c
      if(nscreen.eq.0)then
      open(unit=6,file='minuit.out',status='unknown')
      end if
c
      write(6,*)
      write(6,*)'*****************************************************'
      write(6,*)'This program minimizes the variational Energy for '
      write(6,*)'Hatom in a magnetic field'
      write(6,*)'*****************************************************'
      write(6,*)
      write(6,*)'Magnetic Field Strength:', xB,' au (',Bx,' B_9 )'
      write(6,*)
      write(6,*)
c
      write(*,*)'LIMITS:'
      write(*,*)'-------------------------------------------------'
      write(*,*)
      write(*,*)(RLN(ir), ir=1,nrhoN+1)  ! rho Num limits
      write(*,*)
      write(*,*)(RLD(ir), ir=1,nrhoD+1)  ! rho Den limits
      write(*,*)
      write(*,*)(ZLN(ir), ir=1,nzN+1)    ! z Num limits
      write(*,*)
      write(*,*)(ZLD(ir), ir=1,nzD+1)    ! z Den limits
      write(*,*)
      write(*,*)'-------------------------------------------------'
      write(*,*)
      write(*,*)'EPS:', EPSin, EPSid
      write(*,*)'FACTOR:',FCT
      write(*,*)
c
c     "FLAT" DISTRIBUTION (SAME ACCURACY FOR ALL SUBINTERVALS)
      DO in= 1, 20  ! max regions = 20
      EPNUM(in) = EPSin
      EPDEN(in) = EPSid
      END DO
c
c
      5001   format(1x,5(F10.5,2x))
      5002   format(1x,4(F10.5,2x))
      5003   format(1x,2(F10.5,2x))
c
c     ----------------------------------------
c     Initializing Minuit
c     Establishing unit numbers for data input/output
c     ----------------------------------------
      ird=5          ! Fortran Unit number for reading
      iwr=6          ! Fortran Unit number for writing
      isav=7         ! Fortran Unit number for  saving
      call mninit(ird,iwr,isav)
c     ----------------------------------------
c      ++++++++++++++++++++++++++++++++++++++++
c       Calling to MINUIT
      CALL  MINUIT(FCN,futil)
c
      stop
      end   ! END MAIN PROGRAM
c
c     ***************************************************************
c
      subroutine futil()
      end
c
c     ***************************************************************
c
      SUBROUTINE FCN(NPAR,GR_FVAL,XV,IFLAG,FUTIL)
      IMPLICIT  DOUBLE PRECISION(A-H,O-Z)
      MINUIT parameters and common definitions
```

```
      DIMENSION GR(*),XV(*)
c      .. Parameters for the integration routine D01FCF ...
      INTEGER          NDIM,  MAXPTS,         LENWRK
      PARAMETER       (NDIM=2,MAXPTS=100000000,LENWRK=5000000)
c      .. LOCAL ARRAYS ...
      DOUBLE PRECISION ANUM(NDIM), BNUM(NDIM), ADEN(NDIM), BDEN(NDIM),
     $ WRKSTR(LENWRK), XNU(20), XDE(20)
c      .. COMMON BLOCK FOR INPUT DATA ...
      COMMON / NINPUT3 / nrhoN, nrhoD, nzN, nzD, icorr
      COMMON / XINPUT2 / xB, EPSin, EPSid,  FCT, EPSC
      COMMON / XINPUT1 / RLN(5), RLD(5), ZLN(10), ZLD(10), EPNUM(20)
     $, EPDEN(20)
      COMMON / MONITOR / ebest, icall, icallb
c      .. COMMON BLOCK  FOR WAVE FUNCTIONS PARAMETERS ...
      COMMON / PARM / B, a0, a1, a2, a3, a4, a5, b1, b2, b3, b4, c, d
      COMMON /FLAGS / iqflag
c      .. COMMON BLOCK FOR ABBREVIATIONS ...
      COMMON / ABBR / Bq2, SQRB, FCTR
c      .. INTRINSIC FUNCTIONS ...
      INTRINSIC   ABS
c      .. EXTERNAL FUNCTIONS ...
      EXTERNAL          D01FCF, EVARN, EVARD
c      .. EXECUTABLE STATEMENTS ...
c
      icall = icall + 1
      FVAL  = 0.0D0
      NCEN  = 1
c
c      USEFUL ABBREVIATIONS:   (COMMON)
c      ---------------------------------
      B      = xB
      Bq2    = B*B
      SQRB   = DSQRT(B)
      FCTR   = FCT
c      ---------------------------------
c
      RS = 1.0D0   ! Natural Size of the System set to 1 (H-atom)
c
c      ------------------------------------------------------------------
c      ASSIGNING MINUIT VARIABLES ( VARIATIONAL PARAMETERS )
c
      a0        =  XV(1)
      a1        =  XV(2)
      a2        =  XV(3)
      a3        =  XV(4)/B/B
      a4        =  XV(5)/B
      a5        =  XV(6)/B
      b1        =  XV(7)
      b2        =  XV(8)
      b3        =  XV(9)/B/B
      b4        =  XV(10)/B/B
      c         =  XV(11)
      d         =  XV(12)

c       INSERT COSTRAINTS HERE
      constraint = alpha+beta*B
      IF (constraint.LT.0.D0)then
      FVAL=XB
return
END IF
c
c                      *********************************
c                         VARIATIONAL ENERGY NUMERATOR
c                      *********************************
```

```
c
c
      if(icorr.eq.1)then
      write(*,*)
      write(*,*)
      write(*,*)
      write(*,*)'IREG,␣␣␣␣XNU(IREG),␣␣␣␣EPS,␣␣␣␣␣␣ACC,␣␣␣␣␣␣IFAIL'
      write(*,*)'-----------------------------------------------'
      end if
c
      enernu= 0.0D0
      quadm = 0.0D0
      IREG  = 0
      DO Irho = 1,nrhoN
      DO Iz = 1,nzN
      IREG = IREG+1
      EPS  = EPNUM(IREG)
c
c           NUMERATOR LIMITS    (1)= rho, (2)= z
      ANUM(1)  = RLN(Irho)
      BNUM(1)  = RLN(Irho+1)
      ANUM(2)  = ZLN(Iz)*RS
      BNUM(2)  = ZLN(Iz+1)*RS
c
      MINPTS = 0
      IFAIL  = 1
      FINVN  = 0.0D0
      XNU(IREG) = 0.0D0
c
      CALL D01FCF(NDIM,ANUM,BNUM,MINPTS,MAXPTS,EVARN,EPS,ACC,LENWRK,
     + WRKSTR,FINVN,IFAIL)
c
      XNU(IREG)=FINVN
c
      if(icorr.eq.1)then
      write(*,5004)IREG,XNU(IREG),EPS,ACC,IFAIL
      end if
      5004 format(1x,I4,2x,E12.6,2x,2(E8.3,2x),1x,I2)
c
      enernu = enernu + XNU(IREG)
c
c      ------------------------------------------------------------
c       In this section we calculate the quadrupole moment:
      iqflag = 1   ! flag to calculate Quadrupole Moment
      MINPTS = 0
      IFAIL  = 1
      FINVQ  = 0.0D0
c
      CALL D01FCF(NDIM,ANUM,BNUM,MINPTS,MAXPTS,EVARN,EPS,ACC,LENWRK,
     + WRKSTR,FINVQ,IFAIL)
c
      quadm = quadm + FINVQ
c
      iqflag=0   ! back to numer
c      ------------------------------------------------------------
c
      END DO
      write(*,*)
      END DO
c
c      END NUMERATOR CALCULATION
c      ************************************************************
c
c                      *********************************
```

```
c                        VARIATIONAL ENERGY DENOMINATOR
c                     ***********************************
c
      if(icorr.eq.1)then
      write(*,*)
      write(*,*)'IREG,␣␣␣XDE(IREG),␣␣␣␣EPS,␣␣␣␣␣␣ACC,␣␣␣␣␣␣IFAIL'
      write(*,*)'-----------------------------------------------'
      end if
c
      enerde=0.0D0
      IREG = 0
      DO Irho=1,nrhoD
      DO Iz=1,nzD
      IREG=IREG+1
      EPS  = EPDEN(IREG)
c          LIMITS FOR THE DENOMINATOR
      ADEN(1)   =  RLD(Irho)
      BDEN(1)   =  RLD(Irho+1)
      ADEN(2)   =  ZLD(Iz)*RS
      BDEN(2)   =  ZLD(Iz+1)*RS
c
      MINPTS = 0
      IFAIL  = 1
      FINVD  = 0.0D0
c
      CALL D01FCF(NDIM,ADEN,BDEN,MINPTS,MAXPTS,EVARD,EPS,ACC,LENWRK,
      + WRKSTR,FINVD,IFAIL)
c
      XDE(IREG)=FINVD
      if(icorr.eq.1)then
      write(*,5004)IREG,XDE(IREG),EPS,ACC,IFAIL
      end if
c
      enerde = enerde + XDE(IREG)
c
      END DO
      write(*,*)
      END DO
c
c      END DENOMINATOR CALCULATION
c      ****************************************************************
c
c      ************************
      FVAL = enernu/enerde
c      ************************
c      ************************
      if( FVAL .LE. ebest) then
      icallb = icall
      ebest  = FVAL
      end if
c
c
      quadmo = quadm/enerde
c
      write(*,*)
      write(*,*)
      write(*,*)'␣H-atom␣␣New␣Trial␣(31/07/19)␣␣␣␣␣␣␣␣␣␣␣call:␣',icall
      write(*,*)'****************************************************'
      write(*,*)'␣Variational␣Energy␣␣␣␣␣␣=',FVAL,'␣Ry'
      write(*,*)'␣Binding␣Energy␣␣␣␣␣␣␣␣␣␣=',(xB-FVAL),'␣Ry'
      write(*,*)'␣Magnetic␣Field␣Strength␣=', xB,'␣au'
      write(*,*)'␣␣␣␣␣␣␣␣␣␣␣␣␣␣␣␣␣␣␣␣␣␣␣␣␣(␣', xB*2.35D0,'␣␣B_9␣)'
      write(*,*)'␣Quadrupole␣Moment␣␣␣␣␣␣␣=',quadmo
      write(*,*)
```

```
      write(*,1010)'␣a0␣=',  a0
      write(*,1010)'␣a1␣=',  a1
      write(*,1010)'␣a2␣=',  a2
      write(*,1010)'␣a3␣=',  a3*B*B
      write(*,1010)'␣a4␣=',  a4*B
      write(*,1010)'␣a5␣=',  a5*B
      write(*,1010)'␣b1␣=',  b1
      write(*,1010)'␣b2␣=',  b2
      write(*,1010)'␣b3␣=',  b3*B*B
      write(*,1010)'␣b4␣=',  b4*B*B
      write(*,1010)'␣c␣␣=',  c
      write(*,1010)'␣d␣␣=',  d
      write(*,*)
      write(*,*)'*********************************************'
      write(*,*)'␣␣␣␣␣␣␣␣␣␣␣␣␣␣Ebest=',ebest,'␣call:',icallb
      write(*,*)
c
      1010 format(1x,1A12,1F18.14)
c
c                     ****************************
c                              CORRECTIONS
c                     ****************************
c
c
      if(icorr.eq.1)then
c
      write(*,*)'Calculating␣Relative␣Corrections␣...'
      write(*,*)'␣␣␣␣␣␣␣␣␣␣␣----------␣␣␣␣␣␣␣␣␣␣␣␣␣␣␣'
      write(*,*)
c      1) DeltaRHO NUMER
      ANUM(1)    = RLN(nrhoN+1)
      BNUM(1)    = 2.0D0*RLN(nrhoN+1)
      ANUM(2)    = ZLN(1)*RS
      BNUM(2)    = ZLN(nzN+1)*RS
      EPS        = EPSC
      MINPTS     = 0
      IFAIL      = 1
      FINV       = 0.0D0
      CALL D01FCF(NDIM,ANUM,BNUM,MINPTS,MAXPTS,EVARN,EPS,ACC,LENWRK,
      + WRKSTR,FINV,IFAIL)
      write(*,*)
      write(*,*)'Corrections␣in␣␣rho␣␣␣EPS␣␣␣␣␣␣␣␣␣ACC␣␣␣␣␣␣(NUMER)␣␣␣␣'
      write(*,5005)ABS(FINV/enernu),EPS,ACC
c
      write(*,*)'␣-------------------------------------------------'
c
c      2) DeltaRHO  DENOM
      ADEN(1)    =  RLD(nrhoD+1)
      BDEN(1)    =  2.0D0*RLD(nrhoD+1)
      ADEN(2)    =  ZLD(1)*RS
      BDEN(2)    =  ZLD(nZd+1)*RS
      EPS        = EPSC
      MINPTS     = 0
      IFAIL      = 1
      FINV       = 0.0D0
      CALL D01FCF(NDIM,ADEN,BDEN,MINPTS,MAXPTS,EVARD,EPS,ACC,LENWRK,
      + WRKSTR,FINV,IFAIL)
      write(*,*)
      write(*,*)'Corrections␣in␣␣rho␣␣EPS␣␣␣␣␣␣␣␣␣ACC␣␣␣␣␣␣␣(DENOM)␣␣␣␣'
      write(*,5005)ABS(FINV/enerde),EPS,ACC
c
      write(*,*)'␣-------------------------------------------------'
c
c      3) DeltaZ+ NUMER
```

```
      ANUM(1)    = RLN(1)
      BNUM(1)    = RLN(nrhoN+1)
      ANUM(2)    = ZLN(nzN+1)*RS
      BNUM(2)    = 2.0D0*ZLN(nzN+1)*RS
      EPS        = EPSC
      MINPTS     = 0
      IFAIL      = 1
      FINV       = 0.0D0
      CALL D01FCF(NDIM,ANUM,BNUM,MINPTS,MAXPTS,EVARN,EPS,ACC,LENWRK,
     + WRKSTR,FINV,IFAIL)
      write(*,*)
      write(*,*)'Corrections␣in␣␣z+␣␣␣␣EPS␣␣␣␣␣␣␣␣␣ACC␣␣␣␣␣␣(NUMER)␣␣␣␣'
      write(*,5005)ABS(FINV/enernu),EPS,ACC
c
      write(*,*)'-------------------------------------------------'
c
c     4) DeltaZ+ DENOM
      ADEN(1)    =  RLD(1)
      BDEN(1)    =  RLD(nrhoD+1)
      ADEN(2)    =  ZLD(nZD+1)*RS
      BDEN(2)    =  2.0D0*ZLD(nZD+1)*RS
      EPS        =  EPSC
      MINPTS     =  0
      IFAIL      =  1
      FINV       =  0.0D0
      CALL D01FCF(NDIM,ADEN,BDEN,MINPTS,MAXPTS,EVARD,EPS,ACC,LENWRK,
     + WRKSTR,FINV,IFAIL)
      write(*,*)
      write(*,*)'Corrections␣in␣␣z+␣␣␣␣EPS␣␣␣␣␣␣␣␣␣ACC␣␣␣␣␣␣(DENOM)␣␣␣␣'
      write(*,5005)ABS(FINV/enerde),EPS,ACC
c
      write(*,*)'␣-------------------------------------------------'
c
      end if
c
c
      5005 format(4x,3(E12.6,2x))
c
c      ***************** END CORRECTIONS **********************
c
      RETURN
      END
c      ++++++++++++++++++++++++++++++++++++++++++++++++++++++++++++
c                              END FCN
c
c                            *   *    *
c
c      ****************************************************************
c                            NUMERATOR BEGIN
c      ************************************************************
c              H-atom  in a Magnetic Field  (N=1 centers)
c      ************************************************************
c
c      This SUBROUTINE calculates the INTEGRAND of the ENERGY NUMERATOR
c
c      NOTES
c
c      -- Integration cylindrical coordinates: rho_e and z_e
c      -- Subroutine to be used by the NAG integration routine
c         D01FCF NAG-lib
c
      DOUBLE PRECISION FUNCTION EVARN(NDIM,XN)
      IMPLICIT DOUBLE PRECISION (A-H,O-Z)
c      ...ELECTRON COORDINATES (INTEGRATION VARIABLES)..
c      XN(1)=rhoe    XN(2)=z_e
      DIMENSION XN(NDIM)
c      ...DISTANCES FROM ELECTRON TO EACH CENTER AND OTHER VARIABLES
c      ...COMMON BLOCKS  WAVE FUNCTIONS PARAMETERS
      COMMON / PARM / B, a0, a1, a2, a3, a4, a5, b1, b2, b3, b4, c, d
c
      COMMON /FLAGS / iqflag
c
c      ...COMMON BLOCK FOR ABBREVIATIONS
      COMMON / ABBR / Bq2, SQRB, FCTR
c      .. Intrinsic Functions ..
      INTRINSIC                        DSQRT, DEXP, DCOS
c
c      ------------------------------------------------------------
c
      EVARN = 0.0D0
      ZERO  = 0.1D-10
      NCEN  = 1
c
c      ELECTRON COORDINATES
      rho    = XN(1)
      z      = XN(2)
c
c      ------------------------------------------------------------
c      Distances form the electron to the center:
c      ------------------------------------------------------------
c
      r  = DSQRT(rho**2+z**2)
c
c      Definitions:
c      ----------------------------
      gamma = B  ! magnetic field in a.u.
c
c      Definitions:
      w = dsqrt(1.d0+c*gamma**2*rho**2)
c
      phi = (a0+a1*r+a3*gamma**2*r**2+a4*gamma**2*rho**2+
     & a5*gamma**2*r*rho**2+a2*w)/dsqrt(1+b1*r+b3*gamma**2*r**2+
     & b4*gamma**2*rho**2+b2*w)
c
      pf=(1.d0+b1*r+b3*gamma**2*r**2+b4*gamma**2*rho**2+b2*w)**(-d/2.d0)
      Psi0=pf*dexp(-phi)
c
c
c
c      Quadrupole Moment
      if(iqflag.EQ.1)then
      EVARN=-Psi0*Psi0*(rho**2-2.0D0*z**2)*rho
      RETURN
      end if
c
c      *************** BLOCK FOR GEOMETRICAL TERMS ***************
c
c      ************************************************************
c
c      AUXILIARY FUNCTIONS
c
      w =  dsqrt(1.d0+c*gamma**2*rho**2)
c
      f1 = 1.d0+b1*r+b3*gamma**2*r**2+b4*gamma**2*rho**2+b2*sqrt(1.d0+
     &     c*gamma**2*rho**2)
c
c
c
```

```
c      PARTIAL DERIVATIVES
c
      pa20 = (gamma**2*(4.d0*f1**2*(2*a4+2*a5*r+
     & a2*c*(-((c*gamma**2*rho**2)/(1+c*gamma**2*rho**2)**1.5d0)+
     & 1/w))-2.d0*f1*(2*b4+b2*c*(-((c*gamma**2*rho**2)/(1+
     & c*gamma**2*rho**2)**1.5d0)+1/w))*(a0+a1*r+a3*gamma**2*r**2+
     & a4*gamma**2*rho**2+a5*gamma**2*r*rho**2+a2*w)+
     & (3.d0*gamma**2*rho**2*(a0+a1*r+a3*gamma**2*r**2+
     & a4*gamma**2*rho**2+a5*gamma**2*r*rho**2+a2*w)*(b2*c+
     & 2*b4*w)**2)/w**2-(4.d0*f1*gamma**2*rho**2*(b2*c+
     & 2*b4*w)*(a2*c+2*(a4+a5*r)*w))/w**2))/(4.d0*f1**2.5d0)
c
      pa10 = (gamma**2*rho*(2.d0*a2*c*f1+4.d0*f1*(a4+a5*r)*w-1.d0*(a0+
     & a1*r+a3*gamma**2*r**2+a4*gamma**2*rho**2+
     & a5*gamma**2*r*rho**2+a2*w)*(b2*c+
     & 2*b4*w)))/(2.d0*f1**1.5d0*w)
c
      pa02 = (8.d0*a3*f1**2*gamma**2-4.d0*f1*(b1+2*b3*gamma**2*r)*(a1+
     & gamma**2*(2*a3*r+a5*rho**2))-4.d0*b3*f1*gamma**2*(a0+a1*r+
     & a3*gamma**2*r**2+a4*gamma**2*rho**2+a5*gamma**2*r*rho**2+
     & a2*w)+3.d0*(b1+2*b3*gamma**2*r)**2*(a0+a1*r+a3*gamma**2*r**2
     & +a4*gamma**2*rho**2+a5*gamma**2*r*rho**2+
     & a2*w))/(4.d0*f1**2.5d0)
c
      pa01 = (2.d0*f1*(a1+gamma**2*(2*a3*r+a5*rho**2))-1.d0*(b1+
     & 2*b3*gamma**2*r)*(a0+a1*r+a3*gamma**2*r**2+
     & a4*gamma**2*rho**2+a5*gamma**2*r*rho**2+
     & a2*w))/(2.d0*f1**1.5d0)
c
      pa11 =(gamma**2*rho*(8.d0*a5*f1**2*w-2.d0*f1*(a1+gamma**2*(2*a3*r+
     & a5*rho**2))*(b2*c+2*b4*w)+3.d0*(b1+2*b3*gamma**2*r)*(a0+a1*r
     & +a3*gamma**2*r**2+a4*gamma**2*rho**2+a5*gamma**2*r*rho**2+
     & a2*w)*(b2*c+2*b4*w)-2.d0*f1*(b1+2*b3*gamma**2*r)*(a2*c+2*(a4
     & +a5*r)*w)))/(4.d0*f1**2.5d0*w)
c
c     ------------------------------------------------------
c                        HAMILTONIAN
c      -----------------------------------------------------
c
      VVi = ((-1.d0*b1**2*d*(2+d))/f1**2+(8.d0*b4*d*gamma**2)/f1-
     & 4.d0*pa01**2+4.d0*pa02-4.d0*pa10**2+4.d0*pa20-8.d0/r+
     & (8.d0*pa01)/r-(4.d0*b3**2*d*(2+d)*gamma**4*r**2)/f1**2+
     & (4.d0*pa10)/rho-(8.d0*b4*d*gamma**2*pa10*rho)/f1-
     & (8.d0*pa01*pa10*rho)/r+(8.d0*pa11*rho)/r+gamma**2*rho**2-
     & (8.d0*b4**2*d*gamma**4*rho**2)/f1**2-
     & (4.d0*b4**2*d**2*gamma**4*rho**2)/f1**2-
     & (8.d0*b4*d*gamma**2*pa01*rho**2)/(f1*r)-
     & (2.d0*b2*c**2*d*gamma**4*rho**2)/(f1*(1+
     & c*gamma**2*rho**2)**1.5d0)-
     & (2.d0*b2**2*c**2*d*gamma**4*rho**2)/(f1**2*w**2)-
     & (1.d0*b2**2*c**2*d**2*gamma**4*rho**2)/(f1**2*w**2)+
     & (4.d0*b2*c*d*gamma**2)/(f1*w)-
     & (4.d0*b2*c*d*gamma**2*pa10*rho)/(f1*w)-
     & (8.d0*b2*b4*c*d*gamma**4*rho**2)/(f1**2*w)-
     & (4.d0*b2*b4*c*d**2*gamma**4*rho**2)/(f1**2*w)-
     & (4.d0*b2*c*d*gamma**2*pa01*rho**2)/(f1*r*w)-
     & (4.d0*b3*d*gamma**2*(b2*c*(2+d)*gamma**2*rho**2+2*b4*(2.d0+
     & d)*gamma**2*rho**2*w+f1*(-3+2*pa01*r+
     & 2*pa10*rho)*w))/(f1**2*w)-(2.d0*b1*d*(b2*c*(2+
     & d)*gamma**2*rho**2+2.d0*(f1*(-1.d0+pa01*r+pa10*rho)+(2+
     & d)*gamma**2*(b3*r**2+b4*rho**2))*w))/(f1**2*r*w))/4.d0
c
      EVARN = VVi*Psi0*Psi0*rho
      RETURN
      END
c     ************************************************************
c                          DENOMINATOR BEGIN
c     ************************************************************
c           H-atom in a Magnetic Field  (N=1 centers)
c     ************************************************************
c
c     This SUBROUTINE calculates the INTEGRAND of the ENERGY NUMERATOR
c
c     NOTES
c
c     -- Uses cylindrical coordinates
c     -- Subroutine to be used by the NAG integration routine
c        D01FCF NAG-lib
c
      DOUBLE PRECISION FUNCTION EVARD(NDIM,XD)
      IMPLICIT DOUBLE PRECISION (A-H,O-Z)
      DIMENSION XD(NDIM)
c      ...COMMON BLOCKS  WAVE FUNCTIONS PARAMETERS
      COMMON / PARM / B, a0, a1, a2, a3, a4, a5, b1, b2, b3, b4, c, d
c      ...COMMON BLOCK FOR ABBREVIATIONS
      COMMON / ABBR / Bq2, SQRB, FCTR
c      .. Intrinsic Functions ..
      INTRINSIC                        DSQRT, DEXP , DCOS
c
      EVARD = 0.0D0
      ZERO  = 0.1D-10
      NCEN  = 1
c
c     ELECTRON COORDINATES
      rho    = XD(1)
      z      = XD(2)
c
c      ---------------------------------------------------------------
c      Distances form the electron to the center:
c      ---------------------------------------------------------------
c
      r  = DSQRT(rho**2+z**2)
c
c     Definitions:
c      ----------------------------
      gamma = B  ! magnetic field in a.u.
c
c     Definitions:
      w = dsqrt(1.d0+c*gamma**2*rho**2)
c
      phi = (a0+a1*r+a3*gamma**2*r**2+a4*gamma**2*rho**2+
     & a5*gamma**2*r*rho**2+a2*w)/dsqrt(1+b1*r+b3*gamma**2*r**2+
     & b4*gamma**2*rho**2+b2*w)
c
      pf=(1.d0+b1*r+b3*gamma**2*r**2+b4*gamma**2*rho**2+b2*w)**(-d/2.d0)
      Psi0=pf*dexp(-phi)

c
c   Energy Denominator
      EVARD = Psi0*Psi0*rho
c
c
      RETURN
      END
c
c                       END OF MAIN PROGRAM
c
c
```

Appendix H

Lagrange-Mesh Method for Hydrogen Atom in Magnetic Field: Code

Below it is presented in explicit form the Mathematica Notebook which implements the Lagrange Mesh Method for the hydrogen atom in presence of a uniform and constant magnetic field. The program is optimized to run it directly from the terminal/console.

```
(*This program caculates the energy, wave function,    \
quadrupo lemoment and cusp parameter of the first      \
bound states of the Hydrogen atom in  magnetic field  *)

(*    Load module:  module load Mathematica/11.2      *)

(*       Usage: math -noprompt -run < file.txt        *)

(*Author: Juan Carlos del Valle Nov 19 2019(revisited)*)

(*    ****************************************    *)
                  (*Initial Data Here*)
(*    ****************************************    *)


(*-------------------------------------------------------*)
(*Magnetic Quantum Number*)

m=0;

(*-------------------------------------------------------*)
(*Basis*)

Nr=80;
Ntheta=200;

(*-------------------------------------------------------*)
(*Scaling Parameter*)

h=0.005;

(*-------------------------------------------------------*)
(*Potential*)

V[r_,u_]:= - 2/r + 1/4 gamma^2 (1-u^2)r^2

(*-------------------------------------------------------*)
(*Parity [+1,-1]*)

p=1;

(*-------------------------------------------------------*)

(*Magnetic Field*)

gamma=4000;

(*-------------------------------------------------------*)
```

```
(*Tolerance in Float Numbers*)

dx=0.000000000000000001;
(*-------------------------------------------------------*)
(*    ****************************************    *)
(*                    MAIN PROGRAM                     *)
(*    ****************************************    *)
(*Matrix Elements*)

sols1=NSolve[LaguerreL[Nr,x]==0,x,WorkingPrecision->50];

k=0;

sols1/.{r__Rule}:>Set@@@({r}/.var:x->Subscript[var,++k]);

Clear[k]

(*Ra ces de los polimonios de Legendre*)
sols2=NSolve[LegendreP[Ntheta+Abs[m],Abs[m],u]==0&&\
0<=u<1,u,WorkingPrecision->50];
k=0;

sols2/.{r__Rule}:>Set@@@({r}/.var:u->Subscript[var,++k]);

Do[Subscript[u, -i]=-Subscript[u, i],{i,1,Ntheta/2}]

(*Radial Kinetic Elements*)
Do[For[i=1,i<j,i++,t[i,j]=(-1)^(i-j) (Subscript[x, i]\
+Subscript[x, j])/((Subscript[x, i] Subscript[x, j])^(1/2)\
(Subscript[x, i]-Subscript[x, j])^2);t[j,i]=t[i,j]],{j,1,Nr}];

Do[t[i,i]=(4+(4Nr+2)Subscript[x, i]-Subscript[x, i]^2)\
/(12 Subscript[x, i]^2),{i,1,Nr}];

Clear[i]

(*Angular Kinetic Elements*)
Do[For[i=1,i<j,i++,s[i,j]=(-1)^(i-j) (2(1-Subscript[u, i]^2)\
^(1/2)(1-Subscript[u, j]^2)^(1/2))/(Subscript[u, i]-\
Subscript[u, j])^2;s[j,i]=s[i,j]],{j,1,Ntheta/2}];

Do[s[i,-j]=-(-1)^(i+j) (2(1-Subscript[u, i]^2)^(1/2)\
(1-Subscript[u, -j]^2)^(1/2))/(Subscript[u, i]-\

Subscript[u, -j])^2,{i,1,Ntheta/2},{j,1,Ntheta/2}];

Do[s[i,i]=1/3 (Ntheta+Abs[m])(Ntheta+Abs[m]+1)+(2(m^2-1))\
/(3(1-Subscript[u, i]^2)),{i,1,Ntheta/2}];
```

```
Clear[i]


(*               BLOCK FOR HAMILTONIAN                *)

f[n_,k_]:=(k-1)Nr+n


(*Kinetic Elements*)

T[a_,b_,c_,d_]:=2 1/2 (t[a,c]KroneckerDelta[b,d]+1/\
Subscript[x, a]^2 (s[b,d]+ ps[b,-d])KroneckerDelta[a,c])

Do[Subscript[TT, f[a,b],f[c,d]]=T[a,b,c,d],{a,1,Nr},\
{b,1,Ntheta/2},{c,1,Nr},{d,1,Ntheta/2}]


(*Potential Elements*)

V[a_,b_,c_,d_]:=V[h Subscript[x, a],Subscript[u, b]]\
KroneckerDelta[a,c]KroneckerDelta[b,d]

Do[Subscript[VV, f[a,b],f[c,d]]=V[a,b,c,d],{a,1,Nr},\
{b,1,Ntheta/2},{c,1,Nr},{d,1,Ntheta/2}]


(*Building the Hamiltonian and Diagonalization*)

Ham=Table[Table[ 1/h^2 Subscript[TT, i,j]+ Subscript\
[VV, i,j],{j,1,Nr Ntheta/2}],{i,1,Nr Ntheta/2}];

epsilon=-1+Eigenvalues[IdentityMatrix[(Ntheta
Nr)/2]+Ham,-1,Method->{"Arnoldi","Criteria"\
->"RealPart",MaxIterations->10000000}][[1]];


(*Coefficients for EigenFunctions*)

CF=Eigenvectors[Ham+IdentityMatrix[(Ntheta Nr)/2],-1,\
Method->{"Arnoldi","Criteria"->"RealPart",MaxIterations\
->10000000}];

Do[Subscript[c, (1-r)*Nr+s,r]=Rationalize[CF[[1]][[s]],dx]\
, {r,1,Ntheta/2}, {s,Nr*(r-1)+1,r*Nr}];

(*Quadrupole Moment*)

z2=h*h*2*Sum[Subscript[c, i, j]^2*Subscript[x, i]^2*\
Subscript[u, j]^2,{i,1,Nr},{j, 1,Ntheta/2}];

r2=h*h*Sum[Subscript[c, i, j]^2*Subscript[x, i]^2*\
(1-Subscript[u, j]^2), {i, 1,Nr},{j, 1,Ntheta/2}];
```

```
Q=z2-r2;


Export["B" <> ToString[N[gamma]] <> "_cf.dat", CF[[1]]];


(*Cusp Parameter*)

f[r_, i_] := ((-1)^i*(LaguerreL[Nr, r]/(r - Subscript\
[x, i]))*Exp[-(r/2)])/Subscript[x, i]^2^(-1)

df[y_, i_] := D[((-1)^i*(LaguerreL[Nr, r]/(r - \
Subscript[x, i]))*Exp[-(r/2)])/Subscript[x, i]^2^(-1), r]\
/. r -> y

CuspN=Sum[f[0, i]*df[0, n]*Subscript[c, i, j]*\
Subscript[c, n, j],{i,1,Nr}, {j,1,Ntheta/2}, {n,1,Nr}];

CuspD=Sum[f[0, i]*f[0, n]*Subscript[c, i, j]*Subscript\
[c, n, j], {i,1,Nr}, {j,1,Ntheta/2}, {n,1,Nr}];

Cusp= CuspN/(h*CuspD);


(*                          OUTPUT                       *)

fileName = "B"<>ToString[N[gamma]]<>".dat";

file = OpenWrite[fileName, PageWidth -> Infinity];

WriteString[file,"␣*****************************\n␣"];
WriteString[file,"Hydrogen␣Atom␣in␣Magnetic␣Field␣\n␣"];
WriteString[file,"␣␣␣␣in␣Lagrange␣Mesh␣Method␣␣␣␣␣\n␣"];
WriteString[file,"*****************************\n␣"];
WriteString[file,"␣␣␣␣␣␣␣␣␣␣␣␣␣␣␣␣␣␣␣␣␣␣␣␣␣␣␣␣␣␣␣␣␣\n␣"];
WriteString[file,"␣␣Q.␣␣number␣m␣=␣"<>ToString[m]"\n" ];
WriteString[file,"␣␣␣␣␣␣␣␣␣␣␣␣␣␣␣␣␣␣␣␣␣␣␣␣␣␣␣␣␣␣␣␣␣\n␣"];
WriteString[file,"..............................\n␣"];
WriteString[file,<>ToString[Nr]<>"x"<>ToString[Ntheta]"\n"];
WriteString[file,"␣␣␣␣Scaling␣" <>ToString[N[h]]<>"\n"];
WriteString[file,"..............................\n␣"];
WriteString[file,"␣␣␣␣␣␣␣␣␣␣␣␣␣␣␣␣␣␣␣␣␣␣␣␣␣␣␣␣␣␣␣␣␣\n␣"];
WriteString[file,"Energy␣=␣"<>ToString[epsilon]<>"\n\"];
WriteString[file,"␣␣␣␣␣␣␣␣␣␣␣␣␣␣␣␣␣␣␣␣␣␣␣␣␣␣␣␣␣␣␣␣␣\n␣"];
WriteString[file,"QM="<>ToString[NumberForm[Q,16]]<>"\\␣n"];
WriteString[file,"␣␣␣␣␣␣␣␣␣␣␣␣␣␣␣␣␣␣␣␣␣␣␣␣␣␣␣␣␣␣␣␣␣\n␣"];
WriteString[file,"␣␣Cusp␣Par.␣=␣"<>ToString[Cusp]"\n␣"];
WriteString[file,"..............................\n␣"];

Close[file]
```

Appendix I

Plots of Variational Parameters: Hydrogen Atom in Magnetic Field

Plots of the optimal variational parameters $\{\alpha_{0,1,2,3,4}, \beta_{1,2,3}\}$ for Approximant (12.0.3) as functions of $\log(1+\gamma^2)$ are shown below.

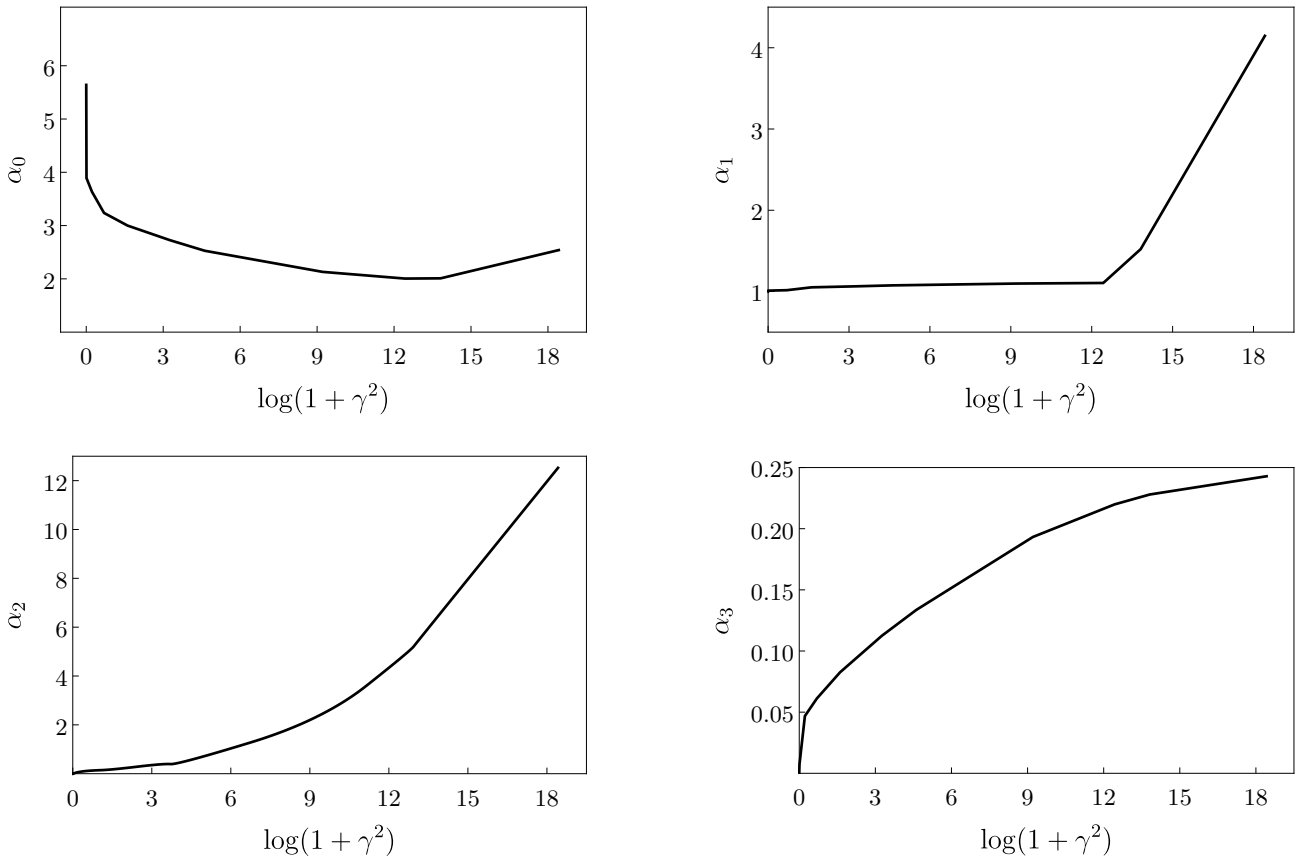

Figure I.1: Optimal variational parameters $\{\alpha_0, \alpha_1, \alpha_2, \alpha_3\}$ of the Approximant (12.0.3) as functions of $\log(1+\gamma^2)$.

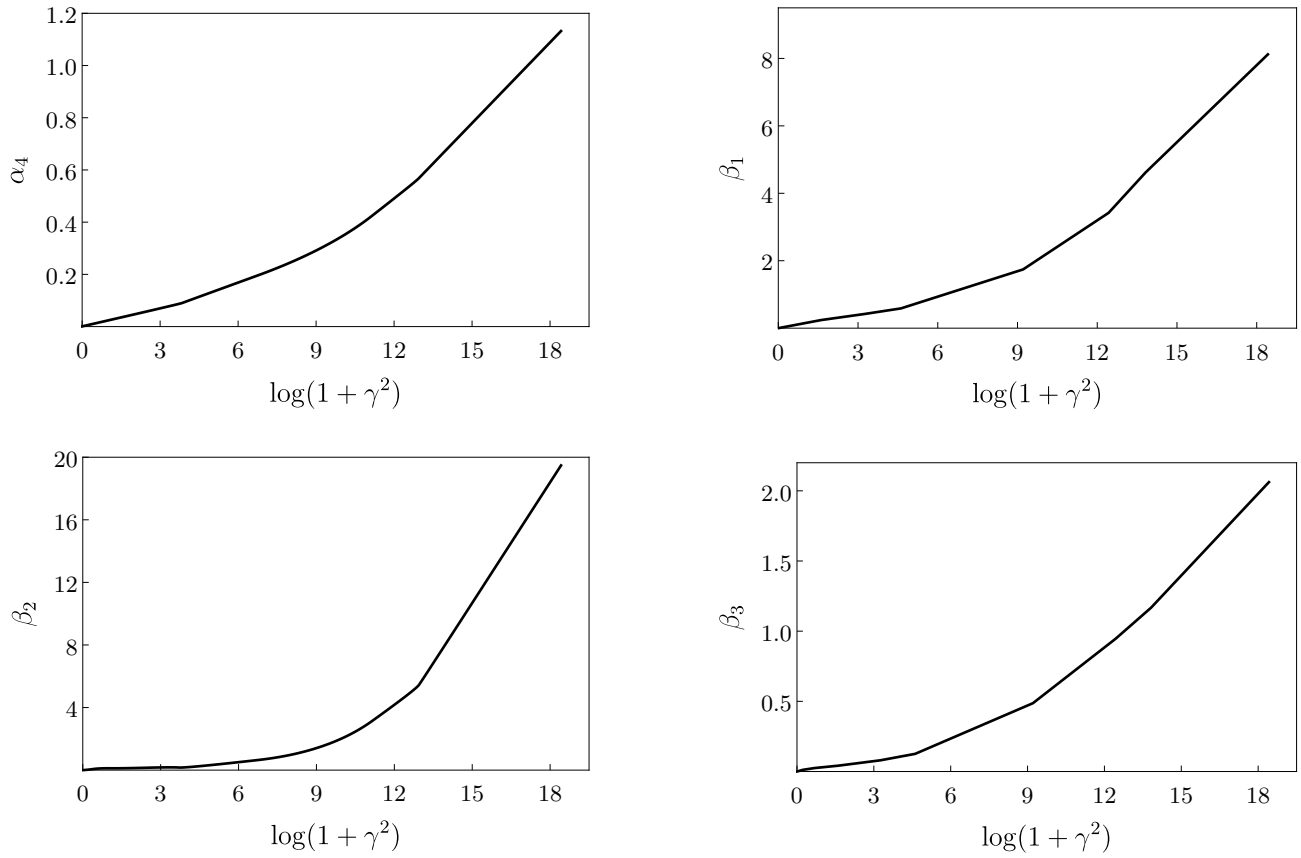

Figure I.2: Optimal variational parameters $\{\alpha_4, \beta_1, \beta_2, \beta_3\}$ of the Approximant (12.0.3) as functions of $\log(1+\gamma^2)$.

Bibliography

[1] L. D. Landau and M. Lifshitz, *Quantum Mechanics, Non-Relativistic Theory*. Pergamon, 1977.

[2] J. J. Sakurai and J. Napolitano, *Modern quantum mechanics; 2nd ed.* San Francisco, CA: Addison-Wesley, 2011.

[3] D. Griffiths, *Introduction of Quantum Mechanics*. Prentice Hall, Inc., 1995.

[4] P. M. Morse and H. Feshbach, "Methods of theoretical physics," *American Journal of Physics*, vol. 22, no. 6, pp. 410–413, 1954.

[5] A. V. Turbiner and J. C. López-Vieyra, *Notas del Curso: La Ecuación de Schrödinger: Teoría y práctica* . Unpublished, 2014.

[6] T. Kato, "On the eigenfunctions of many-particle systems in quantum mechanics," *Commun. Pure Appl. Math.*, vol. 10, 1957.

[7] A. V. Turbiner, "A new approach to the eigenvalue problem in quantum mechanics: Convergent perturbation theory for rising potentials," *J. Phys. A*, vol. 14, no. 7, p. 1641, 1981.

[8] A. V. Turbiner, "The eigenvalue spectrum in quantum mechanics and the nonlinearization procedure," *Phys. Usp.*, vol. 27, no. 9, p. 668, 1984.

[9] J. C. del Valle and A. V. Turbiner, "Radial anharmonic oscillator: Perturbation theory, new semiclassical expansion, approximating eigenfunctions. I. Generalities, cubic anharmonicity case," *Int. J. Mod. Phys. A*, vol. 34, no. 26, p. 1950143, 2019.

[10] J. C. del Valle and A. V. Turbiner, "Radial anharmonic oscillator: Perturbation theory, new semiclassical expansion, approximating eigenfunctions. II. Quartic and sextic anharmonicity cases," *International Journal of Modern Physics A*, vol. 35, no. 01, p. 2050005, 2020.

[11] A. V. Turbiner, M. A. Escobar-Ruiz, and J. C. del Valle, Work in progress.

[12] W. Heisenberg, "Über quantentheoretische Umdeutung kinematischer und mechanischer Beziehungen," *Z. Physik*, vol. 33, no. 1, pp. 879–893, 1925.

[13] E. Schrödinger, "An Undulatory Theory of the Mechanics of Atoms and Molecules," *Phys. Rev.*, vol. 28, pp. 1049–1070, 1926.

[14] E. C. Brinsmade, J. B.; Kemble, "The occurrence of harmonics in the infra-red absorption spectra of diatomic gases," *Proc. Natl. Acad. Sci. U.S.A.*, vol. 3, 1917.

[15] J. L. Dunham, "Intensities in the harmonic band of hydrogen chloride," *Phys. Rev. (Series I)*, vol. 34, 1929.

[16] P. M. Morse and E. C. G. Stueckelberg, "Diatomic molecules according to the wave mechanics I: Electronic levels of the hydrogen molecular ion," *Phys. Rev. (Series I)*, vol. 33, 1929.

[17] P. M. Morse, "Diatomic molecules according to the wave mechanics. II. Vibrational levels," *Phys. Rev.*, vol. 34, pp. 57–64, 1929.

[18] E. C. Kemble, "On the energy required to split HCI into atomic ions," *J. Opt. Soc. Am. (1917-1983)*, vol. 12, no. 1, p. 1, 1926.

[19] E. Fues, "Das Eigenschwingungsspektrum zweiatomiger Moleküle in der Undulationsmechanik," *Ann. Phys.*, vol. 385, no. 12, pp. 367–396, 1926.

[20] C. M. Bender and T. T. Wu, "Anharmonic Oscillator," *Phys. Rev.*, vol. 184, pp. 1231–1260, 1969.

[21] C. M. Bender, "Generalized anharmonic oscillator," *J. Math. Phys.*, vol. 11, 1970.

[22] C. M. Bender and T. T. Wu, "Anharmonic Oscillator. II. A Study of Perturbation Theory in Large Order," *Phys. Rev. D*, vol. 7, pp. 1620–1636, 1973.

[23] A. V. Turbiner, "Anharmonic oscillator and double-well potential: approximating eigenfunctions," *Lett. Math. Phys.*, vol. 74, no. 2, pp. 169–180, 2005.

[24] A. V. Turbiner, "Double well potential: perturbation theory, tunneling, WKB, (beyond instantons)," *Int. J. Mod. Phys. A*, vol. 25, pp. 647–658, 2010.

[25] H. Taşeli and R. Eid, "Eigenvalues of the two-dimensional Schrödinger equation with nonseparable potentials," *Int. J. Quantum Chem.*, vol. 59, no. 3, pp. 183–201, 1996.

[26] E. J. Weniger, "A convergent renormalized strong coupling perturbation expansion for the ground state energy of the quartic, sextic, and octic anharmonic oscillator," *Ann. Phys.*, vol. 246, no. 1, pp. 133–165, 1996.

[27] S. Graffi, V. Grecchi, and B. Simon, "Borel Summability: Application to the anharmonic oscillator," *Phys. Lett. B*, vol. B 32, pp. 631–634, 1970.

[28] H. J. Silverstone, J. G. Harris, J. Čížek, and J. Paldus, "Asymptotics of high-order perturbation theory for the one-dimensional anharmonic oscillator by quasisemiclassical methods," *Phys. Rev. A*, vol. 32, pp. 1965–1980, 1985.

[29] V. Eletsky and V. Popov, "On perturbation theory for the gr^{2N}anharmonic oscillator," *Phys. Lett. B*, vol. 94, no. 1, pp. 65 – 68, 1980.

[30] F. M. Fernández and R. Guardiola, "The strong coupling expansion for anharmonic oscillators," *J. Phys. A*, vol. 30, no. 20, p. 7187, 1997.

[31] J. Loeffel, A. Martin, B. Simon, and A. Wightman, "Pade approximants and the anharmonic oscillator," *Phys. Lett. B*, vol. 30, no. 9, pp. 656 – 658, 1969.

[32] M. R. M. Witwit, "Energy levels of a two-dimensional anharmonic oscillator: Hill determinant approach," *Pramana*, vol. 41, no. 6, pp. 493–502, 1993.

[33] S. N. Biswas *et al.*, "The Hill determinant: an application to the anharmonic oscillator," *Phys. Rev. D*, vol. 4, pp. 3617–3620, 1971.

[34] M. Tater and A. V. Turbiner, "Failure of the Hill determinant method for a sextic anharmonic oscillator," *J. Phys. A*, vol. 26, pp. 697–710, 1993.

[35] P. Lu, "WKB Calculation of the Energy Levels of Anharmonic Oscillators," *J. Chem. Phys.*, vol. 47, no. 2, pp. 815–817, 1967.

[36] F. Hioe, D. Macmillen, and E. Montroll, "Quantum theory of anharmonic oscillators: Energy levels of a single and a pair of coupled oscillators with quartic coupling," *Phys. Rep.*, vol. 43, no. 7, pp. 305 – 335, 1978.

[37] E. Yukalova and V. Yukalov, "Self-similar approximation for an anharmonic oscillator of arbitrary dimensionality," *Phys. Lett. A*, vol. 175, no. 1, pp. 27 – 35, 1993.

[38] N. Ari and M. Demiralp, "Energy levels of a two-dimensional anharmonic oscillator: Characteristic function approach," *J. Math. Phys.*, vol. 26, no. 6, pp. 1179–1185, 1985.

[39] A. D. Dolgov and V. S. Popov, "The anharmonic oscillator and its dependence on space dimensions," *Phys. Lett.*, vol. 86B, pp. 185–188, 1979.

[40] D. J. Doren and D. R. Herschbach, "Spatial dimension as an expansion parameter in quantum mechanics," *Phys. Rev. A*, vol. 34, pp. 2654–2664, 1986.

[41] C. Müller, *Spherical Harmonics*. Springer-Verlag, 1966.

[42] C. Efthimiou and C. Frye, *Spherical Harmonics in p Dimensions*. World Scientific, 2014.

[43] K. D. Granzow, "N-Dimensional total orbital angular-momentum operator," *J. Math. Phys.*, vol. 4, no. 7, pp. 897–900, 1963.

[44] M. A. Escobar-Ruiz, E. Shuryak, and A. V. Turbiner, "Fluctuations in quantum mechanics and field theories from a new version of semiclassical theory.," *Phys. Rev. D*, vol. 93, p. 105039, 2016.

[45] M. A. Escobar-Ruiz, E. Shuryak, and A. V. Turbiner, "Fluctuations in quantum mechanics and field theories from a new version of semiclassical theory. II," *Phys. Rev. D*, vol. 96, p. 045005, 2017.

[46] E. Shuryak and A. V. Turbiner, "Transseries for the ground state density and generalized Bloch equation: Double-well potential case," *Phys. Rev. D*, vol. 98, p. 105007, 2018.

[47] J. C. del Valle and D. J. Nader, "Toward the theory of the Yukawa potential," *J. Math. Phys.*, vol. 59, no. 10, p. 102103, 2018.

[48] R. Lynch and H. Mavromatis, "N-dimensional harmonic oscillator yields monotonic series for the mathematical constant π," *J. Comput. Appl. Math.*, vol. 30, no. 2, pp. 127–137, 1990.

[49] T. I. Banks and C. M. Bender, "Anharmonic oscillator with polynomial self-Interaction," *J. Math. Phys.*, vol. 13, no. 9, pp. 1320–1324, 1972.

[50] F. Dyson, "Divergence of Perturbation Theory in Quantum Electrodynamics," *Phys. Rev.*, vol. 85, pp. 631–632, 1952.

[51] J. Killingbeck, "Renormalised perturbation series," *J. Phys. A*, vol. 14, no. 5, p. 1005, 1981.

[52] A. V. Turbiner and A. G. Ushveridze, "Anharmonic oscillator: Constructing the strong coupling expansions," *J. Math. Phys.*, vol. 29, no. 9, pp. 2053–2063, 1988.

[53] A. V. Turbiner, "A New Approach to finding levels of energy of bound states in quantum mechanics: Convergent perturbation theory," *Soviet Phys. – Pisma ZhETF*, vol. 30, pp. 379–383, 1979.

[54] F. Alarcón, *El estado excitado $2\sigma_g$ del ión molecular H_2^+ en un campo magnético.* Bsc thesis, UNAM, 2004.

[55] H. Medel, *Puntos críticos de sistemas moleculares coulombianos.* PhD thesis, UNAM, 2011.

[56] D. J. Nader, *Existencia de la cadena molecular de hidrógeno H_3 y del ión H_2^- en campos magnéticos intensos.* PhD thesis, UNAM, 2019.

[57] A. Genz and A. Malik, "Remarks on algorithm 006: An adaptive algorithm for numerical integration over an N-dimensional rectangular region," *J. Comput. Appl. Math.*, vol. 6, no. 4, pp. 295 – 302, 1980.

[58] D. Baye, "The Lagrange-mesh method," *Phys. Rep.*, vol. 565, no. Supplement C, pp. 1–107, 2015.

[59] H. Bateman, *Higher Transcendental Functions*, vol. 1. McGraw-Hill Book Company, 1953.

[60] A. D. Dolgov and V. S. Popov, "Higher orders an structure of the perturbation series for the anharmonic oscillator," *Zh. Eksp. Teor. Fiz.*, vol. 75, pp. 668–694, 1978.

[61] A. V. Turbiner, "On perturbation theory and variational methods in quantum mechanics," *Zh. Eksp. Teor. Fiz.*, vol. 79, pp. 1719 – 1745, 1980.

[62] A. V. Turbiner and A. G. Ushveridze, "Anharmonic oscillator: Constructing the strong coupling expansions," *J. Math. Phys.*, vol. 29, no. 9, pp. 2053–2063, 1988.

[63] F. M. Fernández and R. Guardiola, "The strong coupling expansion for anharmonic oscillators," *J. Phys. A*, vol. 30, no. 20, p. 7187, 1997.

[64] E. J. Weniger, "Construction of the strong coupling expansion for the ground state energy of the quartic, sextic, and octic anharmonic oscillator via a renormalized strong coupling expansion," *Phys. Rev. Lett.*, vol. 77, pp. 2859–2862, 1996.

[65] M. Abramowitz and I. A. Stegun, *Handbook of Mathematical Functions with Formulas, Graphs, and Mathematical Tables*. New York: Dover, 1964.

[66] H. Meißner and E. O. Steinborn, "Quartic, sextic, and octic anharmonic oscillators: Precise energies of ground state and excited states by an iterative method based on the generalized Bloch equation," *Phys. Rev. A*, vol. 56, pp. 1189–1200, 1997.

[67] M. R. M. Witwit, "Energy levels of two-dimensional anharmonic oscillators with sextic and octic perturbations," *J. Math. Phys.*, vol. 33, no. 12, pp. 4196–4205, 1992.

[68] W. H. P. Jordan, "Anwendung der Quantenmechanik auf das Problem der anomalen Zeemaneffekte," *Z. Phys.*, vol. 37, 1926.

[69] L. I. Schiff and H. Snyder, "Theory of the quadratic Zeeman effect," *Phys. Rev. (Series I)*, vol. 55, 1939.

[70] R. H. Garstang, "Atoms in high magnetic fields (white dwarfs)," *Rep. Prog. Phys.*, vol. 40, 1977.

[71] J. E. Avron, B. G. Adams, J. Čížek, M. Clay, M. L. Glasser, P. Otto, J. Paldus, and E. Vrscay, "Bender-Wu formula, the SO(4,2) dynamical group, and the Zeeman effect in hydrogen," *Phys. Rev. Lett.*, vol. 43, pp. 691–693, 1979.

[72] C. M. Bender and S. A. Orszag, *Advanced Mathematical Methods for Scientists and Engineers I: Asymptotic Methods and Perturbation Theory*. Springer-Verlag New York, 1 ed., 1999.

[73] J. L. Guillou and J. Zinn-Justin, "The hydrogen atom in strong magnetic fields: Summation of the weak field series expansion," *Ann. Phys.*, vol. 147, no. 1, pp. 57 – 84, 1983.

[74] Y. P. Kravchenko, M. A. Liberman, and B. Johansson, "Exact solution for a hydrogen atom in a magnetic field of arbitrary strength," *Phys. Rev. A*, vol. 54, pp. 287–305, 1996.

[75] D. Baye, M. Vincke, and M. Hesse, "Simple and accurate calculations on a Lagrange mesh of the hydrogen atom in a magnetic field," *J. Phys. B*, vol. 41, no. 5, p. 055005, 2008.

[76] J. H. Wang and C. S. Hsue, "Calculation of the energy levels of a hydrogen atom in a magnetic field of arbitrary strength by using B splines," *Phys. Rev. A*, vol. 52, pp. 4508–4514, 1995.

[77] R. Wallis and H. Bowlden, "Theory of impurity photo-ionization spectrum of semiconductors in magnetic fields," *J. Phys. Chem. Solids*, vol. 7, no. 1, pp. 78 – 89, 1958.

[78] Y. Yafet, R. Keyes, and E. Adams, "Hydrogen atom in a strong magnetic field," *J. Phys. Chem. Solids*, vol. 1, no. 3, pp. 137 – 142, 1956.

[79] A. Galindo and P. Pascual, "Hydrogen atom in a strong magnetic field," *Il Nuovo Cimento B (1971-1996)*, vol. 34, no. 1, pp. 155–168, 1976.

[80] A. V. Turbiner, "The hydrogen atom in an external magnetic field," *J. Phys. A*, vol. 17, no. 4, pp. 859–875, 1984.

[81] A. Y. Potekhin and A. V. Turbiner, "Hydrogen atom in a magnetic field: The quadrupole moment," *Phys. Rev. A*, vol. 63, p. 065402, 2001.

[82] H. Kobori and T. Ohyama, "Variational calculations of energy levels associated with 1s, 2p and 3d states of hydrogenic donors for semiconductors in arbitrary magnetic field," *J. Phys. Chem. Solids*, vol. 58, no. 12, pp. 2057 – 2064, 1997.

[83] E. O. Pokatilov and M. M. Rusanov, "Variational calculation of energy levels of a hydrogen-like system in a magnetic field," *Sov. Phys. Solid State*, vol. 10, p. 2458, 1969.

[84] D. Larsen, "Shallow donor levels of insb in a magnetic field," *J. Phys. Chem. Solids*, vol. 29, no. 2, pp. 271 – 280, 1968.

[85] N. Lee, D. Larsen, and B. Lax, "Exciton levels in a magnetic field," *J. Phys. Chem. Solids*, vol. 34, no. 6, pp. 1059 – 1067, 1973.

[86] P. C. Makado and N. C. McGill, "Energy levels of a neutral hydrogen-like system in a constant magnetic field of arbitrary strength," *J. Phys. C*, vol. 19, no. 6, 1986.

[87] D. Cabib, E. Fabri, and G. Fiorio, "The ground state of the exciton in a magnetic field," *Solid State Commun.*, vol. 9, no. 17, pp. 1517 – 1520, 1971.

[88] G. A. Arteca, F. M. Fernandez, and E. A. Castro, "Summation of the perturbation series for the energy levels of a hydrogen atom in a magnetic field," *Chem. Phys. Lett.*, vol. 102, no. 4, pp. 344 – 353, 1983.

[89] Z. Chen and S. P. Goldman, "Relativistic and nonrelativistic finite-basis-set calculations of low-lying levels of hydrogenic atoms in intense magnetic fields," *Phys. Rev. A*, vol. 45, pp. 1722–1731, 1992.

[90] H. C. Praddaude, "Energy levels of hydrogenlike atoms in a magnetic field," *Phys. Rev. A*, vol. 6, pp. 1321–1324, 1972.

[91] J. C. López-Vieyra and H. O. Pilón, "Hydrogen atom in a magnetic field: electromagnetic transitions of the lowest states," *Rev. Mex. Fis.*, vol. 54, no. 1, pp. 49 – 57, 2008.

[92] W. Rösner, G. Wunner, H. Herold, and H. Ruder, "Hydrogen atoms in arbitrary magnetic fields. I. Energy levels and wavefunctions," *J. Phys. B*, vol. 17, no. 1, pp. 29–52, 1984.

[93] M. V. Ivanov, "The hydrogen atom in a magnetic field of intermediate strength," *J. Phys. B*, vol. 21, no. 3, pp. 447–462, 1988.

[94] J. Xi, X. He, and B. Li, "Energy levels of the hydrogen atom in arbitrary magnetic fields obtained by using B-spline basis sets," *Phys. Rev. A*, vol. 46, pp. 5806–5811, 1992.

[95] H. R. G. Wunner, "Energy levels and electromagnetic transitions of atoms in supertrong magnetic fields," *J. Phys. Colloq.*, vol. 43, 1982.

[96] G. Fonte, P. Falsaperla, G. Schiffrer, and D. Stanzial, "Quadratic Zeeman effect for hydrogen: A method for rigorous bound-state error estimates," *Phys. Rev. A*, vol. 41, pp. 5807–5813, 1990.

[97] C. Stubbins, K. Das, and Y. Shiferaw, "Low-lying energy levels of the hydrogen atom in a strong magnetic field," *J. Phys. B*, vol. 37, no. 10, pp. 2201–2209, 2004.

[98] H. Nakashima and H. Nakatsuji, "Solving the Schrödinger and Dirac equations for a hydrogen atom in the universe's strongest magnetic fields with the free complement method," *Astrophys. J.*, vol. 725, no. 1, pp. 528–533, 2010.

[99] H. Hasegawa and R. Howard, "Optical absorption spectrum of hydrogenic atoms in a strong magnetic field," *J. Phys. Chem. Solids*, vol. 21, 1961.

[100] L. Gorkov and I. Dzyaloshinskii, "Contribution to the theory of the Mott exciton in a strong magnetic field," *Sov. Phys. JETP*, vol. 26, pp. 449–451, 1968.

[101] V. Pavlov-Verevkin and B. Zhilinskii, "Neutral hydrogen-like system in a magnetic field," *Phys. Lett. A*, vol. 78, no. 3, pp. 244–245, 1980.